Role of isoprenylation in the control of cell proliferation and apoptosis in Human Vascular Smooth Muscle Cells in culture

by

Sebnem Unlu

A thesis presented in fulfilment of the requirements of the degree of Doctor of Philosophy

1999

Imperial College School of Medicine

University of London

BIBL
LONDON
UNIV.

I dedicate this thesis to:

To The One who teaches us how to perservere with constancy,

My beloved parents,

My husband,

& Safiye

ABSTRACT

It is now recognised that increased levels of apoptosis and proliferation occur in atherosclerotic or restenotic lesions, and in cultured human vascular smooth muscle (HVSM) cells derived from these sources. The intracellular signals responsible for the regulation of apoptosis in these cells are still not understood. In this study we have used prenyl transferase inhibitors and lovastatin, an HMG-CoA reductase inhibitor, as tools to investigate the possible role of isoprenoids during apoptosis and proliferation of an immortalised HVSM cell line (SM1 cells) in culture and in primary HVSM cells. Lovastatin had no effect on primary, non-transformed cells, although addition of PDGF-BB after growth arrest led to an increase in apoptosis and cell cycle entry. Both apoptosis and S phase entry were inhibited after co-incubation of PDGF-BB with lovastatin. In contrast, addition of lovastatin to SM1 cells led to increased apoptosis in a time- and dose-dependent manner, as confirmed by flow cytometry, TUNEL staining, and DNA ladder assay. There was inhibition of cell proliferation and DNA synthesis after 48 hours. Co-incubation either with the isoprenoid, geranylgeranyl pyrophosphate or with mevalonate prevented the increase in apoptosis and inhibition of DNA synthesis and cell proliferation. In contrast, the addition of other mevalonate derivatives such as farnesyl pyrophosphate, cholesterol, or isopentenyladenosine had no effect on apoptosis. This suggested that geranylgeranylation is essential for the survival and proliferation of these cells. The addition of lovastatin or perillyl alcohol, a putative geranylgeranyl transferase inhibitor, to UVB treated SM1 cells was associated with increased levels of apoptosis and inhibition of DNA synthesis due to UVB alone. However, no significant changes in cell proliferation between the co-treated cultures and cultures treated with UVB alone were seen. Changes in the proportions of some cell cycle phases, as measured by flow cytometry, were also seen. In contrast, the addition of a farnesyl transferase inhibitor, B581, to SM1 cells had no significant effect on apoptosis, DNA synthesis, or cell proliferation. However, there was an increase in percentage total cell viability when B581 was co-incubated with UVB treated cells, with respect to those treated with UVB alone. DNA condensation after DAPI staining in cell cultures treated with B581 and UVB was also clearly absent, unlike those treated with UVB alone, indicating decreased sensitivity to UVB irradiation. No changes in the percentage proportion of any cell cycle phase (with respect to UVB treatment alone) were seen after treatment with B581. These data indicate that inhibition of HMG-CoA reductase or geranylgeranyl transferase is required for apoptosis in SM1 cells, while a selective decrease in farnesylation has no effect on SM1 cell growth or apoptosis. In conclusion, these data provide evidence that isoprenylation is important in the modulation of apoptosis and cell cycle entry in HVSM cells.

ACKNOWLEDGMENTS

Firstly, I am very grateful to Dr. Alun Hughes for his sincere enthusiasm and the kind help he offered whenever it was needed. I must also express my sincere thanks to Dr. N Sawhney for her much needed help with flow cytometry. I am grateful to Dr. X. Lu and Dr. J-K Hsieh, from the Ludwig Institute for Cancer Research, St Mary's Hospital, for helping me with the DNA ladder assay. The help provided by Dr G. Clunn for Phalloidin staining was much appreciated, as well as for valuable discussions for some experiments. I would also like to thank Dr J Lymn and Dr M Patel for their general help in the labs. I would also like to acknowledge the kind help of Dr M Schachter with various issues over the course of my studies. Many thanks goes to Dr C Demoliou-Mason for donating the transformed human VSM cell line, and also for various informative discussions. A lot of thanks goes to Professor P Sever for allowing me to work as a PhD student.

I am also indebted to all my friends and colleagues on the tenth floor of the QEQM wing, St. Mary's Hospital, for their great company and encouragement. Last, but not least, this work would not have been carried out if it were not for the selfless sacrifice and love of my beloved parents.

Finally, I would like to acknowledge with much praise my dear husband, and our daughter, Safiye. They were always there for me whenever I needed help, and constantly encouraged me with their love and enthusiasm. Verily, they deserve more than just to be mentioned on this page.

ABBREVATIONS

bp	Base pairs
cDNA	Complementary deoxyribonucleic acid
DAPI	4, 6-diamidino-2-phenylindole
DMSO	Dimethyl Sulphoxide
FACS	Fluorescence activated cell sorter
GDP	Guanosine diphosphate
GTP	Guanosine 5‘ trisphosphate
GTPase	Guanosine 5‘ trisphosphatase
HEPES	N-[2-hydroxyethyl]piperazine-N‘[2-ethanesulfonic acid]
[^{3}H]-	Tritium (radioactive isotope of hydrogen)
MAPK	Mitogen activated protein kinase
mRNA	messenger Ribonucleic acid
PBS	Phosphate buffered saline
PDGF	Platelet-derived growth factor
PI3K	Phosphatidyl inositol-3-kinase
RNase A	Ribonuclease A
VSM	Vascular smooth muscle

Measurements

^{o}C	Degrees Centigrade
kDa	kiloDalton
M	Molar
M_r	Relative molecular weight
mM	millimolar
µM	micromolar
ml	millilitres
µl	microlitres
µg	microgrammes

INDEX OF FIGURES

		Page no.
Figure 1.1:	Schematic representation of the morphological changes that may be observed once apoptosis has been triggered.	30
Figure 1.2:	Schematic representation of the cell cycle.	31
Figure 1.3:	Diagramatic stick representation of the molecular structure of lovastatin.	32
Figure 1.4:	Schematic representation of the changes which may take place in hepatocytes when endogenous mevalonate synthesis is blocked due to lovastatin.	33
Figure 1.5:	Flow diagram of the mevalonate pathway.	48
Figure 1.6:	Schematic stick representation of the chemical structure of isoprenyl derivatives of mevalonate.	49
Figure 1.7:	Schematic representation depicting the Carboxy-terminal (C-terminal) processing of isoprenylated proteins.	50
Figure 2.1:	Diagrams depicting the gating of a propidium iodide (PI)-stained population to measure the DNA content of the hypodiploid region and the specific cell cycle phases.	72
Figure 2.2:	Diagrams representing the dot plot and the DNA content frequency histograms of a standard population of nuclei, required to calibrate the flow cytometer.	73
Figure 2.3:	Agarose 2% (w/v) gel electrophoresis of DNA extracted from SM1 cells using the standard salting out method.	74
Figure 2.4:	Agarose 2% (w/v) gel electrophoresis of DNA extracted from SM1 cells indicating the negligible prominence of DNA laddering.	75
Figure 2.5:	Agarose gel (2%) electrophoresis of different amounts of DNA weight marker (ϕX174 plasmid DNA *Hae* III digest at 0.04mg/ml, final concentration) to determine the optimal mass of pure DNA to be loaded with SYBR Green I dye.	76
Figure 2.6:	Agarose gel (2%, w/v) electrophoresis of DNA extracted from saos-2 cells after induction with 200nM $ZnCl_2$ in 0.4% (v/v) FBS and incubated for 18 hours, by the Gong J et al., 1994 method.	77
Figure 3.1:	Morphological effects of lovastatin in SM1 cells in culture.	84

Figure 3.2: Cytochemical effects of lovastatin on SM1 cells in culture. 85

Figure 3.3: Dose-dependent changes in the hypodiploid DNA content of SM1 cell cultures after lovastatin treatment. 86

Figure 3.4: Dose-dependent effects of lovastatin on DNA fragmentation. 87

Figure 3.5: Recovery of lovastatin-induced apoptosis when co-incubated with mevalonate. 88

Figure 3.6: Time-dependent effect of lovastatin in serum-free medium on apoptosis in SM1 cells. 89

Figure 3.7: Time-dependent effect of lovastatin in serum-free medium on cell cycle phases in SM1 cells. 90

Figure 3.8: Time-dependent effect of lovastatin in 10 % dialysed (v/v) FBS on apoptosis in SM1 cells. 91

Figure 3.9: Time-dependent effect of 10μM lovastatin on SM1 cell cycle phases as assessed by flow cytometry. 92

Figure 3.10: Time-dependent effects of lovastatin treatment on DNA fragmentation in SM1 cells. 93

Figure 3.11: Recovery of lovastatin-induced increase in the hypodiploid DNA content of SM1 cells with mevalonate or geranylgeranyl pyrophosphate. 94

Figure 3.12: Decrease in lovastatin-induced DNA fragmentation after co-incubation with mevalonate or geranylgeranyl pyrophosphate. 95

Figure 3.13: Effect of lovastatin on cell proliferation of SM1 cells in serum-free medium. 96

Figure 3.14: Effect of lovastatin on SM1 cell proliferation in 10% dialysed (v/v) FBS. 97

Figure 3.15: Lovastatin-induced inhibition of [^{3}H] thymidine incorporation is reversed in the presence of mevalonate (100μM) or geranylgeranyl pyrophosphate (10μM). 98

Figure 3.16: Effect of mevalonate, geranylgeranyl or farnesyl pyrophosphate on lovastatin-induced inhibition of cell proliferation. 99

Figure 3.17: Time-dependent effect of lovastatin on the actin cytoskeleton in SM1 cells. 100

Figure 4.1: The schematic stick representation of the chemical structure of perillyl alcohol. 113

Figure 4.2: Dose- and time-dependent effect of perillyl alcohol on cell proliferation in SM1 cells. 114

Figure 4.3: Effect of perillyl alcohol on % total cell viability in SM1 cells. 115

Figure 4.4: Dose-dependent effect of perillyl alcohol on [^{3}H] thymidine incorporation in SM1 cells. 116

Figure 4.5: Morphological effects of perillyl alcohol in SM1 cells in culture. 117

Figure 4.6: Cytochemical effects of perillyl alcohol on SM1 cells. 118

Figure 4.7: Effects of perillyl alcohol on fluorescent DNA fragmentation in SM1cells. 119

Figure 4.8: Time-dependent effect of perillyl alcohol on % proportion of the hypodiploid. 120

Figure 4.9: Time-dependent effect of 2mM perillyl alcohol on SM1 cell cycle phases as assessed by flow cytometry. 121

Figure 4.10: Time-dependent effect of perillyl alcohol on DNA fragmentation in SM1 cells. 122

Figure 4.11: Differential effects of geranylgeranyl pyrophosphate on lovastatin and perillyl alcohol-induced apoptosis in SM1 cells. 123

Figure 5.1: Effect of UVB irradiation on cell proliferation and cell viability in SM1 cells. 134

Figure 5.2: Morphological effects of UVB irradiation on SM1 cells. 135

Figure 5.3: Cytochemical effects of UVB irradiation on SM1 cells. 136

Figure 5.4: Effects of UVB irradiation on fluorescent DNA fragmentation in SM1cells. 137

Figure 5.5: Time-dependent effect of UVB irradiation on % total proportion of the hypodiploid DNA content in SM1 cells. 138

Figure 5.6: Time-dependent effect of UVB irradiation on SM1 cell cycle phases as assessed by flow cytometry. 139

Figure 5.7: Time-dependent effect of UVB irradiation on DNA fragmentation in SM1 cells. 140

Figure 5.8: Effect of perillyl alcohol, farnesyl transferase inhibitor, B581 and lovastatin co-incubation of UVB treated cells on hypodiploid DNA content. 141

Figure 5.9: Effect of perillyl alcohol, farnesyl transferase inhibitor, B581, and lovastatin co-incubation of UVB treated cells on % proportion of cell cycle phases as assessed by flow cytometry. 142

Figure 5.10: Effect of lovastatin, or the farnesyl transferase inhibitor on UVB-induced increase in DNA fragmentation. 143

Figure 5.11: Cytochemical effects of perillyl alcohol, the farnesyl transferase inhibitor, B581, and lovastatin on UVB-induced DNA condensation in SM1 cells. 144

Figure 5.12: Effect of perillyl alcohol, the farnesyl transferase inhibitor, B581, and lovastatin on UVB-induced inhibition of cell proliferation in SM1 cells. 145

Figure 5.13: Effect of perillyl alcohol, the farnesyl transferase inhibitor, B581, and lovastatin on % total cell viability of SM1 cells exposed to UVB. 146

Figure 5.14: Effect of perillyl alcohol, farnesyl transferase inhibitor, and lovastatin on UVB-induced inhibition of thymidine incorporation in SM1 cells. 147

Figure 6.1: Morphological effects of PDGF-BB in growth-arrested primary human saphenous vein-derived smooth muscle cells in culture. 158

Figure 6.2: Cytochemical effects of stimulation of growth-arrested human VSM cells with PDGF-BB. 159

Figure 6.3: Effects of PDGF-BB on fluorescent DNA fragmentation in growth-arrested human VSM cells. 160

Figure 6.4: Effect of treatment of growth-arrested primary VSM cells with PDGF-BB, and co-incubation with lovastatin on hypodiploid DNA content of cultures. 161

Figure 6.5: The effect of stimulation with PDGF-BB on DNA fragmentation in growth-arrested primary human VSM cells. 162

Figure 6.6: Effect of treatment of growth-arrested primary VSM cells with PDGF-BB, and co-incubation with lovastatin on cell cycle S-phase DNA content of cultures. 163

Figure 6.7: Cytochemical effects of co-stimulation of growth-arrested human VSM cells with PDGF-BB and lovastatin. 164

Figure 6.8: Effects of co-stimulation with both PDGF-BB and lovastatin on fluorescent DNA fragmentation in growth-arrested human VSM cells. 165

Contents

Page no.

Title 1
Dedication 2
Abstract 3
Acknowledgements 4
Abbreviations 5
Index of Figures 6

Chapter 1

INTRODUCTION

1.1.1.1 Background 17

1.1.2.1 History of apoptotic cell death 17

1.1.3.1 Control of tissue function through cell death and proliferation 19

1.2.3.1 Coupling of cell death and proliferation in health and disease 19

1.3.3.1 Cell cycle checkpoints and apoptosis 20

1.4.3.1 Importance of vascular smooth muscle (VSM) cell death and proliferation in the healthy and diseased vasculature 21

1.5.3.1 Is there a role for human vascular smooth muscle (VSM) cell proliferation in the ontogeny of atherosclerotic and restenotic lesions? 24

1.1.4.1 Cardiovascular disease and the beneficial effects of lovastatin 27

1.2.4.1 Lovastatin: structure, source and use 27

1.3.4.1 Effects at the clinical level 28

1.1.1.2 Role of isoprenylation in cell function 34

1.1.2.2 Isoprenoid synthesis 34

1.2.2.2 The Mevalonate pathway 34

1.1.3.2 Isoprenylation as a means of protein modification 35

1.2.3.2 Discovery 35

1.3.3.2 Inhibitors of prenyl transferases 37

1.4.3.2 Functional purpose of isoprenylation 37

1.1.4.2 Potential for opposite, but complementary signaling through Ras and Ras-related small GTPases: cell proliferation or cell death through apoptosis 39

1.2.4.2 Same proteins involved in contrasting pathways 39

1.3.4.2 Common pathways leading to apoptosis or mitosis 41

1.1.5.2 Isoprenoids and cell growth control 43

1.2.5.2 Isoprenylation during cell proliferation 43

1.3.5.2 Cell cycle entry and isoprenylation 45

1.4.5.2 Mevalonate and isoprenylation in the control of apoptosis 46

1.1.6.2 Targeting signal transduction pathways as a means for therapy 47

OBJECTIVES 51

Chapter 2

MATERIALS AND METHODS 52

2.1.1.1 Drugs and Reagents 52

2.2.1.1 Preparation of lovastatin 52

2.3.1.1 Mevalonate and mevalonate derivatives 52

2.4.1.1 Prenyl transferase inhibitors 53

2.5.1.1 Mitogens 53

2.6.1.1 Molecular Biology reagents 53

2.7.1.1 Materials for thymidine incorporation 53

2.8.1.1 Treatments 53

2.1.1.2 Cell culture media and Reagents 54

2.1.1.3 Cell culture 55

2.1.2.3 Cell types used 55

2.1.3.3 Explant technique for isolation of primary HVSM cells 56

2.1.4.3 Culture conditions 56

2.1.5.3 Long term storage of cells 57

2.1.6.3 Thawing of cells frozen in liquid nitrogen 57

2.1.7.3 Dialysis of Foetal Bovine Serum 57

2.1.1.4 DNA Content Flow Cytometric analysis 57

2.1.2.4 Principle of the technique 57

2.1.3.4 Limitations and disadvantages 58

2.1.4.4 Analysis of apoptotic populations by flow cytometry 59

2.1.5.4 Sample preparation 59

2.1.6.4 Calibration of the FACScan ™ 60

2.1.7.4 Acquisition and analysis of data 61

2.1.1.5 Thymidine incorporation 62

2.1.1.6 Optimisation of the DNA "ladder" assay 63

2.1.2.6 Principle of the technique 63

2.1.3.6 Detection of DNA fragmentation in SM1 cells 63

2.1.4.6 Salting out method (adapted from Wyllie A.H. et. al. 1980) 64

2.1.5.6 The Gong J et al., 1994 method 65

2.1.6.6 Final optimized procedure 67

2.1.1.7 Cytochemical techniques 68

2.1.2.7 TUNEL (terminal deoxynucleotidyl transferase-mediated dUTP nick end labeling) assay 68

2.1.3.7 DAPI staining 69

2.1.4.7 Phalloidin staining 69

2.1.1.8 Cell proliferation assay 70

2.1.1.9 Cell Viability assay 70

2.1.1.10 Statistics and Data Analysis 71

Chapter 3

GERANYLGERANYL PYROPHOSPHATE PREVENTS THE PRO-APOPTOTIC AND ANTI-PROLIFERATIVE EFFECTS OF LOVASTATIN ON SV-40 TRANSFORMED HUMAN VSM CELLS IN CULTURE

3.1.1.1 Introduction 78

3.1.1.2 Results 79

3.1.2.2 Effect of lovastatin on apoptosis and changes in cell cycle phases in transformed human VSM cells (SM1 cells) 79

3.1.3.2 Effect of mevalonate derivatives on apoptosis induced by lovastatin 81

3.1.4.2 Effect of lovastatin (10μM) on cell proliferation and viability of SM1 cells 82

3.1.5.2 Effect of isoprenoid derivatives of mevalonate on lovastatin-induced inhibition of cell proliferation and thymidine incorporation in SM1 cells 82

3.1.6.2 The effect of lovastatin on the actin cytoskeleton, as revealed after Phalloidin staining 83

3.1.1.3 Discussion 101

Chapter 4

ACTION OF PERILLY ALCOHOL ON CELL PROLIFERATION AND APOPTOSIS IN SV-40 TRANSFORMED HUMAN VSM CELLS IN CULTURE

4.1.1.1 Introduction 109

4.1.1.2 Results 110

4.1.2.2 Effect of perillyl alcohol on SM1 cell proliferation, DNA synthesis and cell viability 110

4.1.2.3 Effect of perillyl alcohol on changes in apoptosis and the cell cycle phases in SM1 cells 110

4.1.1.3 Discussion 124

Chapter 5

DIFFERENTIAL EFFECTS OF LOVASTATIN, PERILLYL ALCOHOL AND A FARNESYL TRANSFERASE INHIBITOR ON CELL PROLIFERATION AND APOPTOSIS OF SM1 CELLS

5.1.1.1 Introduction 127

5.1.1.2 Results 128

5.1.2.2 Effect of UVB irradiation on cell proliferation and viability in SM1 cells 128

5.1.3.2 Effect of UVB irradiation on apoptosis and the cell cycle phases in SM1 cells 128

5.1.4.2 Effect of lovastatin, perillyl alcohol and a farnesyl transferase inhibitor, B581, on UVB-induced apoptosis and changes in the cell cycle phases 130

5.1.5.2 Effect of lovastatin, perillyl alcohol and B581 on UVB-induced inhibition of cell proliferation, viability and thymidine incorporation 132

5.1.1.3 Discussion 148

Chapter 6

STIMULATION WITH PLATELET-DERIVED GROWTH FACTOR-BB IS ASSOCIATED WITH APOPTOSIS IN CULTURED PRIMARY HUMAN VSM CELLS DERIVED FROM SAPHENOUS VEIN

6.1.1.1 Introduction 154

6.1.1.2 Results 156

6.1.2.2 Cell death and entry into S phase after stimulation of confluent growth-arrested human VSM cells with PDGF-BB 156

6.1.3.2 Effect of lovastatin on PDGF-BB induced apoptosis and S phase entry in human VSM cells 157

6.1.1.3 Discussion 166

CONCLUDING REMARKS and FUTURE WORK 174

BIBLIOGRAPHY 177

Publications relating to this thesis 213

Appendix 214

Chapter 1

INTRODUCTION

1.1.1.1 Background

1.1.2.1 The history of apoptotic cell death

The first description of the effects of tissue loss due to cell death, seen at a gross level as gangrene, were presented in Virchow's Cellular Pathology in 1858 (**Virchow R, 1859**). However, descriptions of regressing tissue, which resulted in a "new, clean, sculpted form" without any tissue degeneration were also described. These descriptions were meant to imply "slow death" or "the death of tissues within the living body". When stains to visualize the nucleus became available in 1885, Walther Flemming (**Flemming W, 1885**) described the first examples of what is now recognized as apoptotic cell death. In his study, he noticed that the nuclei of some cells of the regressing follicle epithelium were fragmented into "half moons" of condensed chromatin; similar observations were reported from studies on cells from lactating mammary glands. **Glucksmann A.** (1951) also saw the same morphological manifestations in the cells of the developing embryo.

Kerr JFR et al., finally coined the term "apoptosis" in 1972. Apoptotic cells were observed after withdrawal of the adrenocorticotrophic hormone from the adrenal gland, and during liver atrophy in the rat after tying off the portal vein. The same observations were also made in untreated malignant neoplasms and during tissue regression following therapy. In all of these cases the ultrastructural changes seen in the cells were essentially the same. These changes indicated that a controlled, defined mode of cell death took place in a wide range of biological systems under various physiological and pathological conditions, characterized by a set of conserved morphological changes irrespective of the stimulus. The authors eventually raised the possibility that this response may be as ubiquitous as cell proliferation and differentiation.

Subsequently, several workers found that the chromatin in irradiated lymphoid tissue and cells *in vitro* was degraded in a distinct internucleosomal manner (**Skalka M. et**

al., 1976). Once a method of DNA extraction was established (**Wyllie AH et al., 1980**), it was used to verify the pattern of DNA degradation (**Yamada T. et al., 1981**) and (**Zhivotovsky BD et al., 1981**). It was **Wyllie et al., in 1984** who correlated the morphological manifestations of apoptotic cells with the internucleosomal degradation of DNA extracted from them.

Hence, a ubiquitous form of cell death was defined with the following sequence of ultrastructural morphological and biochemical manifestations, which, in the majority of cases, can be taken as determinants of cell apoptosis (**Arends M J et al., 1990**):

1) Loss of contact from neighbouring cells as cell shrinkage occurs, the cell becoming rounded up, with increased optical density.
2) Condensation of chromatin into the periphery of the nuclear membrane. Consequently the chromatin appears packed and stains densely with DNA binding dyes.
3) Nuclear fragmentation may then occur, but in most cases the organelles remain intact.
4) Cell membrane budding may be seen where nuclear fragments are packed into vesicular bodies. However, the integrity of the cell membrane appears intact (**Figure 1.1**).
5) At the molecular level, the DNA may become fragmented into multiples of 185bp (internucleosomal distance) oligofragments due to distinct cleavage sites between nucleosomes.
6) In most cases the fragmented DNA, which has exposed 5‘ ends can be probed cytohistochemically with a labelled deoxyUracil tri-phosphate (dUTP) nucleotide analogue, which is incorporated using a terminal deoxynucleotide transferase (**Gavrieli Y et al., 1992**).

Although this is the archetypal description of apoptosis, there are many examples where cell death may not be associated with the sequence of manifestations outlined as above. For example, during brain development (**McConkey DJ et al., 1996**), and during necrotic death of cells under certain chronic pathological conditions, such as the formation of tumours (**Arends MJ et al., 1994**). Necrotic cell death *in vivo* may be associated with an inflammatory response, due to the lysis and leakage of

intracellular contents into the surrounding milieu as the cells are disintegrated. Morphologically, cell death by necrosis may display similar characteristics to apoptotic cell death, but it is generally assumed that the DNA of such cells may be fragmented in a random manner, or not fragmented at all (**Majno G and Joris I, 1995**). Also, unlike the necrotic process, apoptosis has been characterised as an active, energy requiring mechanism, probably necesssary for the synchronised exit of the cell from tissues without any damage to the surrounding area (**Maeda S et al. 1995**). In almost all cases the apoptotic form of cell death was shown to display similar morphological changes. Hence, it is now believed that the key intracellular molecules involved in this process are conserved in most organisms from nematode to man (**McConkey DJ et al., 1996**).

1.1.3.1 Control of tissue function through cell death and proliferation

1.2.3.1 Coupling of cell death and proliferation in health and disease

The selective and precise elimination of specific cells from tissues under normal physiological and developmental conditions represents an important biological principle (**McConkey DJ et al., 1996**). The existence of apoptosis as a complementary counterpart to cell proliferation ensures that an optimum number of cells and hence the three dimensional structure of the tissue is maintained. This is essential because any perturbations in the inherent cell population would otherwise disrupt the structure and the normal function of that tissue. It is therefore not surprising to see that apoptosis *in vivo* is widespread when rapid proliferation is taking place in normal, healthy tissues (**Kerr JFR and Harmon BV, 1991**). Such a tightly regulated mechanism ensures the deletion of certain cells which are not beneficial to the tissue, such as pre-neoplastic, old or damaged cells whilst allowing the survival of those cells that are beneficial. Excessive or uncontrolled proliferation, and the persistence of aberrant cells, mainly due to decreased apoptosis, are clearly seen not only in many tumours (**Corcoran GB et al., 1994**), but also in many other diseases, such as left ventricular hypertrophy in hypertensive patients (**Barr PJ and Tomei LD, 1994**). Furthermore, excessive cell death of

certain cells also seems to be another factor for some diseases such as AIDS. some autoimmune diseases and Alzheimer's (**Barr PJ and Tomei LD, 1994**).

Elimination of cells through apoptosis also takes place after migration of certain cells to an abnormal location, or when cells such as lymphocytes become self-reactive. Both these situations may be harmful, and such cells must be eliminated. Hence, it can be inferred from these examples, that the survival or apoptotic threshold of cells is acutely sensitive to the presence or absence of certain factors outside the cell. These extracellular factors influence the intracellular signals involved in the regulation of survival (**Rudin CM and Thompson CB, 1997**). Thus, the final fate of the cell is determined through the balance of inhibitors and inducers of apoptosis (**MacLellan WR and Schneider MD, 1997**). Under the appropriate conditions, the balance may be tipped towards the pro-apoptotic signals resulting in more cell death or alternatively, fewer cells are deleted when the balance is tipped towards the anti-apoptotic signals. The nature of this balance, however, may be different for different cell types and it may even differ within a cell type depending on the conditions around each cell. The regulation of these signaling cascades appears to be perturbed in some diseases. This can have a direct repercussion on cell-population control and consequently on tissue health. It is therefore imperative to understand what factors are required for determining the final outcome of cell fate in order to find an effective intervention strategy for treatment (**Barr PJ and Tomei LD, 1994**).

1.3.3.1 Cell cycle checkpoints and apoptosis

Successful progression through the cell cycle is required for proliferation of cells. Stimulation of growth arrested or quiescent cells with serum-containing medium results in cell cycle entry. The cell cycle traverse begins by moving from the quiescent G_o/G_1 phase to S-phase where DNA synthesis is initiated; and once the DNA content doubles with respect to the G_1 phase, entry into the G_2/M phase occurs prior to cell division (**Murray A and Hunt T, 1993**). For more details, see **Figure 1.2**).

When aberrant conditions prevail, growth arrest is often initiated at the G_o/G_1 phase. The purpose of this growth arrest is to allow the repair of damage prior to cell

proliferation, or alternatively to initiate apoptosis if cell damage is irrepairable. Effectively, in this case, the aberrant cell is "sacrificed" or eliminated rather than allowed to proceed into the next phase of the cell cycle (**Meikrantz W and Schlegel R, 1995**). The biochemical processes by which such "decisions" are made are increasingly being defined.

Cell cycle entry, progression through S phase, and completion of mitosis, is now known to be dependent on the activity of key enzymes and proteins which act as checkpoints. These include cyclins, cyclin-dependent kinases, endogenous inhibitors of cyclin-dependent kinases, such as p21Cip1/Waf1 and p27Kip1 (**Reed S I, 1997**), certain nuclear immediate-early genes such as *c-myc*, *c-fos* (**Muller R et al. 1984; Thompson NL et al., 1986**) and proliferating cell nuclear antigen (PCNA) (**Murray A, 1994; Elledge SJ, 1996**). Another regulatory gene required for progression from quiescence to cell growth was the phosphorylated retinoblastoma susceptibility gene (RB) (**Reed S I, 1997**). Recent evidence indicates that isoprenylated proteins, such as Ras and Rho small GTPases, are crucial for the determination of cell fate (**Gomez J et al., 1998**) and for cell cycle entry (**Olson MF et al., 1995**).

1.4.3.1 Importance of vascular smooth muscle (VSM) cell death and proliferation in the healthy and diseased vasculature

Depending on the specific internal or external changes in conditions such as somatic growth or altered flow, a dynamic change in the three dimensional structure of vessels occurs *in vivo*. Such changes are required for the maintenance of optimum structure, which is essential for the optimal function of the tissue. This process has been termed vascular remodelling, and has been shown to occur through a fine balance between apoptosis and cell proliferation of smooth muscle cells, for instance during the development of human *ductus arteriosus* (**Slomp J. et al., 1997**), and during neonatal vascular development (**Cho A. et al., 1995**). The majority of studies on VSM cell apoptosis have been *in vitro* (**Bennett M.R. et al., 1994**). Hence the actual role of apoptosis in adult human VSM cells *in vivo* remains largely speculative, although the remodelling of the carotid artery wall in response to altered flow *in vivo* has been demonstrated to involve proliferation and apoptosis (**Cho A et. al., 1997**). Apoptosis is also thought to be involved in vascular diseases like

restenosis and atherosclerosis (**Bennett M R and Boyle J J, 1998**). For example, hypertension is associated not only with increased cell DNA synthesis but also with increased DNA nick end-labeling, in the vessel media and in the target organs, which may be indicative of apoptosis (**Hamet P. et al., 1995b**). Hamet et al., proposed that remodeling represented a new balance of enhanced cell growth and cell death due to the stimulation of both proliferative and apoptotic pathways. They also pointed out that in normal adulthood, this homeostatic mechanism continues to operate at a low rate.

Though only negligible levels of proliferative smooth muscle cell activity has been detected in atherosclerotic and restenotic tissues, abnormal accumulation of smooth muscle cells in the neointima remains a consistent feature of these diseases (**O'Brien E.R. et al., 1993**). Neointimal lesion formation is most probably the result of an imbalance between cell proliferation and cell death. A high rate of DNA nick-end labelling in medial VSM cells was shown to occur immediately after balloon injury of healthy rat, and rabbit arteries (**Perlman H. et al., 1997**). After re-endothelialization, the rate of apoptosis within the neo-intima was reduced (**Bochation-Piallat M. L., et al., 1995**).

Similarly, the presence of a relatively higher percentage of apoptotic VSM cells has been demonstrated in atherectomy specimens from human coronary plaques, as compared to healthy arterial tissue on the basis of DNA nick end-end labeling (**Han D. et al., 1995**). Restenotic lesions in human saphenous vein grafts after by-pass grafting were shown to contain a large number of apoptotic human VSM cells (**Kockx M M et al., 1994**). Similarly, the proportion of DNA nick-end labeling in restenotic tissue was greater with respect to labeling in primary atherosclerotic tissue (**Isner J et al., 1995**). Under serum-free conditions plaque-derived VSM cells *in vitro* were also shown to have 8- to 10- fold greater rates of apoptosis than their healthy counterparts (**Bennett M R et al., 1995**).

It should be noted, however, that the measurement of DNA nick-end labeling provides no direct indication of the 'temporal' window of apoptosis, since the staining is a mere measure of the final, accumulated end-point of the label. Also, DNA nick-end labeling may lead to false positive staining, due to the presence of

endogenous nucleotidyl transferases, required for functional DNA rearrangements (**Smith A and Haaf T, 1998**).

There is as yet no firm information on the temporal pattern of apoptosis, during the development of the disease, although recent evidence indicates that a decrease in the rate of apoptosis may contribute to neointimal hyperplasia. Restenosis after angioplasty was shown to decrease in a rabbit model after suicide gene therapy (**Steg P G et al., 1997**), or after inhibition of *bcl-x* (a gene product known to prevent apoptosis) expression in the neointima (**Pollman M J et al., 1998**). *Fas* ligand gene transfer to the vessel wall was also shown to decrease neointima formation (**Sata M et. al., 1998**), indicating that decreased levels of apoptosis may be involved in neointima formation during vascular disease. The *Fas* receptor is a membrane-bound protein which mediates apoptosis after it is crosslinked with *Fas* ligand (**Kobayashi S and Koike T, 1996**). Thus, neointima formation may be due to the direct accumulation of cells, due to decreased levels of apoptosis, which otherwise would have been eliminated through this process. Evidence to support this hypothesis on neointima formation was shown by **Bauriedel G et al., 1998** who demonstrated lower levels of apoptosis in restenotic tissue with respect to primary lesions.

Acceleration of apoptosis at some stage during the process of primary lesion formation (atherogenesis) may also be a contributing factor to vascular disease. For example, the progressive decrease in "synthetic" VSM cell density could account for the apparent increase in acellular fibrous deposits (**Newby A.C. et. al., 1996**). Interestingly a fall in the number of VSM cells was associated with an increase in lipid filled macrophages (**Davies M. J. et al., 1993**). This may be due to an increased concentration of interleukins, interferon-gamma and TNF-α released from macrophages, shown to promote the loss of the VSM cell population through apoptosis *in vitro* (**Geng Y J et al., 1996**). In 1994, **Schaefer HE** reported that a significant "atrophy" of VSM cells, probably through apoptosis, occurs in the media with advancing age and progress of atherosclerosis. This was to some extent, associated with intra- and extracellular calcification (**Schaefer HE, 1994**). Increased *Bax* immunoreactivity, a pro-apoptotic gene product known to be associated with accelerated apoptosis (**Oltvai Z N et al., 1993**), was also detected in patients who

underwent atherectomy for primary atherosclerosis in the carotid artery, 85% of whom were also hypertensive (**Konstadoulakis M. M. et al., 1998**).

As compared to VSM cells isolated from normotensive vessels, cells from hypertensive vessels were shown to have an increased sensitivity to apoptosis after serum withdrawal (**Tagami M. et al., 1996**). Likewise, increased levels of cell proliferation and of DNA synthesis in VSM cells and in cells of other target organs have been shown to be a feature of hypertension both *in vivo* and *in vitro* (**Walter S.V. and Hamet P. 1986**); **Hadrava V. et al., 1989**; **Yamori Y. et al., 1981**). This increase was shown *in vitro* to parallel that of apoptosis (**Hamet P. et al., 1995b**). The co-existence of both processes was later shown to be persistent in pressure overload-induced heart hypertrophy, suggesting that remodeling during hypertrophy of the cardiac walls may be coupled to hypertension (**Teiger E. et al., 1996**). In this model, the level of apoptosis initially peaked, and then dwindled while cardiac growth persisted for a long period. Hence, in **1996**, **Hamet P. et al.,** proposed a hypothesis whereby an inherent deficiency in apoptosis may be present in neonatal hypertension as in spontaneously hypertensive rat (SHR). This, they inferred, most probably predisposed or contributed towards hyperplasia and hence to hypertrophy, where the rate of apoptosis diminishes below control levels as the mass of the heart increases (**Hamet P. et al., 1996**). This hypothesis was further confirmed by (**Moreau P. et al., 1997**) who demonstrated for the first time that there is an altered balance in the coupling of cell proliferation and cell death in newborn SHR.

Evidence of selective VSM cell death, by apoptosis, was also found to be present in the aneurysmal vessel wall (**Lopez-Candales et al., 1997**), which may be a contributing factor to the eventual rupture of the vessel.

1.5.3.1 Is there a role for human vascular smooth muscle (VSM) cell proliferation in the ontogeny of atherosclerotic and restenotic lesions?

Efforts to understand the mechanisms involved in luminal narrowing after intervention of atherosclerotic and restenotic tissues have mainly concentrated on healthy animal models of vascular injury, such as the rat carotid artery (**Schwartz SM et al., 1995**). There has also been a widespread assumption that the hypothesis of vascular response to injury as put forward by **Ross (1993)** may be applicable to

the response of restenosis after intervention of diseased vessels. Although some pharmacological treatments had an inhibitory effect on intimal thickening after baloon angioplasty in animal models, this was not transferable to human restenosis trials. In the animal models of balloon catheter inflicted injury, there was a dramatic rise in the proliferation of vascular smooth muscle cells (**Clowes AW et al., 1983**). In contrast, various attempts to find a significant quantitative increase in VSM cell replication in human atherosclerotic and restenotic lesions have remained unsuccessful (**Gordon D et al., 1990**; **O'Brien E R et al., 1993**). Although a high labeling frequency of proliferating cell nuclear antigen (PCNA) was found in atherosclerotic plaques, the labeled cells were mainly identified as endothelial cells. Hence, it is still not known whether similar mechanisms are involved in the formation of neointima in animals and humans. Nonetheless, this does not mean that proliferation of vascular smooth muscle cells does not take place at all. It could be that the method of detection of cell proliferation in human tissue may require further improvements. For example, if the proposal that atherosclerotic lesions may be monoclonal is accepted (**Benditt EP, 1977; Schwartz SM and Murry CE, 1998**), this would imply that selective replication of some smooth muscle cells could occur sometime during the formation of the lesions. This event may take place early over a limited time period, or in a more subtle way which ensures the long-term persistence of the plaque. As for restenosis after intervention, the replicative phase may take place shortly after the injury. All these events would be unlikely to be detected with the methods currently used, such as the immunohistochemical staining for PCNA, a marker for cell proliferation, which is applied after several days or even months following intervention.

Indirect evidence for the increased proliferation of smooth muscle cells in vascular disease comes from a study which showed the presence of non-raised fibrous plaques in 2% of children at 6-10 years of age. Fatty streaks and gelatinous plaques in 6% of juveniles between 11 to 15 years were also seen in the same study (**Velican D and Velican C, 1979**). This is an interesting observation, indicating that development of lesions may pertain to certain lifestyle conditions of the individual.

In the swine model fed with a hyperlipidemic diet, it was found that [^{3}H] thymidine labeling indices of lesions (LI) were 3-4 fold greater with respect to the control

intimal cell masses. After a period of 9-18 months on hyperlipidemic diet, lesion size and cell numbers increased further by about 3-fold, whereas if the animal was put on a regression diet for the same period, the growth of lesions stopped completely. This complete regression was primarily accounted for by "turning off" excessive DNA synthesis and restoration to normal levels of intimal cell mass (**Kim DN et al., 1988**). It would appear that these "foci" of increased intimal proliferative activity are sensitive markers of risk factors for atherogenesis. However, whether these patches contain proliferating vascular smooth muscle cells is still unknown. A cytogenetic analysis of primary cell cultures derived from atheromatous plaque has indicated that the cells with clonal chromososme abnormalitites were mainly vascular smooth muscle cells with 100% positivity for vimentin, a cytoskeletal protein considered specific for smooth muscle cells (**Casalone R. et al., 1991**). Other autoradiography and ultrastructural studies on human fibro-atheromatous plaques have indicated the presence primarily of foam cells and monocyte-like cells (**Villaschi S et al., 1983**). However, since the fibrotic plaque is a late stage in atherogenesis, the presence of proliferating VSM cells may not be detected at this stage.

In restenosis, focal proliferation of VSM cells on neointimal surfaces of the coronary artery was evident in a patient who died 17 days after angioplasty (**Austin GE et al., 1985**). In fact it is not surprising that mechanical intervention, endothelial injury and platelet aggregation at the site of the dilatation may further aggravate and enhance the proliferation of VSM cells (**Hanke H and Karsch KR, 1992**). Such an increase in the rate of VSM cell proliferation was also confirmed by comparative studies on restenotic tissue explants and primary lesion explants (**Pickering JG et al., 1992**). Subsequently, it has been reported that restenotic as compared to primary tissue is significantly more likely to contain areas of intimal hyperplasia (**Taylor AJ et al., 1995**). From these observations, it is generally inferred that an early nodal proliferation of smooth muscle cells most probably forms the focal lesions seen in atherosclerosis. Better evidence for a more widespread accumulation or proliferation of intimal vascular cells derives from studies on restenosis after intervention.

Studies of cultured smooth muscle cells have yielded relatively more information and a clearer insight into the underlying factors, which may be involved in these

vascular diseases. For example, certain *in vivo* characteristics of smooth muscle cells isolated from atherosclerotic lesions appear to be retained as intrinsic properties under *in vitro* conditions. These include enhanced proliferative activity and accumulation of lipids (**Orekhov A N et al., 1986**). The effect of various anti-proliferative drugs has been tested on these cells, and it was proposed that such primary cultures may be a useful tool for studying atherosclerosis and its treatment (**Voisard R et al., 1991**). Culture medium from smooth muscle cells derived from atherosclerotic plaques was shown to stimulate the growth of normal aortic smooth muscle cells. This may indicate that greater amounts of certain autocrine/paracrine factors are released from atherosclerotic smooth muscle cells, with respect to normal aortic cells (**Libby P et al., 1988**). Hence, it seems that diseased vascular smooth muscle cells are cytochemically different from vascular cells in normal vessels. The intracellular mechanisms, which may thus be affected, must either be involved in cell proliferation or in cell death or both. Further evidence to support the differences at the cellular level of potentially restenotic and healthy tissue derives from the work of **Chan P et al., 1994**. Human VSM cells derived from intimal hyperplastic regions were shown to have a reduced sensitivity to growth inhibition by heparin *in vitro*, as compared to cells derived from normal vascular tissue. Furthermore a subsequent study (**Refson JS et al., 1998**) showed that individuals whose cells showed reduced sensitivity to growth inhibition by heparin were more likely to suffer graft stenosis over a 18 month follow up period. This may imply some pre-existing defect predisposing cells to proliferate abnormally in some individuals. Whether such a defect is also applicable to factors involved in the regulation of cell death is unknown.

1.1.4.1 Cardiovascular disease and the beneficial effects of Lovastatin

1.2.4.1 Lovastatin: structure, source and use

Lovastatin (mevinolin, Mevacor) is a clinically developed fungal metabolite derived from *Aspergillus terreus* (**Tobert JA et al., 1982**). The chemical structure of lovastatin consists of a lipophilic lactone ring (**Figure 1.3**). It is a competitive,

reversible inhibitor of 3-hydroxy-3-methylglutaryl coenzyme A (HMG-CoA) reductase, the enzyme required to catalyse the generation of mevalonate. This is the first, rate-limiting step in the synthesis of many other mevalonate derived byproducts, including cholesterol (for further details, see later and **Figure 1.7**). Lovastatin is administered in its lactone form in single or divided doses of 20 to 80 mg/day (**Tobert JA, 1987**). Used in hypercholesterolemic patients, it has proved to be a very effective and well-tolerated drug for the lowering of total plasma cholesterol and low density lipoprotein (LDL)-cholesterol.

1.3.4.1 Effects at the clinical level

Lovastatin has been shown to be efficacious in the reduction of cardiovascular morbidity and mortality in clinical trials (reviewed in **Furberg CD et al., 1994 and Ballantyne C M, 1998**). This action is shared by other statin drugs, such as simvastatin and pravastatin, and has been attributed primarily to significant reductions in plasma LDL-cholesterol levels. In humans, cholesterol is a substrate for bile acid synthesis, and is also required for the assembly of very low density lipoprotein in the liver. As a result, there is a high demand for cholesterol in this organ, with respect to other organs. Cholesterol is cleared from the circulation primarily through the LDL receptors on hepatocytes. Intake of a statin leads to inhibition of HMG-CoA reductase and hence a block in intracellular cholesterol biosynthesis. Under normal circumstances, the presence of intracellular cholesterol increases the degradation of LDL receptors. When cholesterol synthesis is blocked, LDL receptors on the surface of cells are upregulated (**Chan PC et al., 1997**), leading to lower circulating levels of blood LDL-cholesterol due to increased uptake of cholesterol from the plasma (**Figure 1.4**).

Recent evidence suggests that effects other than, or in addition to, the reduction in plasma lipid levels may contribute for the beneficial effects seen in heart disease patients (**Massy ZA et al., 1996; Vaughan CJ et al., 1996; Hughes AD, 1996**). This is not a surprising finding, since not only cholesterol but also many other important non-sterol compounds required for proper cell function are derived from mevalonate. Therefore, inhibition of mevalonate synthesis due to HMG-CoA reductase inhibition may be expected to have far reaching, pleiotropic consequences,

compromising many functions. In fact, when whole rats were fed with mevalonate, the systolic blood pressure was decreased with respect to the vehicle fed rats, without a significant change in plasma cholesterol. Lovastatin, however, was associated with the opposite effects (**Roullet J-B, et al., 1993**). Other HMG-CoA reductase inhibitors have been shown to decrease not only plasma concentrations of cholesterol, but also mevalonate, ubiquinone and dolichol (**Pappu AS, et al., 1989**).

Addition of lovastatin to rapidly proliferating tumour and normal mammalian cells in culture, but not to quiescent cells, was associated with growth arrest in the G_1 phase of the cell cycle, which was overcome with mevalonate co-incubation (**Keyomarsi K et al., 1991**). However, co-incubation with cholesterol was ineffective for cell cycle recovery. This fact indicates that certain mevalonate derivatives involved in cell proliferation are turned over at a higher rate, and therefore an inhibition of mevalonate synthesis affects those functions with the highest demands for these derivatives. Quiescent cells were relatively unaffected probably due to the relatively lower turnover rate, and hence a lower demand of mevalonate derivatives in these cells. It is also interesting to note that mevinolin was shown to suppress the growth of murine neuroblastoma cells transfected into mice, without any alterations in serum cholesterol levels (**Maltese WA et al., 1985**).

The intracellular concentrations of these mevalonate derivatives which may be playing crucial roles during cell proliferation are still unknown in the clinical setting. Although the plasma concentrations of the drug in patients in clinical trials are known to be 5-10 times lower than those used for the *in vitro* experiments (**Massy ZA, et al., 1996**), tissue levels of the statin are unknown. In fact, some tissue levels may be higher than the plasma concentrations (**Duggan DE et al., 1989**). It is possible that such higher concentrations of the statin could affect cell function. Tissues with a high cell turnover rate may also be more susceptible to the effects of statins than tissues containing differentiated or quiescent cells (**Massy ZA et al., 1996**).

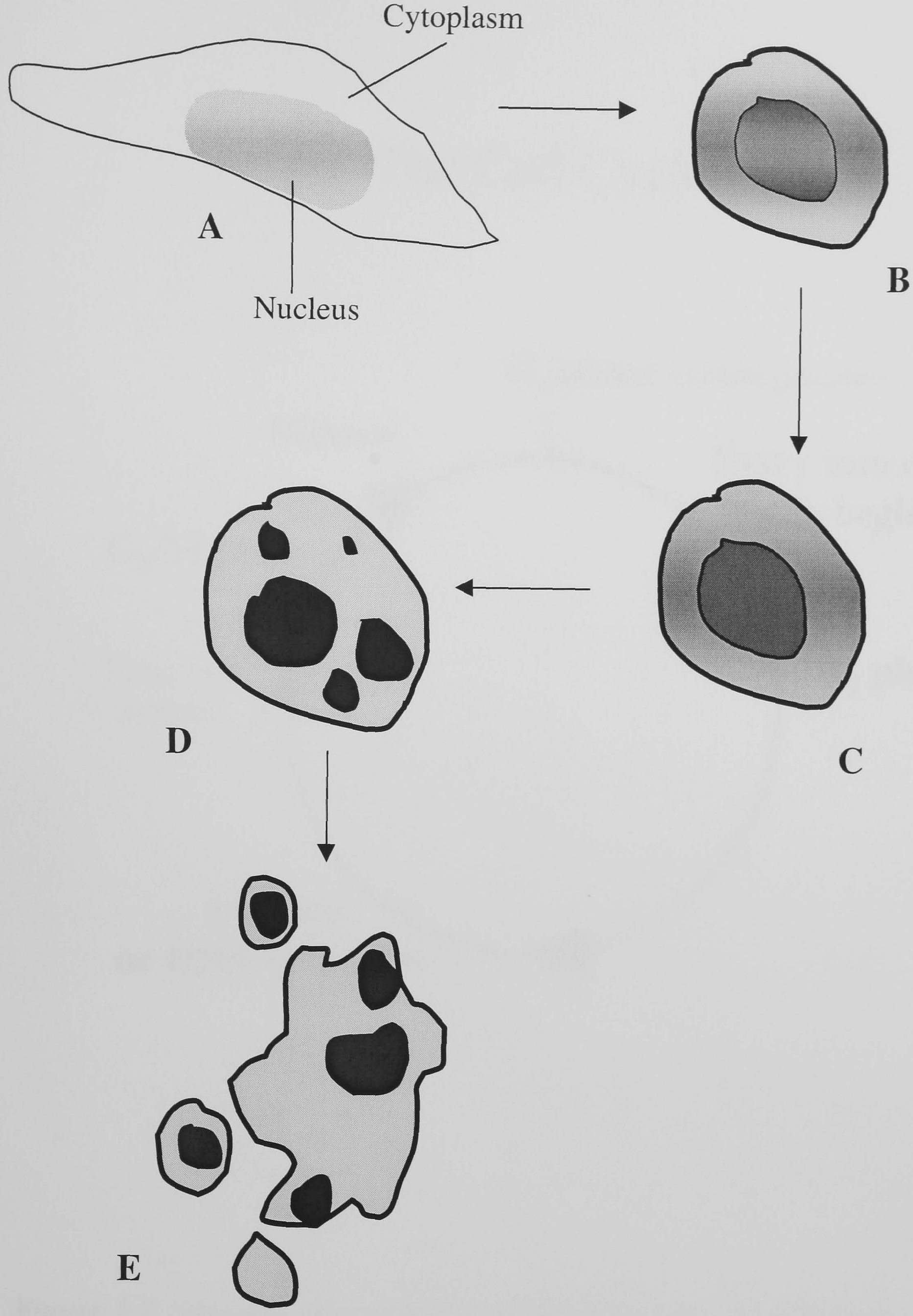


Figure 1.1 Schematic representation of the morphological changes that may be observed once apoptosis has been triggered. The normal cell (**A**) is shown to have an organised, sparse cytoplasm and heterogenous nuclear chromatin. At an early stage in apoptosis, there is rounding up, and loss in cell volume, as seen in (**B**). Later the the cytoplasm may becometightly packed and the chromatin may be condensed, as seen in (**C**). Subsequently, the nucleus may then be fragmented into discrete masses of condensed chromatin (**D**). Finally, fragmentation of the entire cytoplasm into many membrane-bound vesicles (apoptotic bodies) may be observed (**E**). These apoptotic bodies are presumed to be phagocytosed by surrounding cells or passing phagocytes.

Figure 1.2 Schematic representation of the cell cycle. Entry and progression through G_1 phase, the process of DNA synthesis or replication (S-phase), cell division (G_2/M-phase) is dependent on the synchronised and co-ordinated activity of regulatory enzymes, the cylin dependent kinases (cdks) and cyclins. Other proteins, like the small GTPase, Rho, have been shown to be required for a successful entry into S-phase. Cell cycle inhibitory proteins, such as p21Cip1 and p27Kip1, have been shown to be involved in the negative control of these proteins (see discussion of Chapter 6). Completion of the cell cycle, however, requires other proteins, which are probably upregulated when optimal conditions for cell growth exist (see text).

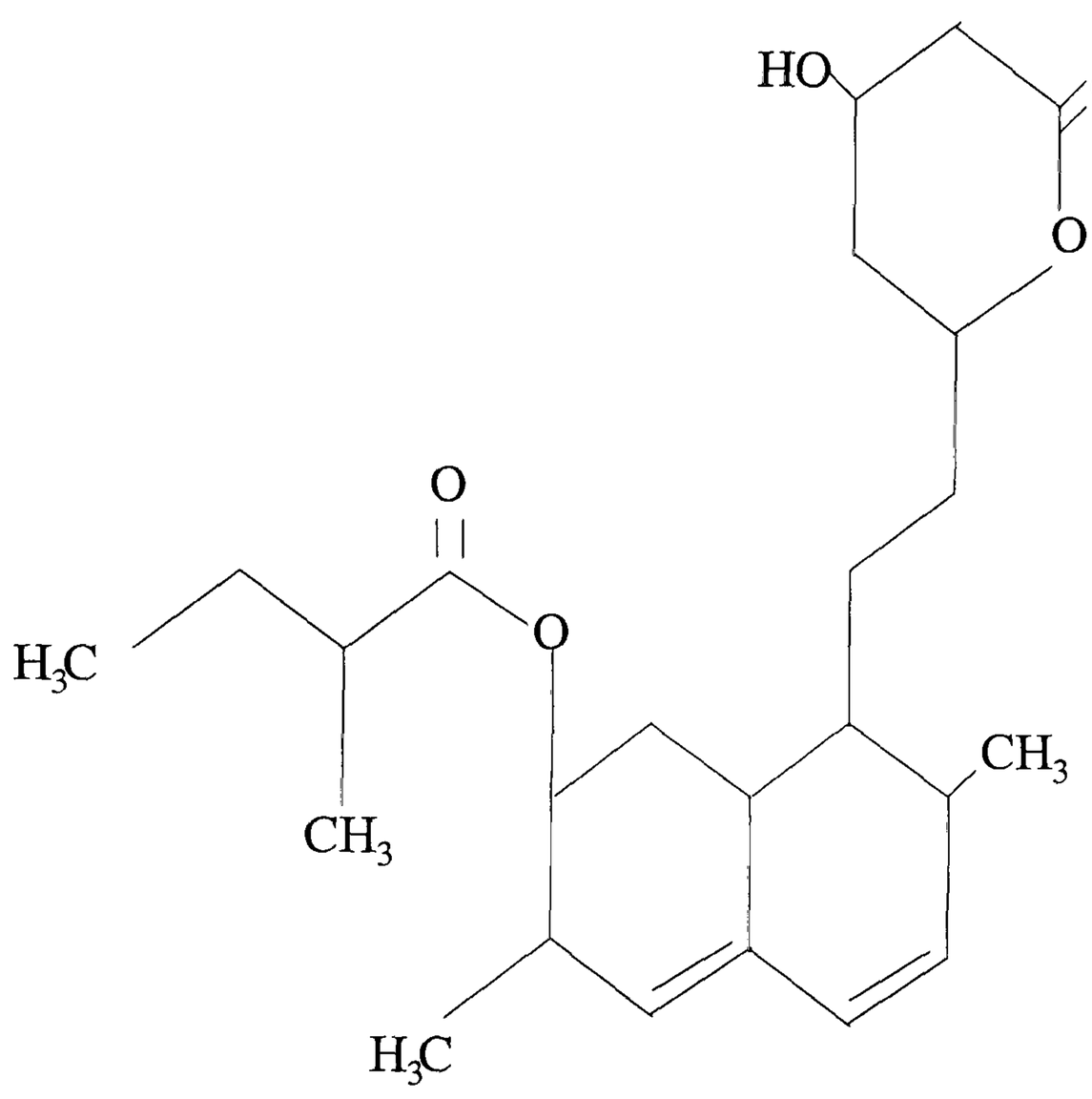


Figure 1.3 Diagramatic stick representation of the molecular structure of lovastatin.

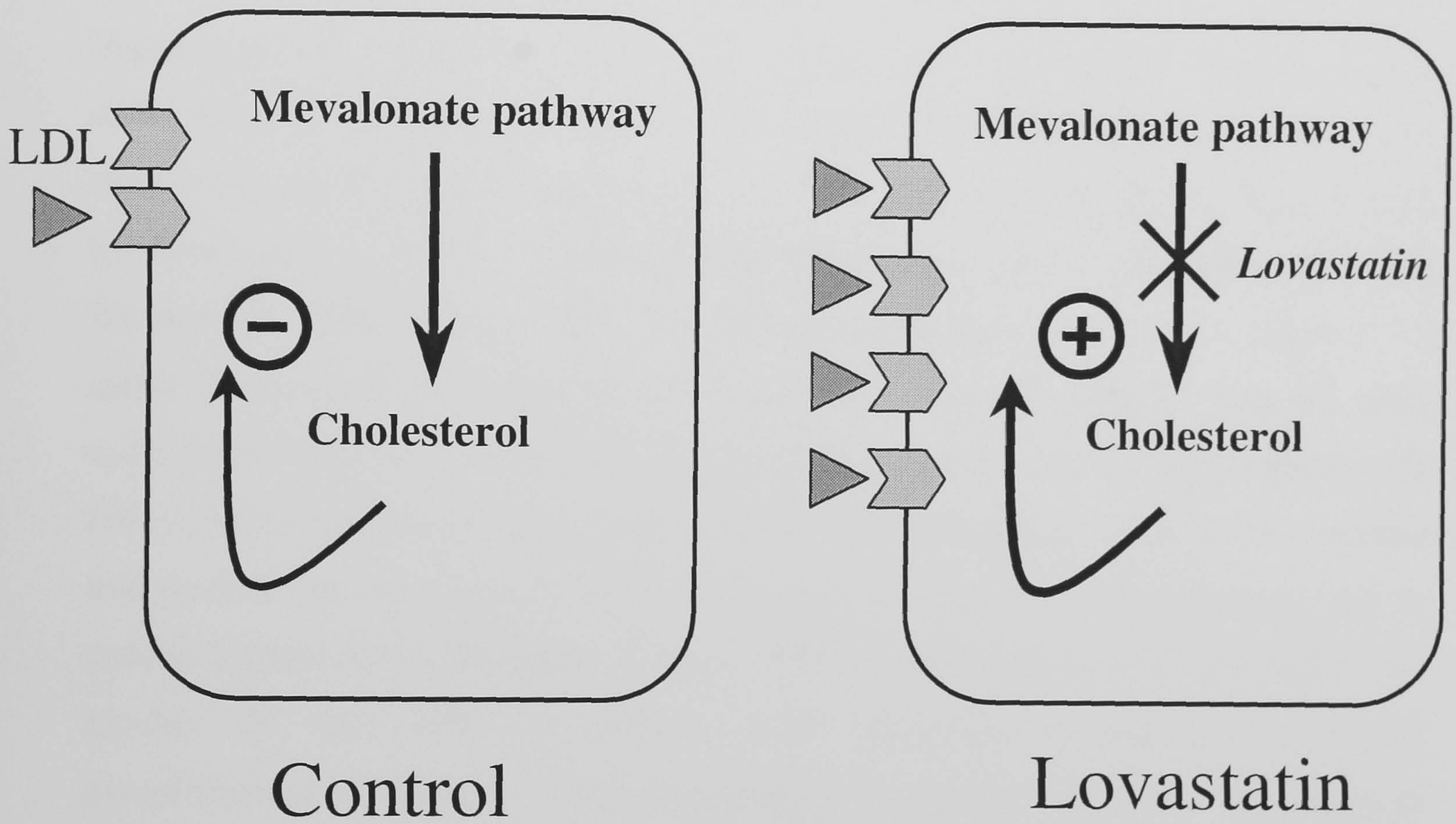


Figure 1.4 Schematic representation of the changes which may take place in hepatocytes when endogenous mevalonate synthesis is blocked due to lovastatin. In order to prevent excessive uptake of exogenous cholesterol through LDL receptor-mediated endocytosis, synthesis of low density lipoprotein (LDL) receptors is negatively regulated when adequate levels of endogenous cholesterol are synthesised *de novo* through the mevalonate metabolic pathway. However, inhibition of HMG-CoA reductase, required for the synthesis of mevalonate and hence endogenous cholesterol, leads to the upregulation of LDL receptors on the surface of hepatocytes. To meet the increased need for endogenous cholesterol, LDL receptors are upregulated for increased uptake of plasma LDL from the bloodstream as a source of exogenous cholesterol. This then results in the lowering of LDL-cholesterol levels in the blood of patients prescribed with lovastatin (see text).

1.1.1.2 Role of isoprenylation in cell function

1.1.2.2 Isoprenoid synthesis

1.2.2.2 The Mevalonate pathway

Endogenous mevalonate is synthesised from HMG-CoA, in the first, rate-limiting step of the pathway through 3-hydroxy, 3-methylglutaryl (HMG)-CoA reductase. After the discovery of compactin (ML-236B), a fungal metabolite, by **Endo A et al., in 1976** as a specific, competitive and reversible inhibitor of HMG-CoA reductase, the importance of mevalonate derivatives other than cholesterol became better understood. It was found that isoprenoids including their derivatives like dolichol and ubiquinone, as well as cholesterol and other sterol-based compounds, such as steroid hormones were in fact the metabolic derivatives of mevalonate (**Goldstein J L and Brown MS, 1990**) (**Figure 1.5**). Mevalonate is converted into 5-carbon units (C5), called isopentenyl pyrophosphate (IPP) (**Grunler J et al., 1994**). Two C5 units combine to form a C10 compound, geranyl pyrophosphate, which then combines with IPP to form farnesol pyrophosphate (Fpp), a C15 compound. FPP is the common intermediate for the biosynthesis of cholesterol, dolichol and ubiquinone as well as protein isoprenylation (**Grunler J et. al., 1994**). Additionally, FPP combines with another C5 unit (IPP) to form a C20 compound, all-*trans*-geranylgeranyl pyrophosphate (GGPP). These conversions are prevented in the presence of lovastatin due to the absence of the IPP units.

Although the bulk end-product of the pathway, cholesterol, is mainly derived exogenously from plasma low-density lipoprotein (LDL) in mammalian cells, some is also synthesised endogenously through the pathway. When cholesterol levels are high, small amounts of mevalonate are synthesised for the non-sterol end-products (**Brown MS and Goldstein J L, 1980**). The enzymes required for the synthesis of the non-sterol by-products of the pathway were shown to have higher affinities for mevalonate-derived substrates than those of cholesterol synthesis (**Brown MS and Goldstein JL, 1980**). However, when mevalonate is limiting, the substrates derived from it are preferentially shunted into the high-affinity non-sterol pathways. Work by **Nakanishi M et. al., 1988** showed that in the presence of compactin, the levels and activity of HMG-CoA reductase were high, even though the cells were saturated with

sterols. Addition of excess mevalonate or smaller amounts of mevalonate along with plasma LDL to the cells treated with compactin, was seen to inhibit the translation of HMG-CoA reductase mRNA, and enhance the degradation of the protein. This indicated that negative feedback inhibition of HMG-CoA reductase mRNA translation was primarily governed by non-sterol derivatives of mevalonate.

The direct incorporation or flux of hydrogen in the form of tritium (^3H) from [^3H]-mevalonate into the two isoprenoid groups, farnesyl and geranylgeranyl pyrophosphate was first demonstrated by (**Lutz, R J et. al., 1992**). This established that isoprenoids were generated directly from mevalonate.

1.1.3.2. Isoprenylation as a means of protein modification

1.2.3.2 Discovery

The first discovery of an isoprenylated molecule came from the studies of **Kamiya et. al.** in **1978** who showed that certain fungal peptide hormones were modified by a 15-carbon farnesylcysteine residue (**Figure 1.6**). This simple isoprene substituent on the protein is made from a chain of carbon and hydrogen atoms.

In groundbreaking experiments in **1984**, **Schmidt RA et. al.,** established that the proteins labelled with [^3H] mevalonate in Swiss 3T3 cells were in fact modified with isoprenoids. Soon after, it was shown that isoprenylation of proteins was in fact a general post-translational modification in mammalian cells (**Maltese WA and Sheridan KM, 1987**). **Farnsworth CC et. al., 1990** subsequently demonstrated that the majority of the proteins in mammalian cells were prenylated with a carbon-20 geranylgeranyl residue (**Figure 1.6**). The idea that proteins involved in eukaryotic cell proliferation may also be prenylated, then led to the discovery of a carbon-15 farnesyl isoprenoid substitute on the p21ras protein, shown earlier to be required for cell proliferation (**Casey P J et. al., 1989**; **Hancock J F et. al., 1989**). However, the majority of the small GTPases (20-30kDa) such as *rac* and *rho*, were later shown to be geranylgeranylated (**Didsbury J R et. al., 1990**; **Yoshida Y et. al., 1991**).

Hence two isoprenyl modifications, namely with farnesyl and geranylgeranyl, are now recognised as ubiquitous modifications of many proteins involved in cell signalling

(**Casey PJ, 1994**). Two endogenous enzymes required for the transfer of these isoprenoids to their respective protein substrates have been recognised, namely protein farnesyl transferase (FTase) and protein geranylgeranyl transferase (GGTase-I) (**Clarke S, 1992; Newman C and Magee AI, 1993**). These enzymes, termed the *CaaX* prenyl transferases, recognise a tetra-peptide sequence on the carboxyl-(C) terminus of a protein onto which the isoprenoid group is transferred (**Figure 1.7**). The isoprenoid was shown to bind as a diphosphate analogue since enzyme denaturation was associated with the release of the intact diphosphate (**Yokoyama K et. al., 1993**). This isoprenoid pyrophosphate molecule was substituted onto a concensus amino acid sequence designated as the -*CaaX*- motif, where "*a*" refers to an aliphatic residue, "*X*" can be any amino acid residue while "C" stands for the amino acid cysteine (**Clarke S, 1992**). The amino acid cysteine is absolutely required for isoprenylation. However, the amino acid "*X*" specifies whether the protein will be farnesylated (methionine or serine) or geranylgeranylated (leucine or phenylalanine) by the appropriate enzyme (**Clarke S, 1992**). This scheme is generally found in most cells, but exceptions do occur (**Rowell C A et al., 1997**). Substrates for FTases include the Ras GTPases, and other large proteins not involved in cell signalling such as the nuclear lamins (**Clarke s, 1992**). Known targets of GGTaseI include mainly the Ras-related small GTPases, such as members of the Ras and Rac/Rho families (**Casey PJ and Seabra MC, 1996**).

Although *CaaX* prenyltransferases have been shown to be relatively selective for their respective protein substrates, some cross-reactivity and relative flexibility in their substrate binding has been observed (**Moores SL, et. al., 1991; James GL et. al., 1995a**). Such a capacity to modulate alternate substrates most probably has some kind of biological significance (**Casey PJ and Seabra MC, 1996**). For example, a specific form of Ras protein, K-Ras, has been shown to be a substrate for both FTase and GGTase-I (**James GL et. al., 1995b**). A potent GGTase I inhibitor was shown to inhibit K-Ras processing and oncogenic signaling (**Lerner EC et. al., 1995**). The GGTase-I enzyme was shown to mediate the transfer of either isoprenoid onto a Ras-related protein, RhoB (**Armstrong SA et. al., 1995**).

1.3.3.2 Inhibitors of prenyl transferases

An important property of both FTase and GGTaseI is that short peptides containing the -*CaaX*- motif are bound onto the enzymes with equal affinity as the native protein substrates (**Reiss Y et al., 1990**). Hence, such peptides have been used to design other cell-permeable, peptidomimetic compounds that are specific, competitive inhibitors of these enzymes. One such peptide, CVFM, was found to serve as a basis for the design of specific FTase inhibitors, which may be used both *in vitro* and *in vivo*. Treatment of many oncogenic Ras-transformed, cancerous cells with these compounds was found to result in the reversion of the transformed phenotype (**James GL et. al., 1993**), indicating that FTase inhibitors may be beneficial as chemotherapeutic agents. Such an absolute need for farnesylation in oncogenic Ras transformation led to increased efforts in the development of many FTase inhibitors as anti-cancer drugs (**Casey PJ and Seabra MC, 1996**).

1.4.3.2 Functional purpose of isoprenylation

The possible biochemical and functional consequences of isoprenylation of proteins involved in signal transduction is of especial interest. Recent evidence indicates that the prenyl modification of certain proteins is essential for their proper biological function, probably being involved in membrane and protein-protein interactions (**Spiegel AM et. al., 1991**) and (**Marshall CJ, 1993**). The precise role of these modifications in the function of each protein is not properly understood. It is still unknown whether the prenyl substituted cysteine residue in prenylated proteins acts as a hydrophobic anchor for the association of the respective protein with membranes or with other specific proteins. However, it has been generally assumed that such a hydrophobic/lipidic modification may serve to enhance or direct membrane association. Experiments done by **Perez-Sala, D.** (cited in **Rando RR, 1996**), have indicated that the hydrophobicity of geranylgeranylated cysteine derivatives were about 85-fold higher than farnesylated cysteine derivatives. It was also shown that methylation and mild proteolysis of a 1kDa fragment from the C-terminal fragment from several small GTPases was enough to prevent cell membrane association (**Yamane HK et. al., 1989**).

Nonetheless, many prenylated proteins studied after subcellular fractionation were found to be located in the cytosol (**Maltese WA and Sheridan, KM, 1987**). Another study showed the distribution of several isoprenylated proteins was heterogenous, i.e. proteins with the same prenylation were found in a variety of subcellular locations or membranes (**Maltese WA, 1990**). For example, the geranylgeranylated *rap1B* protein was found in the supernatant fraction in inactivated platelets but in platelets that had been aggravated with alpha-thrombin and the calcium ionophore, A23187, it was found in the cytoskeletal fraction (**Fischer T H et al., 1990**). Likewise, the G25K protein, also shown to be geranylgeranylated (**Yamane H K et al., 1991**) was found predominantly in the cytosol of murine erythroleukemia cells (**Maltese WA and Sheridan KM, 1990**). These observations indicated that the prenylation of a particular protein does not necessarily result in cell membrane association.

The small GTPase proteins, Ras and Rho, were shown to be involved in the control of cell proliferation and apoptosis (**Lacal JC, 1997**). For example, the *ras* protein was shown to be involved in growth control signalling (**Bourne HR et. al., 1991**) and (**Gomez J et. al., 1996**). Recent work has identified a protein kinase, *raf*, a cytosolic second messenger, as the target of farnesylated and methylated *ras* (**Stokoe D et al., 1994**). However, when *raf* itself was farnesylated through the engineering of a concensus prenylation motif (-*CaaX*-) into it, the resulting *raf* was activated in the absence of *ras* through direct association with the membrane. These experiments indicate that prenylation of proteins is not only needed to facilitate association with membranes, but is also required for binding to effector proteins permitting functional activity. Hence, farnesylation of, for example, the *ras* protein may be required for its coupling to certain effector proteins. In fact, when the cysteine residue essential for the isoprenylation process is substituted with another residue, such as serine, then the resulting *ras* protein remains inactive in its unprocessed form (**Gutierrez L et. al., 1989**). In *Xenopus* oocytes, prenylation of p21 *ras* was shown to be necessary for the activation of the mitogen-activated protein kinase pathway (**Kuroda Y et. al., 1993**). All this evidence also suggests that certain prenyl "receptor" molecules may be present on membranes for each prenylated protein, since it has been predicted that the branched structure of the prenyl group may not be able to undergo direct insertion into membranes (**Marshall CJ, 1993**).

Evidence that isoprenylation may be required for functions other than membrane attachment comes from studies on the Ras superfamily of small GTPases, which are known to be regulated through reversible guanidine nucleotide (GTP) binding. The small GTPases "cycle" between an active guanosine triphosphate (GTP)-bound and an inactive guanosine diphosphate (GDP)-bound form. In the GDP-bound form, interaction with exchange factors that regulate GDP release takes place, whereas in the GTP-bound state, the proteins interact with effector proteins and GTPase-activating proteins (**Marshall CJ, 1993**). This interaction, however, may take place completely in the cytosol, without the requirement of any membrane binding. The *Rap1* protein serves as an example of this. *Rap1* has been shown to be involved in mitogenic pathways (**Altshuler DL and Ribeiro-Neto, 1998**) and as a negative regulator of the *Ras* signalling pathway (**Wani MA et. al., 1997**). Competition studies with peptides encompassing the C-terminus of *rap1A*, a geranygeranylated protein, have been shown to inhibit its interaction with a GDP/GTP exchange protein (**Shirataki H et al., 1991**). The p21 *rho A* protein was also shown to require a prenylated C-terminus for activation with a stimulatory GTP/GDP exchange protein (**Mizuno T et. al., 1991**). Geranylgeranylation of Rac proteins were recently shown to be essential for association with RhoGDI (Rho-GDP dissociation inhibitor) (**Hancock JF and Hall A, 1993**).

1.1.4.2. Potential for opposite, but complementary signaling through Ras and Ras-related small GTPases: cell proliferation or cell death through apoptosis

1.2.4.2 Same proteins involved in contrasting pathways

Some *Ras* proteins, like *Ki-Ras*, has been shown to be modified either with a geranylgeranyl or a farnesyl residue *in vivo* (**Rowell C A et. al., 1997**). In these experiments, *Ki-Ras* was demonstrated to be increasingly modified, in a dose-dependent manner, with a geranylgeranyl residue in the presence of increasing concentrations of farnesyl transferase (FTase) inhibitors, B956 or B957. Additionally, a Ras-related protein implicated in cytoskeletal organisation, RhoB, was shown to be modified by either farnesyl or geranylgeranyl (**Adamson P et. al.,**

1992a). The significance of these modifications, however, is still not understood, but may possibly be related to the fact that these proteins seem to be involved in signalling pathways determining cell fate. **Chen CY and Faller DV, 1995** have demonstrated that Ras molecules were involved during the stimulation of both apoptosis and cell proliferation.

It is also interesting to note that the majority of *rho* proteins, mainly *rhoA* and *rhoC* are geranylgeranylated, and yet they are generally localised in the cytosol (**Adamson P et. al., 1992b**). *rhoB* proteins which can be found in farnesyl modified form, are mainly localised on intra-cellular membranes. This is a very interesting observation, since the longer carbon-20 isoprenoid group is known to be more hydrophobic, and hence would be more likely to be expected in association with membranes than the carbon-15 moiety.

Rac1 proteins, which are geranylgeranylated (**Didsbury J R et. al., 1990**) have been shown to be involved in pro-apoptotic signalling (**Brenner B et. al., 1997**), in anti-apoptotic signalling (**Eves EM et. al., 1998**), as well as in cell cycle progression (**Moore K A et. al., 1997**). The *cdc42* protein, which is also known to be geranylgeranylated (**Ziman M et al., 1993**) was shown to be involved not only in the initiation of an apoptotic signalling pathway (**Chuang TH et al., 1997**), but also in cell cycle progression (**Bordoulous S et al., 1998**). Finally, the γ subunit of heterotrimeric G proteins, also known to be geranylgeranylated (**Mumby S M et al., 1990**) have been demonstrated to be involved in apoptotic signalling (**Giambarella U et al., 1997**) as well as in signalling for mitogenesis (**Crouch MF and Simson L, 1997**).

These data provide further evidence that the specific isoprenyl groups attached onto proteins involved in control of cell growth and apoptosis may govern crucial protein-protein interactions during signal transduction. This means that the isoprenylated proteins may potentially interact with a plethora of downstream effector proteins and may therefore be involved in differential signals determining cell fate.

1.3.4.2 Common pathways leading to apoptosis or mitosis

Since the final morphological changes seen in a diverse number of apoptotic cell types seem to be conserved, it was inferred that a conserved, common, final pathway of cell death may be triggered in all cells. Such a proposal would be comparable to the specific pathways that are involved in mitosis and cell proliferation (**Vaux DL, 1993**). This concept was first proposed in a crude way by **Raff M. (1992)**. It has been supported through further evidence, such as the protective effect of gene products like *Bcl-2* in response to a variety of cell death-inducing stimuli, like growth-factor withdrawal and UV-irradiation. Likewise, a number of molecules like *Bax*, which promote apoptosis have also been identified. Thus increasing evidence suggests that both promoter and inhibitory molecules are involved in the regulation of a final common apoptotic pathway. When exposed to a cell-death stimulus, the signals invoked finally lead to the activation of the cell death machinery, in which case all the house-keeping functions of the cell are irreversibly switched off in an ordered manner (**Kroemer G. et. al. 1995).** These include proteolysis of certain proteins through a conserved set of proteases called caspases (**Nunez G et. al., 1998**), release of cytochome c from mitochondria and mitochondrial transmembrane depolarisation (**Green DR and Reed JC, 1998**). Under normal conditions, such as quiescence, differentiation or proliferation, the entry into this final pathway is inhibited. However, increasing evidence suggests that a co-ordinated regulation of both cell death and cell proliferation signalling machinery may be involved (**King K L and Cidlowski J A, 1998**), at least at some stage during the lifespan of the cell.

The *Ras* protein was shown to be involved in Fas-induced cell death (**Gulbins E. et. al. 1996**), and in TNF-α-induced apoptosis (**Trent J C et. al., 1996**). Likewise, *R-Ras* has been implicated in growth factor-deprivation induced apoptosis (**Wang HG et. al., 1995**). Equally, the *ras* protein was implicated in signalling required for inhibition of apoptosis (**Kauffman-Zeh A. et. al. 1997**; **Kinoshita T et. al., 1995**) and (**Gardner A M and Johnson G L, 1996**), as well as in cell proliferation signalling (**Malumbres M et al., 1998**). **Kauffman-Zeh A. et. al.**, demonstrated clearly that the interaction of the *Ras* protein with phosphatidyl inositol kinase (PI-3K) inhibited cell death due to *c-myc*-induced apoptosis, while association with *Raf*

promoted apoptosis of the same cells. It is also interesting to note that human *ras* protein over-expression often leads to malignant or metastatic tumours in rats (**Wyllie A H et al., 1987**) and in humans (**Sun XF et. al., 1998**), possibly due to the inhibition of apoptosis.

The messenger RNA (mRNA) of low molecular weight GTP-binding protein *RhoB* was also shown to be transcriptionally upregulated not only after UVB irradiation and also after serum re-stimulation (**Fritz G et. al. 1995; Jahner D and Hunter T, 1991**). *rhoB* mRNA was also demonstrated to be rapidly and transiently upregulated after EGF stimulation (**Decremoux P et al., 1994**). Hence, the molecules normally involved in signalling for cell proliferation may not necessarily be "cell proliferation" gene products, although inhibition of their activity may lead to an inhibition of cell proliferation, depending on the prevailing conditions. Likewise, all the molecules used for signalling to trigger cell death may not necessarily be "cell death promoter" gene products, although inhibition of their activity may promote cell survival, depending on the prevailing circumstances (**Vaux DL, 1993**). Hence, it can be concluded from such observations that by and large, the same molecules involved in activation of cell death may also be involved in cell proliferation. Therefore most of the signals evoked in each process may essentially be the same. For example, it is interesting to know that *rho* is required for the induction of apoptosis (**Esteve P et. al., 1995**), while the same protein is also required for inhibition of apoptosis through *Bcl-2* (**Gomez J et. al., 1997**; **Bobak D et. al., 1997**). In fact, activation of *rho* proteins with *Escherichia coli* cytotoxic necrotizing factor 1 (CNF 1) has been shown to lead to an inhibition of apoptosis in epithelial cells (**Fiorentini C et. al., 1997**).

Likewise, there are several cases of apoptosis-induced *de novo* gene expression which are also associated with cell cycle re-entry, such as the transient induction of *c-myc* and *c-fos* in castration-induced prostate regression (**Buttyan R. et. al. 1988**). In fact, antisense oligonucleotides against *c-myc* mRNA were found to decrease thymocyte apoptosis (**Shi Y. et. al. 1992**).

If certain molecules used for either process (apoptosis or proliferation) are the same, then differential signalling by a molecule may be due to specific protein-protein interactions and so their differential binding with specific downstream proteins may

determine the final outcome of the pathway. It has recently been shown that some protein-protein interactions are governed through differential isoprenylation (**Zhang FL and Casey PJ, 1996**). This suggests that the interaction of a protein with another downstream effector protein may depend on its differential modification with certain isoprenoids. Since there are two alternative isoprenoids, i.e. farnesyl and geranylgeranyl, then each of these lipophilic modifications may confer unique properties to the modified protein resulting in changes in protein-protein binding and hence in signaling to opposite cell fates (**Resh MD, 1996**).

It has already been shown that certain *Ras* proteins are alternatively geranylgeranylated in cells treated with protein farnesyl transferase inhibitors (FTI's) (**Whyte DB et. al., 1997**). The questions that would then be posed are**:** what would be the effect of such a modification on cell fate in the presence of an apoptotic stimulus?. Also, what would be the effect of a geranylgeranyl transferase inhibitor or an HMG-CoA reductase inhibitor on cell fate under the same circumstances?

1.1.5.2 Isoprenoids and cell growth control

1.2.5.2 Isoprenylation during cell proliferation

The important need for mevalonate in the regulation of cell growth was first implied by the work of **Chen HW et al. in 1974**. These workers used relatively non-specific, oxygenated derivatives of cholesterol to inhibit the activity of HMG-CoA reductase. This was shown to result in an inhibition of cell growth. In **1977, Kandutsch AA and Chen HW** noticed that after incubation of L-cells with oxygenated cholesterol derivatives, the activity of this enzyme declined, and the consequences included a dramatic inhibition of DNA synthesis. In the absence of exogenous cholesterol, endogenous mevalonate synthesis was greatly increased (**Goldstein JL and Brown MS, 1977**). Inhibition of this endogenous supply of mevalonate with compactin or any other HMG-CoA reductase inhibitor, led to growth arrest (**Astruc M et al., 1978; Quesney-Huneeus V et al., 1979; Habenicht A J R et al., 1980**). Under these conditions, the HMG-CoA reductase protein was upregulated by 200-fold (**Brown MS et al., 1978**) and the growth of human fibroblasts was inhibited unless adequate

amounts of mevalonate were present. The mevalonate requirement was also reduced but not completely abolished in the presence of exogenous cholesterol in the form of low density lipoprotein (LDL).

An isoprenoid requirement during cell growth was first demonstrated by **Maltese WA and Sheridan KM** in **1985b**. These workers demonstrated that high concentrations of mevinolin induced growth arrest in G_1 phase of the cell cycle and inhibition of cell proliferation in neuroblastoma cells, which was recovered by mevalonate but not by cholesterol, dolichol, ubiquinone or isopentenyl adenine. They also found that [^{3}H] acetate labelling of cholesterol, dolichol and ubiquinone was suppressed at all the concentrations of mevinolin. These results showed for the first time that flux through the cholesterol synthesis pathway is shunted away from the least required substrates for cell growth, and directed towards the isoprenoids which are required for cell proliferation. Isoprenylated proteins were then detected during cell proliferation by **Maltese WA and Sheridan KM in 1987**. They showed that in C1300 murine neuroblastoma cells pre-labelled with [^{14}C] mevalonate in the presence of lovastatin, a derivative of mevinolin, and then deprived of exogenous mevalonate, there was a 50-60% decline in the concentration of protein-bound isoprenoid label. However, there was little change in the radioactivity from the sterol, dolichol or ubiquinone fractions. The timing of decline in the label of the isoprenoid-bound protein also preceded the decline in DNA synthesis. These results indicated that the rate of isoprenoid turnover from labelled proteins in growing cells is very high, implying that they are substrates continually required for signalling pathways in growth control. Further evidence to suggest that mevalonate derivatives are required for the proliferation of cells came from studies with 6-fluoromevalonate (Fmev), an inhibitor of mevalonate pyrophosphate decarboxylase (**Cuthbert JA and Lipsky PE, 1990**; **Sawamura M et al., 1993**). Under these circumstances, it was found that addition of mevalonate to cell cultures treated with both lovastatin and fluoromevalonate, restored [^{3}H] thymidine incorporation. The role of the isoprenoids farnesol and geranylgeraniol in smooth muscle cell proliferation was clearly demonstrated by **Corsini A et al., in 1993**. They showed that addition of mevalonate was fully effective in the prevention of lovastatin-induced inhibition of cell proliferation in arterial myocytes, while addition of the isoprenoids farnesol or geranylgeraniol was partially effective in restoring proliferation.

Other HMG-CoA reductase inhibitors, like mevinolin, were shown to be effective in the inhibition of neuroblastoma cell growth (**Maltese W A et al., 1985a**). These workers demonstrated that increased HMG-CoA reductase activity correlated with a marked increase in tumour weight and DNA content. This was later found to be associated with deregulated feedback inhibition of HMG-CoA reductase activity (**Azrolan NI et al., 1989**). In **1993 Bennis F et al.,** showed that in fact about 40% of the reductase activity was devoted to non-sterol synthesis in a human lung adenocarcinoma cell line, A549, while in normal fibroblasts this was about 15-20%.

1.3.5.2 Cell cycle entry and isoprenylation

Mevalonate was shown to be required for DNA synthesis and proliferation in cells, but exactly at which stage or phase of the cell cycle this requirement was fulfilled was shown by **Quesney-Huneeus V et al., in 1983**. They demonstrated that addition of cholesterol to compactin growth-arrested cells during early G_1 or addition of mevalonate in late G_1 allowed the progression through the G_1 and S phases. This indicated that there was a specific need for mevalonate at the G_1/S boundary. This is in keeping with the observation of **Roussillon S et al., 1983,** that the peak in HMG-CoA reductase activity during early-to-mid G_1 precedes the rise in thymidine incorporation in embryonic rat fibroblasts. Further corroborative evidence for a specific mevalonate requirement at a critical point during the cell cycle was made by **Fairbanks K P et al., in 1984.** They demonstrated that compactin induced growth-arrest in human fibroblasts was abrogated only when mevalonate was present during the period of from 10-20 hours after PDGF-BB addition, but not before or after this time period. Also, interestingly, when compactin was added to the cells 10 hours after the addition of PDGF-BB, DNA synthesis was inhibited as fully as in cells where compactin was added at zero time. However, when compactin was added at 20 hours, DNA synthesis assayed at 24 hours was not at all inhibited (**Fairbanks KP et al., 1984**). In fact, it was also shown that both HMG-CoA reductase activity and endogenous cholesterogenesis were downregulated in parallel during late G_1, just before S-phase entry, suggesting that the flux of carbon from mevalonate was shunted towards the isoprenoids, required at this stage of the cell cycle (**Larsson O, 1987**).

Later in **1985**, **Sinensky M and Logel J** demonstrated that DNA synthesis was inhibited at a unique point in the cell cycle due to mevalonate starvation. Entry into S phase was correlated with increased labelling of mevalonate into post- or co-translationally modified isoprenylated proteins. Subsequently, **Sepp-Lorenzino et al., 1991** found a cell-cycle-phase-dependent pattern of mevalonate incorporation into the 24-20 kDa proteins in HepG2 cells. There was a baseline level of [^{3}H] mevalonate incorporation into these proteins already present at early G_1 phase, which was seen to peak around mid G_1 and then decline again to basal levels by around mid S phase. Also, the [^{3}H] acetate incorporated into the isoprenyl alcohols, farnesol and geranylgeraniol, increased markedly by early G_1 and peaked upon entry into S-phase.

These observations were finally confirmed by the results of (**Noguchi Y et al., 1998**). They observed that cell cycle entry was associated with the dissociation of *RhoA* from the cell membranes of rat thyroid FRTL-5 cells by early G_1, whereupon newly synthesised *RhoA* was detected in the cytosol. *RhoA* was subsequently detected on the membranes in late G_1. However, pravastatin, an HMG-CoA reductase inhibitor, which inhibited the isoprenylation of *RhoA* prevented the return of *RhoA* back to the membranes. Consequently, all the *RhoA* remained in the cytosol and growth arrest resulted. Interestingly though, in the presence of geranylgeranyl pyrophosphate with pravastatin, *RhoA* was restored to the membrane. These observations indicate that *rho* proteins may cycle on and off membranes, depending on their specific function under different circumstances. This preferential change in the isoprenylation of the protein most likely dictates its interactions with other effector proteins as well as its binding to the membrane, since the protein was initially present on the membrane before its modification with a geranylgeranyl moiety.

1.4.5.2. Mevalonate and isoprenylation in the control of apoptosis

It has been shown that direct inhibition of endogenous cholesterol synthesis with a squalene epoxidase inhibitor does not have an effect on apoptosis in cell cultures (**Matzno S et al., 1997**; **Flint O P et al., 1997a**). However, there is considerable evidence in the literature to suggest that HMG-CoA reductase inhibitors, such as lovastatin, lead to increased levels of apoptosis in some cultured cells (**Bansal N et al., 1989**). In 1994, **Perez-Sala D and Mollinedo F** made the first reported case of

isoprenoid inhibition leading to apoptosis in human promyelocytic HL-60 cells. It was also shown by **Padayatty S J et al., 1997** that only co-incubation of mevalonate or geranylgeraniol with lovastatin was adequate for the inhibition of lovastatin-induced apoptosis in cancerous prostate stromal cells. In **1997 Flint OP et al.**, showed that [^{3}H] mevalonate and [^{3}H] farnesyl pyrophosphate labeling of three protein bands with relative molecular weights 26.6, 27.7 and 28.9 kDa was markedly inhibited at concentrations higher than 1μM lovastatin. In contrast though, these proteins were equally well labelled with [^{3}H] geranylgeraniol pyrophosphate at all the lovastatin concentrations tested, suggesting that isoprenylation of these proteins is crucially dependent on geranylgeranylation. In fact, the [^{3}H]geranylgeranyl pyrophosphate labeling of the 27.8 and especially of 28.9 kDa proteins seemed to increase after 1μM lovastatin. Such an effect of lovastatin was attributed to increased levels of myotoxicity in cell cultures, which was abrogated either with mevalonate or geranylgeraniol co-incubation (**Flint O P et. al., 1997a**). This was an extremely interesting observation, indicating that when mevalonate synthesis is inhibited, the high demand for geranylgeranylation is met through the shunting of isoprenoid synthesis away from farnesyl isoprenoid synthesis, in an effort to complete the geranylgeranylation of crucial signalling proteins.

1.1.6.2 Targeting signal transduction pathways as a means for therapy

It is now recognized that many diseases, including cardiovascular diseases, may be direct consequences of aberrant alterations in the molecular machinery of signaling pathways. Novel drugs are being designed to inhibit or promote certain signals within the cells of the tissues in question. Many of these drugs are either used to inhibit cell proliferation or enhance cell death. However, they may also be used as valuable tools to understand the subtle principles inherent in the working of these signals (**Levitzki A, 1994**). This thesis will concentrate on the relevance of isoprenylation as a factor involved in the modulation of signalling cascades leading to cell proliferation or cell death by apoptosis in human VSM cells.

The mevalonate pathway

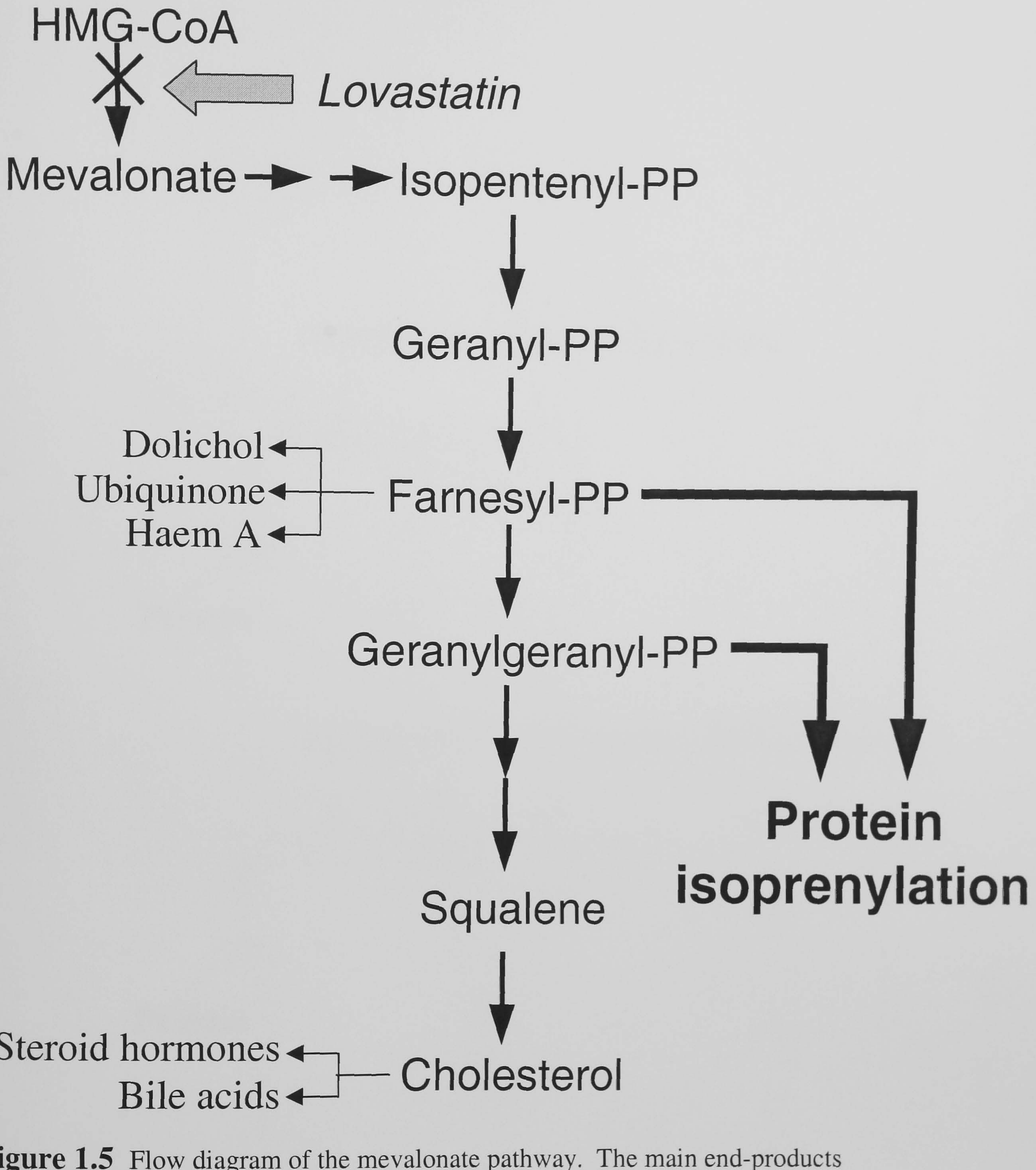
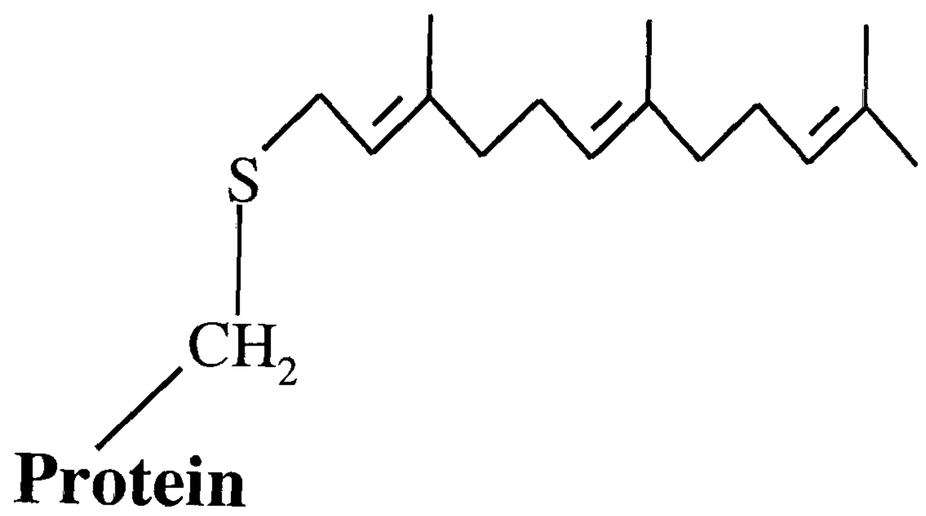


Figure 1.5 Flow diagram of the mevalonate pathway. The main end-products of the pathway are cholesterol and the non-sterol isoprenoids. Cholesterol, the main bulk product, is required for the synthesis of many sterol-derived biological compounds like the steroid hormones, and the bile acids. The isoprenoid derivative of mevalonate, farnesyl pyrophosphate, is not only required for the synthesis of other compounds like ubiquinone, dolichol, and Haem A, but is also required for the post-translational modification of certain proteins, such as Ras. It is also a precursor of geranylgeranyl pyrophosphate, which is another isoprenoid required for the isoprenylation of specific proteins in the cell.

S-farnesyl cysteine (15-Carbon)



S-geranylgeranyl cysteine (20-Carbon)

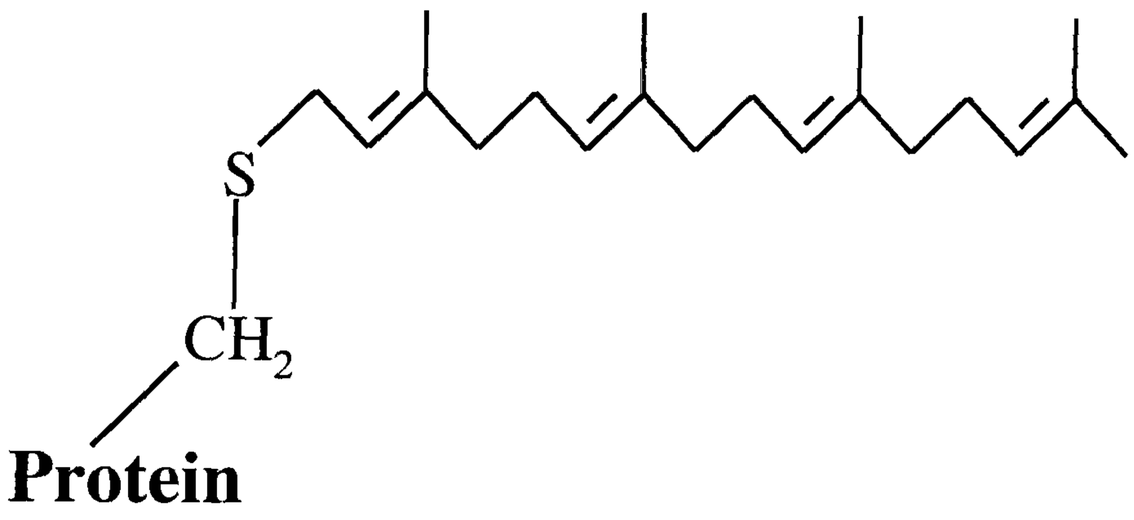


Figure 1.6 Schematic stick representation of the chemical structure of isoprenyl derivatives of mevalonate. Farnesyl (15 Carbons), and geranyl geranyl (20 Carbon) moieties are covalently attached onto the C-terminal Cysteine residue, found in the amino acid consensus motif, -*CaaX*-, of many isoprenylated proteins (see text).

BIBL
LONDON
UNIV.

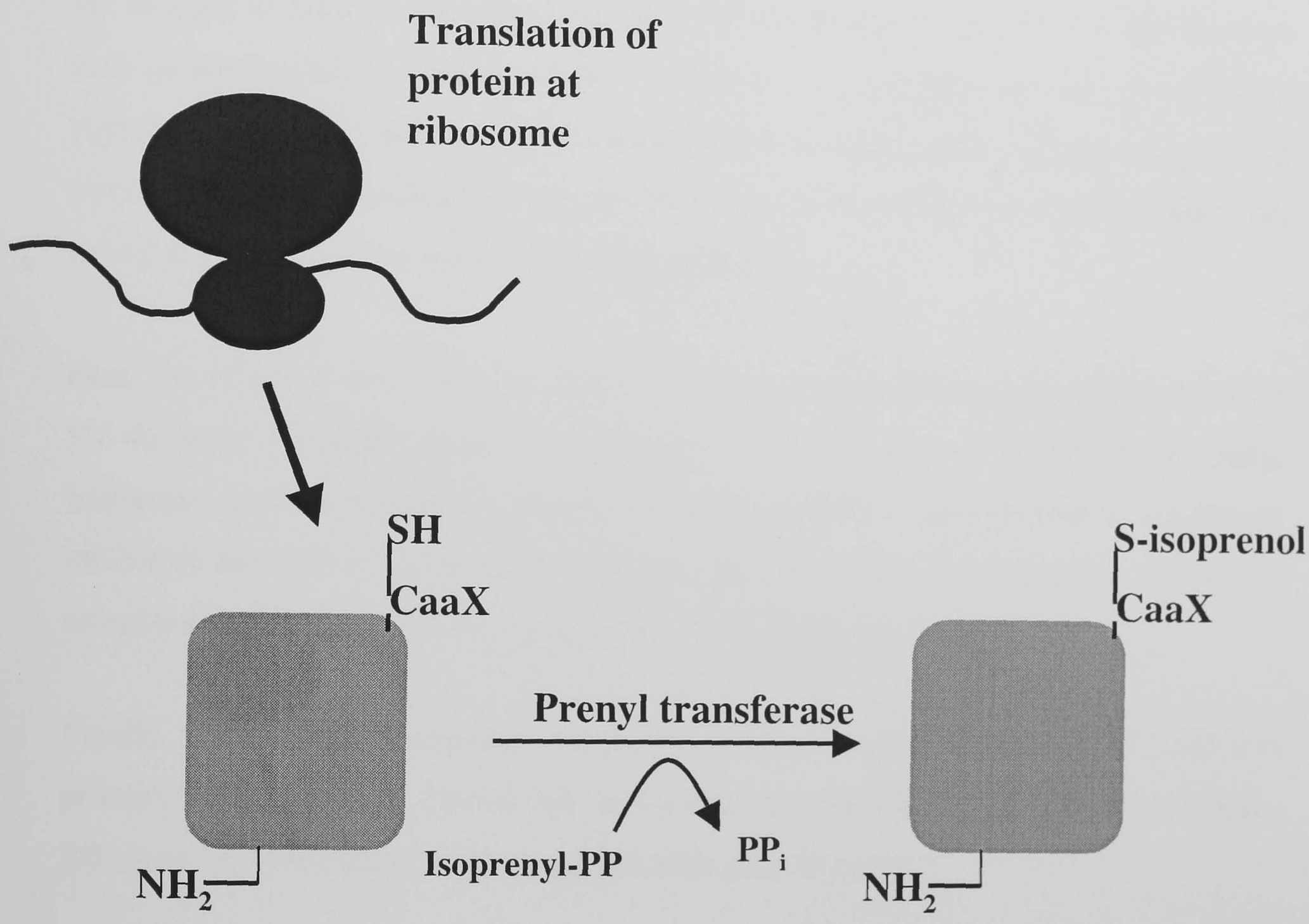


Figure 1.7 Schematic representation depicting the Carboxy-terminal (C-terminal) processing of isoprenylated proteins. First, the protein with the consensus amino acid motif, -*CaaX*-, are synthesised at the ribososmes after translation of the respective mRNA for the protein. The isoprenyl moiety, usually found as a pyrophosphate in cells, is then transferred onto the respective protein by a prenyl transferase (either a farnesyl or a geranylgeranyl transferase) onto the Sulphur atom on the side group of the Cysteine residue. This reaction is coupled to the release of a reduced pyrophosphate group (PPi).

OBJECTIVES

A substantial amount of evidence in the literature points to the fact that certain Ras-related small GTPases that are prenylated, are involved in signalling pathways which mediate apoptosis or cell proliferation, depending on circumstances.

This study was conducted to directly investigate the role that isoprenylation may play in the control of apoptosis and cell proliferation in human VSM cells. These cells are thought to play an important role in the development of certain vascular diseases such as atherosclerosis and restenosis. Although a lot of attention has been given to signalling pathways involved in the proliferation of these cells, an in-depth study of possible signalling involved in the control of their survival, as an essential counterpart to cell proliferation, has not been carried out thus far.

First, the effect of lovastatin, an HMG-CoA reductase inhibitor, was examined in an SV-40 large T antigen transformed human VSM cell line. The effects of prenyl tranferase inhibitors, such as perillyl alcohol (possibly a geranylgeranyl transferase inhibitor) and B581, a farnesyl transferase inhibitor, were also looked at in control, untreated cells and in cells that were exposed to UVB irradiation.

Finally, the effect of lovastatin on growth-arrested human saphenous-vein derived primary VSM cells was carried out, as well as the effect of stimulation with PDGF-BB alone or co-incubated with lovastatin after growth arrest.

The effects were measured through DNA content analysis using flow cytometry, DNA ladder assays, cell proliferation assays, cell viability assays through Trypan Blue exclusion, cytochemical techniques, including staining with the TUNEL reagent and the DNA-binding fluorescent dye, DAPI. DNA synthesis was also measured as $[^3H]$ thymidine incorporation.

Chapter 2

MATERIALS AND METHODS

2.1.1.1 Drugs and Reagents

2.2.1.1 Preparation of lovastatin

Lovastatin in powder form, as the lactone, was kindly donated by Merck, Sharp and Dohme (Hoddesdon, UK). The powder was hydrolysed to the active carboxylate (acid form) by dissolving 8mg of it in 0.4ml absolute ethanol to which was added 0.6 ml of 0.1 M sodium hydroxide (NaOH) and heated at 50^0C for 2 hours. This solution was adjusted to pH7.4 by adding 0.3 ml of 0.1M hydrochloric acid and made up to a final volume of 2ml with deionised water. This 10mM stock solution was diluted to the required working concentration in culture medium. The relevant controls were treated with an equivalent concentration of lovastatin vehicle (0.4ml absolute ethanol, 0.6ml of 0.1M NaOH and 0.3ml of 0.1M hydrochloric acid made up to 2mls).

2.3.1.1 Mevalonate and mevalonate derivatives

Mevalonic acid lactone (Sigma, St. Louis) was hydrolysed in a similar manner to lovastatin, for a stock concentration of 100mM. Farnesyl and geranylgeranyl pyrophosphates (Sigma, St. Louis) were dissolved directly into the culture medium at final concentrations of 10μM. The isoprenoid derivative, Ubiquinone Q10 (Sigma) was emulsified into the culture medium by ultrasonication with Soniprep 150 (using an amplitude set at 15 microns) with equimolar amounts of phosphatidylcholine (Sigma). Isopentenyladenosine (Sigma) at a stock concentration of 1mM was made up in deionised water (dH_2O) and diluted to 1μM. "Water soluble" cholesterol, which is a water-soluble ester of cholesterol, called Polyoxyethanyl-cholesteryl sebacate, from Sigma was made up in dH_2O at a stock concentration of 25mg/ml and diluted to 10μg/ml in the culture media.

2.4.1.1 Prenyl transferase inhibitors

The farnesyl transferase inhibitor, B581, was purchased from Biomol Research Labs. Inc., USA and stored at –20°C as a 2 mg/ml solution in dH_2O.

The other farnesyl transferase inhibitor, BZA-5B, was a gift of Dr James Masters from GenenTech, USA. The dry powder was dissolved in DMSO to a stock concentration of 100mM and stored as aliquots at –20°C.

R-(+)-Perrilyl alcohol (99%) was purchased from Aldrich Chemical Co, USA and stored at 4^0C.

2.5.1.1 Mitogens

Human recombinant PDGF-BB (stock concentration at 20µg/ml) was purchased from Gibco Life Technologies (Paisley, UK). This was diluted to a working concentration of 20ng/ml or 100ng/ml, stored as aliquots at –20°C and thawed immediately before use.

2.6.1.1 Molecular Biology reagents

All the reagents used for DNA extraction were of Molecular Biology (MB) grade from Sigma Chem. Co., Ltd., UK (see Appendix II)

2.7.1.1 Materials for thymidine incorporation

10% (w/v) of trichloroacetic acid was prepared a couple of hours before use by dissolving the acid in powder form in dH_2O and stored on ice or at 4^0C.

2.8.1.1 Treatments

Lovastatin or vehicle, with or without the isoprenoid derivatives was added to defined NCTC-109 serum-free medium supplemented with BSA, fraction V (2.5mg/ml) (Boehringer Mannheim, W. Germany), G418, L-Glutamine (final concentration 4mM) and HEPES (final concentration 25mM) or 10% (v/v) dialysed FBS (dFBS).

The serum was dialysed to ensure the medium was mevalonate-free, so that exogenous mevalonate does not become available to the cells in culture. This ensured that the effects of lovastatin in serum-containing medium were not counteracted by an exogenous source of mevalonate.

UVB irradiation was carried out in an AXL-1000 UV crosslinker (Spectronics Corporation). UVB intensity between 0-200 J/m^2 was used.

B581 at 2mg/ml (or a stock concentration of 4.2mM) was diluted to a final working concentration of 100μM in the cell culture medium.

R-(+)-Perillyl alcohol (with a stock concentration of 6.3M) was diluted to a working concentration of 2mM, in 10% (v/v) FBS supplemented with G418. It was freshly prepared and placed into the humidified incubator at 37°C, usually 24 hours before use.

Primary human vascular smooth muscle cells were growth arrested for up to 7 days with NCTC-109 serum-free medium, supplemented with BSA. They were then induced with PDGF-BB at 20ng/ml, with or without Lovastatin (10μM).

2.1.1.2 Cell Culture Media and Reagents

All cell culture media were purchased from Gibco Life Technologies, (Paisley, UK). See Appendix I for the recipes.

1. Serum free NCTC-109 medium supplemented with BSA and G418 for transformed SM1 cells

2. Serum free NCTC-109 medium supplemented with BSA for the primary cells

3. Standard DMEM supplemented with 10% (v/v) FBS or 10% dialysed FBS and G418 for the SM1 cells

4. Standard DMEM supplemented with 15% (v/v) FBS for the primary cells

5. Standard DMEM serum free medium supplemented with transferrin, insulin, and selenium, without BSA

Trypsin-EDTA at 0.25% (w/v) in 1mM EDTA and PBS-A solution

2.1.1.3 Cell Culture

2.1.2.3 Cell types used

1. SV-40 Large T (LT) antigen transformed human vascular smooth muscle cell line (SM1 cells)

This is a novel immortalised human vascular smooth muscle cell (SMC) line obtained after G418 selection of human saphenous vein-derived SMC conditionally transformed with a retroviral recombinant plasmid expressing a temperature-sensitive mutant of SV40 large T-antigen (LT-antigen). Only cells at passages between P89 and P122 were used for experiments. They were kindly donated by
Dr. C. Demoliou-Mason.

2. *Primary non-transformed human vascular smooth muscle cells derived from surplus human saphenous vein*

Cells were derived from surplus human saphenous vein and cultured using an explant technique. Tissues were acquired after coronary by-pass grafting operations. Passage 3 cells were utilised for all experiments.

3. *Human osteosarcoma cell line (saos-2 cells)*

These are a transformed human osteosarcoma cell line, kindly donated by Dr X. Lu of the Ludwig Institute for Cancer Research, St. Mary's Hospital Medical School.

2.1.3.3 Explant technique for the isolation of primary HVSM cells

In this method, small pieces of human saphenous vein are laid down onto the culture flask in culture medium, and incubated at 37^0C for a couple of weeks. Under these circumstances, medial smooth muscle cells migrate out from the pieces of tissue onto the surrounding surface, where a monolayer of cells is formed.

Surplus saphenous vein from individual coronary artery bypass grafting (CABG) operations stored in transport medium (see Appendix I) was placed into fresh, sterile medium containing fresh and conditioned culture medium from passage 2 primary cell cultures in a 1:1 ratio (v/v). Using sterile scalpel and tweezers, the adventitia of the veins was carefully scraped off. After cutting the vein longitudinally to expose the luminal side, endothelial cells were scraped off. Using a scalpel or scissors, the resultant inner media containing almost exclusively vascular smooth muscle cells (**Munro E et. al., 1994**) was cut into small pieces. These explants were then placed in 7-8 ml of conditioned medium in an 80 cm^2 culture flask, incubated under standard conditions, without being disturbed for 2 weeks. After 2 weeks, the explant tissue was fed with condition medium twice a week. When enough cells had migrated from the media of the explants and attached onto the substratum, the explants were trypsinised with 0.25% (w/v) trypsin-EDTA solution and the primary HVSM cells were subcultured as passage 1. Passage 2 cells were obtained after the latter were subcultured and used for experiments as appropriate.

2.1.4.3 Culture conditions

The routine growth and maintenance of SM1 cells was carried out in standard nutrient medium, comprising Dulbecco's modified Eagle's medium (Life Technologies, Inc.) supplemented with 10% (v/v) FBS (Life Technologies Inc.), and Geneticin at 100mg/ml (G418) from Life Technologies, Inc. The primary cells were maintained in standard nutrient medium, comprising Dulbecco's modified Eagle's medium (Life Technologies, Inc.) supplemented with 15% (v/v) FBS, and Gentamicin (10µg/ml) from Life Technologies, Inc. The cells were routinely maintained in a humidified incubator at 37^0C with 5% CO_2.

2.1.5.3 Long term storage of cells

Cell stocks at about $2x10^6$ cells/ml in 10% Dimethyl sulfoxide (Sigma Chem. Co., UK) made up in foetal bovine serum (FBS) were stored under liquid nitrogen. Before storage, they were gradually cooled to -70^oC overnight and then submerged in liquid nitrogen the following day.

2.1.6.3 Thawing of cells frozen in liquid nitrogen

The vials were removed carefully from the liquid nitrogen dewars, and gently placed in a 37^0C-water bath for a few minutes until thawing just begins. The surface of the vial was swabbed with 70 % ethanol and then opened. The concentrated suspension of cells was then placed into the culture flask and diluted drop by drop with 10%(v/v) FBS culture medium. The flask of cells was then placed into the humidified incubator. After 4 hours the medium was replaced with fresh culture medium.

2.1.7.3 Dialysis of Foetal Bovine Serum

Fresh serum was dialysed against PBS in a $14x10^3$ kDa cut-off dialysis tubing for 3 to 4 days at 4^oC. The serum was filter-sterilised before use in cell culture.

2.1.1.4 DNA content flow cytometric analysis

2.1.2.4 Principle of the technique

This is an established technique used to allow rapid and very accurate measurements of changes in DNA content of a given cell population. Simultaneous analysis of large cell populations allows the discrimination of distinct subgroups with specific differences. Each subpopulation may then be quantified as a percentage of the total population.

DNA content analysis of cells and the respective distribution of the total DNA in the cell within the G_1, S and the G_2/M phases of the cell cycle has been one of the earliest

applications of flow cytometry (**Rabinovitch P S, 1995**). It is a simple, yet a powerful method used in quantifying cell cycle phase proportions and apoptosis. The distinctive feature involves the mathematical analysis of single parameter (univariate) DNA content histograms. A specific DNA-binding fluorescent dye, such as Propidium Iodide, is used to tag the DNA of the cells. All quiescent and non-replicative cells have a basal DNA content, termed G_1 or G_0. During cell replication however, DNA synthesis occurs and the quantity of the DNA and hence the fluorescence due to Propidium Iodide binding to DNA increases above the G_o level, this phase is termed the S phase. During this period DNA content is increased continually until it is double the content of the diploid DNA (or double the basal level of DNA at the G_0/G_1 phase), this phase is designated as G_2/M, after which mitosis takes place. Hence, in a growing cell population, the distribution of the DNA content as measured from the fluorescence emitted by the respective phases consists mainly of cells in the G_1 phase and in the G_2/M phase, with a broadly distributed S phase in between (**Figure 2.1**).

2.1.3.4 Limitations and disadvantages

This technique is very useful in identifying apoptotic cells along with revealing their ploidy and/or the cell-cycle distribution of the non-apoptotic cell population. However, the hypodiploid peak can represent, in addition to apoptotic cells, debris from mechnically damaged cells, cells with lower DNA content, such as those that are in the process of mitosis where the degree of staining with DNA may be diminished (**Cotter TG and Martin SJ, 1996**). Another disadvantage stems from the fact that isolation of nuclei as described below, may result in fragmented parts of the nucleus (apoptotic bodies) being released from a single apoptotic cell. Hence the proportion of the hypodiploid region as measured by FACS represents the amount of nuclear DNA released from the cells, and not the number of apoptotic cells. The changes in the amount of DNA content of this region give us an idea as to the relative changes in the number of apoptotic cells, and therefore must not be relied upon as an absolute measure.

However, there are other disadvantages posed by such a single parameter analysis for apoptosis. For example, decreased DNA content (as a result of apoptosis) of a cell

containing the DNA of a nucleus at the G_2/M phase of the cycle, may be recorded as an event containing the same amount of DNA as a normal cell at S phase of the cell cycle. This may result in an underestimation of the measure of apoptosis in the cell population. Hence, for a better measure of apoptosis in the population, cells may be stained with a DNA binding dye, such as propidium iodide, and another specific stain for apoptotic cells, such as a TUNEL reagent stain.

2.1.4.4 Analysis of apoptotic populations by flow cytometry

As discussed earlier, one of the relatively specific hallmarks of apoptosis is the endonucleosomal cleavage of DNA into low molecular weight 180-200bp multimers (**Telford WG et al., 1991**; **Arends MJ et al., 1990**). When cells are fixed or permeabilised, this fraction of low molecular weight, fragmented DNA is thought to leak out of the cytoplasm (**Afanasyev VN et. al., 1993**). These cells therefore would have less DNA than the DNA content of the diploid G_o/G_1 phase, and hence fluorescence staining of these cells would be reduced (**Darzynkiewicz Z et al., 1992**). Such decreased staining of DNA accounts for the appearance of fluorescence events below the G_o/G_1 peak, designated as the hypodiploid (A_o) region after treatment of cells with various cytotoxic agents. It has in fact been considered a marker of apoptotic cell death (**Nicoletti I et al., 1991**). This region of the DNA content histograms has been shown to increase in a dose-dependent and time-dependent manner with respect to many cytotoxic agents (**Telford WG et al., 1991**). The proportion of events in the hypodiploid region was also correlated with the amount of fragmented DNA extracted from the same population observed after agarose gel electrophoresis (**Crompton T et al., 1992**). Additionally, the chromatin of this subpopulation of sorted cells appears to be fragmented, compared with the chromatin of the cells sorted from the G_o/G_1 phase (**Ormerod M G et al., 1992**). This apoptotic subpopulation was also shown to represent morphologically intact cells (**Zamai L et al., 1993**).

2.1.5.4 Sample preparation

In order to assess the relative amount of DNA in each cell cycle phase and the hypodiploid region (A_o), SM1 cells were plated at a density of ~$14x10^3$ cells/cm^2 or

about $800x10^3$ cells per petri dish, which had been pre-coated with poly-L-Lysine. After an overnight incubation, they were exposed to lovastatin at the required concentration in either NCTC-109 medium (supplemented with BSA) or in 10%dFBS for up to 24 or 48 hours. The cells were then scraped off the dishes and resuspended in the culture medium used for treatment, thus including any detached cells. They were centrifuged at 2000rpm for 5 minutes, washed once with PBS-A, and then permeabilised to isolate clean nuclei, which were stained with Propidium Iodide using the CycleTest PLUS^{TM} DNA reagent kit (Becton Dickinson). The samples were then stored on ice, covered with foil, until analysis.

The principle of the kit is to allow the cell membrane to dissolve due to the presence of a non-ionic detergent. The cell cytoskeleton and the nuclear proteins are then digested with trypsin, while the RNA is digested with the RNase. The nuclear chromatin is also stabilised with the cationic macromolecule, spermine, present in the solutions. Propidium Iodide then binds stoichiometrically to the clean, isolated nuclei or fragmented DNA.

2.1.6.4 Calibration of the FACScan^{TM}

A Beckton Dickinson (San Jose, CA, USA) FACScan ^{TM} Flow Cytometer equipped with a 15mV argon ion laser emitting an excitation wavelength of 488nm was used. Red fluorescence (580-650nm) emitted from Propidium Iodide (PI)-stained nuclei was detected by the FACScan's fluorescence 2 (FL-2) detector, equipped with a 585/42 bandpass filter, which analyses wavelengths between 564 and 606nm. The emission fluorescence of PI is known to be between 550-640nm. The data from 10^4 cells, run at a 'LO' rate of about 60 events/second were collected in the 'List mode' for each sample and the signals for red fluorescence were recorded using the linear amplifications or scales, i.e. the data were registered on a linear scale.

The instrument was first calibrated to setup the photomultiplier tube (PMT) voltages and amplifier gains of the fluorescence detectors, as well as to provide information regarding instrument linearity and resolution. To do this certain quality control nuclei are used, which are provided by the manufacturer. Standard Chicken Erythrocyte Nuclei (CEN) are run using the CellFIT^{TM} software on the Hewlett-Packard (HP 9000

model 340) Platform. This preparation contains single nuclei, doublets, triplets, and some larger aggregates. When stained with PI they result in four or more reference peaks in the FL-2 fluorescence area (**Figure 2.2**). The first four FL-2A histogram peaks represent the singlets, doublets, triplets, and quadruplets respectively. If the instrument response is linear and the nuclei have been correctly stained, the channel values of the means should be approximately 2, 3 and 4 times greater than the singlet peak. The resolution of each peak, as determined by the % coefficient of variation (% CV) should be less than or equal to 3%, where:

$$\% \text{ Coefficient of Variation (CV)} = \frac{\text{Standard deviation of peak}}{\text{Mean}} \times 100$$

The linearity of the instrument is the relationship between the channel number (i.e. fluorescence intensity or DNA content) and the number of events it measures (i.e. the cell counts). Hence, in terms of the DNA content histograms, the channel number (FL2-A on the x-axis) of the doublet peak in the CEN profile should be twice that of the singlet peak. Likewise for the G_o/G_1 peak and the G_2/M peak in any normal cell population. Hence, the integrated area of the red fluorescence (FL-2A parameter) from PI-stained nuclei must be directly proportional to the DNA content.

2.1.7.4 Acquisition and analysis of data

Once the instrument was calibrated, then the DNA content data of each sample is acquired using the CellFIT^{TM} Software following the manufacturer's instructions.

Each sample comprising a PI-stained suspension of clean nuclei is run through the instrument, as 10^4 events are acquired. Acquisition is carried out in a cytogram of integrated fluorescence area versus fluorescence width, i.e., FL2-Area (on the Y-axis) vs. FL2-Width (on the X-axis). Hence, the DNA fluorescence of the singlet nuclei derived from single cells will increase linearly in fluorescence area without a significant increase in the fluorescence width (**Figure 2.1**). However, the cell doublets and other larger aggregates will display an increased signal width at each cell cycle phase (**Fraker PJ et al., 1996**). The DNA content of the nuclei at G_o/G_1 phase, as measured on the FL2-A axis, will roughly be half the amount of the DNA at the

G_2/M phase. Apoptotic nuclei will give a fluorescent region which is on the left of the G_0/G_1 peak. A DNA fluorescence gate, which includes almost all the events from this region through to the singlet G_2/M peak, is carefully drawn. The events on the far left near the Y-axis (the debris) and all the aggregates on the right are excluded. Thus, the gate should contain greater than 85% of all the DNA fluorescence events, which have been acquired.

Once the gate is drawn, then the percentage proportion of total DNA content in each of the cell cycle phases and the hypodiploid region (in the gated area) is calculated from the integrated DNA fluorescence area histogram (**Figure 2.1**). For a reproducible and accurate calculation, the SOBR algorithm was used. This mathematical model fits a broadened (Gaussian convolved) rectangle to the S-phase region, while the peaks are fitted by Gaussian curves and the cell cycle percentages are calculated by integrating the areas under the respective curves. The MANL model was then used to measure the proportion of events in the hypodiploid region (A_o) as a percentage proportion of total number of events on the histogram. The hypodiploid region is marked manually from the beginning of the sub-diploid "apoptotic" peak, excluding the debris on the far left, i.e. those with a very low DNA content or less than channel 10, up to the area near the G_o/G_1 peak (**Nicoletti I, et. al, 1992**).

2.1.1.5 Thymidine incorporation

SM1 cells were seeded into 96-well plates at a subconfluent density of $30x10^3$ cells/ml, 0.2ml/well. After overnight incubation, they were stimulated with 10% (v/v) dFBS containg lovastatin or vehicle, supplemented with the relevant isoprenoid derivatives. After an incubation period of 22 hours, stock [Methyl-^{3}H]-Thymidine in 70% ethanol at 1mCi/ml (from ICN Flow, Thame, UK) was diluted as follows: after preparing a 40μCi/ml concentration in supplemented serum-free medium (standard DMEM) supplemented with Transferrin (4mg/ml), Selenium (100μM), and Insulin (1μM). The volume used depended on the number of wells pulsed. A volume of 25μl (of 40μCi/ml [^{3}H]-Thymidine/well) was added to each well just below the meniscus to give around 5μCi/ml final concentration and incubated at 37^0C for a further 4 hours. The experiment was terminated by washing the cells once with ice-cold PBS

and twice (15 minutes. each wash) with 200µl ice-cold 10% (w/v) trichloroacetic acid (Fisher Scientific, Loughborough, UK) to remove acid-soluble nucleotides. All the acid was removed and the cells were then lysed overnight at room temperature using 1M sodium hydroxide solution (0.2ml/well) and acidified with 70µl 4M Hydrochloric acid (Fisher Scientific) to precipitate the remaining DNA prior to harvesting with a cell harvester onto glass fibre filters (Packard, USA). Radioactivity was counted using a Matrix 96 direct β-counter (Canberra Packard, Pangbourne, UK).

2.1.1.6 Optimisation of the DNA "ladder" assay

2.1.2.6 Principle of the technique

Since the DNA of apoptotic cells is cleaved at the internucleosomal (linker) regions, then this characteristic can be used to identify apoptotic cells in a population (**Wyllie A H, 1980**; **Compton MM, 1992**). If the total DNA of a given apoptotic population is extracted and run on a conventional agarose electrophoresis gel, the appearance of a "ladder" of bands representing 180-200 bp fragments and multiples of this unit becomes obvious. This type of analysis, which is qualitative, has become the most common biochemical method to be used for the detection of apoptosis. Hence, it is often considered the biochemical hallmark of apoptosis (**McConkey D J et. al., 1989**).

However, although oligonucleosomal cleavage accompanies apoptosis in most cases, some workers have reported the morphological appearance of apoptosis in the absence of DNA ladders (**Ucker D S et. al., 1992; Oberhammer F et. al., 1993**). Therefore, it is important to use other corroborative methods to verify the occurrence of apoptosis.

2.1.3.6 Detection of DNA fragmentation in SM1 cells

Two standard methods for DNA extraction were tried in order to detect the DNA ladders after electrophoresis of the extracted DNA from treated SM1 cells.

Subsequently, a methodology combining elements of both standard assays was used to optimise the assay for SM1 cells.

2.1.4.6 Salting out method (adapted from Wyllie AH et. al., 1980 and modified by Dr X Lu, Ludwig Institute for Cancer Research, St Mary's)

Initially, a methodology based on the protocol by **Wyllie A H (1980)** was used, with minor changes. Both attached and floating cells were pooled, after the former were trypsinised off the culture dishes and resuspended in 10 % (v/v) FBS. The cells were spun down at 2000rpm for 5minutes, washed once with PBS-A and resuspended in lysis buffer (see Appendix II) at $10x10^6$ cells/ 0.5 ml. After incubation on ice for 10 minutes, a final concentration of 50µg/ml Proteinase K (Sigma Chem Co., UK) was added for 1 hour on ice. 0.5 ml of Phenol: Chloroform (1:1) was added, and the mixture was vortexed, and centrifuged at 14000 rpm for 5 minutes. The clear aqueous phase at the top was transferred to a clean tube, and extraction process repeated a further two times. Chloroform (400µl) was added to the aqueous phase, the mixture vortexed and spun at 14000 rpm for 10 minutes. 5M Sodium Chloride (NaCl) was then added to the crude extract at 1:10 (v/v) and the total volume made up to 1ml with 80% (v/v) isopropanol. The extract was incubated at –20°C overnight. The tubes were spun at 14000 rpm at 0°C for 20 minutes, the alcohol discarded, and the pellet was washed with 1ml ice-cold 70 % (v/v) ethanol for 2 minutes at 14000rpm. After leaving to dry in open air, the pellet was dissolved in 15µl of TE/RNase A at 10µg/ml, pH 8.0. After incubation at 37°C for 15 minutes, the tubes were plunged into ice and loaded with 1:5 (v/v) of gel loading buffer (GLB) (see Appendix II). A 2% (w/v) agarose gel was made up using 1x TAE buffer and a final concentration of 0.5mg/ml of Ethidium Bromide (Appendix II) was added to stain the gel. A *Hae* III digest of ϕX174 DNA weight marker was also run at 80V for 1 hour.

The above methodology, was designed for the detection of DNA "laddering" in saos-2 cells (a transformed human osteosarcoma cell line).

One of the major disadvantages with this method was the large number of SM1 cells (about $10x10^6$) required to achieve a detectable amount of "laddering". Another

disadvantage was that it proved extremely difficult to digest all the RNA in SM1 preparations. This can be seen in as the prominent bands at the bottom of the gel, shown in **Figure 2.3**. Increasing RNase concentration or incubation time had little effect on the amount of RNA. Hence, although in the example shown (**Figure 2.4**) 50µg of nucleic acid was loaded onto the gel a proportion of this was likely to be RNA and led to inconsistencies in loading of actual DNA onto gels. It is unclear why it proved impossible to digest all the RNA, possibly it is a consequence of very high levels of RNA in SM1 cells, or protection of RNA from RNase by some protein in SM1 cells. However, this question was not examined further.

In order to enhance the detection and prominence of the bands and so reduce the number of cells required for the assay, a DNA binding dye with greater sensitivity than Ethidium Bromide, called SYBR^{TM} Green I, was tried. This dye is approximately 25 to 100 times more sensitive than Ethidium Bromide. The use of this dye allowed us to use smaller quantities of DNA (**Figure 2.5**), however, SYBR^{TM} Green I is more sensitive to overloading, such that in the presence of excess DNA, bands did not run straight down the gels (**Figure 2.5**). Nevertheless, it was considered that the benefits in terms of increased sensitivity outweighed the potential difficulties associated with overloading and this dye was used for subsequent studies.

2.1.5.6 The Gong J et. al., 1994 method

In order to further increase the sensitivity of the DNA ladder assay a procedure first described by Gong J et al., 1994 was used. This is a relatively rapid and selective procedure for extracting the internucleososmally degraded low molecular weight DNA fragments from "apoptotic" cells. Several advantages of this method over the conventional method (salting out method) include:

1) DNA extracted from 1 to 2 x10^6 cells, of which as few as 8% are apoptotic (**Gong J et. al., 1994**) yield discontinuous DNA bands or a "ladder" upon gel electrophoresis, since the procedure allows the concentration of the DNA fragments.

2) Cells may be stored in 70% ethanol for at least several weeks before analysis without any significant DNA degradation.

3) Treatment with ethanol inactivates endogenous enzymes, preventing autolysis after sample collection.

The procedure employed was adapted from Gong J et al., 1994, with some modifications, and is as follows:

About 2 x 10^6 cells were harvested and centrifuged at around 2000rpm for 5 minutes. The cells were re-suspended in 1 ml of HBSS (Hank's Buffered Salt Solution) into tubes on ice containing 10 ml of 70% ethanol in deionised water. The cells were stored in this way at -20^0C usually for 48 hours or longer. For DNA extraction, cells were centrifuged at 2000rpm for 5 minutes. The ethanol was removed, and the cell pellets resuspended in 300µl of phosphate-citrate (PC) buffer, pH 7.8 (see Appendix II) in 1.5 ml Eppendorf tubes at room temperature for about 1.5 hours (at least 30 minutes). After centrifugation at 4500rpm in a microfuge for 5 minutes, the supernatant containing the dissolved low molecular weight (LMW) fragments was transferred to new Eppendorfs and concentrated by vacuum in a SpinVac concentrator for 30 minutes. A 5µl aliquot of 0.25% IGEPAL (see Appendix II) made up in deionised water was added, followed by 5µl of a solution of RNase A (1mg/ml in deionised water). After 30 minutes of incubation at 37°C, 5µl of a solution of Proteinase K (1mg/ml) was added and the extract was incubated for an additional 30 minutes at 37°C. The DNA in each aliquot was quantified spectrophotometrically using a UV/Visible spectrophotometer, Ultrospec 2000 (Pharmacia Biotech, UK) after diluting the DNA sample by 1:151 in TE buffer (pH 8.0). Appropriate quantities from each sample were mixed with 2.5µl of gel loading buffer (GLB), and all the contents of the tube were loaded onto the 2% (w/v) agarose gel stained with SYBR green I dye. The gel was then run at 4.5V/cm.

Gels run with samples of DNA obtained using this method still did not contain prominent bands (**Figure 2.6**).

It was then decided that a combination of the two methods, which combines phenol: chloroform extraction, and the concentration step from the Gong method may be better. This latter method sometimes gave inconsistent results, and was not reproducible. The inconsistency in the method was finally solved when the pellet was dried in a SpinVac, before the addition of RNase.

2.1.6.6 Final optimised procedure

About $2x10^{-6}$ SM1 cells were seeded down onto 9cm diameter petri dishes in 10% (v/v) FBS (supplemented with BSA and G418) and incubated overnight. The same number of primary human VSM cells were also seeded onto petri dishes, but the cultures were allowed to become overconfluent, so that enough DNA may be extracted for a detectable degree of "laddering" or DNA fragmentation. The cells were then exposed to the relevant dose of lovastatin or vehicle for 24 or for 48 hours in serum-free medium. At the specified time point the cell culture medium was removed and kept on ice, and the cells on the petri dish were washed once with PBS, trypsin-EDTA (0.25% (w/v)) was added, and once the cells were detached from the substratum. The detached cells were then resuspended with the culture medium which was kept on ice. The suspension was centrifuged at 2000rpm for 5 minutes and the supernatant discarded. The pellet was resuspended in 1ml of ice-cold Hanks` buffered salt solution (HBSS) (Life Technologies, Inc.) and transferred into universal vials containing 10 ml of 70% ethanol, on ice. The cells were then stored in the fixative at –20°C for 3 days or less. The samples were then centrifuged at 2000rpm for 5 minutes to pellet the fixed cells and the ethanol was thoroughly removed. The pellets were then resuspended at room temperature in 300µl of phosphate-citrate buffer, consisting of 192 parts 0.2M Na_2HPO_4 and 8 parts of 0.1M citric acid (pH 7.8) (Sigma, St. Louis) in Eppendorfs (see Gong J. et. al. 1994). The tubes were rotated on a blood tube rotor SB1 (Stuart Scientific, UK) for at least 1 hour. After centrifugation, the supernatant was transferred to clean tubes and incubated in 200µl of 1mg/ml proteinase K (Sigma, St. Louis) at 37°C for about 1 hour. Standard phenol:chloroform extraction was carried out three times alternately and finally once with chloroform (Sigma, St.Louis). The DNA was then precipitated overnight at –20°C in 1:10 (v/v) of 5M Sodium Chloride (Sigma, St. Louis) and about 600µl of 80%

Isopropanol-2 (BDH, Poole, England). The tubes were centrifuged at $14x10^3$ rpm at 4°C for 20 minutes and the supernatant disposed. The pellet was washed once in ice-cold 70% ethanol for 2 minutes at the same temperature and the tubes dried under vacuum in a SpinVac concentrator (Heto) for about 5 minutes at 40°C. The pellet was dissolved in 15µl TE/RNase (1mg/ml), pH 8.0 (Sigma, St. Louis) and incubated at 37°C for 30 minutes. The amount of DNA present was measured spectrophotometrically (Pharmacia Biotech, UK), after a 1:151 dilution of the DNA solutions and about 2-3µg of DNA was loaded in 2µl of Gel Loading Buffer (Sigma, St. Louis), along with 5µl (at 0.4µg/ml) of ϕX174 plasmid Hae digest DNA marker (Life Technologies, Inc.). The samples were run on a 2% agarose (Life Technologies, Inc.) gel which was cast along with 1:10000 dilution of stock SYBR Green I dye (Flowgen, UK) at about 4 V/cm for about an hour. The DNA in the gel was visualised under UV light and captured and saved on a Gel Doc 1000 system (BioRad, UK).

2.1.1.7 Cytochemical techniques

2.1.2.7 TUNEL (Terminal deoxynucleotidyl transferase-mediated dUTP nick end labeling) assay

Cleavage of genomic DNA during apoptosis may sometimes yield double-stranded, low molecular weight DNA fragments (mono- and oligonucleosomes) as well as single strand breaks ("nicks") in high molecular weight DNA. These DNA strand breaks can be identified after the free 3`-hydroxyl termini are modified with nucleotides in an enzymatic reaction. In this technique, a terminal deoxynucleotidyl transferase (TdT), which catalyes the polymerisation of a deoxynucleotide conjugated with a fluorescein label onto the free 3`-hydroxyl DNA ends, is used to label DNA strand breaks. These were then detected as green fluorescence under the epifluorescence microscope, using the blue filter.

Cells were seeded onto sterile coverslips in 10% (v/v) FBS at around 42×10^3 cells per well in a 24 well plate and incubated overnight. Next day the cells were washed once with PBS and 100µM lovastatin or vehicle was added in defined NCTC-109

serum-free medium for 24 and 48 hours. Fixation was carried out at room temperature in 4% Paraformaldehyde (Sigma, St. Louis) for 30 minutes. The coverslips were rinsed once in PBS and permeabilised in 0.1% Triton X-100, 0.1% Sodium Nitrate (Sigma, St.Louis) for 2 minutes on ice. After rinsing the coverslips twice with PBS, and once with deionised water, the area around the sample was dried and the TUNEL kit from Boehringer Mannheim was used to label the cells according to the instructions. The cells were mounted with CitiFluor (AGAR, UK) mountant. The samples were visualised using an epifluorescent microscope (MC80 Zeiss, Germany) with a blue filter, FT510, LP520.

2.1.3.7 DAPI staining

DAPI is a fluorescent dye, which binds specifically to DNA. Upon exposure to UV light, a blue fluorescence at around 480nm is emitted. The dye was used to stain the nuclei of the cells after treatment with the pro-apoptotic reagent. It is used to reveal the condensation of apoptotic DNA, which stains brighter than normal, uncondensed genomic DNA.

The same fixation procedure as per the TUNEL staining method was used. However, a mountant containing DAPI from Vector Laboratories, UK was used and visualised under the UV light source of an epifluorescence microscope (MC80 Zeiss, Germany).

2.1.4.7 Phalloidin staining

Phalloidin is a toxin extracted from the mushroom *Amanita Phalloides* that irreversibly binds the filamentous (F) actin fibres within permeabilised cells. Labelled with a green fluorescent probe, it is used to visualise the structure of the actin cytoskeletal network within cells. Organised or polymerised F actin usually stains as distinct, long fibres.

SM1 cells were seeded in 10% (v/v) FBS (supplemented with G418) onto sterile coverslips placed in a 24 well plate at around $28x10^3$ cells/well and incubated overnight. They were then exposed to lovastatin or vehicle at 10μM in defined

NCTC-109 medium (supplemented with BSA and G418) for 24, 48 and 72 hours, respectively. At each time point, the cells were washed once with PBS-A, fixed in 100% ethanol on ice for 5 minutes and stored at 3-4°C until staining. TRITC labelled Phalloidin (Sigma, St. Louis, MO) was made up at 20µg/ml in DMSO and stored at –20°C in 100µl aliquots, was diluted 1:10 (v/v) to 2µg/ml in deionised water. The coverslips were placed on a flat surface in a fume cupboard and 100µl of the final concentration was applied onto the coverslips and left for 10-15 minutes. The phalloidin was removed by washing thoroughly in dH_2O to minimise non-specific staining. The coverslips were then left to dry completely and finally mounted with CitiFluor (AGAR, UK) and viewed on x400 or x200 magnification on the epifluorescence microscope (MC80 Zeiss, Germany).

It is acknowledged that the above method was kindly developed by Dr. G. Clunn (Clinical Pharmacology, NHLI, ICSM)

2.1.1.8 Cell Proliferation assay

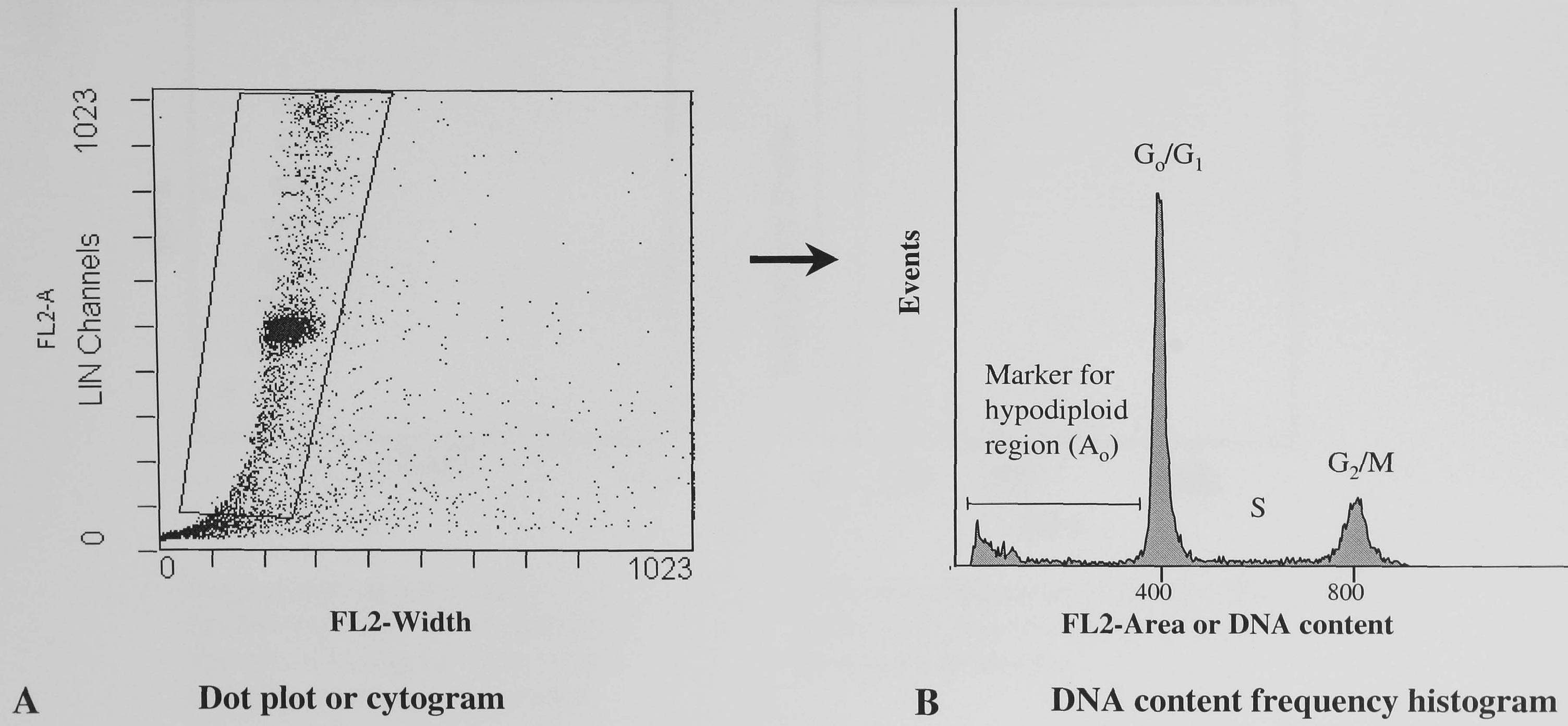
Cells were seeded at $28x10^3$ cells/well in a 24-well plate in 10% (v/v) FBS. After an overnight incubation, the cells were washed once with PBS and exposed to 10µM lovastatin with or without the isoprenoids or mevalonate derivatives or vehicle either in defined NCTC-109 medium or 10% (v/v) dFBS for upto 3 to 5 days. The medium was replenished every day with fresh medium with or without the reagents added. The cells were trypsinised in 1x Trypsin/EDTA (Life Technologies, Inc.) at 0.25% (v/v) and counted on the Coulter Counter Z1 (Coulter Electronics Ltd., England).

2.1.1.9 Cell viability assay

Cell viability was determined after trypsinising the attached cells, resuspending in the culture medium used for treatment (containing the floating cells) and centrifuging each sample at 2000rpm for 5 minutes. The pellet was then resuspended in 10% (v/v) FBS and Trypan Blue in 1:1 ratio (v/v) and the % viability in the whole population calculated (**Pollard JW and Walker JM, 1989**) after counting using the Improved Neubauer Haemocytometer (Weber Scientific International Ltd., England).

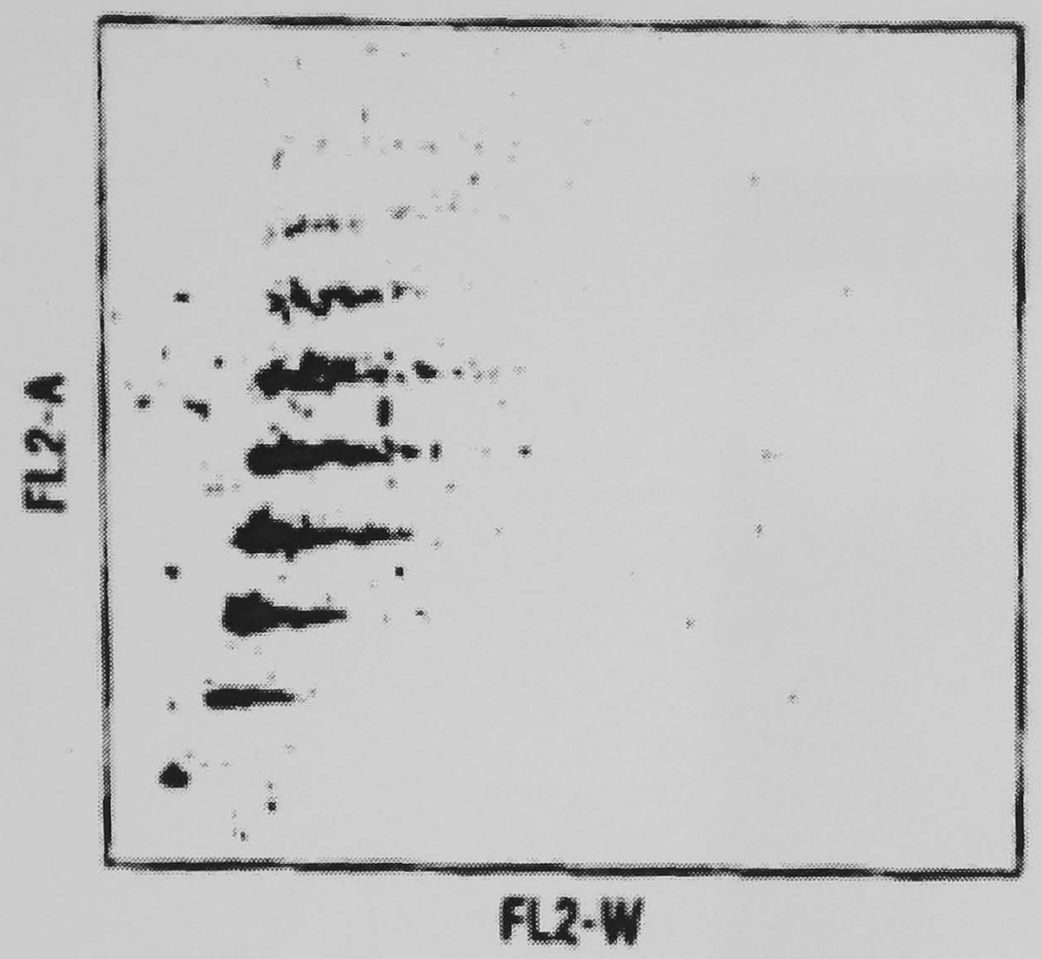
2.1.1.10 Statistics and Data Analysis

The data are presented as the mean ± SEM (standard error of mean) derivedfrom the mean of *n* observations. In order to determine a statistical difference between two groups, 2 tailed Student`s t test was used (paired or unpaired) as appropriate, using Microsoft Excel. Where multiple groups were compared, ANOVA (analysis of variance) was performed using GraphPad Instat software. This was followed by Tukey-Kramer multiple comparisons test to assign *p* values to particular differences (**Motulsky H, 1995**). $p<0.05$ was considered significant.

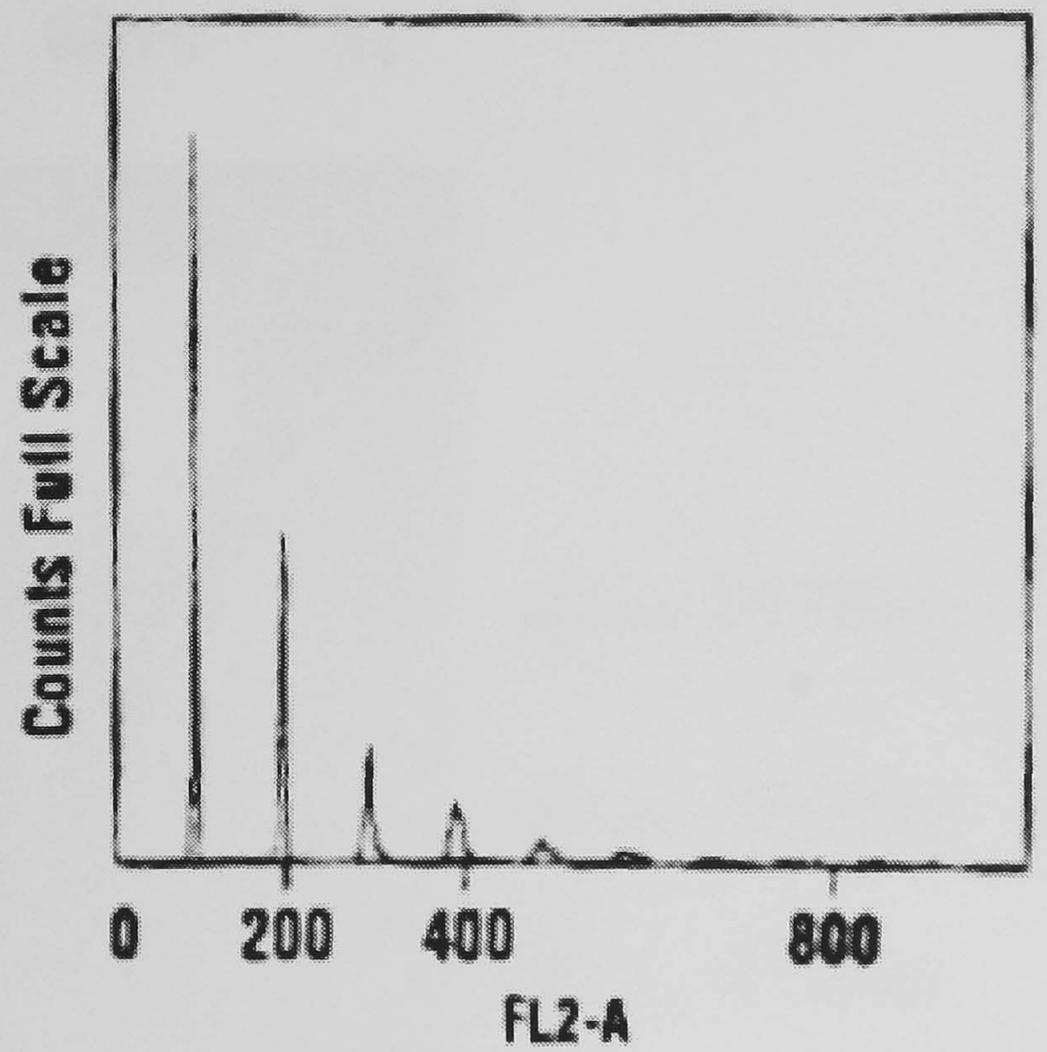


A **Dot plot or cytogram** **B** **DNA content frequency histogram**

Figure 2.1 Diagrams depicting the gating of a propidium iodide (PI)-stained population to measure the DNA content of the hypodiploid region and the specific cell cycle phases. Once 10^4 of events of a given sample are acquired on the CellFit software, then the subpopulation of singlet (not the aggregates) events are gated (A) to give a DNA content frequency histogram (B). From this, using the SOBR algorithm, the % proportion of the hypodiploid DNA content as well as the % proportion of total DNA content in each of the cell cycle phases are calculated. The area under each peak is proportional to the % proportion of cells with a specific amount of DNA. Hence, usually cells or nuclei with a DNA content that corresponds to the amount which would be present if cells were in the G_0/G_1 phase of the cell cycle are the most abundant.



Dot plot of PI-stained Chicken Erythrocyte Nuclei (CEN) aggregates. The dots which appear on the right in each subpopulation are aggregates.



DNA content histogram of the same PI-stained CEN population demonstrating resolution and linearity.

Figure 2.2 Diagrams representing the dot plot and the DNA content frequency histograms of a standard population of nuclei, required to calibrate the flow cytometer. The PI-stained CEN are run through until the fluorescent detectors for the optimal detection of red fluorescence from PI-stained nuclei are set. From this, a DNA content frequency histogram is acquired through the software, to calculate the % coefficient of variation of each peak. For optimal resolution, this value should be less than or equal to 3%. Once the fluorescence detectors are set, then the samples can be run.

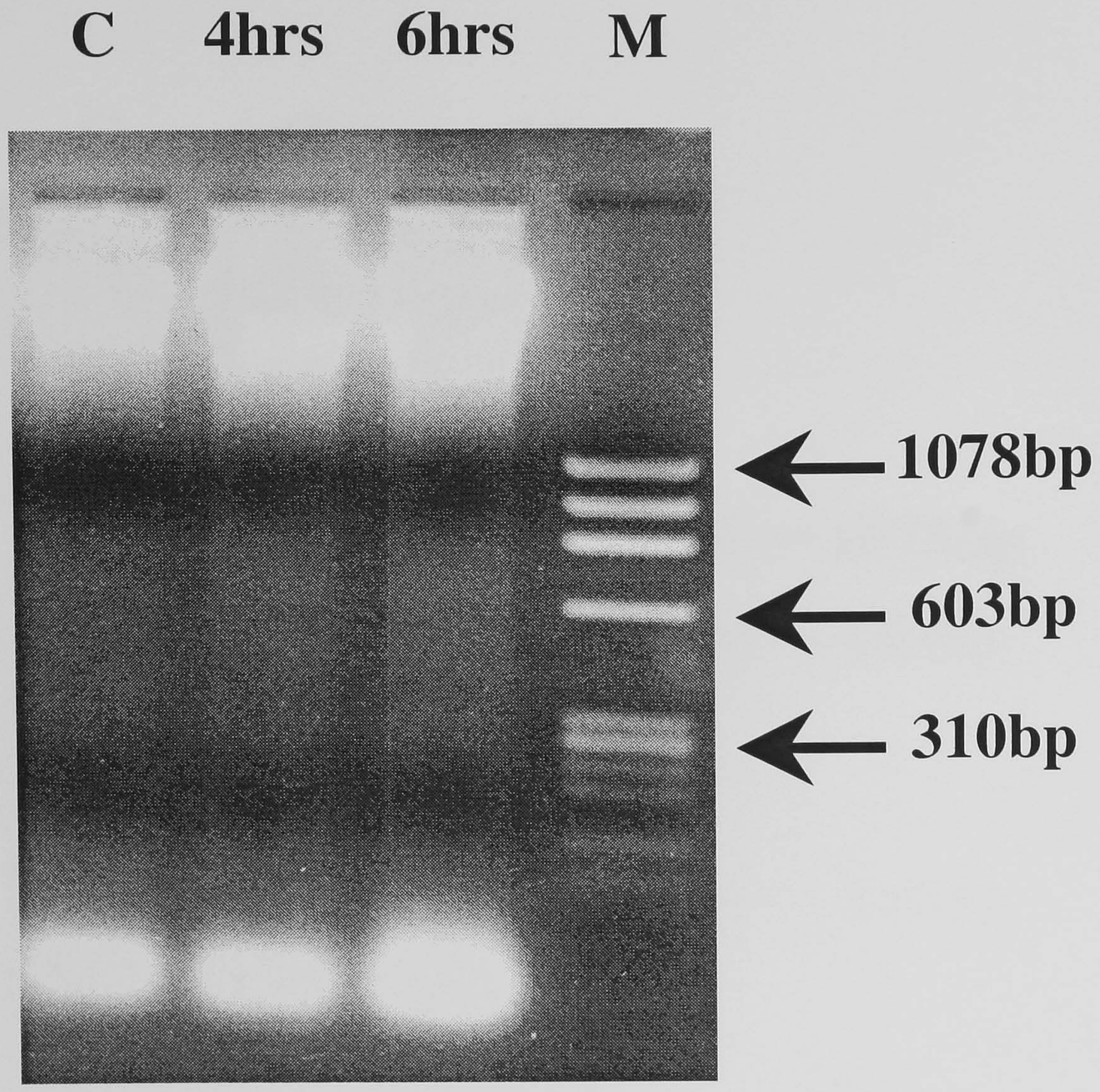


Figure 2.3 Agarose 2% (w/v) gel electrophoresis of DNA extracted from SM1 cells using the standard salting out method. The picture indicates the extremely large amounts of RNA in the samples, which appeared to accumulate at the bottom of each sample lane. SM1 cell cultures were irradiated with 50 J/m^2 in 10% (v/v) FBS, and the DNA was isolated after 4 and 6 hours of incubation. Around 50μg of nucleic acid was loaded per lane.

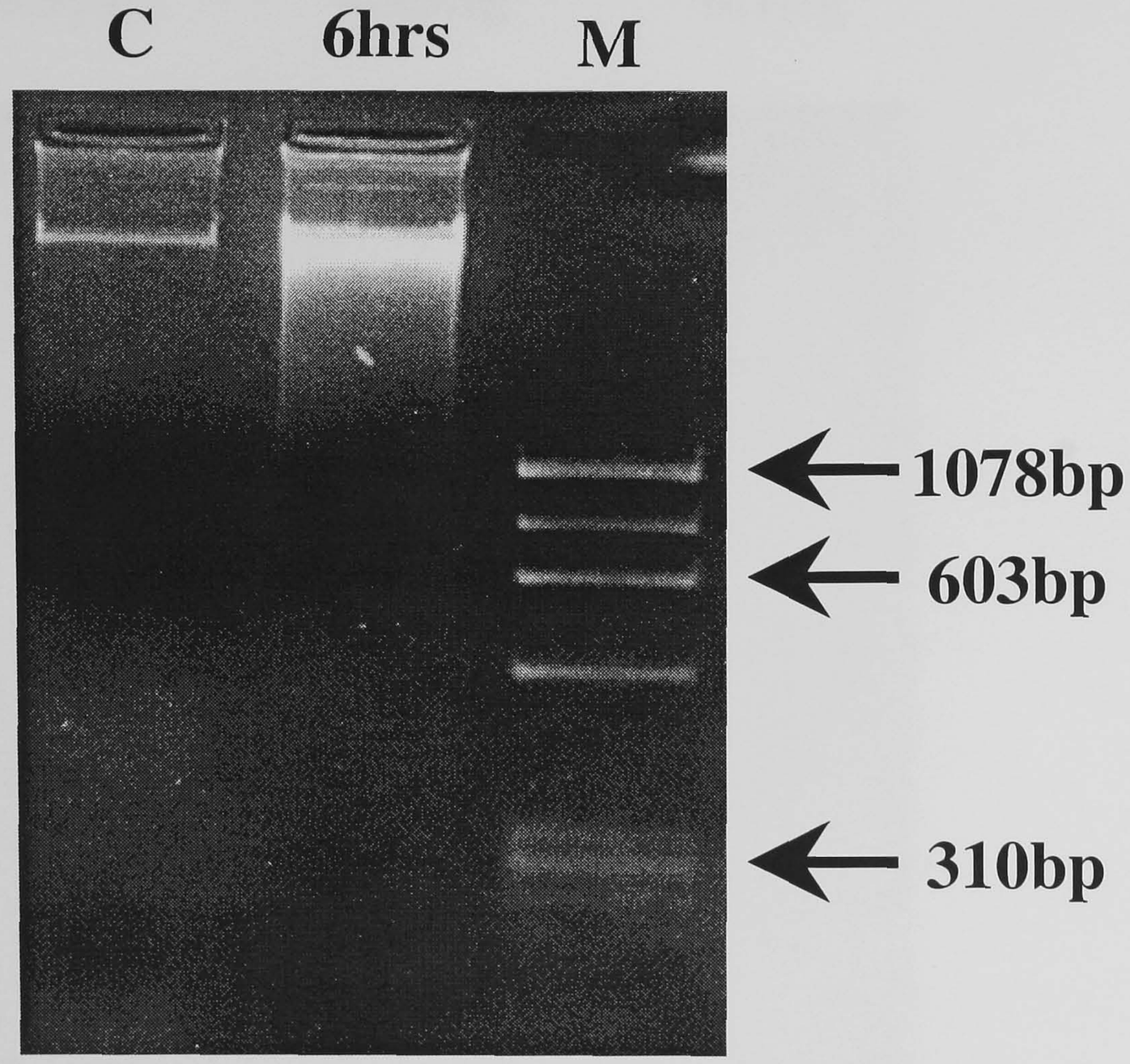


Figure 2.4 Agarose 2% (w/v) gel electrophoresis of DNA extracted from SM1 cells indicating undetectable DNA laddering. SM1 cell cultures were either not treated (lane C) or irradiated with 50 J/m^2 in 10% (v/v) FBS, and the DNA was isolated after 6 hours (lane 6 hrs) of incubation. In this case, around 20μg of nucleic acid was loaded. When less than 50mg of nucleic was loaded onto the gels, the prominence and the detection of bands was much decreased.

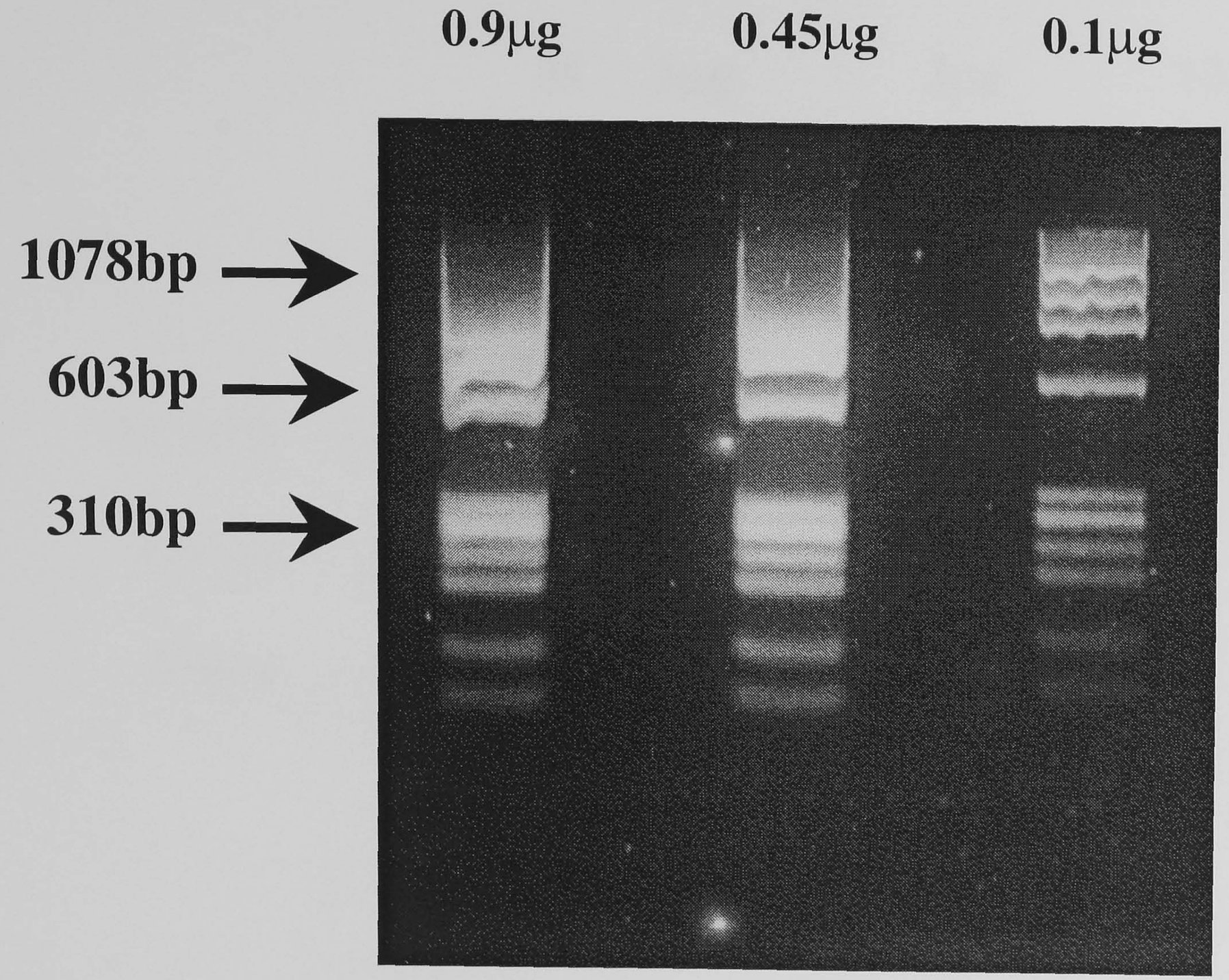


Figure 2.5 Agarose gel (2%) electrophoresis of different amounts of DNA weight marker (ϕX174 plasmid DNA *Hae* III digest at 0.04mg/ml, final concentration) to determine the optimal mass of pure DNA to be loaded with SYBR Green I dye. Lanes show DNA loaded at 0.9, 0.45 and 0.1μg, respectively. Under overloading conditions, the resolution of the bands were cosiderably decreased.

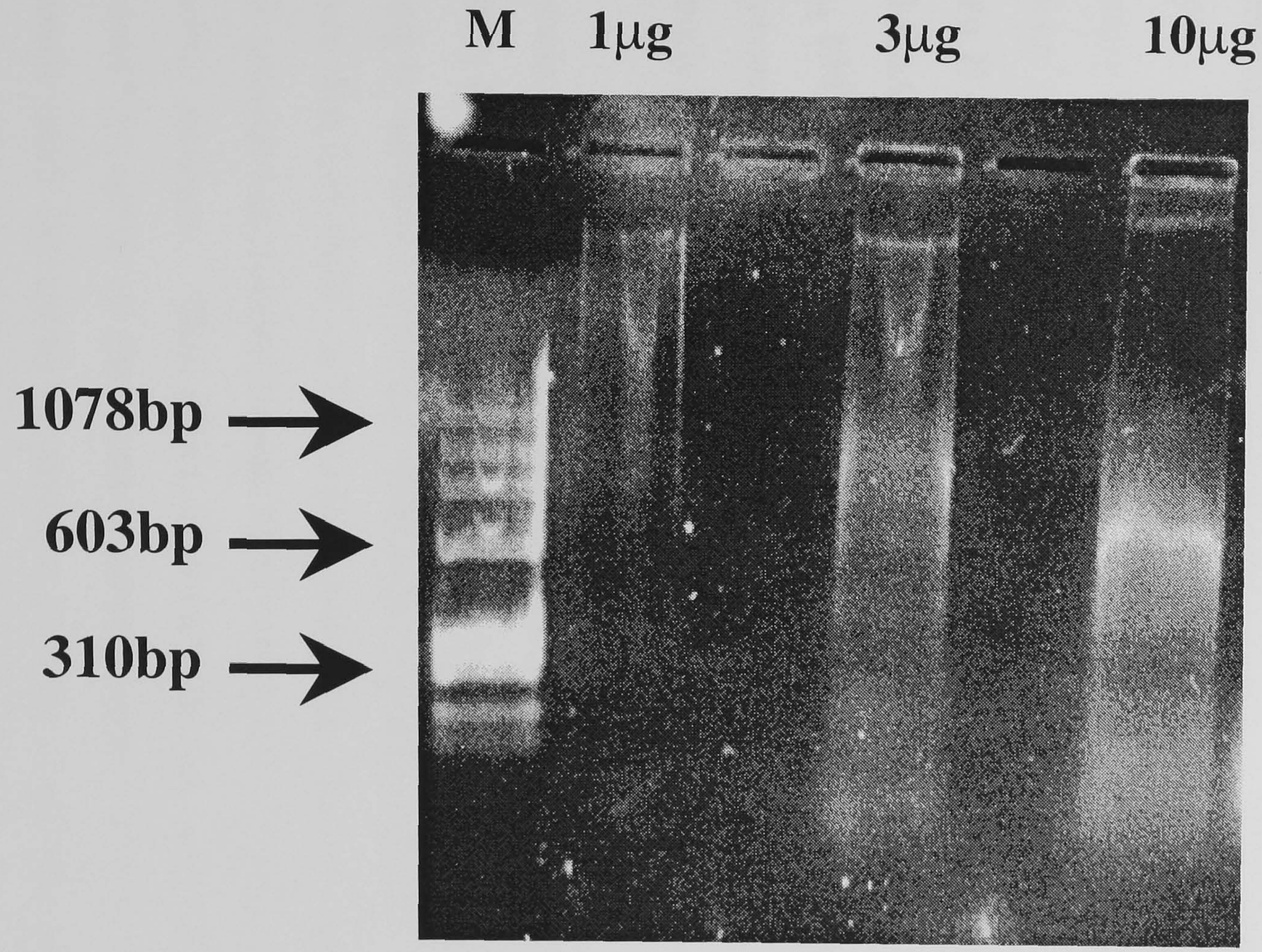


Figure 2.6 Agarose gel (2%, w/v) electrophoresis of DNA extracted from saos-2 cells after induction with 200nM $ZnCl_2$ in 0.4% (v/v) FBS and incubated for 18 hours, by the Gong J et. al., 1994 method. Lanes show DNA loaded with 1, 3, and 10μg of DNA, respectively. Saos-2 cells were chosen since DNA laddering in these cells was relatively more easily detectable with respect to SM1 cells. Around 3μg of nucleic acid seemed to be optimal for the ladder assay, but any more led to overloading, while less than this was inadequate. Hence, almost all the other agarose gels were loaded with about 3μg of nucleic acid. Lane M indicates the molecular weight marker ϕX174 plasmid DNA *Hae* III digest at 0.04mg/ml, final concentration.

Chapter 3

Geranylgeranyl pyrophosphate prevents the pro-apoptotic and anti-proliferative effects of lovastatin on SV-40 transformed human VSM cells in culture

3.1.1.1 Introduction

Although apoptosis of VSM cells has been shown to play an important role in the normal and diseased vasculature, very little is known or understood regarding the mechanisms involved in the control of VSM cell apoptosis. Since the development of atherosclerosis and restenosis is associated with increased migration and proliferation of VSM cells (**Ross R, 1999**), a lot of attention has been given to these aspects of VSM cell biology. The inhibitory effects of HMG-CoA reductase inhibitors (or statins) on VSM cell proliferation has been shown in many different VSM cell models in culture (**Corsini A et. al., 1991; Munro E et. al., 1994; Choi KH et. al., 1995**). Likewise, the inhibitory effects of other HMG-CoA reductase inhibitors on VSM cell migration has been demonstrated (**Hidaka Y et. al., 1992; Corsini A et. al., 1996**). Furthermore, the inhibition of these phenomena has been proposed as potential mechanisms of action involved in the effects of these drugs, at least early in atherogenesis.

Lovastatin was associated with increased apoptosis in a variety of cell lines (**Ghosh PM et al., 1997; Iimura O et al., 1997**). Despite its relevance, no attempts to study the effect of this drug on apoptosis in human VSM cells have been reported. In this chapter, we provide evidence that lovastatin, an HMG-CoA reductase inhibitor, induces apoptosis in a SV-40 large T antigen transformed human VSM cell line in the presence of serum-containing and serum-free medium. This effect of lovastatin was abrogated in the presence of the isoprenoid derivative of mevalonate, geranylgeranyl pyrophosphate (GGpp), as well as mevalonate itself, but not in the presence of farnesyl pyrophosphate (Fpp). Such an effect suggests a role for small GTPases of the Ras superfamily, which are mainly modified with a geranylgeranyl moiety, in the control of lovastatin-induced apoptosis in human VSM cells. We also provide evidence that lovastatin-induced inhibition of cell proliferation and thymidine incorporation were abrogated in the same cells when GGpp but not Fpp, was co-incubated with lovastatin.

3.1.1.2 Results

3.1.2.2 Effect of lovastatin on apoptosis and changes in cell cycle phases in transformed human VSM cells (SM1 cells)

To evaluate whether the HMG-CoA reductase inhibitor, lovastatin, induces apoptosis of human VSM cells, exponentially growing subconfluent SM1 cells were exposed to increasing concentrations of the drug for 24 and 48 hours in serum-free medium (NCTC-109, supplemented with BSA).

Treatment with 10μM lovastatin was associated with cell rounding, increased granularity, and detachment from the petri dish substratum and surrounding cells, as assessed by light microscopy (**Figure 3.1**).

Staining with the DNA-binding fluorescent dye, DAPI and also with the TUNEL reagent revealed that treatment with lovastatin was associated with genomic DNA condensation and fragmentation, characteristic of apoptosis (**Figure 3.2**).

To quantitate the degree of apoptosis induced in the cells, the cell DNA content was assessed using flow cytometry (FACS). Treatment with lovastatin was associated with the appearance of a subpopulation with hypodiploid DNA content, an established marker for apoptosis (**Figure 3.3**). Increasing concentrations of the drug from 0-100μM, was associated with a significant increase in the proportion of cells with hypodiploid DNA content in a dose-dependent manner. The percentage proportion of the hypodiploid region increased from 23%±5% in vehicle treated cultures to 46%±0% ($p=0.05$, $n=6$) in lovastatin (30μM) treated cultures. Likewise, there was a significant increase in the proportion of the hypodiploid region from 21.5±1% in vehicle treated cultures to 56±6% in lovastatin (50μM) cultures at 24 hours ($p=0.03$, $n=6$) (**Figure 3.3**).

Dose-dependent increase in hypodiploid cell DNA content was also associated with the appearance of DNA fragmentation into multiples of 180-200bp bands upon agarose gel electrophoresis, constituting a typical "laddering" pattern characteristic of apoptosis (**Figure 3.4).**

Co-incubation of lovastatin treated cell cultures with mevalonate (100mM) completely prevented the pro-apoptotic effect of lovastatin, as assessed by DNA content analysis by FACS, (**Figure 3.5**), and DNA fragmentation in terms of the "ladder" assay (**Figure 3.9**). There was a significant decrease in the percentage of apoptosis from 22±2% in lovastatin treated cultures to 15±2% in lovastatin and mevalonate co-treated cultures (p=0.005, n=5) The percentage of the hypodiploid region in vehicle treated cultures was 17±2% (**Figure 3.5**). This suggests that the effects of lovastatin were indeed related to the inhibition of endogenous mevalonate synthesis.

We next assessed the kinetics of apoptosis over a period of 48 hours due to 10μM lovastatin. Subconfluent, exponentially growing SM1 cells were exposed to 10μM lovastatin in serum-free (NCTC-109) medium or in 10% dialysed FBS (dFBS), and apoptosis in cultures was assessed by FACS analysis at 0, 24 and 48 hours after the addition of lovastatin. **Figure 3.6 and Figure 3.8** depict the time course of the effect of lovastatin on the hypodiploid region in serum-free medium and in 10% dialysed FBS, respectively. There was a significant increase in apoptosis to 205±2% of control, from 18±2% in control cultures to 37±4.5% (p=0.01, n=4) at 48 hours after treatment of cultures with lovastatin in serum-free medium (**Figure 3.6**). In cultures treated with lovastatin in 10% dialysed FBS, apoptosis increased significantly to 144.5±7.5% of control, from 20±1% to 29±3% (p=0.008, n=6) (**Figure 3.8**). Increased DNA fragmentation into oligofragments of 180-200bp was also evident after electrophoresis of DNA extracted from cultures at 0, 6, 10, 18, and 24 hours after treatment with 100μM lovastatin in serum-free medium (**Figure 3.10**).

DNA content analysis of each cell cycle phase was also assessed by FACS analysis (using the SOBR algorithm) after treatment with 10μM lovastatin in serum-free medium and 10% dFBS over the 48 hour period of treatment. There was no significant difference in G_o/G_1 phase, between the control, vehicle treated cultures at 24 hours and the lovastatin treated cultures at 24 hours. No significant difference in G_o/G_1 phase was seen between vehicle treated, control cultures and lovastatin treated cultures at 48 hours. Equally, there were no significant differences in S phase between the lovastatin treated cultures and the vehicle, control cultures either at 24 hours or at 48 hours after treatment. Likewise, no significant

difference in G_2/M phase between the untreated cultures were seen with respect to cultures treated with lovastatin for 48 hours (**Figure 3.7**).

In cultures treated with lovastatin in 10% (v/v) dialysed FBS, there was no significant difference in G_o/G_1 phase between the lovastatin treated and vehicle treated cultures at 24 hours. At 48 hours, however, there was a significant increase ($p=0.01$, $n=6$) in G_o/G_1 phase by 20±10% from 56±3% in vehicle treated cultures to 67±2% in lovastatin treated cultures. At the same time, S phase decreased ($p=0.001$, $n=6$) by 34±1%, from 32±2% in vehicle treated cultures to 21±1% in lovastatin treated cultures at 48 hours (**Figure 3.9**). There was no significant difference in G_2/M phase between the lovastatin treated and vehicle treated cultures at 24 hours, or at 48 hours (**Figure 3.9**).

3.1.3.2 The effect of mevalonate derivatives on apoptosis induced by lovastatin

To evaluate which of the mevalonate derivatives may be depleted, and hence is important for the induction of apoptosis by lovastatin, SM1 cells were co-incubated with lovastatin and other mevalonate derivatives for 24 hours in serum-free medium. Apoptosis was assessed through quantifying the DNA content of the hypodiploid region using FACS analysis. **Figure 3.11** indicates that the percentage proportion of the hypodiploid region of lovastatin-exposed cultures when co-incubated with mevalonate (18±1%, $p=<0.01$, $n=3$) or the isoprenoid geranylgeranyl pyrophosphate (GGpp) (24±3%, $p=<0.05$, $n=3$) was significantly less than in cultures treated with lovastatin alone (34±3%, $n=3$). The control levels of apoptosis were 20.5±3%, $n=3$. Co-incubation with cholesterol, isopentenyladenosine, or ubiquinone did not significantly prevent apoptosis induced by lovastatin (30±2% for cholesterol and lovastatin, $n=3$). This suggests the increase in apoptosis was not due to the depletion of these compounds. Similarly, co-incubation with the isoprenoid farnesyl pyrophosphate (Fpp) did not have any effects on lovastatin-induced apoptosis. DNA fragmentation was also reduced when lovastatin treated cultures were co-incubated with GGpp, but not with FFpp (**Figure 3.12**).

3.1.4.2 Effect of lovastatin (10μM) on cell proliferation and viability of SM1 cells

To evaluate the effect of lovastatin on the rate of SM1 cell proliferation, 10□M of lovastatin was added to subconfluent, exponentially growing SM1 cells in serum-free medium and in the presence of 10% dialysed (v/v) FBS. Addition of 10μM lovastatin in serum-free NCTC-109 medium to SM1 cells led to a time-dependent reduction in cell numbers over a period of 5 days (**Figure 3.13**). Cell numbers had decreased by 91±4% in lovastatin treated cultures ($p<0.01$, $n=4$) with respect to control cultures at 5 days. Interestingly, cell numbers increased by 3-fold after 5 days in control, vehicle treated cultures despite the absence of serum. However, co-incubation of lovastatin treated cultures with mevalonate (100μM) failed to prevent the decline in cell numbers seen at 4 and 5 days although increase in cell numbers at 2 and 3 days appeared to be particularly preserved by mevalonate.

There was no significant difference in percentage total viability of SM1 cells in vehicle treated, control cultures with respect to lovastatin treated cultures for 5 days in serum-free medium (**Figure 3.13**).

Cell proliferation assays carried out in the presence of 10% (v/v) dialysed (d) FBS, showed a similar pattern to experiments in the absence of serum with lovastatin appearing to prevent the increase in cell number over 5 days. This did not achieve statistical significance by ANOVA probably due to the limited number of experiments conducted (**Figure 3.14**).

Although incubation with lovastatin (10μM) appeared to be associated with a small reduction in cell viability at 3 and 4 days, the % total viability of cells did not differ statistically during lovastatin treatment with respect to vehicle control (**Figure 3.14**).

3.1.5.2 The effect of isoprenoid derivatives of mevalonate on lovastatin-induced inhibition of cell proliferation and thymidine incorporation in SM1 cells

To evaluate whether these isoprenoid derivatives had any effect on the inhibitory effects of lovastatin (10μM) on cell proliferation and thymidine incorporation, GGpp and FFpp were

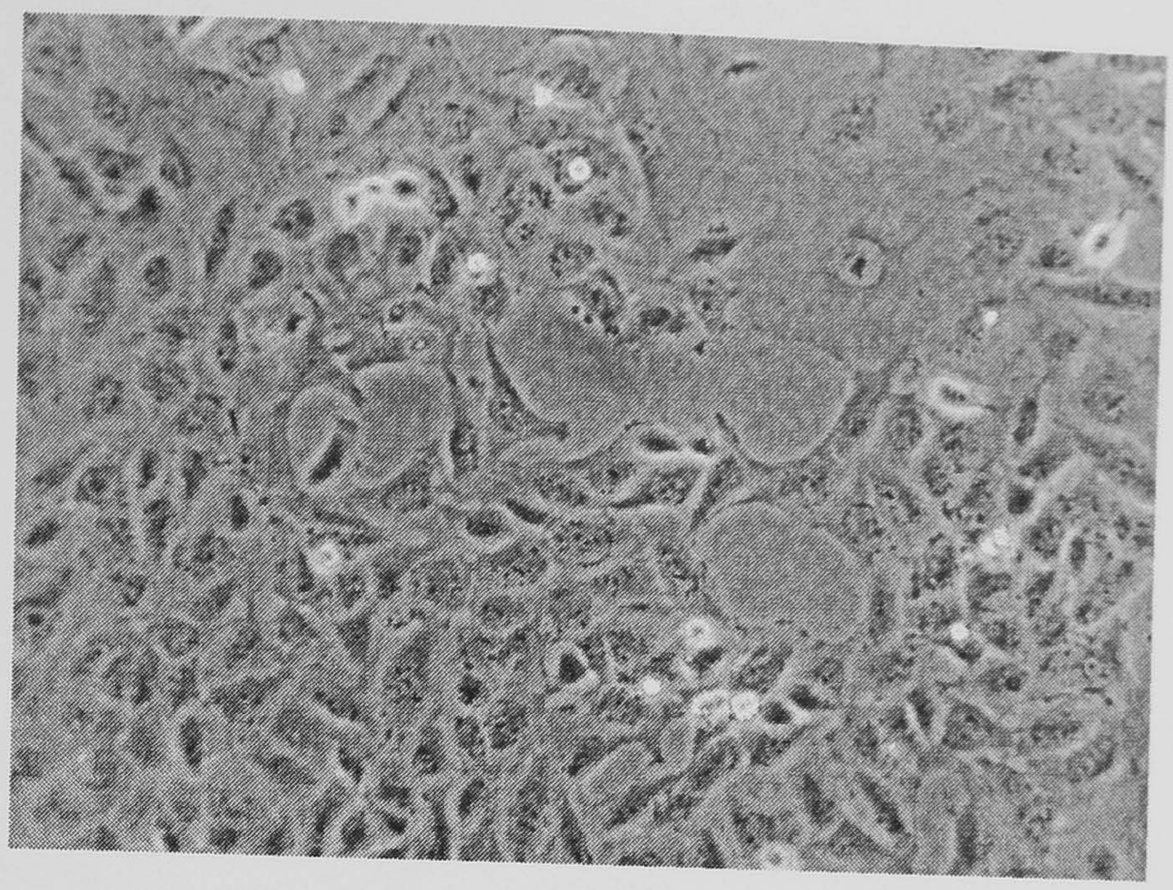
co-incubated with or without lovastatin. [^{3}H]-thymidine incorporation was carried out in 10% dialysed FBS over a period of 72 hours. **Figure 3.15** shows that at 48 hours, there was a significant inhibition of [^{3}H] thymidine incorporation by 79.5±0.5% from 1727±544 cpm in control, vehicle treated cultures to 351±101 cpm in lovastatin treated cultures (p=0.03, n=4). At 72 hours there was a significant decrease in [^{3}H] thymidine incorporation by 87% from 2196±363 cpm in control, vehicle treated cultures to 276±46.5 cpm in lovastatin treated cultures (p=0.002, n=4). There was also a significant decrease in [^{3}H] thymidine incoporation by 86.5% from 2196±363 cpm in control cultures to 308±107 cpm in lovastatin and farnesyl pyrophosphate (10μM) co-treated cultures (p=0.002, n=4). However, there was a significant increase in [^{3}H] thymidine incoporation by about 5 fold from 276±46.5 cpm in lovastatin treated cultures to 1500±176 cpm in cultures co-incubated with lovastatin and geranylgeranyl pyrophosphate (10μM) (p=0.002, n=4).

Addition of GGpp to lovastatin treated cells, also increased cell numbers (**Figure 3.16**) by about 3 fold from $19.2x10^3 \pm 5.4x10^3$ cells in lovastatin treated cells to $61.8x10^3 \pm 8.4x10^3$ cells in cultures co-incubated with both lovastatin and GGpp (p=0.01, n=3). However, there was no significant increase in cell numbers in cultures co-incubated with lovastatin and FFpp, with respect to the lovastatin-treatment alone.

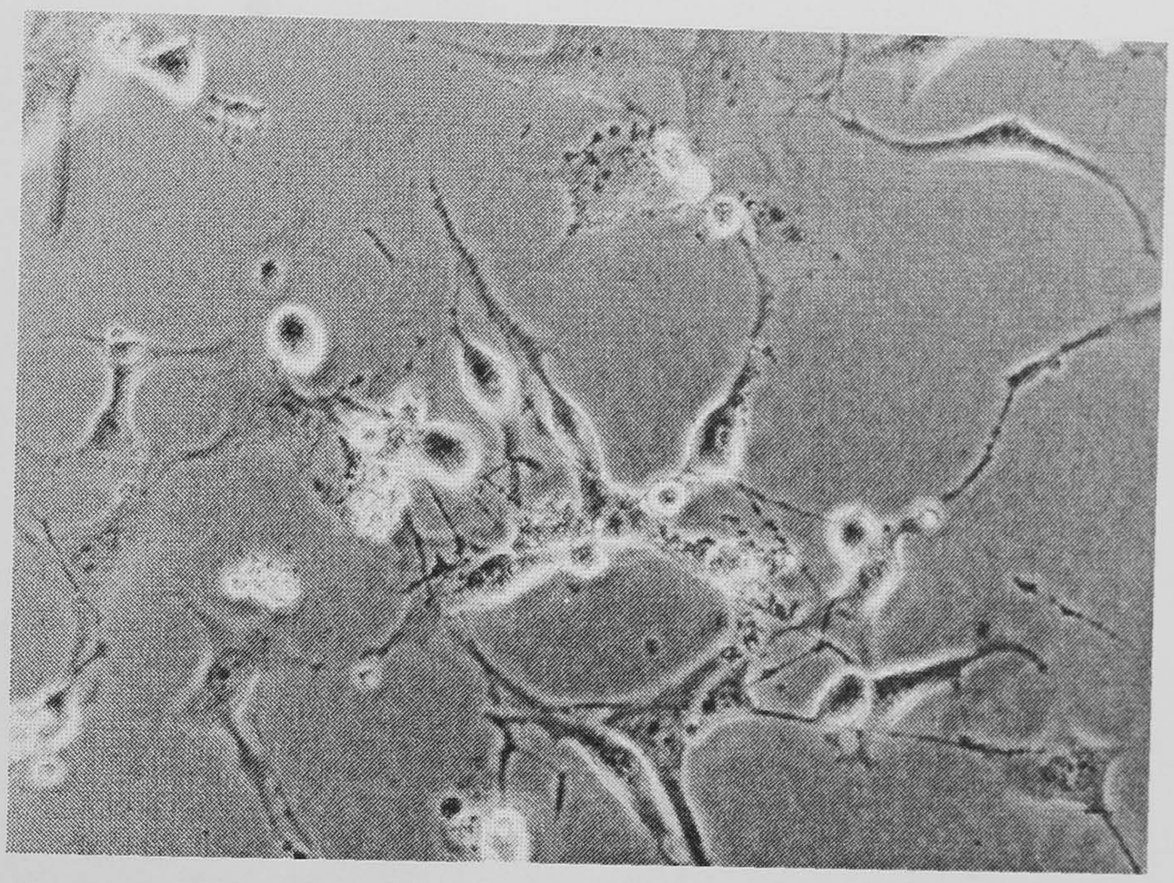
3.1.6.2 The effect of lovastatin on the actin cytoskeleton, as revealed after Phalloidin staining

SM1 cells were exposed to lovastatin (10μM) in serum-free medium for a period of upto 72 hours, and the cells were washed and fixed as described in the materials and methods. The fixed cells were then stained with TRITC-labelled Phalloidin to assess the organisation of the F actin cytoskeletal network. The collapse of the cytoskeletal network was very apparent by 24 hours after exposure (**Figure 3.17**).

A



B



C

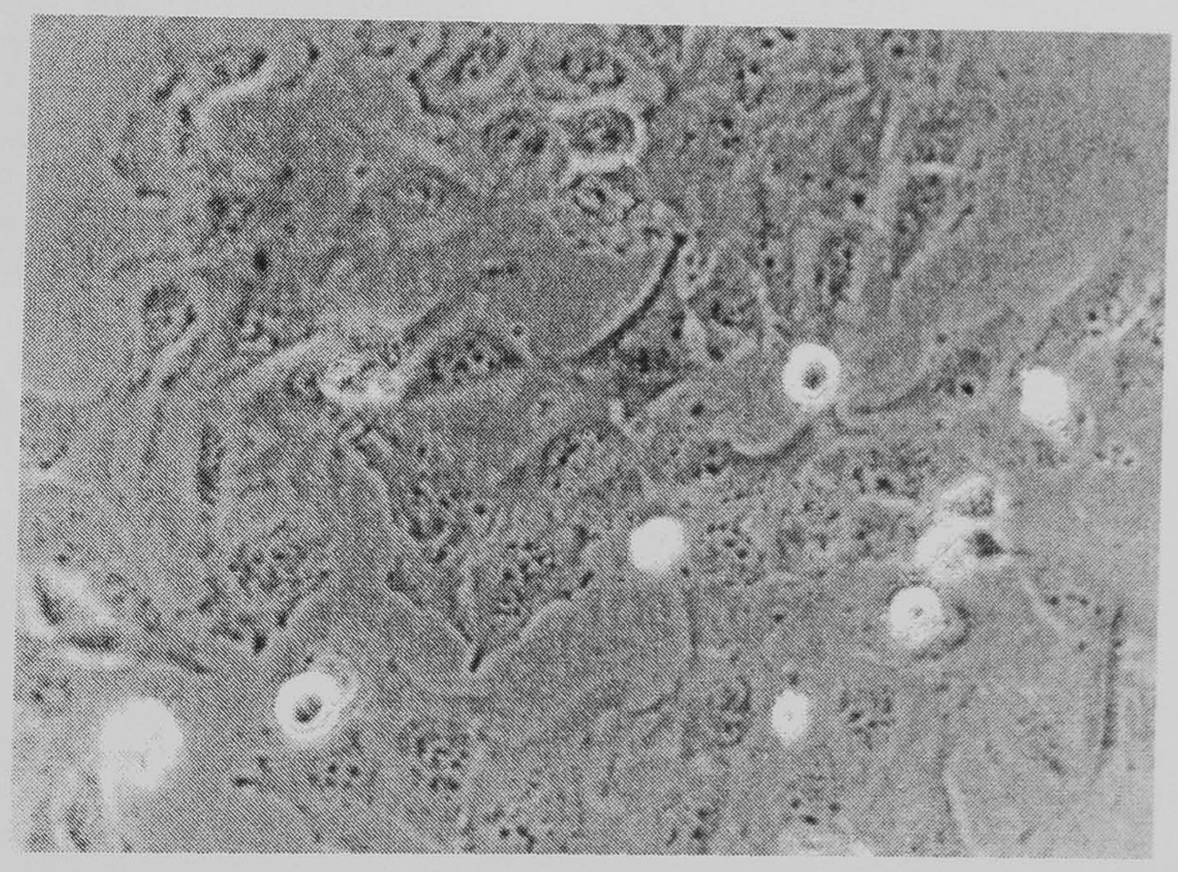
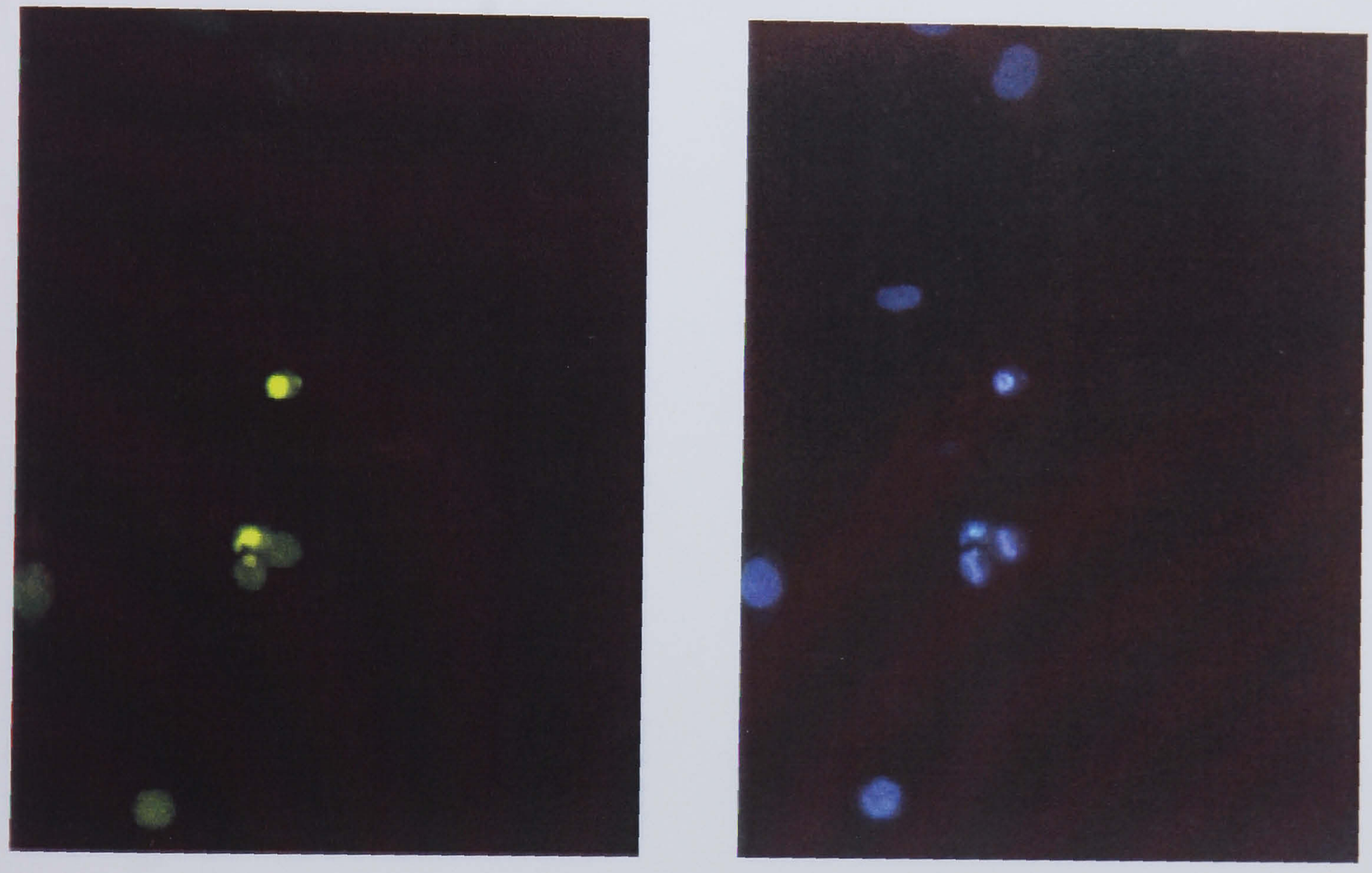


Figure 3.1 Morphological effects of lovastatin in SM1 cells in culture. Light microscopy photomicrographs of lovastatin-treated SM1 cells, indicating common morphological features of apoptosis, such as barely attached or floating, rounded up cells with condensed cytoplasm. SM1 cells were induced with 10μM of **A**) vehicle (original magnification x100) **B**) lovastatin **C**) lovastatin and 100μM of mevalonate (original magnification x200, respectively) for 48 hours in dialysed 10% (v/v) FBS.



TUNEL staining

DAPI staining

Figure 3.2 Cytochemical effects of lovastatin on SM1 cells in culture. Fluorescence photomicrographs of SM1 cells that have been treated with 100μM lovastatin in serum-free medium for 24 hours. The cells were first stained with the TUNEL (transferase-mediated dUTP nick-end labelling) reagent, as described in the Materials and Methods, and finally counterstained with the DNA-binding fluorescent dye, DAPI (originalmagnification x400). The bright green stains indicate the apoptotic, TUNEL positive nuclei with DNA fragmentation, while the bright blue staining corresponds to nuclei with DNA condensation.

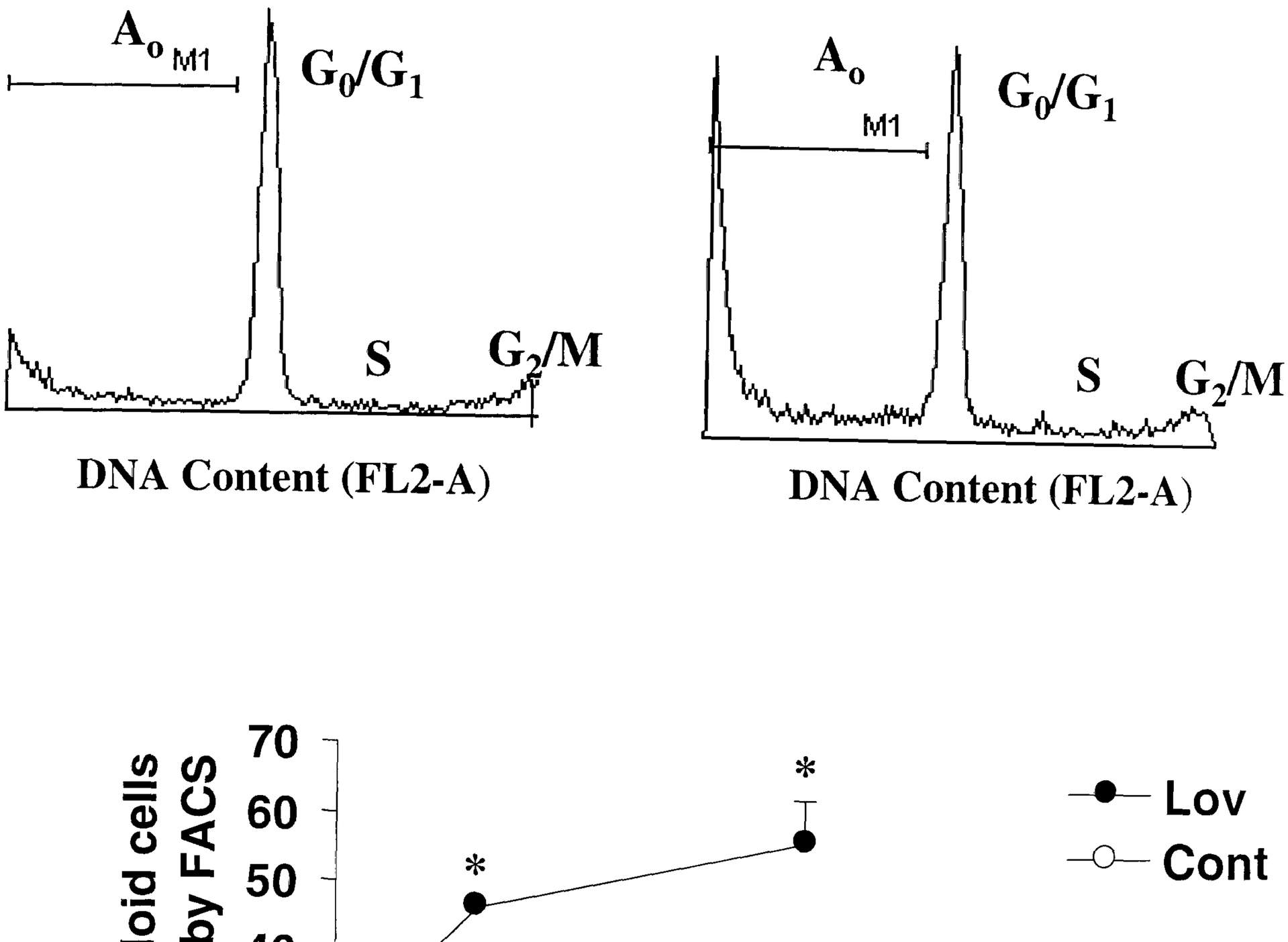


Figure 3.3 Dose-dependent changes in the hypodiploid DNA content of SM1 cell cultures after lovastatin treatment. **A)** Representative DNA histograms depicting the specific peak (or frequency) of nuclei or cells containing DNA which corresponds to the amount of DNA contained at the G_0/G_1, S and the G_2/M phase of the cell cycle, respectively. The hypodiploid region is marked by a marker, and the area beneath this region gives the % proportion of events with that specific DNA content. Treatment with 30μM lovastatin is associated with an increased proportion of cells with hypodiploid DNA content. **B)** Exponentially growing SM1 cells were treated with increasing concentrations of lovastatin (Lov) or vehicle (Cont) in serum-free medium for 24 hours, and the % proportion of the hypodiploid region measured for each sample by FACS analysis (flow cytometry) after propidium iodide staining. Lovastatin treatment was associated, in a dose-dependent manner, with increased proportion of cells with hypodiploid DNA content. The results represent the mean ± SEM of six experiments. Statistical significance was assessed by the Student`s t test, where * = $p<0.05$ vs control.

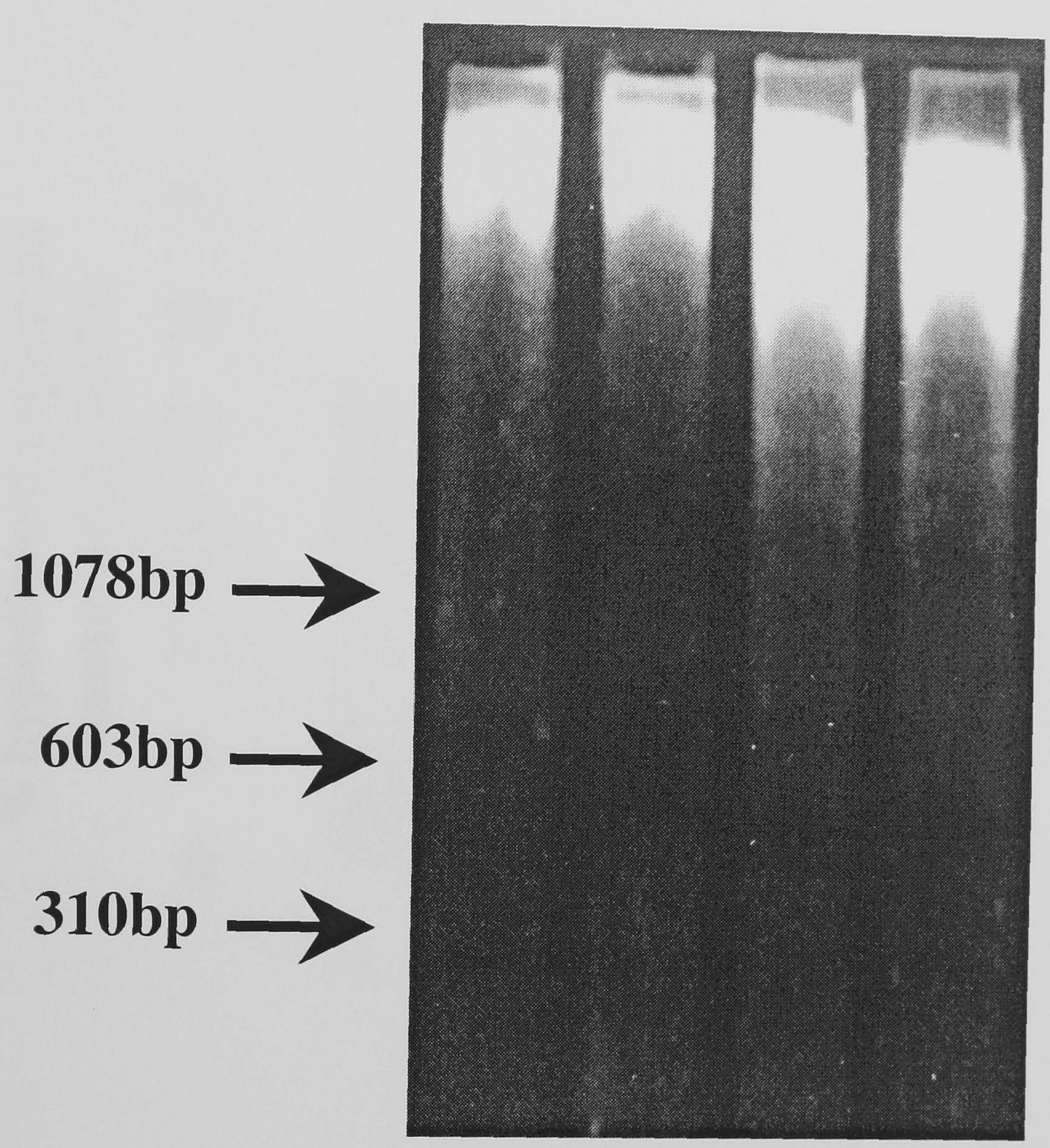


Figure 3.4 Dose-dependent effects of lovastatin on DNA fragmentation. Agarose gel (2%) (w/v) electrophoresis of DNA extracted from SM1cells treated with increasing concentrations of lovastatin (3, 10 and 30μM) for 24 hours in serum-free medium, and with vehicle (Cont) for 24 hours. Treatment with increasing concentrations of lovastatin was associated with increased levels of DNA fragmentation, resulting in high molecular weight fragments. Lane M indicates the DNA size marker, ϕX174 plasmid cut with *Hae* III (0.04mg/ml). The final optimised procedure was used to extract the DNA from the cells. About 2 μg of nucleic acid was loaded, and the gel was cast with 1:10000 dilution of SYBR Green I dye.

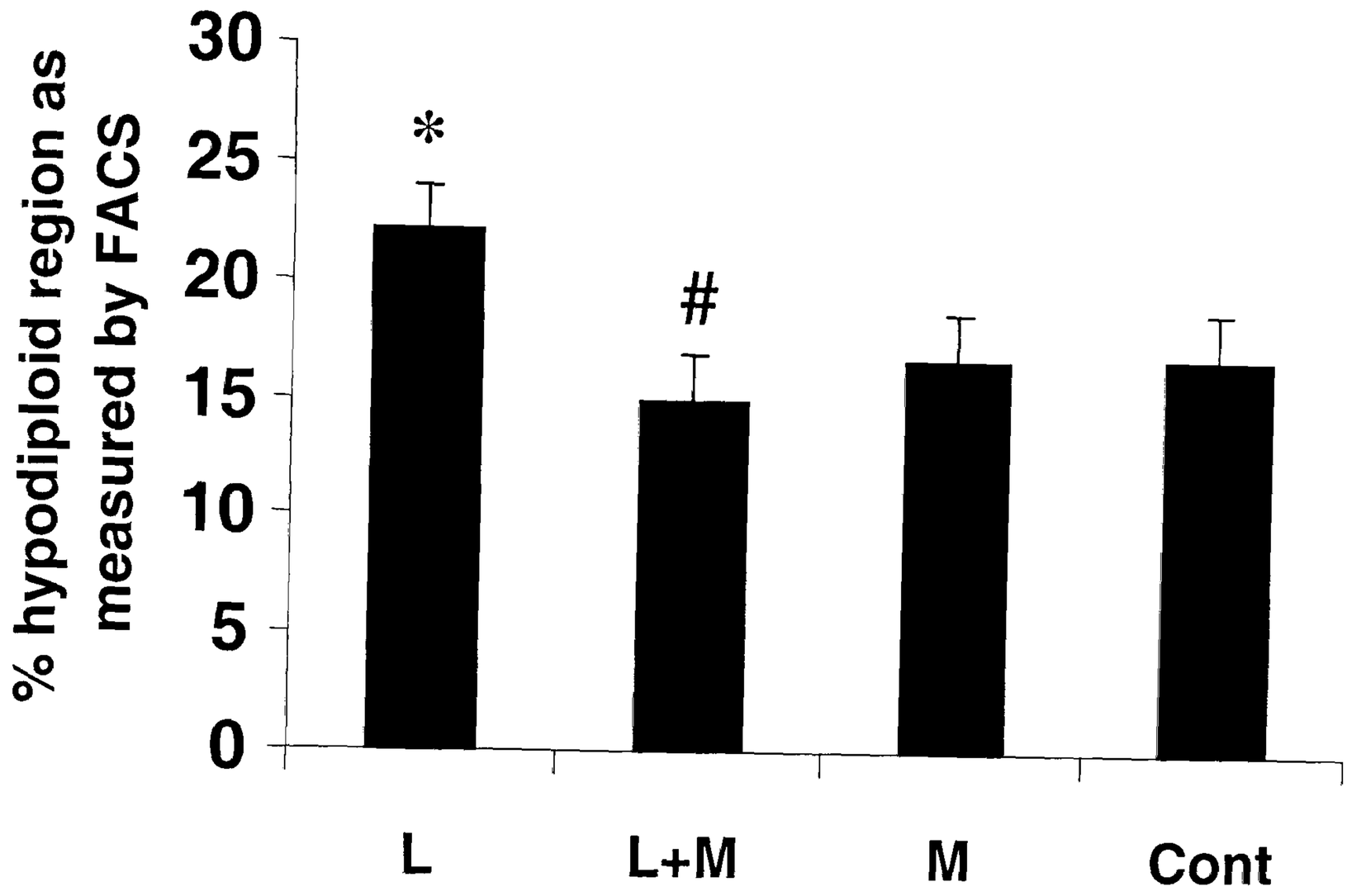


Figure 3.5 Recovery of lovastatin-induced apoptosis when co-incubated with mevalonate. Graph indicating the decrease, with respect to lovastatin alone treated cultures, in the % total proportion of the hypodiploid region, as measured after propidium iodide staining by flow cytometry, when exponentially growing SM1cells were co-treated with 10μM lovastatin (L) and mevalonate (L+M) or incubated with the vehicle (Cont) in NCTC-109 serum-free medium for 24 hours. This indicated a consequent decrease in apoptosis in the same cell cultures (see Figure 3.1). Results represent the mean ± SEM of five experiments. Statistical significance was assessed by ANOVA, followed by the Tukey-Kramer multiple comparisons test where * =$p < 0.01$ vs control and # =$p < 0.001$ vs lovastatin.

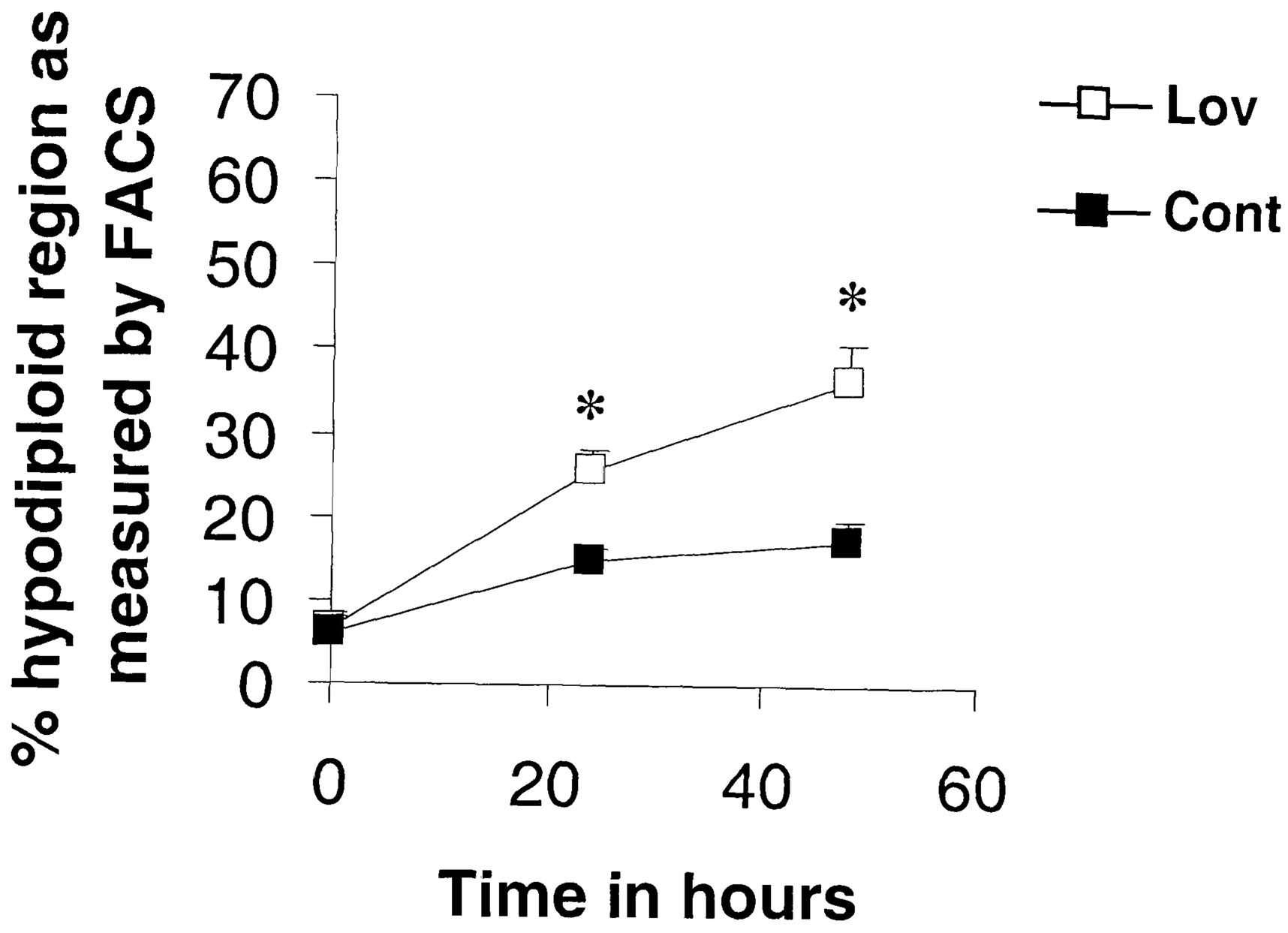


Figure 3.6 Time-dependent effect of lovastatin in serum-free medium on apoptosis in SM1 cells. Exponentially growing SM1 cells were treated with 10μM of lovastatin (Lov) and vehicle (Cont) for upto 48 hours in NCTC-109 serum-free medium. Cultures were harvested, stained with propidium iodide and analysed by flow cytometry at 0, 24, and 48 hours. The graph indicates a time-dependent increase in % total proportion of the hypodiploid region of the DNA histogram, a characteristic feature of apoptosis, after exposure to lovastatin. Results represent the mean ± SEM of four experiments. Statistical significance was assessed by the Student`s t test. where *=$p<0.05$ vs control.

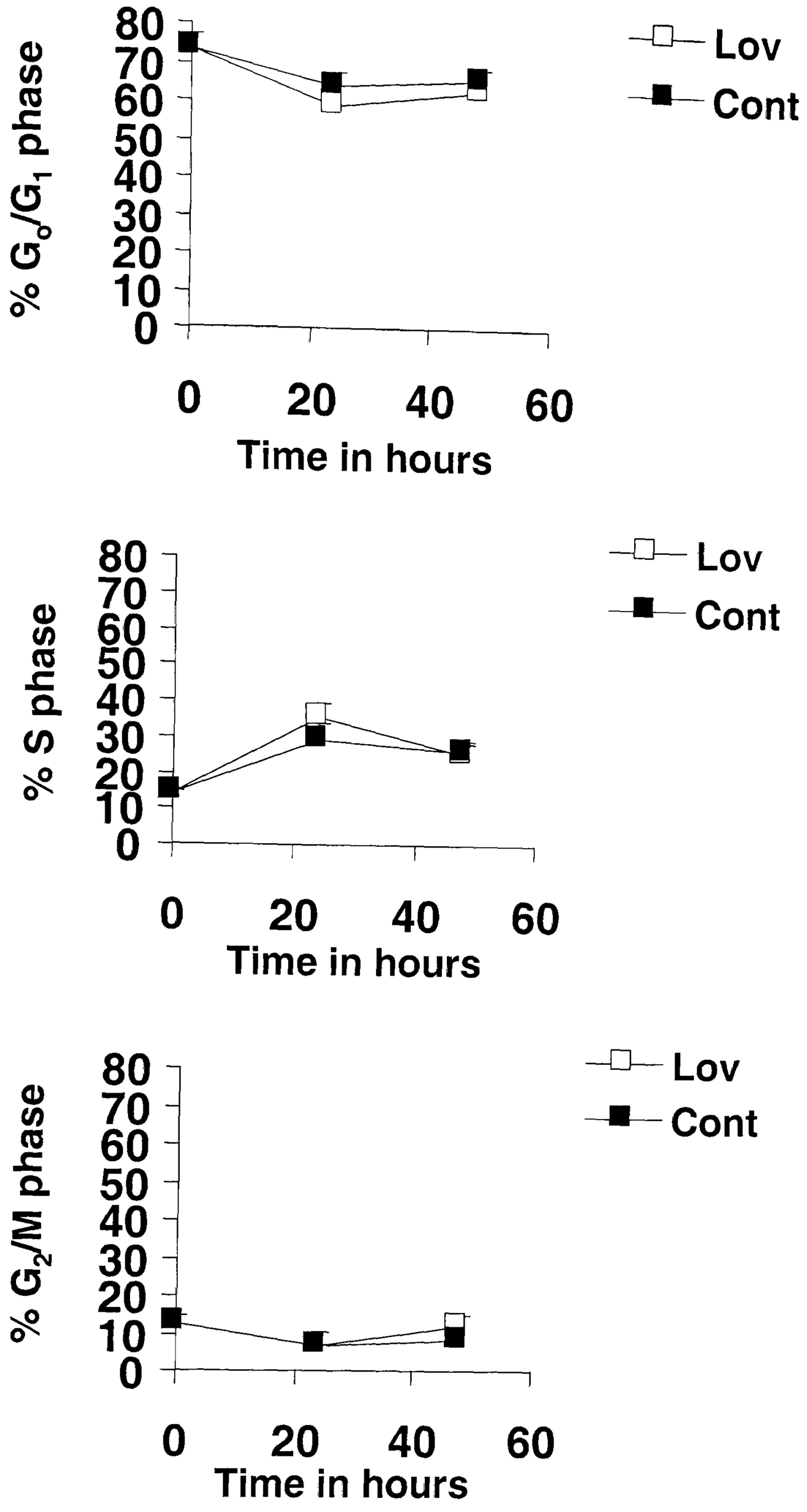


Figure 3.7 Time-dependent effect of lovastatin in serum-free medium on cell cycle phases in SM1 cells. Exponentially growing SM1 cells were treated with 10μM of lovastatin (Lov) and vehicle (Cont) for upto 48 hours in NCTC-109 serum-free medium. Cultures were harvested, stained with propidium iodide and analysed by flow cytometry at 0, 24, and 48 hours. The graphs indicat time-dependent changes in % total proportion of each cell cycle phase of the DNA histogram, measured using the SOBR algorithm, as part of the DNA content analysis software. Results represent the mean ± SEM of four experiments.

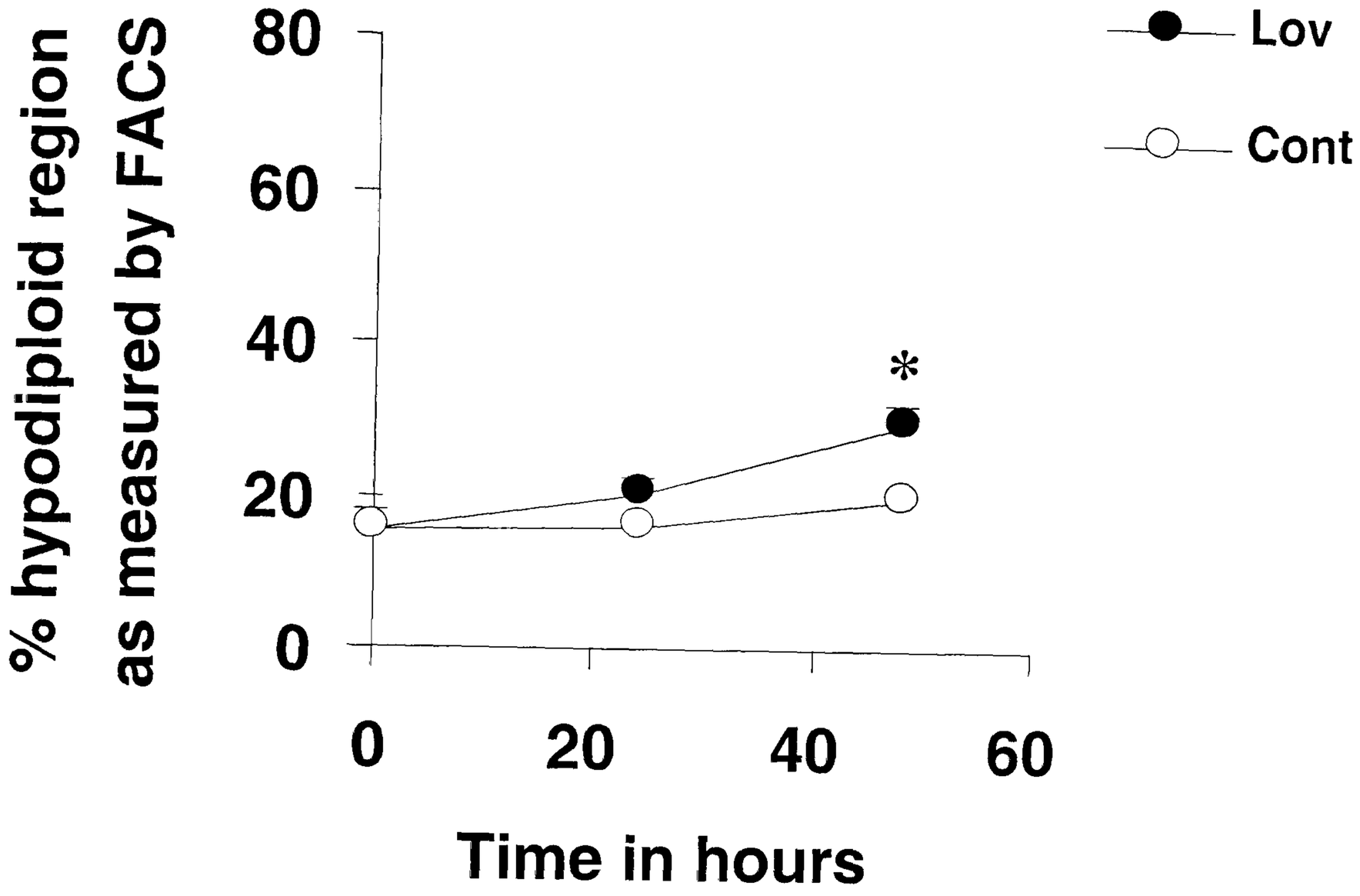


Figure 3.8 Time-dependent effect of lovastatin in 10 % dialysed (v/v) FBS on apoptosis in SM1 cells. Exponentially growing SM1 cells were treated with 10μM of lovastatin (Lov) and vehicle (Cont) for upto 48 hours in dialysed 10% (v/v) foetal bovine serum. Cultures were harvested, stained with propidium iodide and analysed by flow cytometry at 0, 24, and 48 hours. The graph indicates a time-dependent increase in % total proportion of the hypodiploid region of the DNA histogram, a characteristic feature of apoptosis, after exposure to lovastatin. Results represent the mean ±SEM of five experiments. Statistical significance was assessed by the Student`s t test, where *=$p<0.05$ vs control.

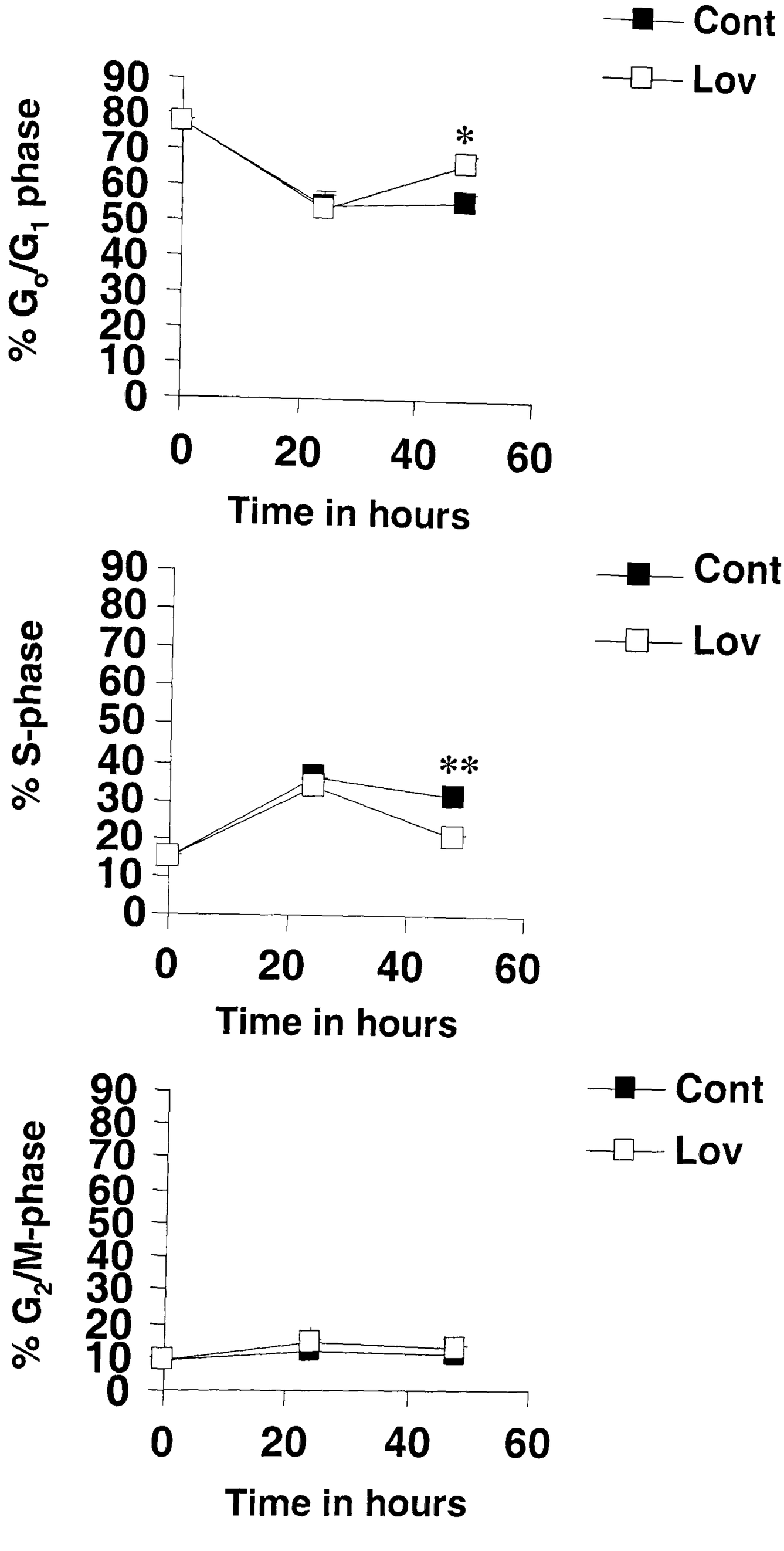


Figure 3.9 Time-dependent effect of 10μM lovastatin on SM1 cell cycle phases as assessed by flow cytometry. Exponentially growing, subconfluent SM1 cells were treated with lovastatin (Lov) or vehicle (Cont) in 10% (v/v) dialysed FBS for 48 hours. The cells were harvested, stained with propidium iodide and analysed by FACS. The % total proportion of each cell cycle phase was measured using the SOBR algorithm, which is part of the DNA content analysis software. The results represent the mean±SEM of five experiments. Statistical significance was assessed by the Student`s t test, where *=$p<0.05$ vs control and **=$p<0.01$ vs control.

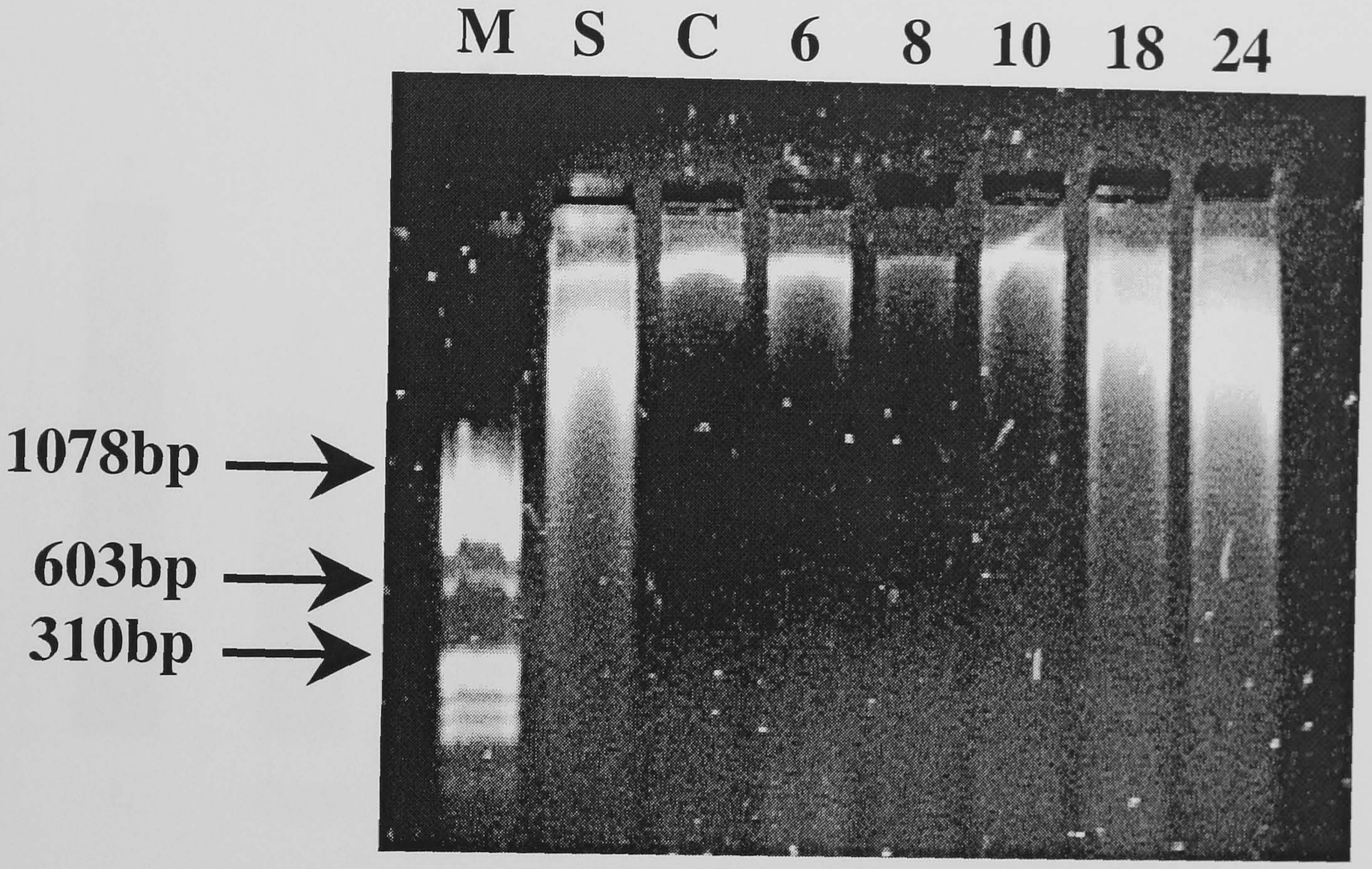


Figure 3.10 Time-dependent effects of lovastatin treatment on DNA fragmentation in SM1 cells. Agarose gel (2%) (w/v) electrophoresis of DNA extracted from SM1cells treated with 100μM lovastatin for 0, 6 ,8, 10, 18 and 24 hours in serum-free medium. Treatment with lovastatin was associated, in a time-dependent manner, with increased levels of DNA fragmentation, resulting in high molecular weight fragments. Lane S indicates a positive control sample of DNA extracted from a transformed human osteosarcoma cell line, saos-2 cells, treated with 200nM Zinc Chloride ($ZnCl_2$) in 0.4% (v/v) FBS for about 18 hours. Lane M indicates the DNA size marker, ϕX174 plasmid cut with *Hae* III (0.04mg/ml). The final optimised procedure was used to extract the DNA from the cells. About 3 μg of nucleic acid was loaded, and the gel was cast in 1:10000 dilution of SYBR Green I dye.

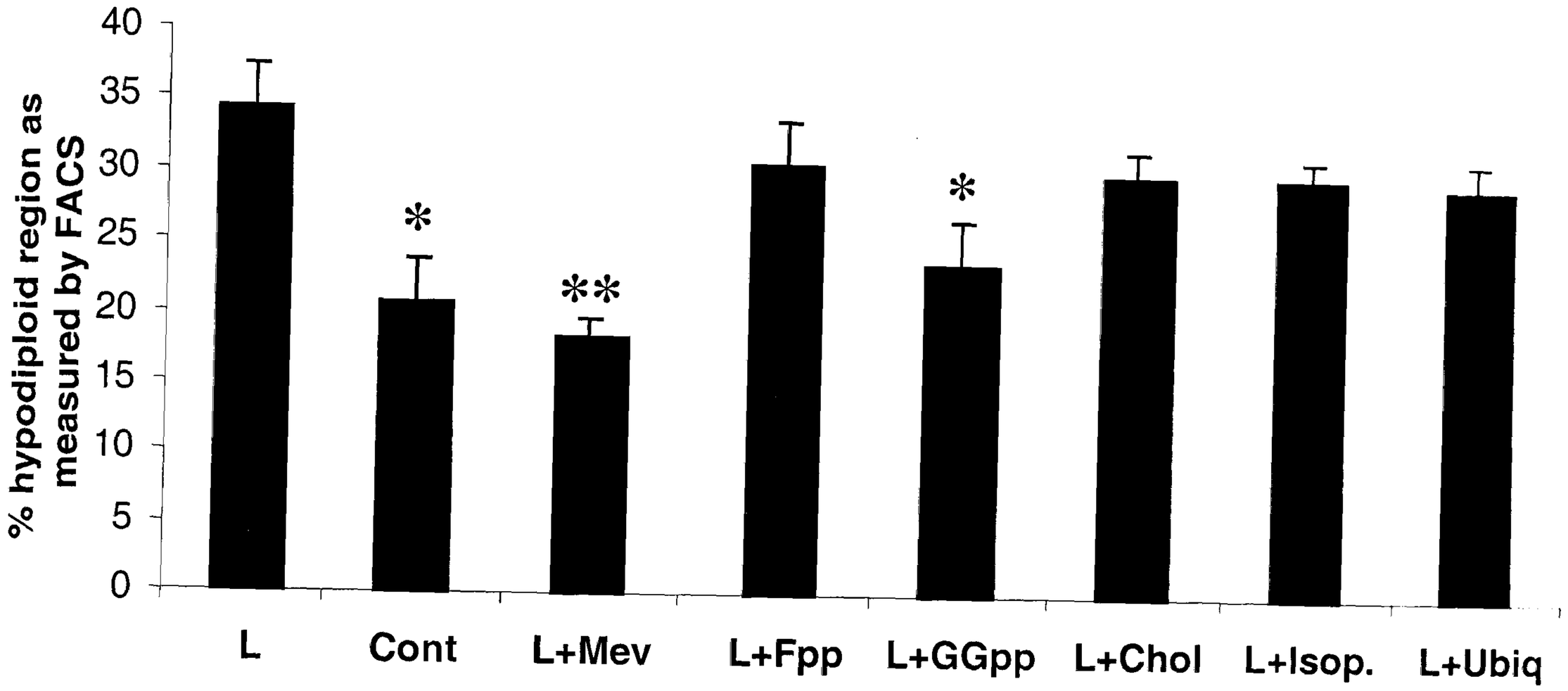


Figure 3.11 Recovery of lovastatin-induced increase in the hypodiploid DNA content of SM1 cells with mevalonate or geranylgeranyl pyrophosphate. Graph indicating the decrease in the % total proportion of the hypodiploid region, with respect to lovastatin treated cultures, when SM1 cells were co-incubated with lovastatin (10μM) and other mevalonate derivatives, such as 100μM mevalonate (Mev), 10μM farnesyl pyrophosphate (Fpp), 10μM geranylgeranyl pyrophosphate (Gpp), cholesterol (Chol), isopentenyladenosine (Isop), and ubiquinone (Ubiq). Co-incubation with either mevalonate or geranylgeranyl pyrophosphate, was associated with a decrease in the proportion of cells with reduced DNA content, that was otherwise increased when cells were treated with lovastatin alone. Results represent the mean ± SEM of three experiments. Statistical significance was assessed by ANOVA, followed by theTukey-Kramer multiple comparisons test, where *=$p<0.05$ and **=$p<0.01$ vs lovastatin).

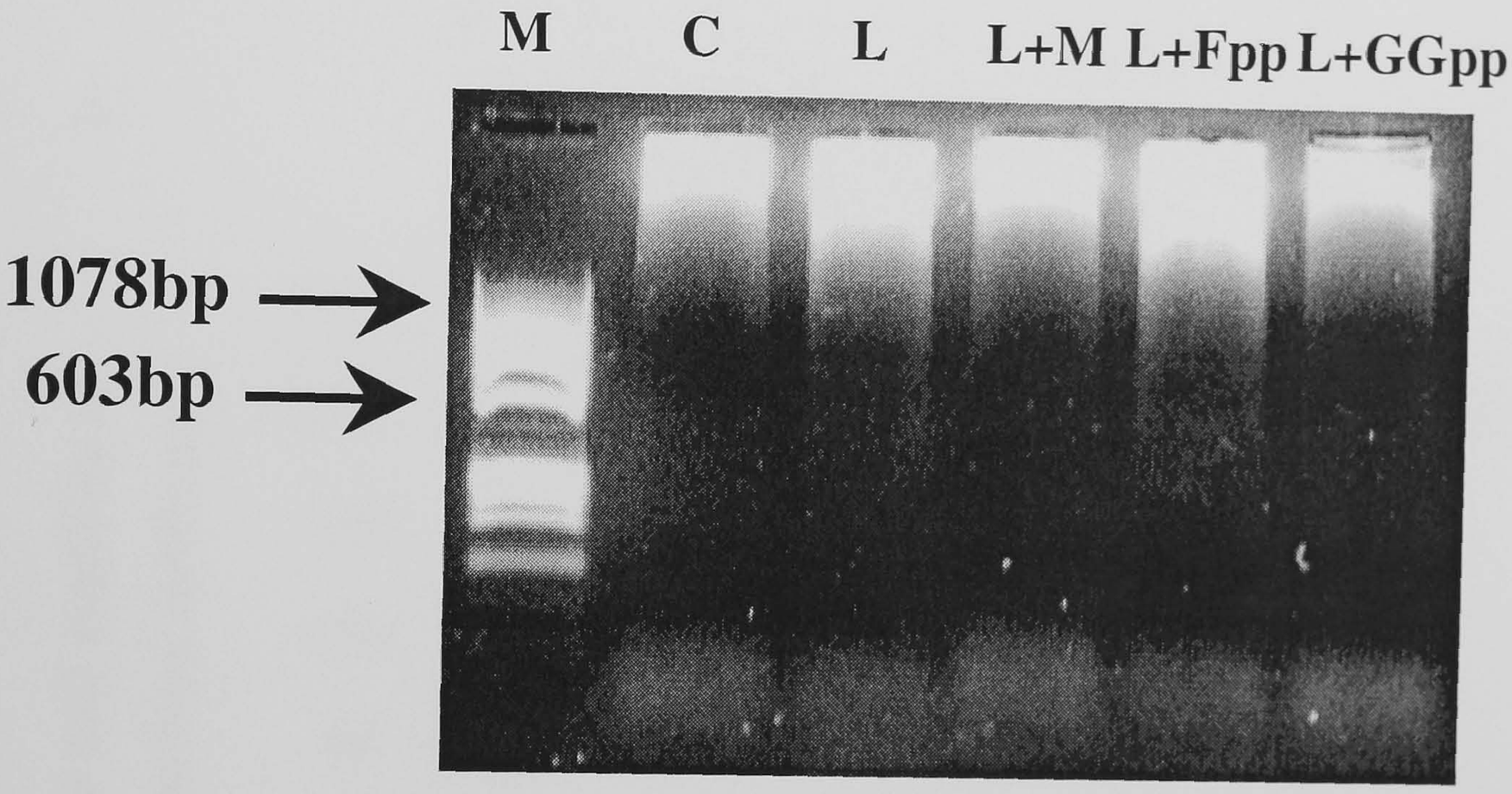


Figure 3.12 Decrease in lovastatin-induced DNA fragmentation after co-incubation with mevalonate or geranyl geranyl pyrophosphate. Agarose gel (2%) (w/v) electrophoresis of DNA extracted from SM1 cells treated with 10μM lovastatin (L) or vehicle (C) in serum-free medium for 48 hours, indicating the decrease in DNA fragmentation when lovastatin treated cells were co-incubated either with 100μM mevalonate (L+M) or 10μM geranylgeranyl pyrophospahte (L+GGpp). Co-incubation of lovastatin treated cells with farnesyl pyrophosphate (L+Fpp) did not seem to have an effect on DNA fragmentation due to lovastatin. Lane M indicates the DNA size marker, ϕX174 plasmid cut with *Hae* III (0.04mg/ml). The final optimised procedure was used to extract the DNA from the cells. About 3 μg of nucleic acid was loaded, and the gel was cast in 1:10000 dilution of SYBR Green I dye.

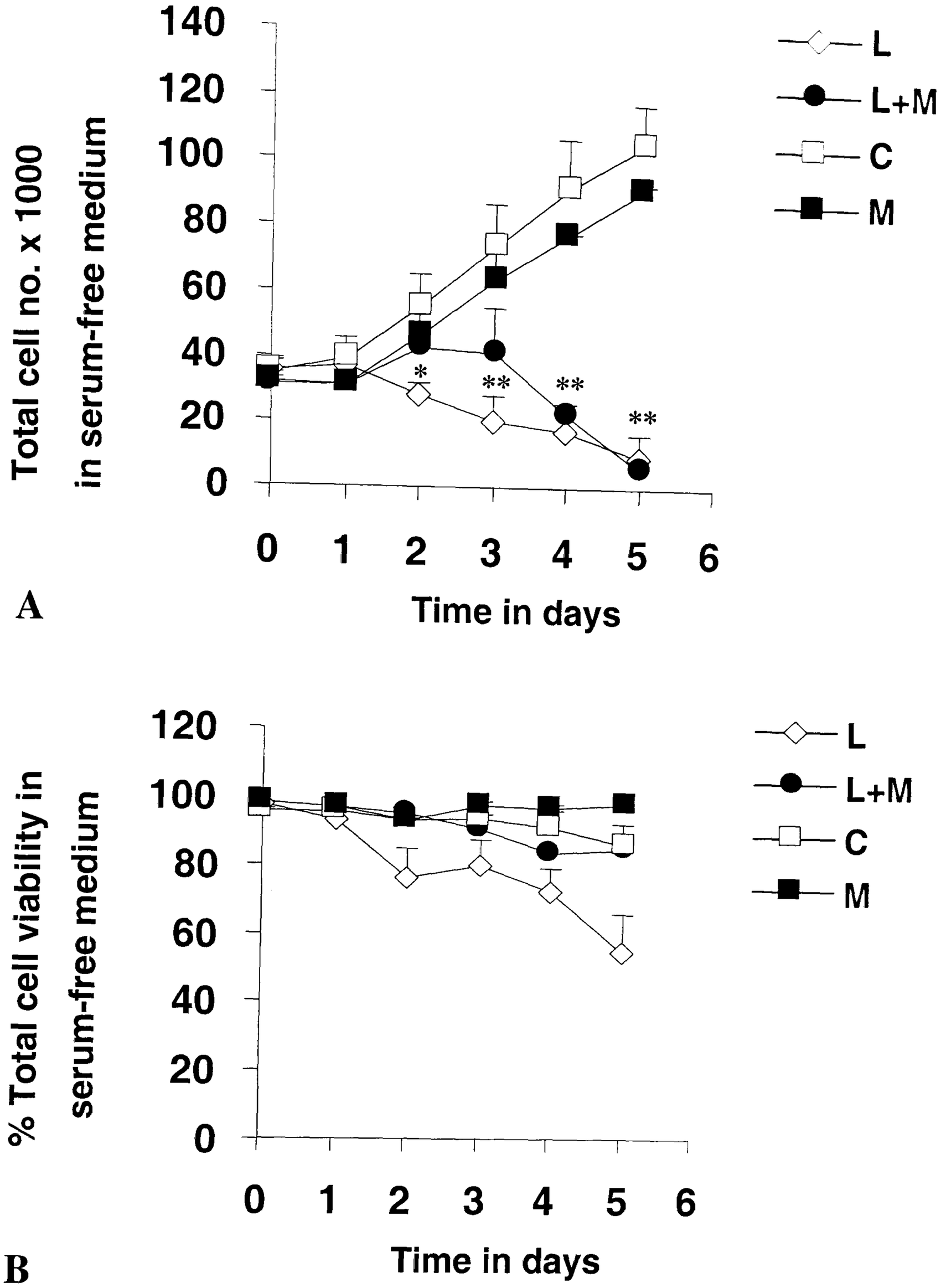


Figure 3.13 Effect of lovastatin on cell proliferation of SM1 cells in serum-free medium. Both cell proliferation and % total cell viability of SM1 cells decreased in the presence of 10μM lovastatin (L), with respect to vehicle (C) treated cultures, in serum-free medium over a 5 day period. However, there was no recovery in cell proliferation when cells were co-incubated with both lovastatin and 100μM mevalonate (L+M). All the respective treatments were replenished every day. Cell numbers were counted every day after the addition of the treatments using the Coulter Counter Z1, as described in the Materials and Methods. Percentage total cell viability was also calculated every day after both the attached and the detached cells were pooled, spun down and resuspended in a 1:1 ratio (v/v) of Trypan blue : 10% (v/v) FBS. The number of viable cells (exclusion of Trypan blue) were calculated as a % proportion of the total number of cells using the Neubauer Haemocytometer. Results represent the mean ± SEM of three separate experiments. Statistical significance was assessed by ANOVA, followed by the Tukey-Kramer multiple comparisons test, where *=$p<0.05$ and **=$p<0.01$ vs. control.

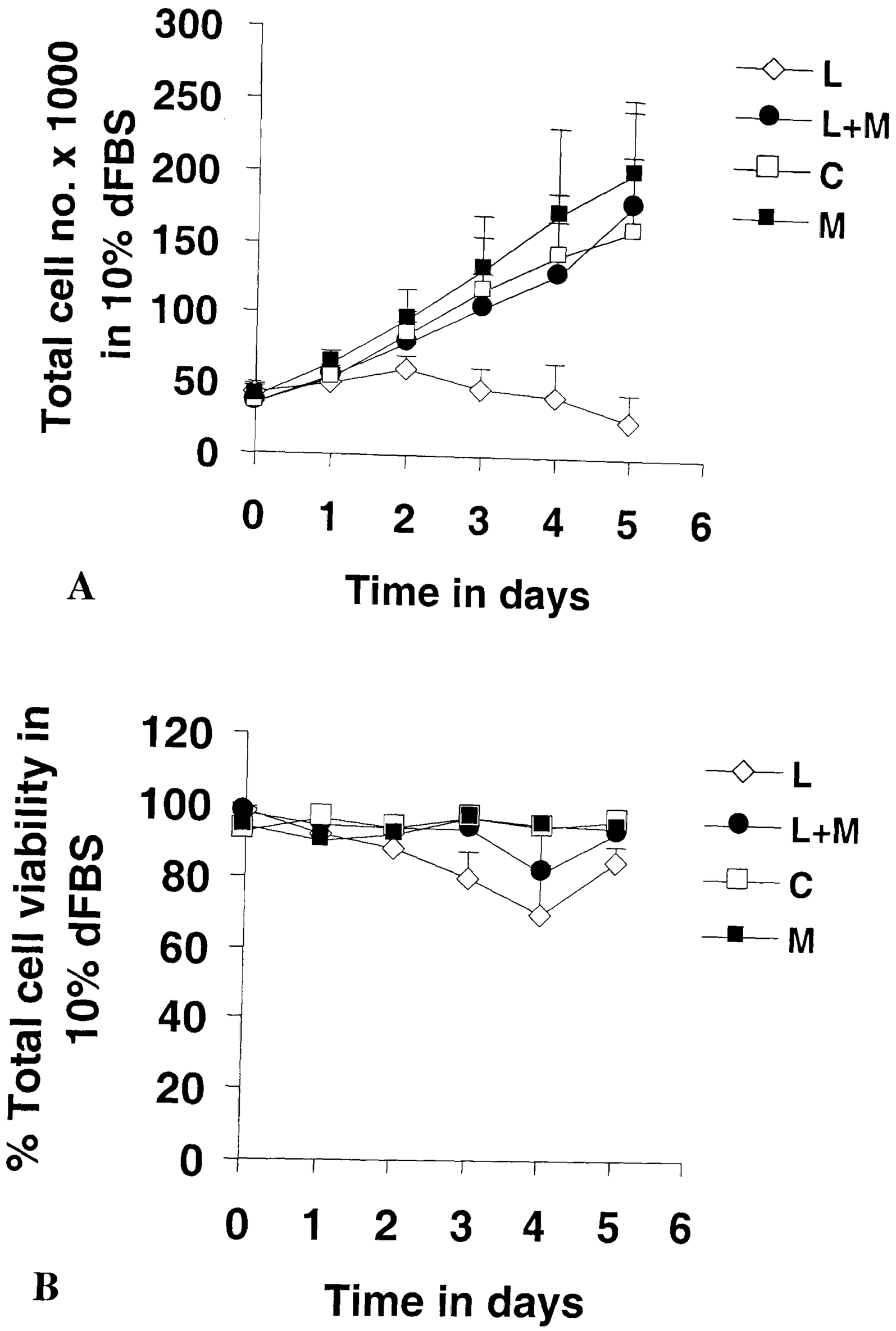


Figure 3.14 Effect of lovastatin on SM1 cell proliferation in 10% dialysed (v/v) FBS. Both cell proliferation and % total cell viability of SM1 cells in 10% dialysed (v/v) FBS was decreased, in a time-dependent manner, in the presence of 10μM lovastatin (L), with respect to vehicle (C) treated cells over a 5 day period. However, both were recovered in the presence of lovastatin and 100μM mevalonate (L+M). The respective treatments were replenished everyday. Cell numbers were counted every day after the addition of the treatments using the Coulter Counter Z1, as described in the Materials and Methods. Percentage total cell viability was also calculated every day after both the attached and the detached cells were pooled, spun down and resuspended in a 1:1 ratio (v/v) of Trypan blue : 10% (v/v) FBS. The number of viable cells (exclusion of Trypan blue) were calculated as a % proportion of the total number of cells using the Neubauer Haemocytometer. Results represent the mean ± SEM of three separate experiments. Statistical significance was assessed by ANOVA.

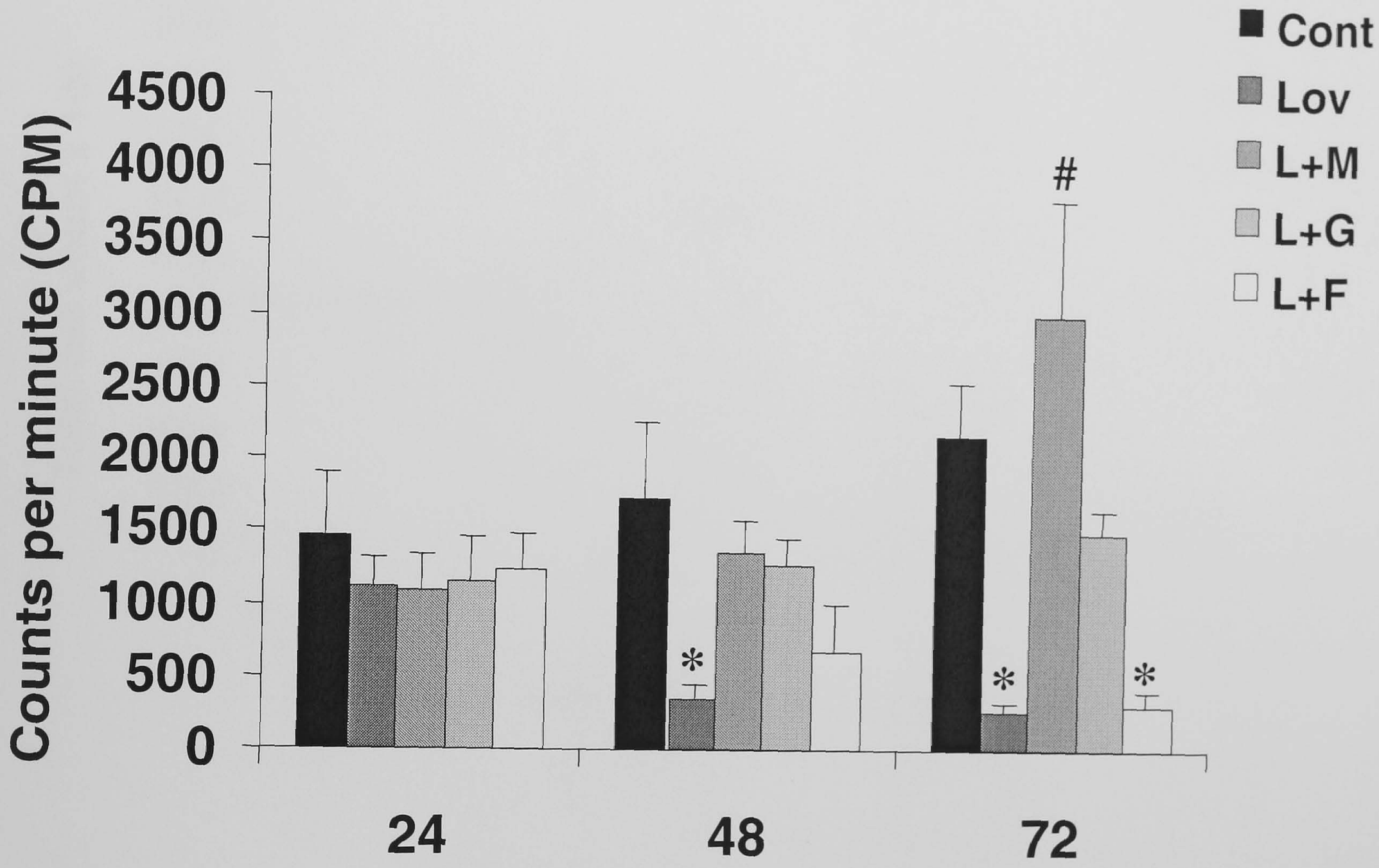


Figure 3.15 Lovastatin-induced inhibition of [^{3}H] thymidine incorporation is reversed in the presence of mevalonate (100μM) or geranylgeranyl pyrophosphate (10μM). [^{3}H] thymidine incorporation was decreased, in a time-dependent manner, with respect to the control, vehicle (C) wells, in SM1 cells treated with 10μM lovastatin (L) at 48 hours. Recovery of thymidine incorporation was seen in the presence of lovastatin and mevalonate (L+M), lovastatin and geranylgeranyl pyrophosphate (L+G), but not in the presence of lovastatin and farnesyl pyrophosphate (L+F) in 10% dialysed (v/v) FBS after 48 hours. Results represent the mean ± SEM of four separate experiments. Statistical significance was assessed by ANOVA, followed by the Tukey-Kramer multiple comparisons test, where *=$p<0.05$ vs control and #=$p<0.01$ vs lovastatin.

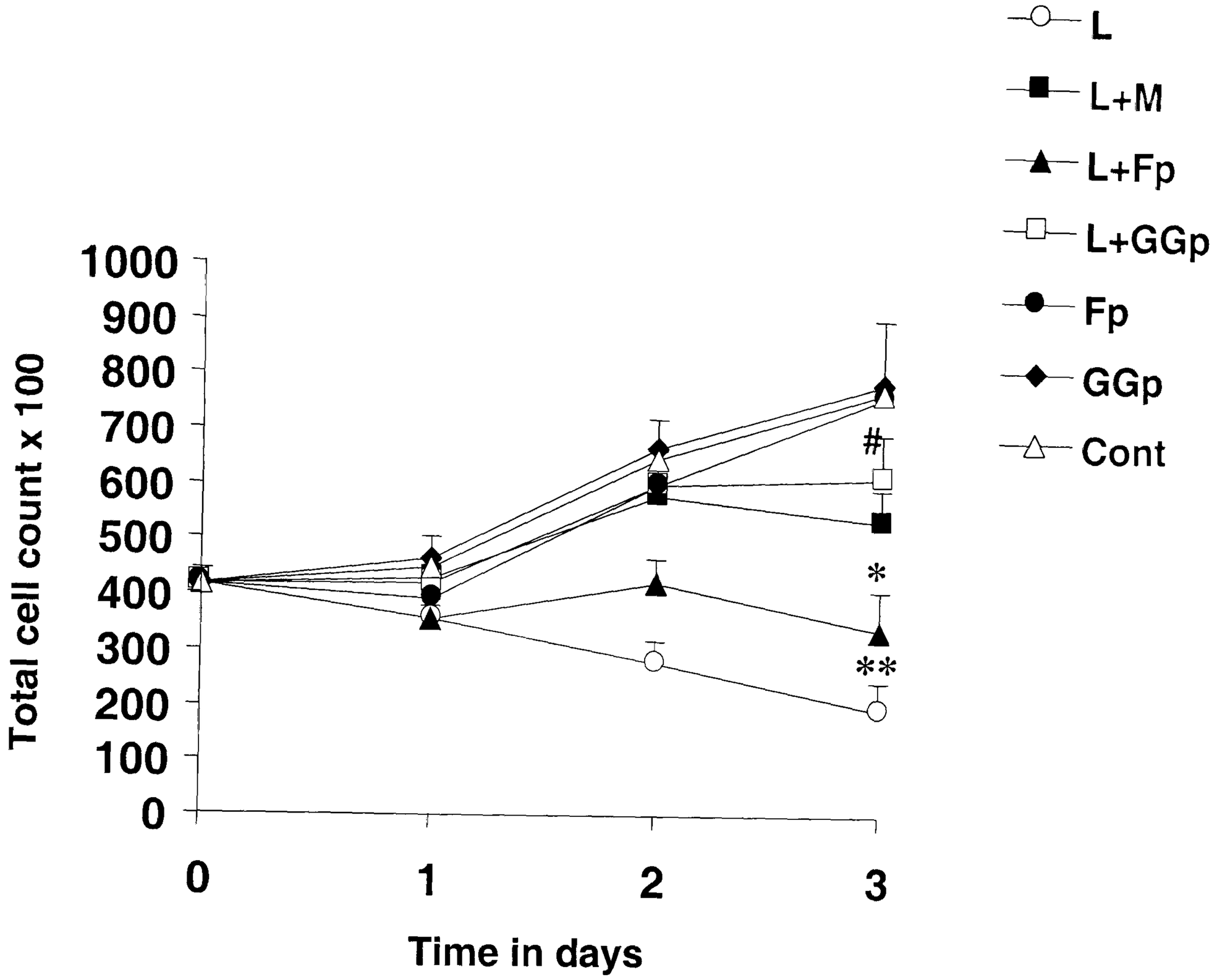
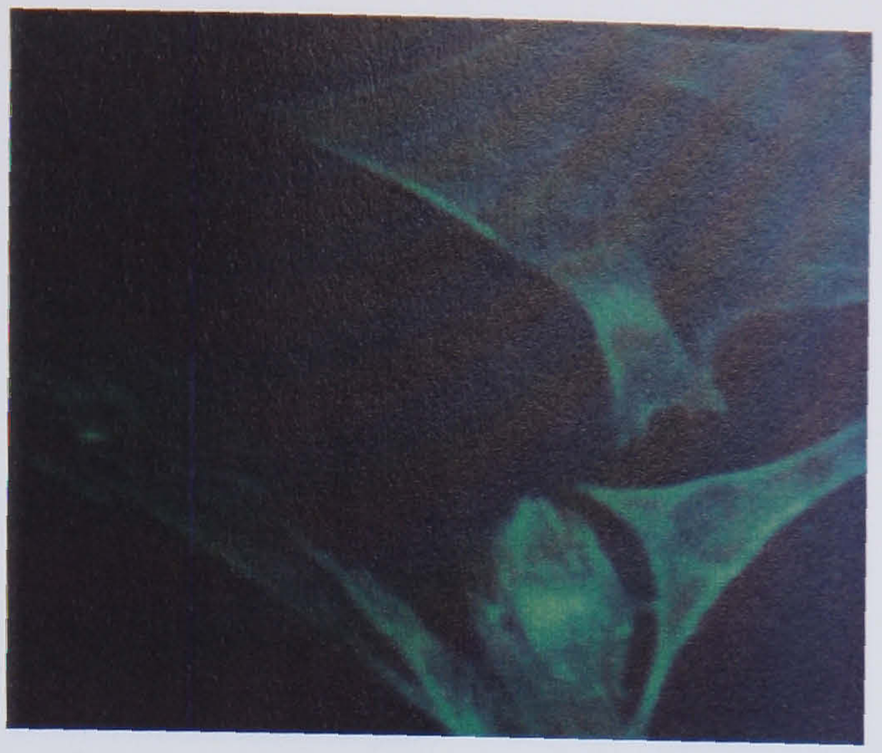
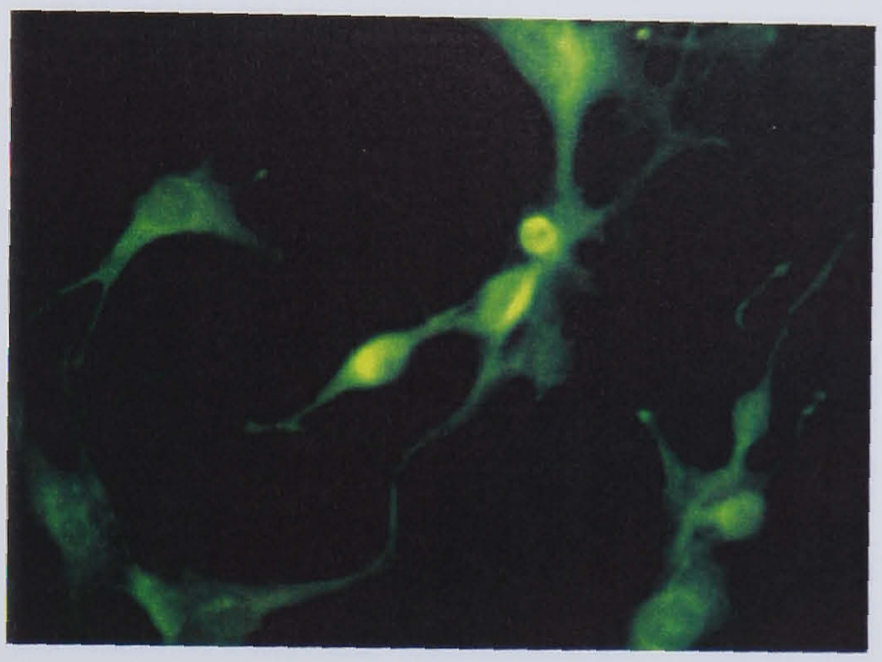


Figure 3.16 Effect of mevalonate, geranylgeranyl or farnesyl pyrophosphate on lovastatin-induced inhibition of cell proliferation. Cell proliferation was inhibited, in a time-dependent manner, in the presence of lovastatin (L, 10mM) in serum-free medium. This inhibition was reversed when lovastatin treated cells were co-incubated with mevalonate (M, 100μM) or geranylgeranyl pyrophosphate (Gpp, 10μM). Co-incubation with farnesyl pyrophosphate (Fpp, 10μM), however, did not lead to a significant degree of recovery from lovastatin-induced inhibition of cell proliferation. Results indicate mean ± SEM from three separate experiments. Statistical significance was assesed by ANOVA, followed by the Tukey-Kramer multiple comparisons test, where *=$p<0.05$, **=$p<0.01$ vs control and #=$p<0.05$ vs lovastatin.

A



B



C

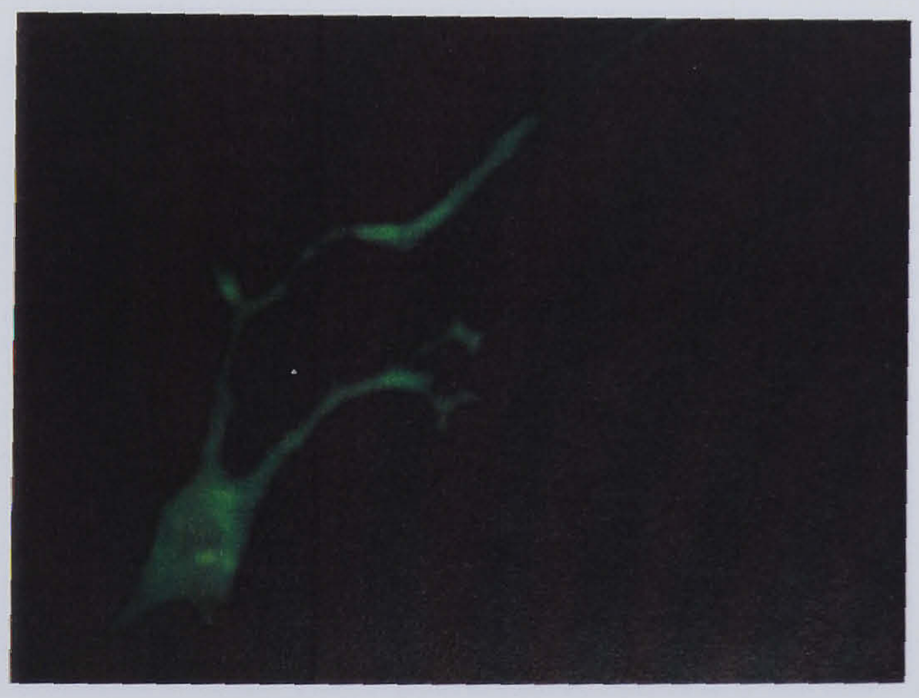


Figure 3.17 Time-dependent effect of lovastatinon the actin cytoskeleton in SM1 cells.
Changes in the actin cytoskeleton associated with lovastatin-treated SM1 cells. Fluorescence photomicrographs of Phalloidin stained SM1 cells that have been treated with vehicle for **A)** 72 hours and lovastatin (10μM) for **B)** 24 hours and **C)** 72 hours (original magnification x 400). After incubation for the respective period of time, the cells were washed with PBS and fixed in 100% absolute ethanol. The cells were then exposed to TRITC labeled Phalloidin, to reveal the organisation of the F actin cytoskeleton.

3.1.1.3 Discussion

The results presented in this chapter show for the first time that lovastatin, an HMG-CoA reductase inhibitor, promotes apoptosis, as assessed by flow cytometry, cytochemical staining, and gel electrophoresis of the extracted DNA, in an SV-40 large T antigen transformed human VSM cell line, termed SM1 cells. The same drug was associated with a marked inhibition of cell proliferation in serum-free medium, and a marked decrease in serum-stimulated DNA synthesis.

Mevalonate has been shown to be essential for cell proliferation of several cell types, including that of VSM cells (**Habenicht A J et. al., 1980; Falke P et. al, 1989**). Lovastatin has recently been shown to lead to apoptosis in VSM cells derived from other species (**Stark WW Jr, et. al., 1998; Guijarro C et. al., 1998**). Another "statin", atorvastatin, was also associated with apoptosis in stimulated rabbit SM cells (**Baetta R et al., 1997**).

A certain number of non-sterol isoprenoid compounds, along with cholesterol are derivatives of mevalonate: ubiquinone, and isopentenyladenine as well as farnesyl pyrophosphate and geranylgeranyl pyrophosphate. Although ubiquinone is known to be essential for respiration as part of the electron transport chain found in mitochondria (**Stryer L, 1995**), and isopentenyladenine is incorporated into some transfer-RNAs (tRNAs) (**Goldstein J L and Brown M S, 1990**), replenishing these compounds to lovastatin treated cultures does not seem to affect the degree of apoptosis in these cells, with respect to those treated with lovastatin alone (**Figure 3.11**). The reduced synthesis of these compounds is unlikely to be the reason for lovastatin-induced effects on SM1 cells, probably because relatively large cellular pools of these products are found in most eukaryotic cells (**Goldstein J L and Brown M S, 1990**). Although a similar observation in the presence of these compunds was confirmed indirectly in terms of morphology changes in Swiss 3T3 cells due to compactin (**Schmidt R A et. al., 1982**), it had not been measured in terms of their effects on apoptosis due to an HMG-CoA reductase inhibitor. Likewise, cholesterol, the main end-product of the mevalonate metabolic pathway, was shown to be required for cell membrane synthesis (**Cheng S et. al., 1979**). However, when cholesterol was

added in serum-free medium to mevalonate deprived SM1 cells, lovastatin-induced apoptosis was not prevented in these cells.

Members of the Ras superfamily of small GTPases such as K-Ras (**Rowell CA et. al., 1997**), H-Ras (**Hancock J F et. al., 1989**) and N-Ras, are known to be involved in the control of signalling pathways determining cell fate. Although these proteins are normally farnesylated *in vitro*, they have been demonstrated to be geranylgeranylated *in vitro* under some circumstances, through a geranylgeranyl transferase (GGPTase) (**Zhang F L et. al., 1997**). Whether this also takes place *in vivo*, and under which circumstances, is unknown, as well as what the direct consequences of this post-translational modification may be on cell growth and the determination of cell fate.

Under the conditions of the experiments used by us, it is unknown whether the farnesylation of Ras proteins is affected when SM1 cells are treated with lovastatin. Whether modification of Ras proteins is affected by lovastatin will depend on the size of the endogenous farnesyl pyrophosphate pool, and the rate of turnover or new synthesis of Ras proteins, since only the function of newly sythesised Ras protein will be affected by inhibition of isoprenylation. As a result, the above may be one of the reasons why co-incubation of lovastatin treated cells in serum-free medium with farnesyl pyrophosphate did not have a significant effect on lovastatin-induced changes (**Figure 3.11, 3.12, 3.15, 3.16**). In contrast, co-incubation of lovastatin treated cells with geranylgeranyl pyrophosphate resulted in a recovery from lovastatin-induced apoptosis, DNA synthesis and cell proliferation (**Figure 3.11, 3.15 and 3.16**). A reason for the latter result is consistent with evidence from other studies that the labelling of the 21-28 kDa proteins with the [^{3}H] geranylgeranyl pyrophosphate was far greater than their labelling with [^{3}H] farnesyl pyrophosphate (**Danesi R et. al., 1995**), indicating that the post-translational modification requirement for these proteins with this moiety was far greater than for the latter. Depletion of this isoprenoid would probably have dramatic consequences on the processes that may depend on it. Equally, co-incubation of lovastatin treated cells with mevalonate led to a decrease in apoptosis by 46+/-2%, while co-incubation with 10μM geranylgeranyl pyrosphate led to a decrease in apoptosis by 29.5±2.5% (**Figure 3.11**). These results

indicate that the protective effects of mevalonate are largely or wholly mediated via the geranylgeranyl isoprenoids.

These results also indicate that depletion of geranylgeranyl isoprenoids severely undermines the survival and hence the cell proliferation signalling processes in these cells. Treatment of neonatal rat skeletal muscle cells with lovastatin for more than 8 hours has been shown to lead to depletion of both the farnesyl and the geranylgeranyl isoprenoid pools (**Flint OP et. al., 1997**). Whether the level of the farnesyl isoprenoid in SM1 cells is also decreased is unknown, but if any changes have taken place, they do not seem to affect the signalling processes determining cell fate in these cells. Although in the presence of farnesyl protein transferase inhibitors (FPTase), compensatory prenylation of otherwise farnesylated proteins has been shown, such that even the Ras proteins become geranylgeranylated (**Wyte DB et. al., 1997**), it is still unknown whether the same changes are taking place in the presence of lovastatin. However, when geranylgeranyl isoprenoids become depleted, the demand for them cannot be substituted through an alternative modification (**Danesi R et. al., 1995**). These data are in agreement with the results obtained by **Flint O P et. al., 1997**, who found that [^{3}H]geranylgeranyl pyrophosphate incorporation was similar in the presence or in the absence of the HMG-CoA reductase inhibitor, again suggesting the constant need for geranylgeranylation at all times in rat muscle cells. Hence, one can conclude from these observations that only the end-products of the mevalonate pathway with the highest rate of turnover (geranylgeranyl pyrophosphate) will become affected as a result of a block in endogenous mevalonate synthesis.

Other workers have obtained similar results with respect to the effect of geranylgeraniol. For example, **Corsini A et. al., 1993** showed that cell proliferation inhibited due to a HMG-CoA reductase inhibitor, simvastatin, in arterial myocytes was largely recovered when there was co-incubation with geranylgeraniol and/or mevalonate and to some extent, with farnesol. In **1997, McGuire TF and Sebti SM** reported that addition of geranylgeraniol prevented lovastatin-induced cytotoxicity in H-Ras transformed cells. In C6 glioma cells, addition of geranylgeraniol was shown to overcome the block in cell proliferation and DNA synthesis induced by lovastatin (**Crick DC et. al., 1998**). Entry into the cell cycle of UT-2 cells, a mutant clone of Chinese hamster ovary cells deficient in HMG-CoA reductase, in the absence of mevalonate was shown to be promoted in the presence of geranylgeraniol, (**Crick D**

C et. al., 1997). However, very little cell proliferation was observed when the culture medium was supplemented with farnesol. Similarly, geranylgeranyl pyrophosphate but not farnesyl pyrophosphate was required to restore the inhibitory effects of pravastatin, another HMG-CoA reductase inhibitor, in human peripheral blood mononuclear cells (PBMC) on cell cycle progression and DNA synthesis (**Tatsuno I et. al., 1997**).

Recent studies have indicated that the geranylgeranylated proteins Rho, Rac and Cdc42 may be important in cell-cycle progression (**Olson M F et. al., 1995**). Based on these results, **Olson M F et. al, 1995** have in fact proposed that activation of c-jun N-terminal kinase (JNK) through Ras may be mediated through Rac, a geranylgeranyl modified protein. Work by **Hirai A et. al., 1997**, showed that geranylgeranylated small Rho GTPases were essential for the degradation of another cyclin-dependent kinase inhibitor, p27Kip, to facilitate the progression from G_1 to S phase in growth-stimulated rat FRTL-5 cells. In their experiments, pravastatin, an HMG-CoA reductase inhibitor, was shown to lead to the accumulation of this protein, and to growth arrest. However, addition of geranylgeranyl pyrophosphate, but not farnesyl pyrophosphate, was associated with the degradation of the protein, and entry into S phase. Treatment of NIH3T3 cells either with lovastatin or with a GGTase I inhibitor (GGTI-298) was shown to lead to G_0/G_1 phase arrest (**Vogt A et. al., 1996**). Furthermore, lovastatin-induced block in G_0/G_1 was released upon co-incubation with mevalonate and was reversed upon co-incubation with GGTI-298, but not with the farnesyl transferase inhibitor, FTI-277 (**Vogt A et. al., 1996**). The geranylgeranylated Rho proteins have additionally been shown to be essential for induction of another cell-cycle associated gene, cyclin E (**Tanaka T et. al., 1998**). The Rac and Cdc42 proteins were demonstrated to be potent stimulators of retinoblastoma (RT) susceptibility gene product hyperphosphorylation, required for S-phase traverse (**Gjoerup O et. al., 1998**). This also confirmed the results of **Peeper D S et. al., 1997,** who showed that Ras signalling was directly linked to the cell-cycle machinery through the retinoblastoma protein.

Our results in serum-free medium indicate that the G_o/G_1 phase of SM1 cells was not affected or inhibited in the presence of lovastatin, with respect to the untreated, control cultures (**Figure 3.7**). Likewise, under the same conditions, the percentage

proportion of S phase or G_2/M phase were not significantly affected in the presence of lovastatin. One of the reasons why neither cell cycle phase was affected due to lovastatin, may be that the depletion of mevalonate derivatives has less effect on cell growth due to the lower turnover rate of Ras proteins required for cell cycle phase transitions under these circumstances. Apoptosis, on the other hand, is more sensitive to isoprenoid depletion since it is seen very early under serum-free conditions.

Equally, the cell numbers of SM1 cell cultures co-incubated with lovastatin-and farnesyl pyrophosphate were lower with respect to the control, untreated cultures than those co-incubated with lovastatin and geranylgeranyl pyrophosphate, especially after 72 hours or more of incubation in serum-free medium (i.e. in the absence of exogenous mevalonate) (**Figure 3.16**). These results indicate that limited growth of lovastatin treated SM1 cells in the absence of exogenous mevalonate was most probably due to inadequate amounts of geranylgeranyl pyrophosphate for the isoprenylation of one or more proteins essential for survival (**Figure 3.16**). This would result in a direct decrease in cell number due to high levels of cell death under these circumstances.

When SM1 cells were treated with lovastatin in the presence of 10% (v/v) dialysed foetal bovine serum (FBS), however, a marked increase in G_o/G_1 phase resulted at 48 hours of lovastatin treatment, indicating growth arrest at this time point (**Figure 3.9**). Hence, this increase or accumulation in G_o/G_1 phase was associated with a direct decrease in the proportion of S phase (**Figure 3.9**). This result confirmed that entry into S phase was not affected at 24 hours, but there was a significant decrease by 48 hours of treatment, as was confirmed through [^{3}H] thymidine incorporation (**Figure 3.15**).

Treatment of SM1 cells with lovastatin (10μM) in 10% (v/v) dialysed FBS indicated a clear inhibition of cell growth due to lovastatin, with respect to the vehicle treated cultures (**Figure 3.14A**). However, analysis by ANOVA indicated that the difference in cell numbers between lovastatin treated and the vehicle treated cultures was not quite significant ($p=0.08$), probably due to the small sample numbers.

It has been established for some time now that direct inhibition of Ras function is associated with inhibition of smooth muscle cell proliferation, such as shown by **Indolfi C et. al., 1995**. The latter demonstrated that direct inhibition of Ras function through transdominant negative mutants resulted in inhibition of smooth muscle cell proliferation. The results of **McGuire TF and Sebti SD, 1997**, also clearly indicate that incubation of NIH3T3 cells with lovastatin for 2 days was associated with a mobility shift of the H-Ras protein, which indicates a change in its molecular weight, it was also associated with apoptosis. Co-incubation of these cells with geranylgeraniol was shown to prevent cell death, but not the shift in mobility. All these observations are consistent with the proposal that geranylgeranylated regulatory proteins play an important function in signalling pathways determining apoptosis and hence the rate of cell proliferation. However, whether the activity or the mobility of Ras proteins was inhibited in SM1 cells treated with lovastatin under the conditions we used, is unknown. Also, even if Ras activity or mobility was reduced or affected (for which we have no evidence) that reduction might be insufficient to affect Ras-dependent growth.

It is also interesting to note the significant difference in the degree of recovery in cell proliferation when cells were co-incubated with lovastatin and mevalonate under serum-free conditions. In the presence of lovastatin, there was an increase in cell numbers only for 2 days but not thereafter. This may indicate that other survival and growth factors derived from serum must be present for optimal cell proliferation, and the presence of mevalonate alone is inadequate for prevention of all of the inhibitory effects of lovastatin, even though the cultures were replenished with fresh mevalonate (100μM) every day (**Figure 3.13**). This could imply that lovastatin has actions not recoverable by mevalonate. Alternatively, there may still be a possibility that such a concentration of mevalonate may have been insufficient to complete the isoprenylation of certain proteins in the cell. In contrast, co-incubation with mevalonate was associated with prevention of lovastatin-induced inhibition of cell growth in the presence of 10% dialysed foetal bovine serum (FBS) (**Figure 3.14A**). This could be taken to indicate a reduced requirement for mevalonate under these circumstances, increased uptake or supply of mevalonate in the presence of serum, or

possibly, lack of modification for some other lovastatin inhibitable factor under these conditions.

If the isoprenylation of certain proteins crucial for cell survival and proliferation are inhibited due to inhibition of endogenous mevalonate synthesis, then it is not surprising that this will have a pleiotropic effect on many other processes within the cell. One of these changes seems to be the disappearance of filamentous (F-) actin, as reported by (**Fenton R G et. al., 1992; Seronie-Vivien S et. al., 1995**) when cells have been treated with an HMG-CoA reductase inhibitor. Our observations suggest that the collapse of the actin architecture seems to occur at around the same time-period, as the morphological manifestations of apoptosis (**Figure 3.17**). Likewise, the association of actin cytoskeleton breakdown with apoptosis induced by other agents has been reported by other workers (**Rufini S et. al., 1997**), and appears to be a general manifestation of cells undergoing apoptosis. Interestingly, proteolytic cleavage of actin fibre proteins during apoptosis was reported by (**Brown SB, et. al., 1997; Guenal I et. al., 1997**). Likewise, another group reported a marked decrease in the amount of F-actin, as measured by flow cytometry, in apoptotic human leukemia cells (**Endresen P C et. al., 1995**).

Although lovastatin-induced morphological changes were reversed when cells were co-incubated with mevalonate, this has been associated with a rapid repolymerisation of the actin cytoskeleton (**Fenton RG et. al., 1992**). A breakdown in the actin framework may be due to the inhibition of certain isoprenylated proteins, but it may also be associated with, or be a characteristic of the apoptotic morphology itself. Evidence from the literature suggests Rho proteins may be required for the appropriate organisation of the cytoskeleton under different circumstances. For example, lovastatin-treated, rounded up Swiss NIH3T3 cells reverted back to a flat morphology when microinjected with dominant active RhoA (Val14RhoA) (**Koch G et. al., 1997**), while addition of *Escherichia coli* cytotoxic necrotizing factor (CNF1) to the cells, known to lead to activation of Rho proteins, was associated with flattening of round, lovastatin treated NIH 3T3 cells.

A reorganisation of the actin cytoskeleton was shown to be required for early cell membrane blebbing seen during apoptosis (**Huot J et. al., 1998**). This was shown to

be regulated through the Rho proteins as well, such that the *Clostridium botulinum* exoenzyme C3 transferase which ADP ribosylates and inhibits Rho led to inhibition of apoptotic cell membrane blebbing (**Mills J C et. al., 1998**). However, interestingly, direct disruption of the cytoskeleton was associated with an inhibition of the blebbing process (**Mills J C et. al., 1998**), suggesting a more complex role for Rho in blebbing associated with apoptosis. In view of these findings, it seems plausible to suggest that at least part of the action of lovastatin in SM1 cells may involve inhibition of geranylgeranylation of Rho proteins accounting for disruption of actin cytoskeleton and possibly increased apoptosis.

In conclusion, the results presented in this chapter indicate that certain, specific proteins dependent, possibly on isoprenylation with a geranylgeranyl moiety, are required for the survival and cell proliferation of transformed human VSM cells in culture.

Chapter 4

Action of perillyl alcohol on cell proliferation and apoptosis in SV-40 transformed human VSM cells in culture

4.1.1.1 Introduction

Perillyl alcohol (**Figure 4.1**) is a simple monoterpene compound, found naturally in the oil of citrus fruit peel (**Crowell PL, 1997**). It has been used as an antitumour agent against many pre-neoplastic cancer types, such as mammary cancers in rodents (**Haag J D et. al., 1994**). Recently, it has been used in phase I clinical trials in patients with advanced malignancies (**Ripple GH et. al., 1998**). The chemopreventative action of perillyl alcohol toward liver and colon tumours was shown to be mediated through apoptosis (**Mills J J et. al., 1995; Reddy BS et. al., 1997**). Additionally, it has been associated with cell cycle inhibition in G_1 phase and prevention of S phase entry in lymphocytes (**Schulz S et. al., 1994**). Recently, oral perillyl alcohol administration in a rabbit model was shown to be effective in the reduction of vein graft intimal hyperplasia (**Fulton G J et. al., 1997**).

The molecular mechanism of action of this drug was found to include inhibition of protein isoprenylation, through the inhibition of prenyl transferases (**Crowell PL et. al., 1994; Gelb MH et. al., 1995**). It is interesting to note that the action of the drug was very selective, such that proteins with a molecular weight between 20-26 kDA seemed to be preferentially affected, indicating that Ras-related small GTPases are the primary targets (**Crowell P L et. al., 1994**). Recently, perillyl alcohol was shown to inhibit geranylgeranyl transferases relatively selectively in NIH3T3 cells (**Ren Z et al., 1997**), while another group of workers showed that protein farnesyl transferase (FPTase) was not inhibited by monoterpenes *in vivo* (**Hohl R J and Lewis K, 1995**).

In chapter 3 it was shown that geranylgeranyl pyrophosphate, but not farnesyl pyrophosphate, was required for the prevention of apoptosis and promotion of cell proliferation in lovastatin treated SM1 cells. In this chapter, we show that perillyl alcohol also leads to inhibition of cell proliferation and promotion of apoptosis in these cells. However, this effect of perillyl alcohol was not recovered with geranylgeranyl pyrophosphate (GGpp) nor with farnesyl pyrophosphate (Fpp), as would be anticipated if this agent acts as a prenyl transferase inhibitor.

4.1.1.2 Results

4.1.2.2 Effect of perillyl alcohol on SM1 cell proliferation, DNA synthesis and cell viability

To evaluate the effect of perillyl alcohol on cell proliferation, SM1 cells were treated with a range of concentrations between 0-3mM in 10 % (v/v) FBS for 3 days at each concentration. There was a dose-dependent and time-dependent decrease in cell numbers. Cell numbers decreased significantly from $13.7x10^3 \pm 360$ in control cultures to $8.1x10^3 \pm 5.7x10^3$ cells in cultures treated with 2mM perillyl alcohol after 3 days ($p=0.005$, $n=3$) (**Figure 4.2**). However, treatment of cells with 3mM perillyl alcohol appeared to have a cytotoxic effect, resulting in almost no detectable cells by 24 hours after exposure. 2mM perillyl alcohol was not associated with such an effect and appeared to be the maximum concentration of this agent that can be used with these cells.

Percentage total cell viability estimated by Trypan Blue exclusion assay also decreased significantly by 38±3% ($p=0.05$, $n=3$) from 91±1% in control cultures to 56.5±3.5% in cultures at 48 hours after exposure to 2mM perillyl alcohol (**Figure 4.3**).

There was no significant dose-dependent decrease in thymidine incorporation after 24 hours of exposure to perillyl alcohol (concentrations between 0-2mM). However, there was a significant dose-dependent decrease in thymidine incorporation after 48 hours of exposure to perillyl alcohol. Counts decreased by 66.5±12.5% from 1592±59 cpm at 0mM perillyl alcohol to 547±219 cpm at 2mM of perillyl alcohol, after 48 hours ($p=0.01$, $n= 3$) (**Figure 4.4**).

4.1.2.3 Effect of perillyl alcohol-induced changes in apoptosis and the cell cycle phases in SM1 cells

Since there was a significant decrease in SM1 cell viability after treatment with perillyl alcohol, but an insignificant effect on DNA synthesis (after 24 hours of

treatment with 2mM perillyl alcohol), we hypothesised that inhibition of cell growth due to this drug may be accounted for by the stimulation of apoptosis.

Perillyl alcohol at a concentration of 2mM was used to evaluate whether there is any apoptosis in the cell cultures, since this concentration resulted in a marked decrease in the rate of cell growth and was not overtly toxic. Treatment with 2mM perillyl alcohol in 10% (v/v) FBS for 24 hours was associated with cell rounding, increased granularity, and detachment from the petri dish substratum and surrounding cells, as assessed by light microscopy (**Figure 4.5**).

Staining with the DNA-binding fluorescent dye, DAPI and also with the TUNEL reagent revealed that perillyl alcohol treatment was associated with genomic DNA condensation and fragmentation, characteristic of apoptosis (**Figure 4.6 and Figure 4.7**).

To quantitate the degree of apoptosis induced in the cells, the cell DNA content was assessed using flow cytometry (FACS). SM1 cells were treated with 2mM perillyl alcohol in 10% (v/v) FBS and harvested after 24 and 48 hours for FACS analysis. There was a significant increase in the proportion of the hypodiploid region, characteristic of apoptosis, by 261±67% of control, from 12±5% ($p=0.01$, $n=3$) in control cultures to 28±5% in cultures treated with perillyl alcohol after 48 hours (**Figure 4.8**).

We also assessed the time-dependent changes in the DNA content of each cell cycle phase with FACS analysis, using the SOBR algorithm (see Materials and Methods). The same cell cultures were treated as discussed above, and analysed through flow cytometry. There was a significant decrease ($p=0.04$, $n=4$) in G_o/G_1 phase by 11±2% from 75±3% in control cultures to 67±1% in perillyl alcohol treated cultures at 48 hours (**Figure 4.9**). There was no significant difference in S phase between the perillyl alcohol treated cultures at 48 hours and the control cultures at 48 hours. There was also no significant change in G_2/M phase after 48 hours of treatment with perillyl alcohol, with respect to control cultures (**Figure 4.9**).

A time-dependent increase in hypodiploid cell DNA content was also associated with the appearance of DNA fragmentation into multiples of 180-200bp bands upon agarose gel electrophoresis, constituting a typical "laddering" pattern characteristic of apoptosis (**Figure 4.10**).

To evaluate which of the isoprenoids may have become depleted and hence whether there will be any recovery (or prevention) of perillyl alcohol-induced apoptosis, perillyl alcohol treated cells were co-incubated with geranylgeranyl pyrophosphate (GG) or with farnesyl pyrophosphate (F) alone. There was no significant difference in levels of hypodiploid DNA content in cultures co-incubated with the isoprenoid pyrophosphates (Poh+GG or Poh+F) compared to cultures treated with perillyl alcohol alone. This was in direct contrast to lovastatin-induced apoptosis, where co-incubation of lovastatin with geranylgeranyl pyrophosphate led to a significant decrease in the levels of apoptosis (**Figure 4.11**).

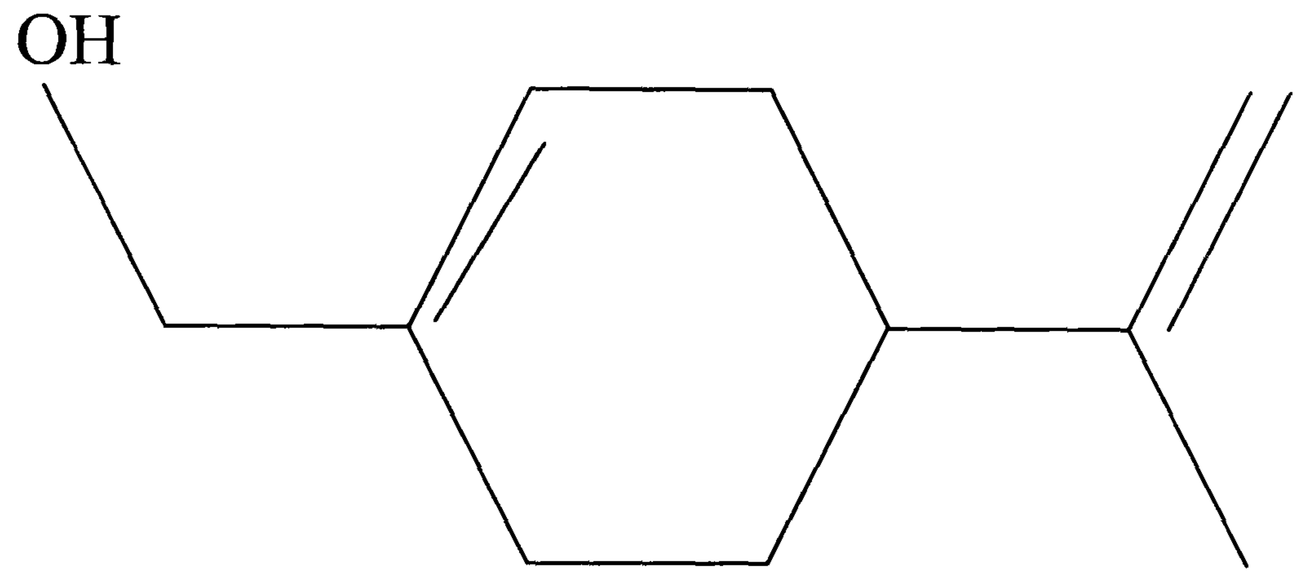


Figure 4.1 The schematic stick representation of the chemical structure of perillyl alcohol.

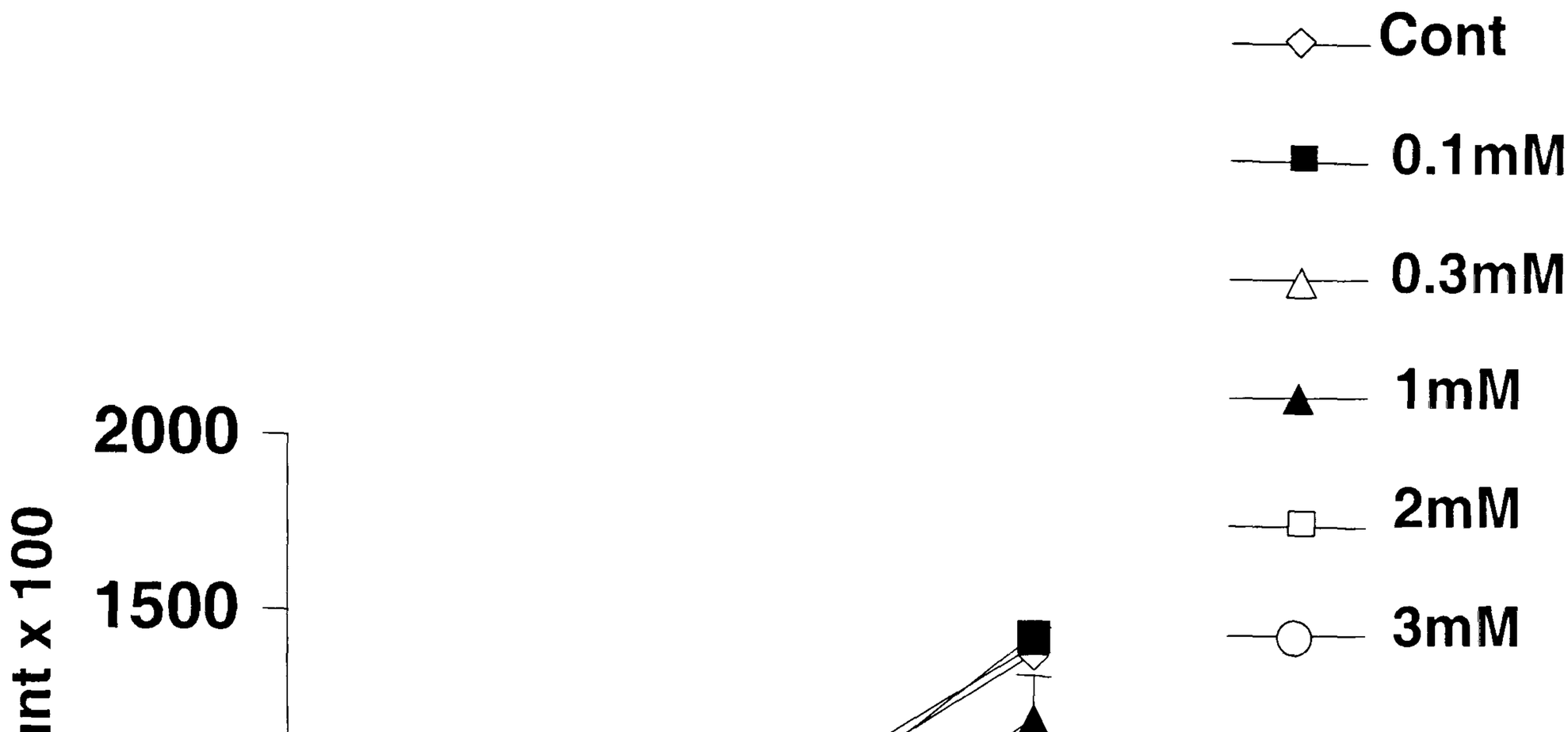


Figure 4.2 Dose- and time-dependent effect of perillyl alcohol on cell proliferation in SM1 cells. Exponentially growing SM1 cells were exposed to increasing concentrations of perillyl alcohol in 10 % (v/v) FBS from 0, 0.1, 0.3, 1, 2, and 3mM for upto 3 days at each concentration, and the cell numbers were counted with the Coulter Counter Z1 each day. Cell proliferation decreased progressively in perillyl alcohol treated cultures, but there was optimal growth in untreated cultures over the same time period. Results represent the mean±SEM of three separate experiments. Statistical significance was assessed by ANOVA, followed by the Tukey-Kramer multiple comparisons test, where **=$p<0.01$ vs control.

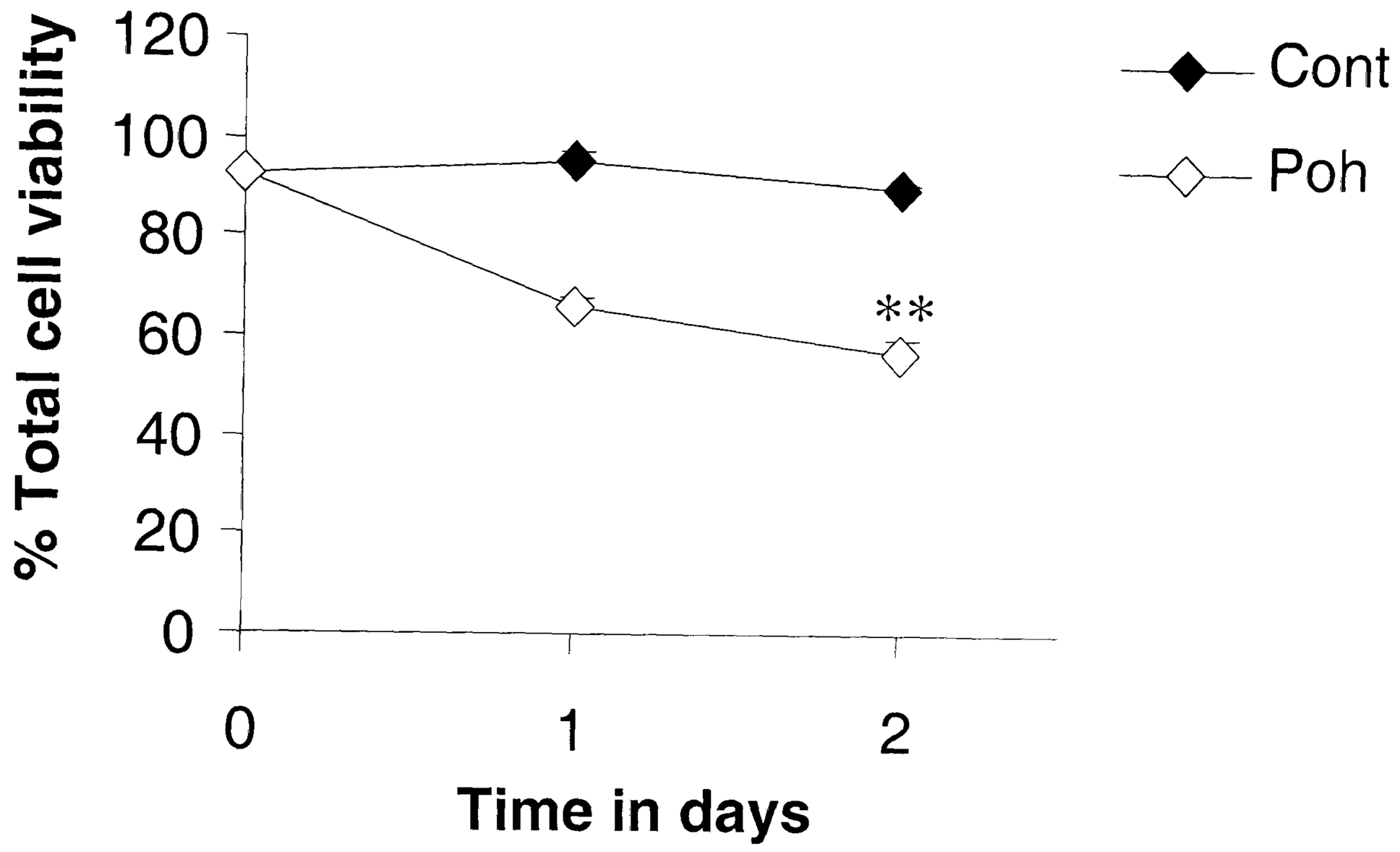


Figure 4.3 Effect of perillyl alcohol on % total cell viability in SM1 cells. Exponentially growing SM1 cells were exposed either to 2mM perillyl alcohol (Poh) or to control (Cont), regular 10% (v/v) FBS for 2 days. Percentage total cell viability was calculated every day after both the attached and the detached cells were pooled, spun down and resuspended in a 1:1 ratio (v/v) of Trypan blue : 10% (v/v) FBS. The number of viable cells (exclusion of Trypan blue) were calculated as a % proportion of the total number of cells using the Neubauer Haemocytometer. Results represent the mean ± SEM of three separate experiments. Statistical significance was assessed by the Student`s t test, where **=$p<0.01$vs control.

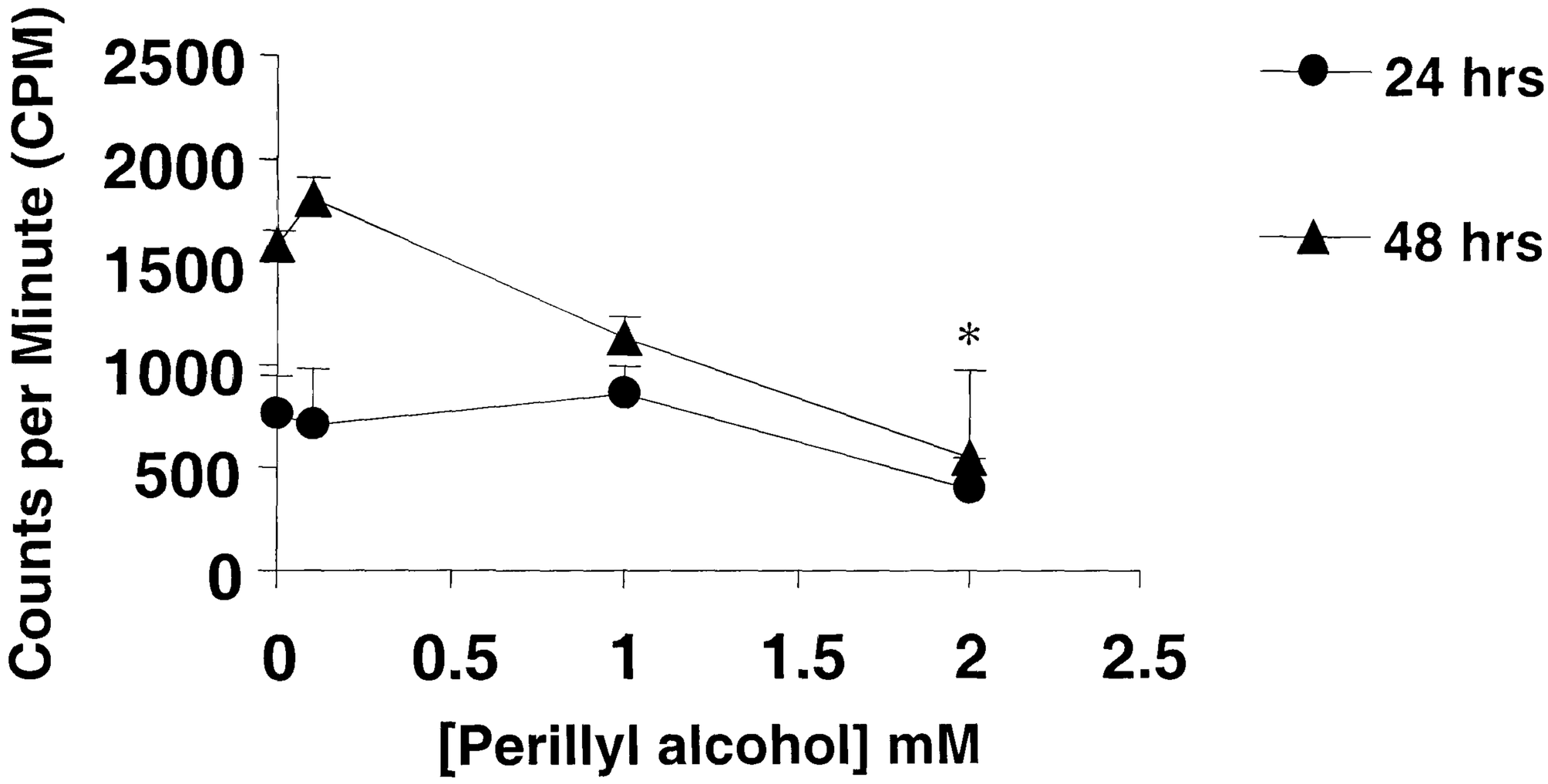
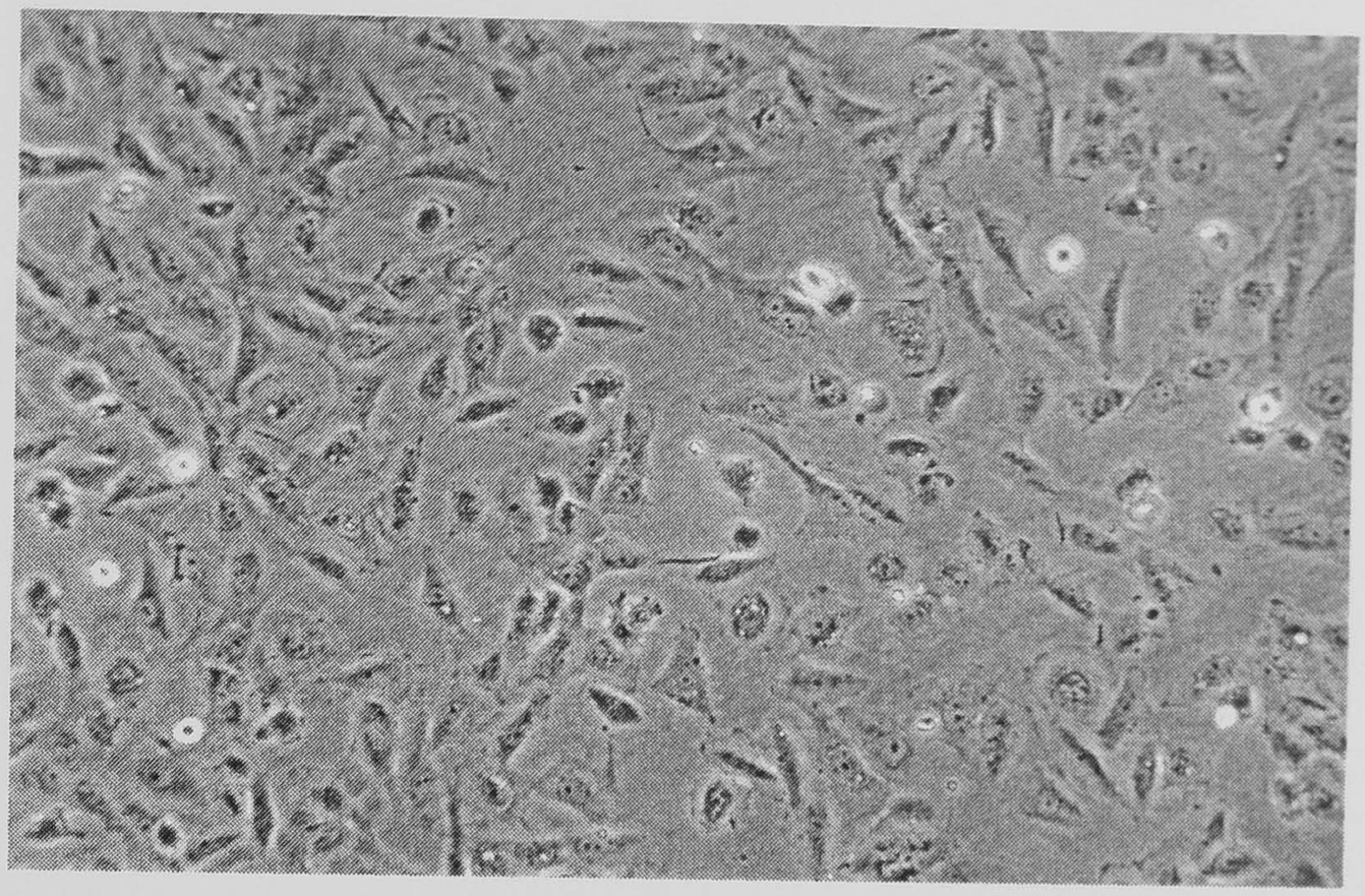
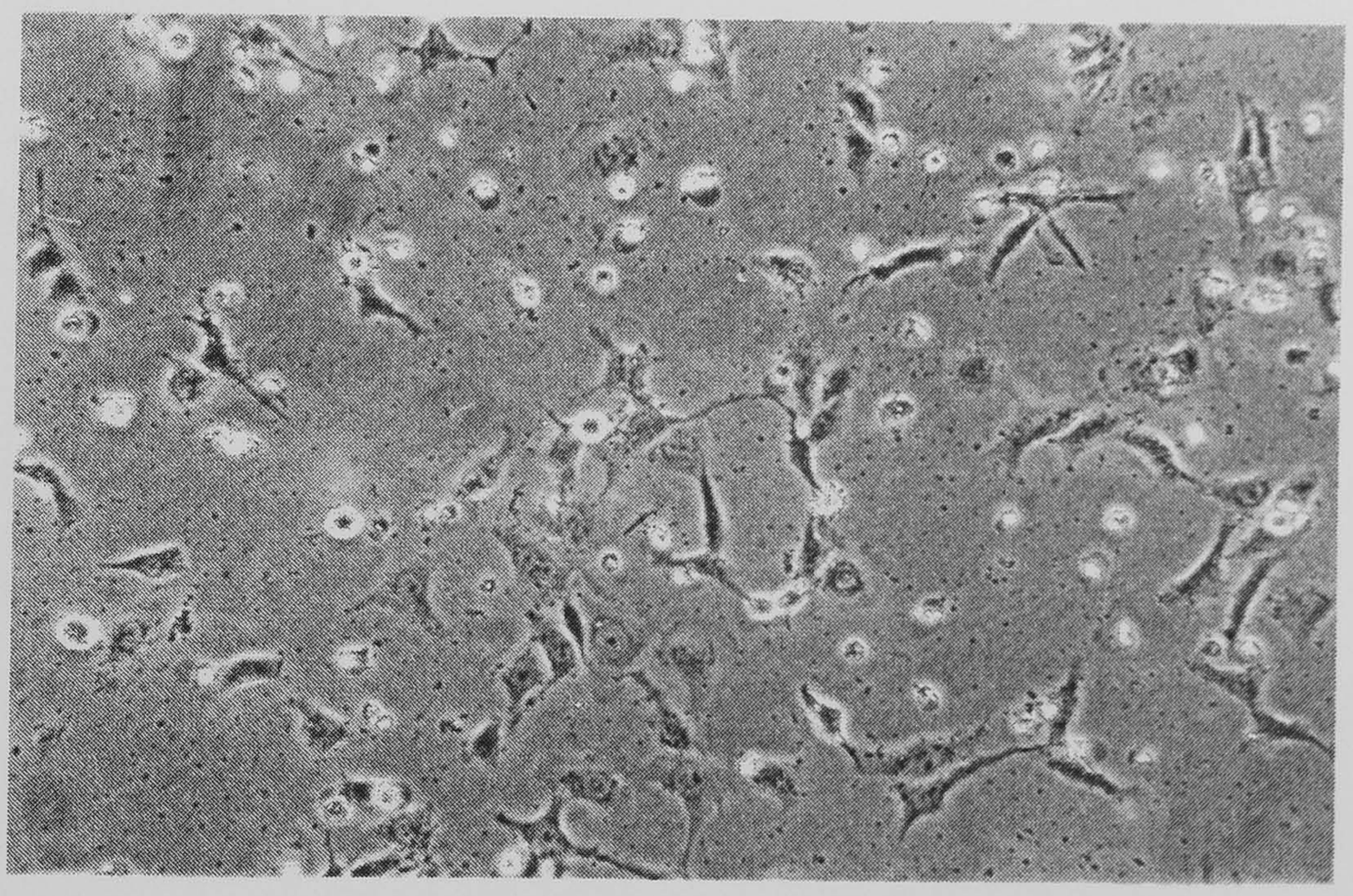


Figure 4.4 Dose-dependent effect of perillyl alcohol on [^{3}H] thymidine incorporation in SM1 cells. Exponentially growing SM1 cells were exposed to increasing concentrations of perillyl alcohol (0, 0.1, 1, and 2mM), and thymidine incorporation was measured either after 22 or 44 hours (24 and 48 hours, respectively) of treatment with the respective concentration of perillyl alcohol in 10% (v/v) FBS. The cells were pulsed with [^{3}H] thymidine for 4 hours. The results represent the mean±SEM of three separate experiments. Statistical significance was assessed by ANOVA, followed by the Tukey-Kramer multiple comparisons test, where *=$p<0.05$ vs 0mM perillyl alcohol at 48 hours.



A



B

Figure 4.5 Morphological effects of perillyl alcohol in SM1 cells in culture. Light microscopy photomicrographs of perillyl alcohol-treated SM1 cells, indicating common morphological features of apoptosis, such as barely attached or floating, rounded up cells with condensed cytoplasm **A**) SM1 cells in the absence of any treatment, in 10% (v/v) FBS **B**) after 48 hours of treatment with 2mM perillyl alcohol (original magnification x100, respectively).

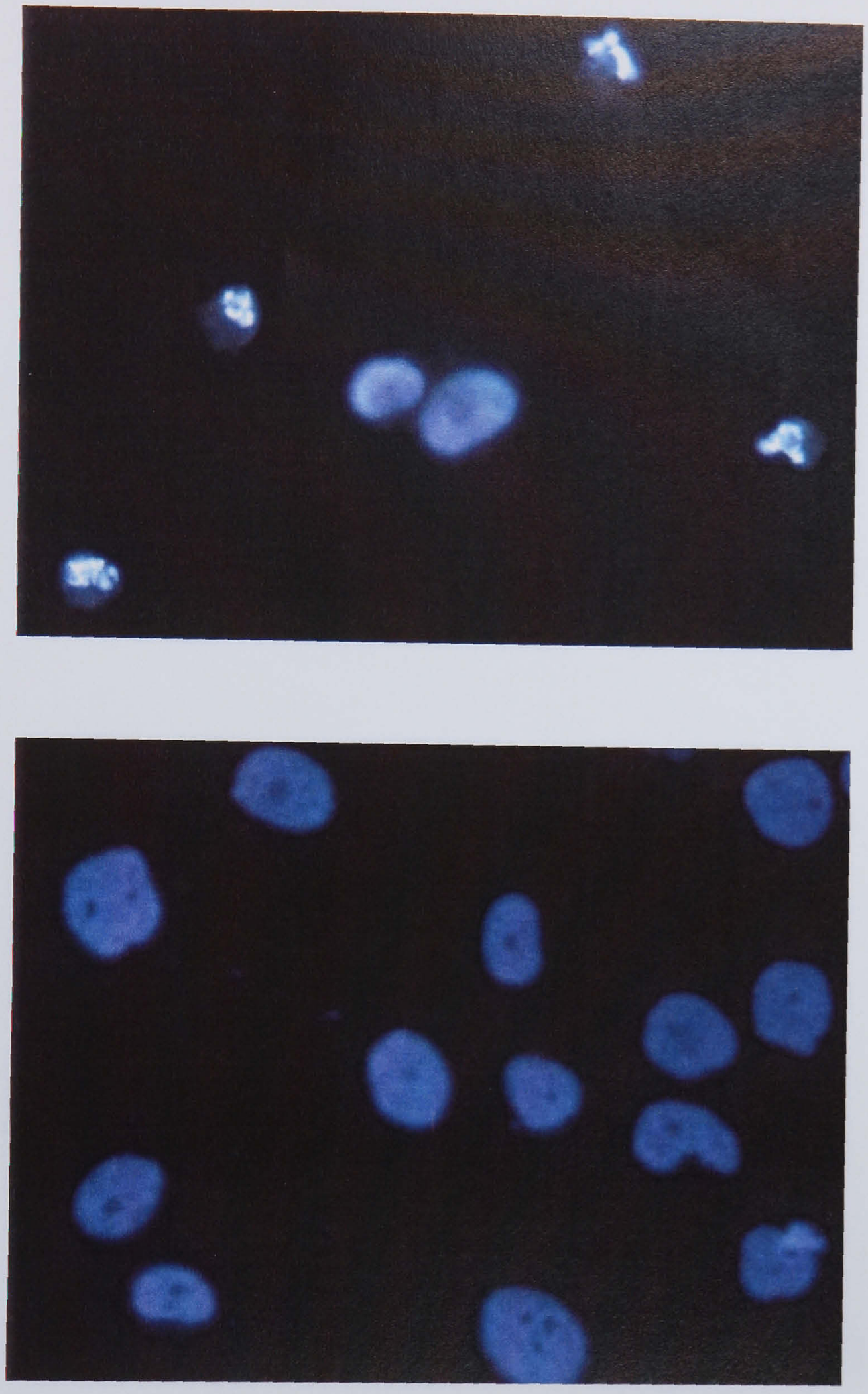
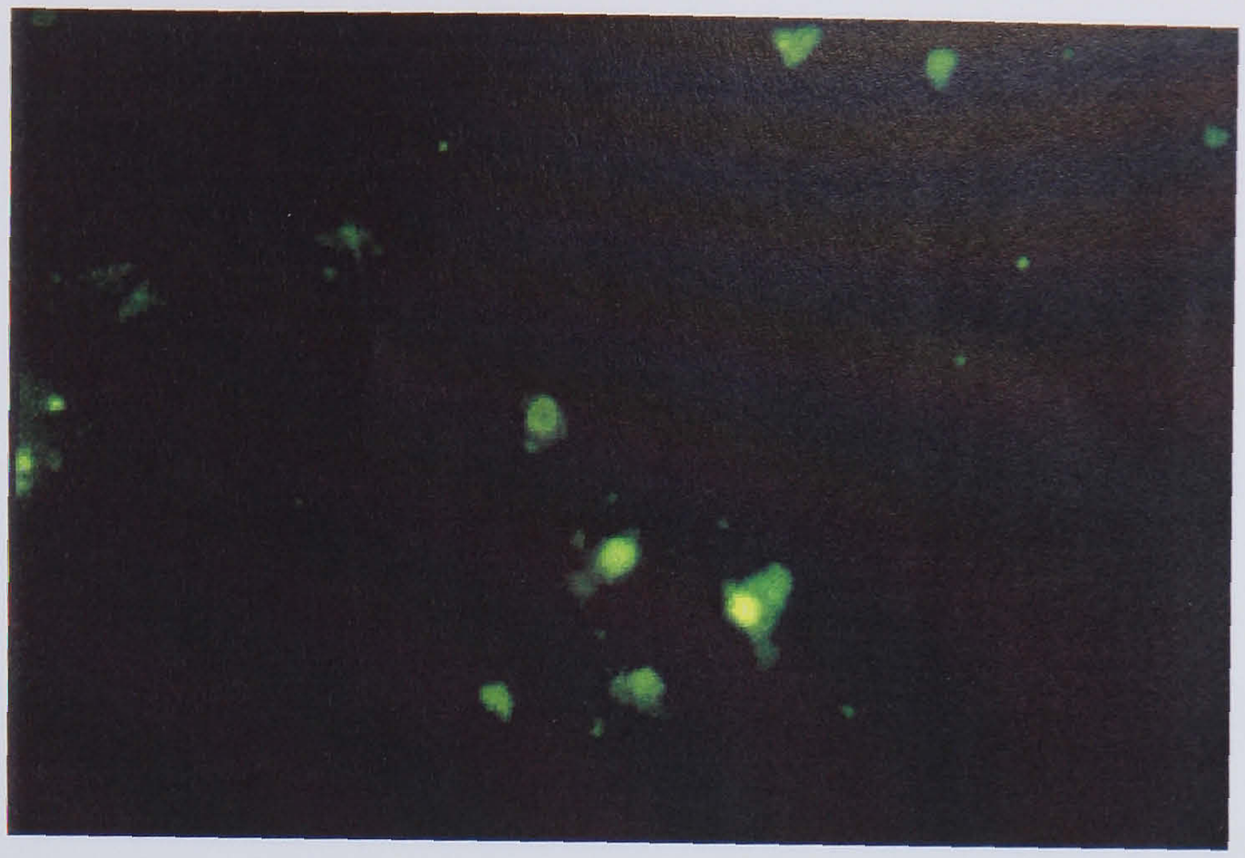


Figure 4.6 Cytochemical effects of perillyl alcohol on SM1 cells. Fluorescent photomicrographs of SM1 cells that have been stained with the fluorescent DNA-binding dye, DAPI, after treatment with **A)** 2mM perillyl alcohol **B)** or normal treatment for 48 hours in 10% (v/v) FBS (original magnification x400. The bright blue staining indicate areas of nuclear DNA condensation, usually a characteristic of apoptotic cells.

A



B



Figure 4.7 Effects of perillyl alcohol on fluorescent DNA fragmentation in SM1cells. Exponentially growing SM1 cells were exposed to **A)** 2mM perillyl alcohol in 10% (v/v) FBS for 48 hours, and stained with the TUNEL reagent (transferase-mediated dUTP end-labelling) **B)** no treatment (original magnification x400). The bright green stains indicate the TUNEL-positive, apoptotic nuclei with DNA fragmentation. Positive staining is absent in the control samples.

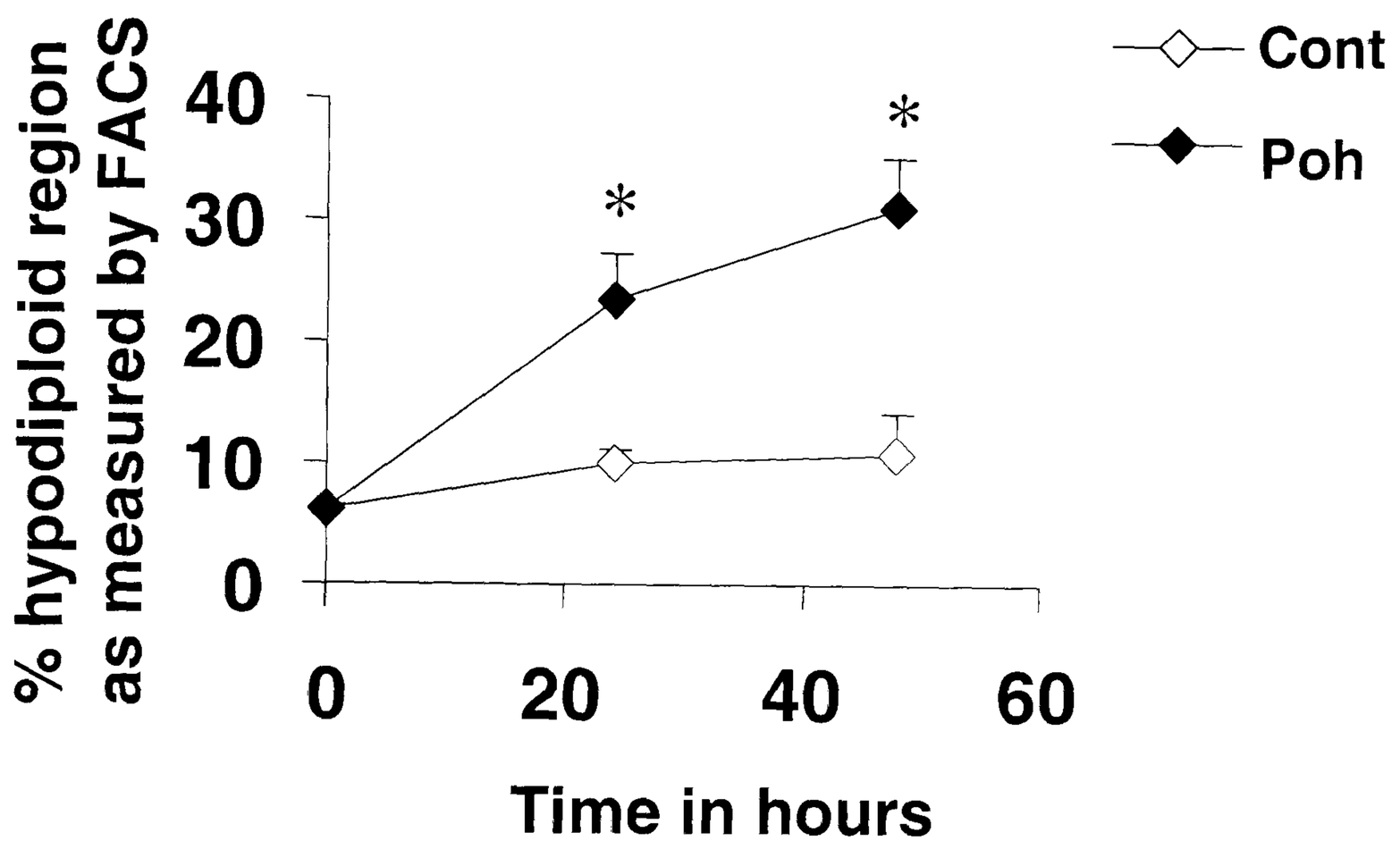


Figure 4.8 Time-dependent effect of perillyl alcohol on % proportion of the hypodiploid DNA content of SM1 cells. Exponentially growing SM1 cells were treated either with 2mM perillyl alcohol (Poh) or without (Cont) in 10% (v/v) FBS for 48 hours. The cells were harvested, stained with propidium iodide (PI) and analysed with flow cytometry. Exposure to perillyl alcohol was associated with a time-dependent increase in the % total proportion of cells with hypodiploid DNA content. Results represent the mean±SEM of four experiments. Statistical significance was assessed using the Student`s t test, where *=$p<0.05$ vs control.

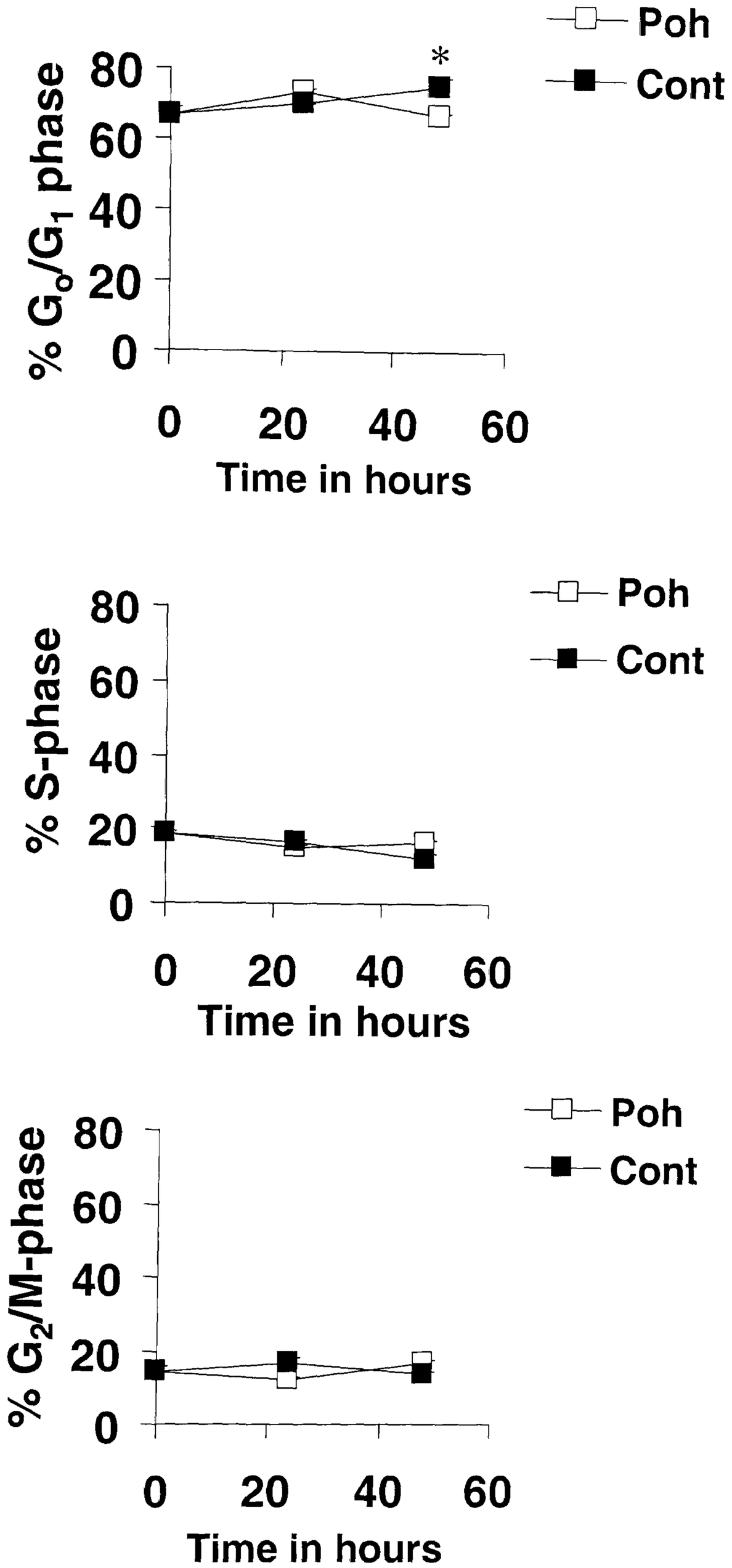


Figure 4.9 Time-dependent effect of 2mM perillyl alcohol on SM1 cell cycle phases as assessed by flow cytometry. Exponentially growing cells were exposed to perillyl alcohol (Poh) or vehicle (Cont) for 48 hours. The cells were harvested, stained with propidium iodide and analysed by FACS. The % proportion of each cell cycle phase was measured using the SOBR algorithm, which is part of the DNA content analysis software. The results represent the mean±SEM of four experiments. Significance was assessed using the Student`s t test, where *=$p<0.05$ vs control.

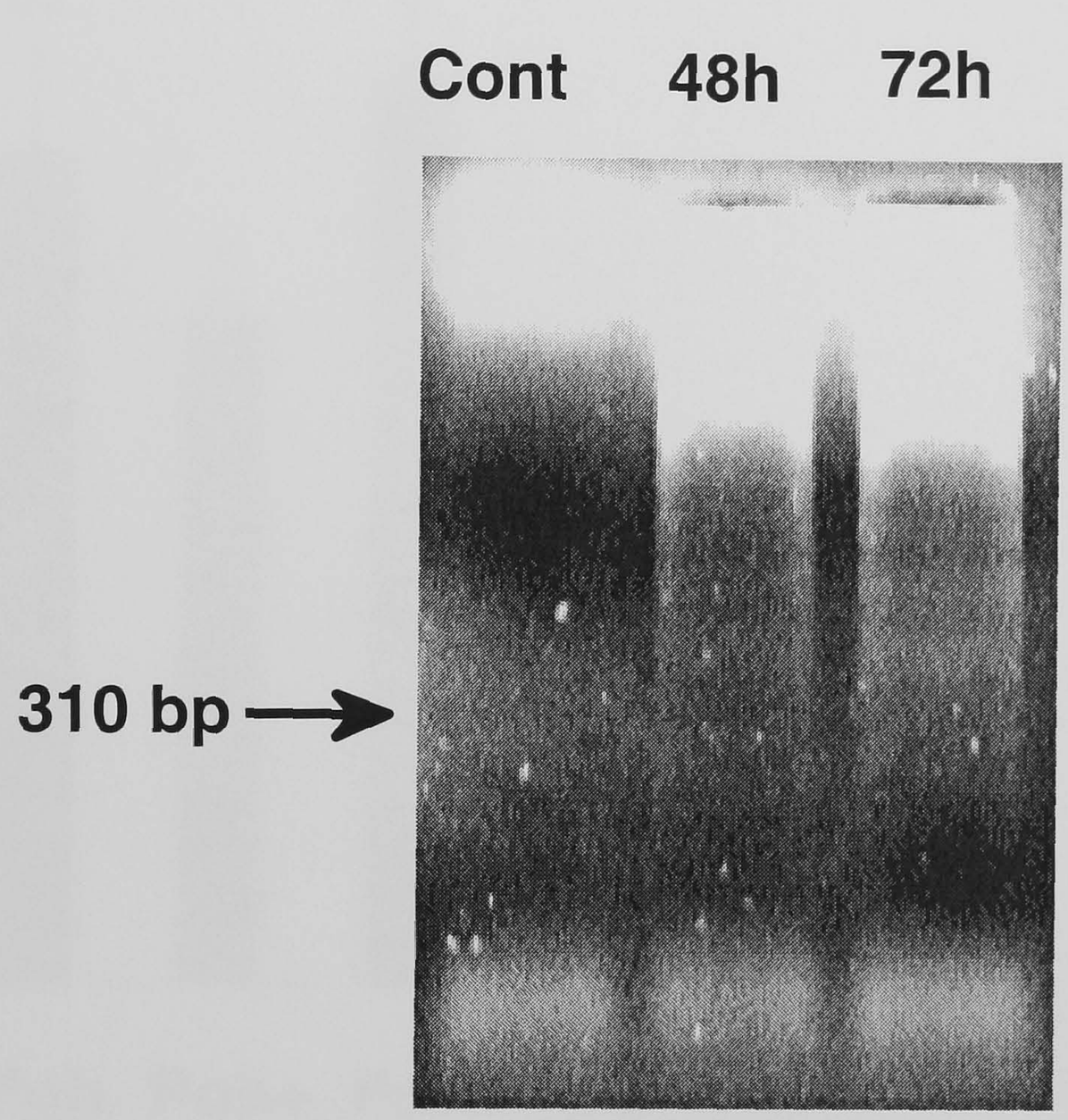


Figure 4.10 Time-dependent effect of perillyl alcohol on DNA fragmentation in SM1 cells. Agarose gel (2%) (w/v) electrophoresis of DNA extracted from SM1cells treated with 2mM perillyl alcohol for 48 and 72 hours in 10% (v/v) FBS. Treatment was associated with a time-dependent increase in levels of DNA fragmentation, resulting in multiples of 180-200 base pair molecular weight fragments. Lane M indicates the DNA size marker, ϕX174 plasmid cut with *Hae* III (0.04mg/ml). The final optimised procedure was used to extract the DNA from the cells. About 3μg of nucleic acid was loaded, and the gel was cast with 1:10000 dilution of SYBR Green I dye.

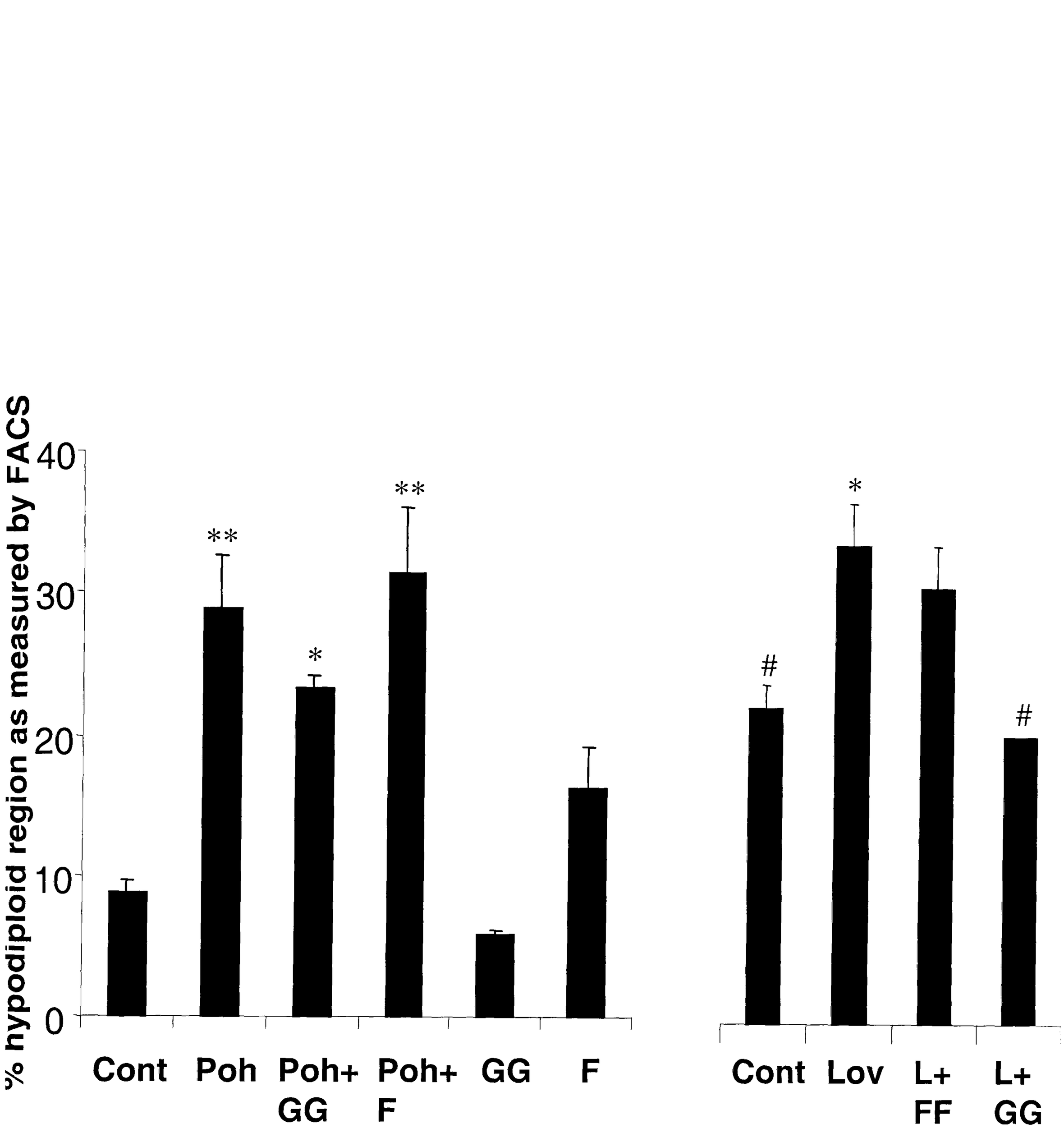


Figure 4.11 Differential effects of geranylgeranyl pyrophosphate on lovastatin and perillyl alcohol-induced apoptosis in SM1 cells. **A)** Farnesyl (F) and geranylgeranyl pyrophosphate (GG) both at 10μM were co-incubated with 2mM perillyl alcohol (Poh) for 48 hours, indicated as P+F and P+GG, respectively **B)** with 10μM lovastatin (Lov), indicated as L+FF or as L+GG, respectively for 48 hours. Control cultures for lovastatin were treated with vehicle. The samples were then harvested, stained with propidium iodide and analysed using flow cytometry. Co-incubation of lovastatin treated cells with GG decreased the % total proportion of hypodiploid DNA content, but co-incubation of perillyl alcohol-treated cells with GG had no effect on the hypodiploid DNA content. Results represent the mean±SEM of three experiments. Statistical significance was assessed by ANOVA, followed by the Tukey-Kramer multiple comparisons test, where *=$p<0.05$ vs control, **=$p<0.01$ vs control, and #=$p<0.05$ vs lovastatin.

4.1.1.3 Discussion

The results in this chapter provide evidence that perillyl alcohol treatment of SM1 cells is associated with increased apoptosis, a decrease in the rate of cell proliferation and inhibition of thymidine incorporation.

The data obtained through flow cytometry indicate a large increase in the proportion of the hypodiploid region after treatment with 2mM of perillyl alcohol, an established marker of apoptosis in cultures. The cell cycle phase analysis of SM1 cells treated under the same conditions indicate a slight, but significant reduction in the G_o/G_1 phase of perillyl alcohol treated SM1 cells, predominantly at 48 hours after treatment (**Figure 4.10**). This decrease may be accounted for through a selective increase in apoptosis of cells in G_o/G_1 phase at the same time point. Although these results do not conform with those of (**Schulz S et. al., 1994**; **Bardon S et. al., 1998**) who observed an accumulation of lymphocytes and human breast cancer cells, respectively, in the G_o/G_1 phase of the cell cycle, indicating growth arrest, the outcome may be dependent on the cell type used. In fact, the inhibition of [^{3}H] thymidine incorporation (**Figure 4.4**) seen after 48 hours, but not so much at 24 hours, indicates that entry into S phase (DNA synthesis) is not affected *per se*, but is indirectly decreased due to loss of cells in G_o/G_1 phase through apoptosis.

The mechanism of action of the monoterpene, perillyl alcohol, was shown to involve an inhibition of geranyl geranyl transferases in NIH3T3 cells (**Ren Z et. al., 1997**), and was also associated with decreased levels of antigenic Ras in human-derived myeloid and lymphoid cell lines (**Hohl RJ and Lewis K, 1995**). These authors demonstrated that levels of [^{3}S] methionine-labelled Ras were less than the [^{3}S] methionine-labelled Ras proteins from untreated cultures. However, they have not shown whether this effect on Ras protein levels is a direct effect of possible geranylgeranyl transferase inhibition. It may be possible that inhibition of this enzyme may affect Rho function, which may lead to a down-regulation of Ras protein levels or activity, although there is as yet no evidence on this.

It is interesting to note, however, that in contrast to the above group, **Ren Z et. al., 1997** did not see any differences in the levels of this protein after treatment with

perillyl alcohol. This may have been because they had carried out some of their experiments in the presence of lovastatin, so that the Ras and Ras-related proteins in the cells would be labelled with [^{3}H] mevalonolactone, a lactone derivative of mevalonic acid. Hence, to conclusively differentiate the effect of lovastatin from that of perillyl alcohol on members of the Ras superfamily of small GTPases would be a problem (for comments see, **Hohl RJ and Lewis K, 1995**). **Ren Z et. al, 1997**, however, studied the effects of treating cells with perillyl alcohol alone, so their results would be easier to interpret. Antigenic levels of Ras protein were shown to decrease with increasing concentrations of perillyl alcohol. In contrast, however, the antigenic levels of another protein, G_α, the α-subunit of heterotrimeric G proteins were not affected, indicating that the action of perillyl alcohol was specific. Such an effect due to perillyl alcohol was in direct contrast to the effect of lovastatin, which resulted in a mobility shift of the Ras protein (slower migrating) band. This change in mobility is interpreted as being due to loss of isoprenyl modification. It is interesting to note, however, that very low levels of antigenic Ras were associated with cytotoxicity, as measured by uptake of Trypan blue, in cells treated with perillyl alcohol (**Hohl RJ and Lewis K, 1995**). The possibility that cytotoxicity seen reflected apoptosis of these cells was not explored.

Although the authors did not look at the possible effect of perillyl alcohol on antigenic levels of other Ras-related proteins, such as Rho, it is possible that the apoptotic effect of perillyl alcohol seen in our experiments may be due to a direct reduction of Ras protein levels. Such an effect would probably have a direct bearing on the anti-apoptotic activity of proteins like Rho or Rac, as these proteins have been shown to be downstream effector proteins of Ras (**Yang Y et al., 1999**). Indeed, direct inhibition of (normal) Ras activity with dominant negative mutant Ras molecules (**Sakai N et. al, 1994**), with anti-p21 ras antibodies (**Nobes CD and Tolkovsky AM, 1995**), and with antisense oligonucleotides to Ras (**Chen CY et. al., 1998**) have all been associated with apoptosis. Alternatively, the effects of perillyl alcohol may be accounted for by a direct inhibition of small GTPase protein geranylgeranylation, especially of those proteins which are dependent on this modification, such as most forms of Rho and Rac. Similarly, although lovastatin treatment for 2 days lead to inhibition of Ras protein farnesylation (**McGuire T F and Sebti S D, 1997**), the

geranylgeranylation of crucial survival and growth-related molecules like Rho and Rac may have been equally affected.

One reason why we do not see any recovery from perillyl alcohol-induced apoptosis when co-incubated with geranylgeranyl pyrophosphate may be due to the direct inhibition of geranylgeranyl transferase enzymes (GGTase), where addition of the isoprenoid would have no effect (**Figure 4.12**). This would be unlike the effect of lovastatin, which results merely in a depletion of this isoprenoid due to the block in endogenous mevalonate synthesis, and hence would be recovered after the isoprenoid is replenished. Indeed, we do not see a recovery from perillyl alcohol-induced apoptosis, but we do see a recovery in lovastatin-induced apoptosis, when cells are co-incubated with geranylgeranyl pyrophosphate (**Figure 4.12**). Hence, it may be that perillyl alcohol leads to inhibition of crucial survival and growth signals through a direct inhibition of geranylgeranylation in the cell, which may also be coupled to a decrease in Ras protein levels, but that the effect of lovastatin is directed at the inhibition of geranylgeranyl synthesis from mevalonate.

In conclusion, these results are consistent with perillyl alcohol activity as a direct inhibitor of GGTase. However, other effects of perillyl alcohol cannot be excluded, eg. reduction in Ras levels or another factor mediating the effects which would result in SM1 cell apoptosis.

Chapter 5

Differential effects of lovastatin, perillyl alcohol and a farnesyl transferase inhibitor on UVB-induced effects on cell proliferation and apoptosis of SM1 cells

5.1.1.1 Introduction

Although exposure to UVB irradiation has been associated with apoptosis in many cell lines (**Rattis FM et. al., 1998; Shindo Y et. al., 1998**), it was also associated with the upregulation of many gene products seen during cell proliferation, such as *c-fos* and *c-jun* (**Kramer M et. al., 1990; Ghosh R et. al., 1993**). These gene products were shown to be coupled to an activation of the Ras signalling pathway as part of the UV response, which is conserved from yeast to mammals (**Engelberg D et. al., 1994**). Recently, the Ras-related small GTP-binding protein RhoB was reported to be immediate-early gene inducible by DNA damaging treatments (**Fritz G et. al., 1995**). Expression of platelet-activating factor (PAF) receptors was associated with enhanced UVB irradiation-induced apoptosis in a human epidermal cell line (**Barber LA et. al., 1998**), suggesting that the signals evoked from PAF receptors may in fact be complementary to those evoked due to UVB irradiation, leading to enhanced apoptosis. Similar observations were also reported in the presence of PDGF, by **Kim HE et. al., 1997**, in human prostate cancer cells. UVB irradiation, however, has also been associated with marked inhibition of DNA synthesis, upregulation of a cell cycle checkpoint protein, p21/Waf1, and prolonged growth arrest at G_1 and S phases of neonatal rat keratinocytes (**Petrocelli T, et. al., 1996**).

In the previous chapter we provided evidence that perillyl alcohol, a putative prenyl transferase inhibitor leads to apoptosis in SM1 cells. Lovastatin, an HMG-CoA reductase inhibitor, was also associated with apoptosis in these cells. In this chapter we describe the effects of a farnesyl transferase inhibitor, B581, perillyl alcohol (a putative GGTase inhibitor) and lovastatin on UVB-induced apoptosis, inhibition of cell proliferation and DNA synthesis in SM1 cells.

5.1.1.2 Results

5.1.2.2 Effect of UVB irradiation on cell proliferation and viability in SM1 cells

To evaluate the effect of another agent known to induce apoptosis in other cell types, subconfluent, exponentially growing SM1 cells were irradiated with increasing doses of UVB (0-200J/m^2) in 10% (v/v) FBS and cell numbers counted after 24 and 48 hours post-irradiation.

Figure 5.1 shows the dose-dependent decrease in cell numbers after UVB irradiation. Cell numbers decreased significantly by 53.4±4.5% ($p<0.01$, n=3) from 449x10^3+/-69x10^3 cells in control cultures to 204x10^3+/-12x10^3 cells at 24 hours after a UVB dose of 50J/m^2. There was a similar percentage decrease in cell numbers after 48 hours in control cultures, with respect to those treated with 50J/m^2 after the same time period (**Figure 5.1**). After irradiation with a UVB dose of 100J/m^2, cell numbers significantly decreased by 67.5±5.5% ($p<0.01$, n=3) from 449x10^3±69x10^3 cells in control cultures after 24 hours to 151x10^3±47x10^3 cells at 24 hours.

Total percentage viability, measured by Trypan Blue exclusion also decreased significantly by 31±1% ($p<0.001$, n=3) from 94±1% in control cultures at 48 hours to 62±2% in cultures irradiated with a 50 J/m^2 dose of UVB after the same time period (**Figure 5.1**).

This dose of UVB was then selected to evaluate the effect of UVB irradiation on the kinetics of apoptosis in SM1 cells by FACS analysis.

5.1.3.2 Effect of UVB irradiation on apoptosis and the cell cycle phases in SM1 cells

To evaluate whether UVB irradiation increased apoptosis in SM1 cell cultures, SM1 cells were irradiated with a UVB dose of 50J/m^2 and incubated for 48 hours. Various corroborative methods for detecting apoptosis were used.

Treatment with UVB was associated with cell rounding, increased granularity, and detachment from the petri dish substratum and surrounding cells, as assessed by light microscopy (**Figure 5.2**).

Staining with the DNA-binding fluorescent dye, DAPI and also with the TUNEL reagent revealed that treatment with UVB was associated with genomic DNA condensation and fragmentation, characteristic of apoptosis (**Figure 5.3 and Figure 5.4**).

To quantitate the degree of apoptosis induced in cultures, the cell DNA content was assessed using flow cytometry (FACS). Irradiation with UVB was associated with the appearance of a subpopulation with hypodiploid DNA content, an established marker for apoptosis. Cells were stained with PI and the hypodiploid region quantified after 0, 24 and 48 hours of UVB treatment (50 J/m^2). There was a significant increase in the percentage proportion of hypodiploid DNA content by 157.5±5.5% of control, from 9.2±1% in untreated cultures to 15±0.5% in UVB treated cultures at 24 hours ($p=0.002$, $n=3$) (**Figure 5.5**).

The DNA content of each cell cycle phase, as a % proportion of the total amount, was also assessed, using the SOBR algorithm as part of the DNA content analysis software (see materials and methods). There was a significant decrease in G_o/G_1 phase ($p=0.01$, $n=3$) by 42±3% from 45±1% in untreated cultures at 24 hours to 26±2% in cultures after 24 hours of exposure to UVB. Likewise, there was a significant decrease in G_o/G_1 phase by 50.5±0% ($p=0.004$, $n=3$) from 50±4% in control cultures to 25±2% in UVB treated cultures at 48 hours. Interestingly, there was a significant increase in S phase ($p=0.0003$, $n=3$) by about 2 fold from 30±2% in control cultures at 24 hours to 60±2% in UVB treated cultures at the same time. In addition, there was a significant increase in G_2/M phase ($p=0.002$, $n=3$) by 225±25% from 11±1% in control cultures at 48 hours to 25±5% in UVB treated cultures at the same time period (**Figure 5.6**).

A time-dependent increase in hypodiploid DNA content was also associated with increased DNA fragmentation into oligofragments of 180bp, resulting in a typical

apoptotic hallmark of "laddering" upon electrophoresis of the extracted DNA (**Figure 5.7**)

5.1.4.2 The effect of lovastatin, perillyl alcohol, and a farnesyl transferase inhibitor, B581, on UVB-induced apoptosis and changes in the cell cycle phases

Since isoprenylation has been shown to be important in the regulation of SM1 cell apoptosis, we next evaluated the effects of lovastatin, and other prenyl transferase inhibitors, such as perillyl alcohol and farnesyl transferase inhibitor, B581 on UVB-induced apoptosis in SM1 cells. UVB (at 50J/m^2) was used to induce apoptosis in exponentially growing, subconfluent SM1 cell cultures. Lovastatin at 10μM in 10% (v/v) dFBS, perillyl alcohol at 2mM in 10% FBS, or farnesyl transferase inhibitor, B581 at 100μM in 10% (v/v) FBS was co-incubated with SM1 cells exposed to UVB (50J/m^2) and incubated for 48 hours. Apoptosis was quantified as the percentage proportion of the hypodiploid region, A_o, as a characteristic marker. Apoptosis in cells exposed to UVB increased significantly from 25±1% in UVB exposed cultures to 41±0.3% ($p<0.01$, $n=3$) in UVB and lovastatin co-treated cultures. Likewise, apoptosis in lovastatin treated cultures increased from 30±1% to 41±0.3% in UVB and lovastatin co-treated cultures ($p<0.05$, $n=3$). Apoptosis was also increased from 25±1% (in UVB cultures, $p<0.01$, $n=3$) and from 31.5±4% (in perillyl alcohol treated cultures) to 58±1.5% ($p<0.001$, $n=3$) in UVB and perillyl alcohol co-treated cultures. In contrast, there was no significant change in the degree of apoptosis, with respect to UVB treated cultures, when cells were co-treated with UVB and 100μM B581 (**Figure 5.8**).

The respective changes in the % proportion of the cell cycle phases, were assessed by FACS analysis using the SOBR algorithm, which is part of the DNA content analysis software. There was no significant difference in G_o/G_1 phase of cell cultures when co-treated with UVB and 100μM B581, or when cultures were treated with B581 alone. No significant difference in G_o/G_1 phase between UVB alone treated cultures and cultures treated with both UVB and 2mM perillyl alcohol was seen . However, a significant decrease in G_o/G_1 phase by 38±2% from 63±1% in perillyl alcohol (2mM) treated cultures to 39±2% in UVB and perillyl alcohol co-treated cultures ($p<0.001$,

n=3). Equally, a significant decrease in G_o/G_1 phase by 78±1% from 72±1% in lovastatin treated cultures to 16±1% in UVB and lovastatin co-treated cultures ($p<0.001$, n=3) was observed. A significant decrease was also seen ($p<0.05$, n=3) in G_o/G_1 phase by 44±4%, from 29±4% in UVB treated cultures to 16±1% in UVB and lovastatin co-treated cultures (**Figure 5.9**).

There was no significant change in S phase in UVB alone treated cultures, with respect to UVB and 100μM B581 co-treated cultures, as well as in cultures treated with B581 alone at 48 hours. Co-incubation of cultures with UVB and 2mM perillyl alcohol led to a significant decrease ($p<0.001$, n=3) in S phase by 55±2% from 47±0% in UVB treated cultures to 21±1% in UVB and 2mM perillyl alcohol co-treated cultures. However, there was no significant difference in S phase between cultures treated with perillyl alcohol alone and cultures co-treated with UVB and perillyl alcohol. In contrast, the proportion of S phase in UVB and lovastatin co-treated cultures was not significantly different from cultures treated with UVB alone. Also in contrast to perillyl alcohol treated cultures, the S phase proportion in lovastatin treated cultures increased from 12±0% to 55±3% in UVB and lovastatin co-treated cultures ($p<0.001$, n=3) (**Figure 5.9**).

With respect to changes in G_2/M phase, there was no significant difference in cultures treated with UVB alone and cultures co-treated with both UVB and 100μM B581. There was also no significant difference in G_2/M phase in cultures treated with 100μM B581 alone, with respect to the untreated, control cultures. In contrast, there was a significant decrease ($p<0.01$, n=3) in G_2/M phase by 52±2% from 21±1% in UVB alone treated cultures at 48 hours to 10±0% in UVB and 2mM perillyl alcohol co-treated cultures at 48 hours. However, there was a significant increase ($p<0.05$, n=3) in G_2/M phase by 138±3%, from 21±1% in UVB alone treated cultures to 29±2% in cultures co-treated with UVB and 10μM lovastatin. Equally, a significant increase in G_2/M phase was seen in lovastatin treated cultures from 15±0.5% to 29±2% in UVB and lovastatin treated cultures ($p<0.001$, n=3) (**Figure 5.9**).

Increase in hypodiploid DNA content, a marker of apoptotic cell death, was associated with an increase in DNA fragmentation as assayed by the DNA ladder

assay (**Figure 5.10**). However, this assay proved inadequate for distinguishing the difference in the degree of apoptosis between UVB treated and other co-treated populations.

Cytochemical DAPI staining was also carried out revealing increased levels of apoptosis in cultures that have been co-treated with lovastatin and perillyl alcohol, with no apparent changes in B581 co-treated cultures (**Figure 5.11**). The photomicrographs revealed a large number of bright blue staining, indicating DNA condensation, in the UVB alone treated cultures (**Figure 5.11A**), and especially in those cultures that were co-treated with UVB and 10μM lovastatin (**Figure 5.11B**) or 2mM perillyl alcohol (**Figure 5.11D**). Interestingly, there were very little, if any, staining in the UVB and B581 co-treated cultures (**Figure 5.11C**).

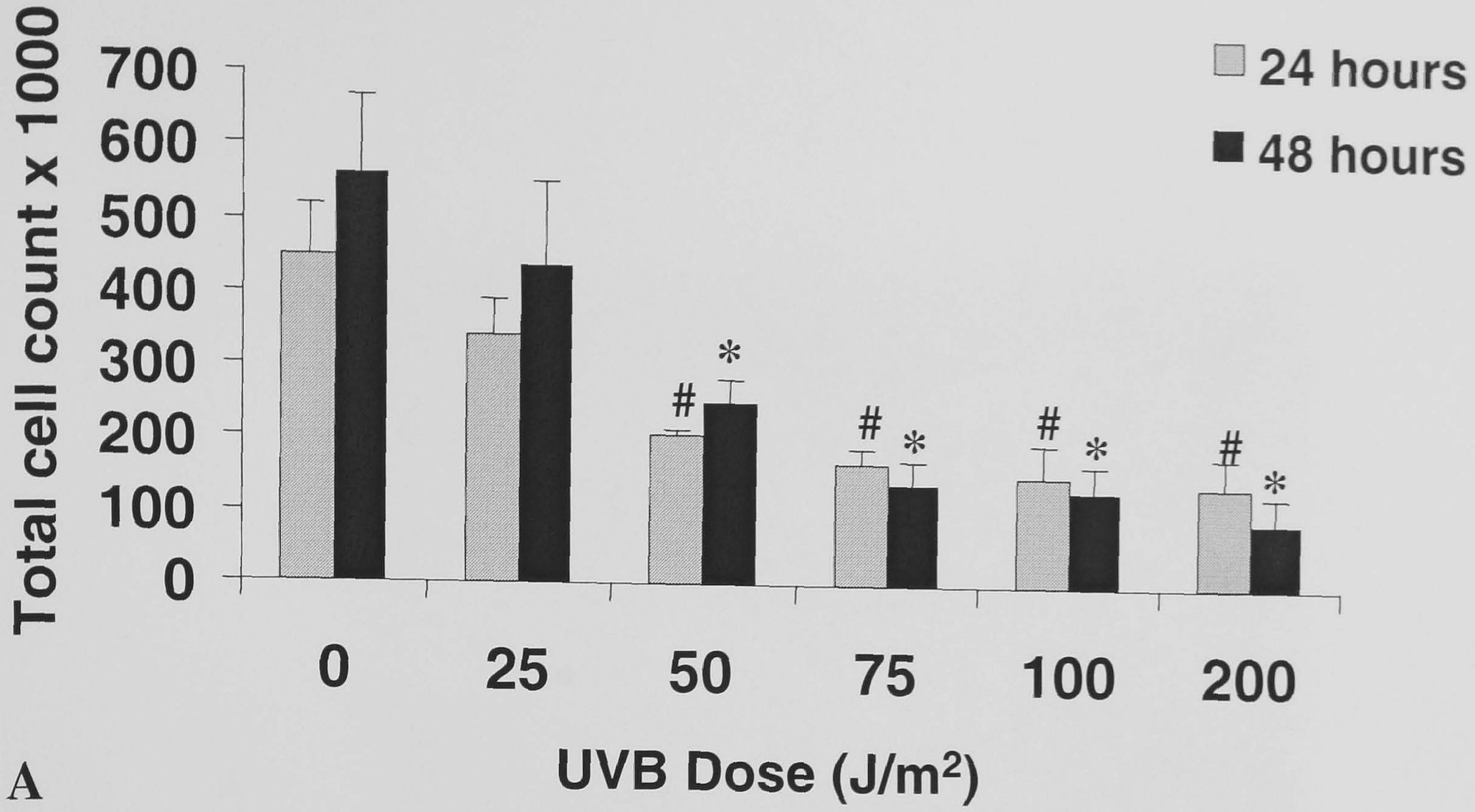
5.1.5.2 Effect of lovastatin, perillyl alcohol, and B581, on UVB-induced inhibition of cell proliferation, viability and thymidine incorporation

To evaluate the effect of these inhibitors on the rate of cell proliferation in SM1 cells after UVB irradiation, the same concentrations as discussed above were incubated with cells which had been exposed to UVB for 48 hours. There were no significant differences in total cell counts with respect to cultures that were exposed to UVB alone, and cultures co-treated with either B581, lovastatin or perillyl alcohol (statistical analysis by ANOVA, and Tukey-Kramer multiple comparisons post test) (**Figure 5.12**). Treatment of cells with B581 alone had no significant effect on cell proliferation, with respect to the control, vehicle treated cells.

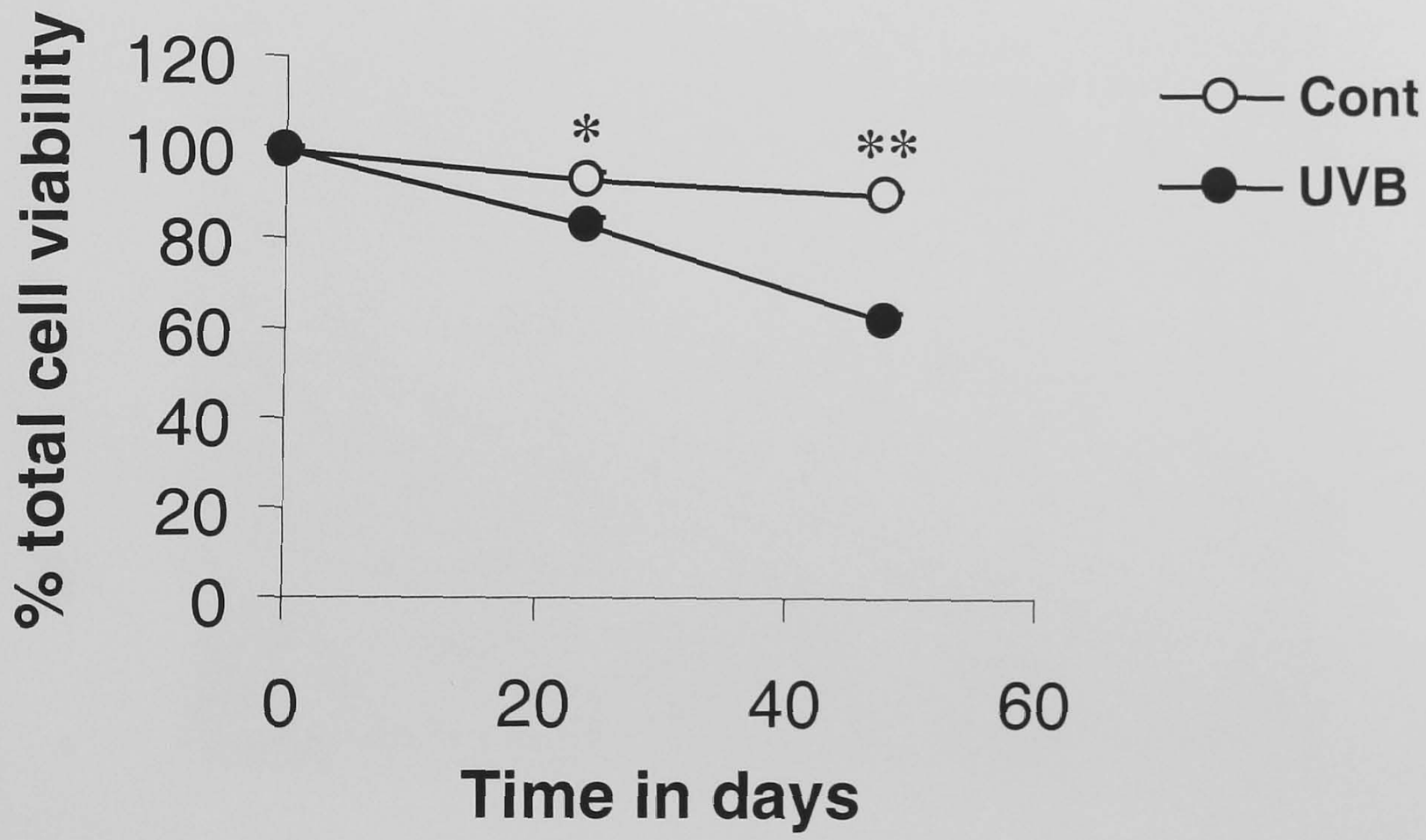
Total percentage viability also decreased significantly from 60±1% in UVB irradiated cultures to 42±2% in UVB and lovastatin co-treated cultures ($p<0.01$, $n=3$). The percentage viability of lovastatin treated cells also decreased from 84±2% to 42±2% in UVB and lovastatin co-treated cultures ($p<0.001$, $n=3$). Additionally, there was a significant decrease in cell viability in UVB treated cultures from 60±1% to 3±0% in UVB and perillyl alcohol co-treated cultures ($p<0.01$, $n=3$). There was also a significant decrease in % total cell viability in perllyl alcohol treated cultures from 53±5% to 3±0% in cultures co-treated with both UVB and perillyl alcohol ($p=<0.001$,

n=3). In contrast, however, cell viability increased significantly from 60±1% in UVB alone treated cells to 76±-1% in UVB and B581 co-treated cells ($p<0.01$, n=3) (**Figure 5.13**).

Changes in thymidine incorporation were also assessed after SM1 cells were co-treated with UVB and B581, lovastatin and perillyl alcohol respectively. All treatments with lovastatin were carried out in 10% (v/v) dFBS, while all the rest of the treatments were carried out in 10% (v/v) FBS. The cells in the 96-well plates were UVB irradiated ($50J/m^2$), and lovastatin, perillyl alcohol and the farnesyl transferase inhibitor (B581) at 10μM, 2mM and 100μM, respectively were added to the cells. After an incubation period of about 46 hours, the cells were exposed to tritiated thymidine for 4 hours as described in Material and Methods. There was a significant decrease in thymidine incorporation by 83.5±-0.5% from $5.7x10^3$±317 cpm in UVB treated cultures to 948±82 cpm in UVB and lovastatin co-treated cultures ($p<0.001$, n=3). A significant decrease in thymidine incorporation by 93±2% from $5.7x10^3$±317 cpm in UVB treated cells to 409±149 cpm in UVB and perillyl alcohol treated cultures ($p<0.001$, n=3). There was no significant increase in thymidine incorporation between UVB treated cultures and cultures co-treated with UVB and B581 (**Figure 5.14**).



A



B

Figure 5.1 Effect of UVB irradiation on cell proliferation and cell viability in SM1 cells. **A)** Exponentially growing SM1 cells were exposed to increasing doses of UVB (0, 25, 50, 75,100, and 200 J/m^2) and incubated for 24 or 48 hours, respectively in 10% (v/v) FBS. The cell numbers were then measured using the Coulter Counter Z1. Results represent the mean±SEM of three experiments. Statistical significance was assessed by ANOVA, followed by theTukey-Kramer multiple comparisons test, where *=$p<0.05$ vs 0 J/m^2 and #=$p<0.01$ vs 0 J/m^2. **B)** The decrease in % total cell viability was measured in cultures exposed to UVB or untreated (Cont) after staining with a 1:1 (v/v) of Trypan blue : 10% (v/v) FBS using a Neubauer Haemocytometer. Results represent the mean±SEM of three experiments. Statistical significance was assessed by the Student`s t test, where *=$p<0.05$ vs control, and **=$p<0.001$ vs control.

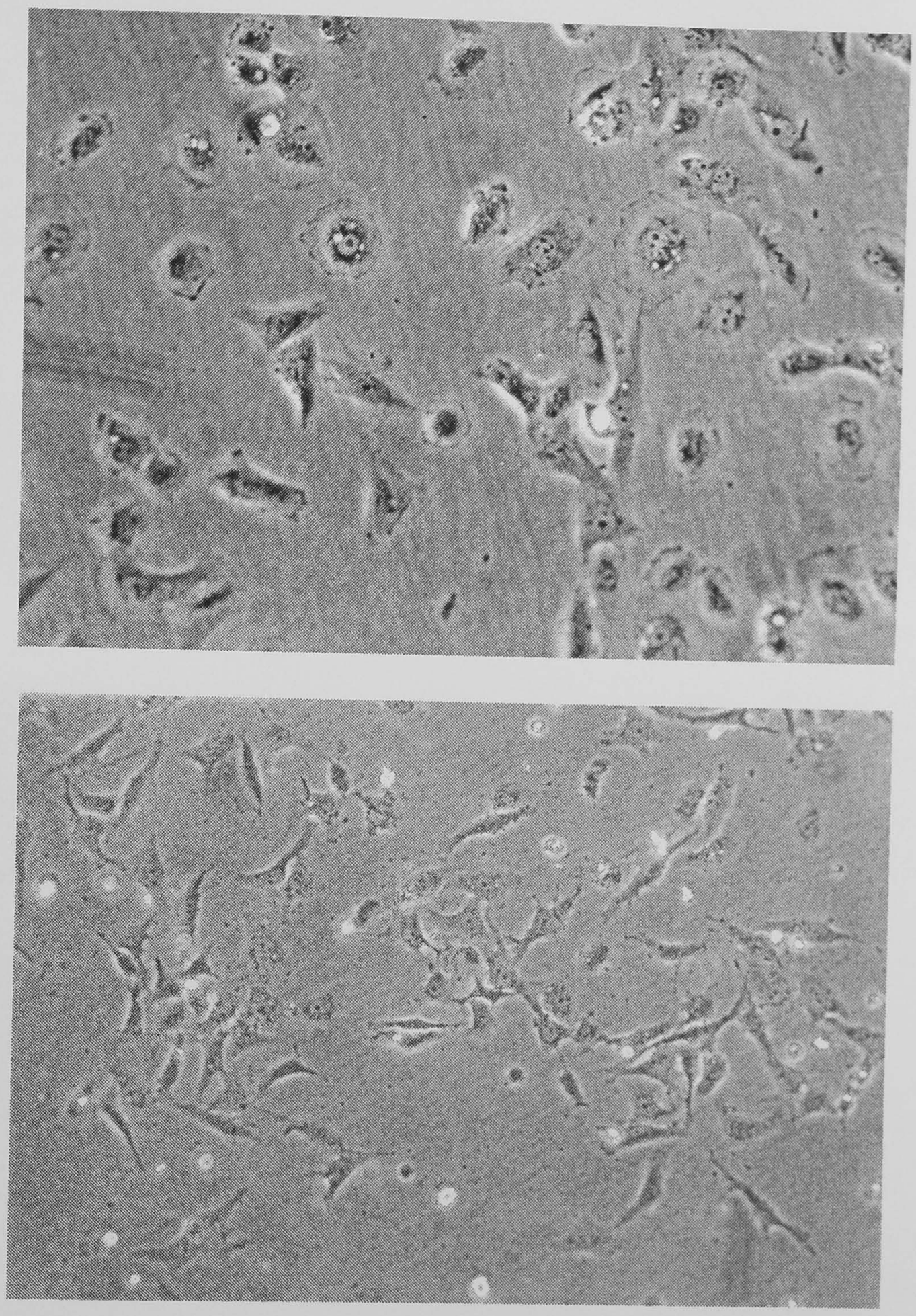
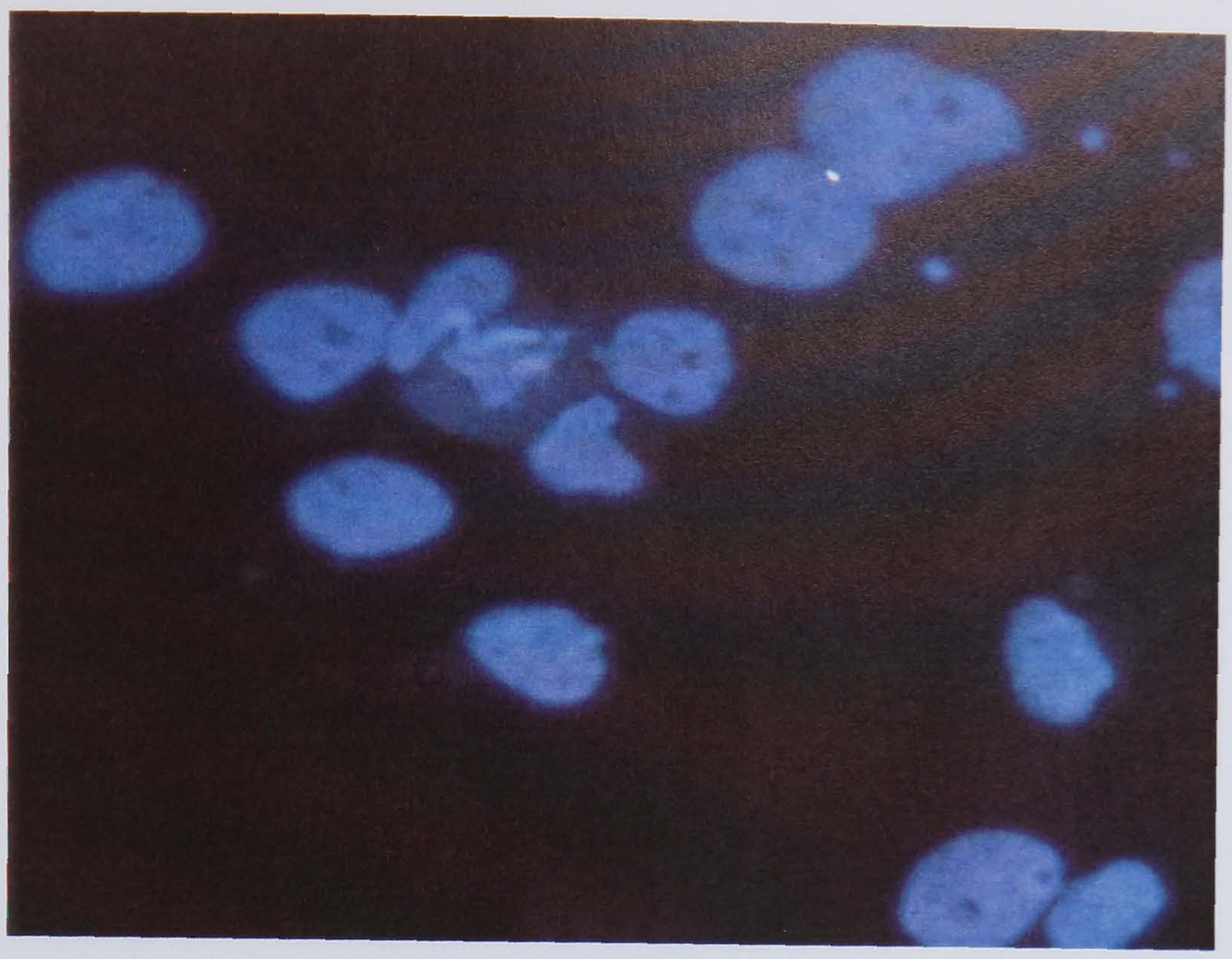
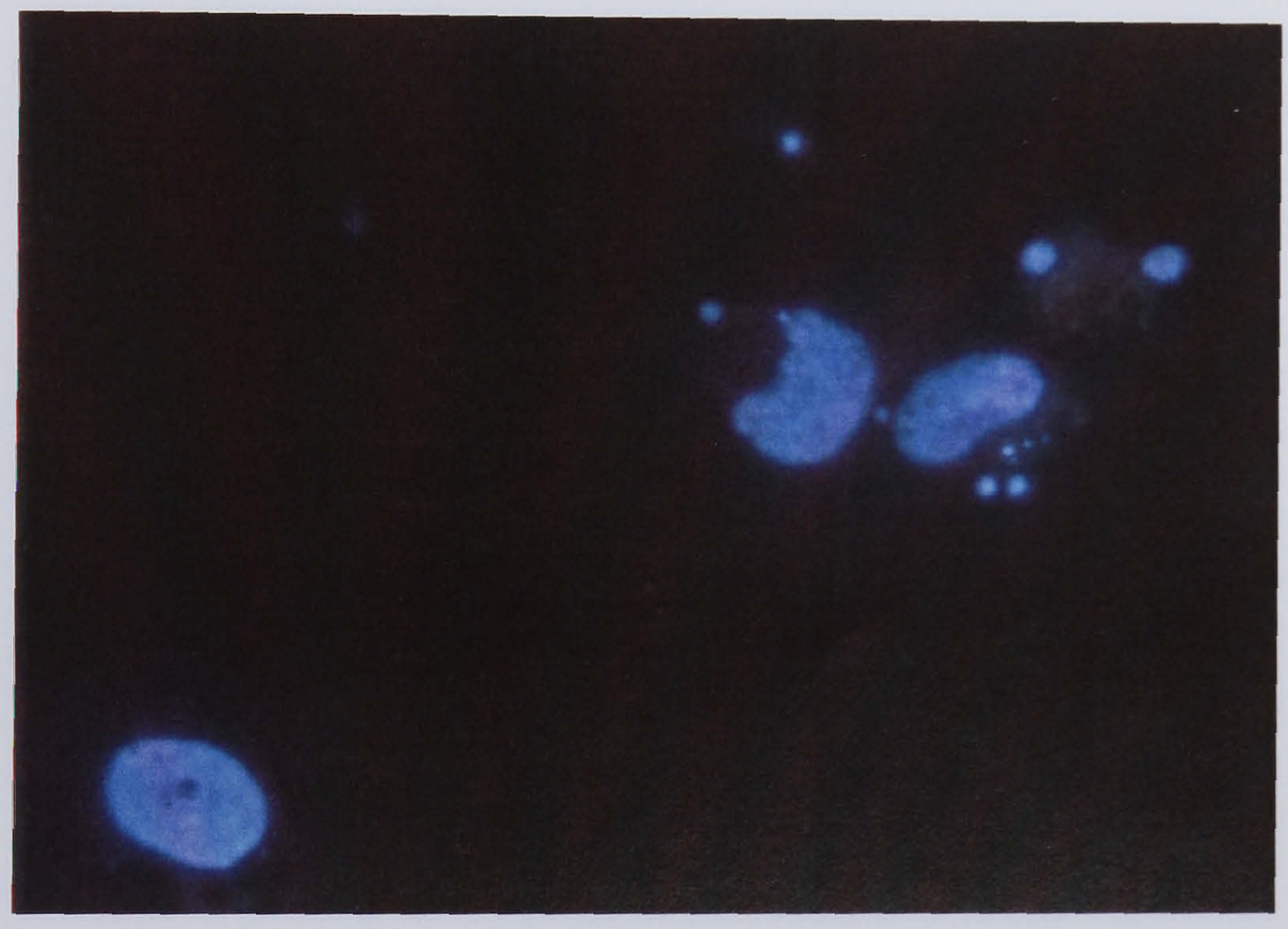


Figure 5.2 Morphological effects of UVB irradiation on SM1 cells. Light microscopy photomicrographs of UVB-treated SM1 cells, indicating common morphological features of apoptosis, such as barely attached or floating, rounded up cells with condensed cytoplasm **A)** SM1 cells as they appear under normal conditions in 10 % (v/v) FBS (original magnification x200) **B**) after exposure to 50 J/m^2 of UVB irradiation for 48 hours (original magnification x100) in regular 10% (v/v) FBS.

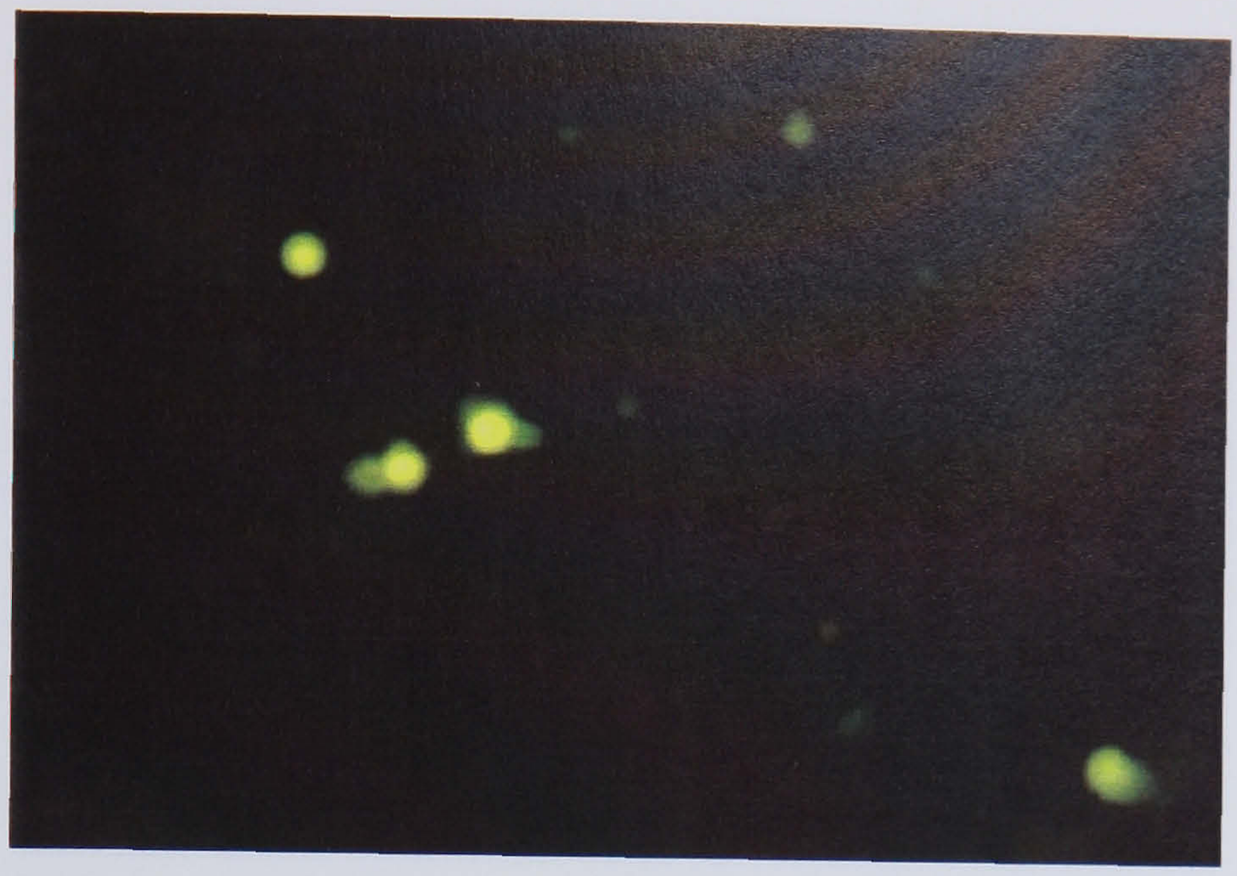


A



B

Figure 5.3 Cytochemical effects of UVB irradiation on SM1 cells. Fluorescent photomicrographs of SM1 cells that have been stained with the fluorescent DNA-binding dye, DAPI **A)** under normal circumstances **B)** after exposure to 50J/m^2 of UVB for 48 hours in 10% (v/v) FBS(original magnification x400). The bright blue staining indicate areas of nuclear DNA condensation, usually a characteristic of apoptotic cells.



A



B

Figure 5.4 Effects of UVB irradiation on fluorescent DNA fragmentation in SM1cells. Exponentially growing SM1 cells were either exposed to **A)** 50J/m^2 of UVB in 10% (v/v) FBS for 48 hours, and stained with the TUNEL reagent (transferase-mediated dUTP end-labelling) **B)** not exposed to any irradiation (original magnification x400). The bright green stains indicate the TUNEL-positive, apoptotic nuclei with DNA fragmentation. Positive staining is absent in the control samples.

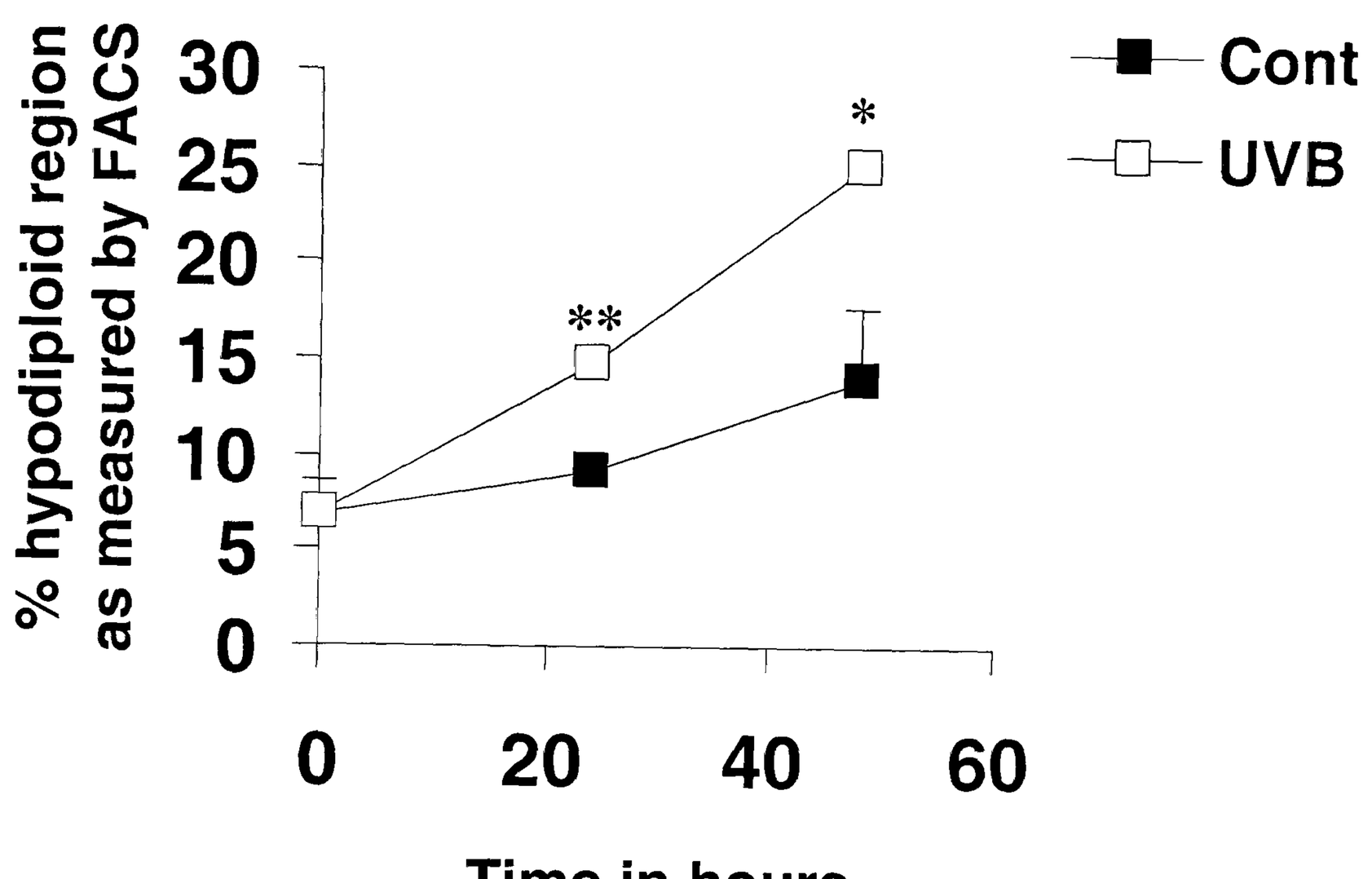


Figure 5.5 Time-dependent effect of UVB irradiation on % total proportion of the hypodiploid DNA content in SM1 cells. Exponentially growing SM1cells were treated either with 50J/m^2 UVB or without (Cont) in 10% (v/v) FBS for 48 hours. The cells were harvested, stained with propidium iodide (PI) and analysed with flow cytometry. Exposure to UVB irradiation was associated with a time-dependent increase in the % total proportion of cells with hypodiploid DNA content. Results represent the mean±SEM of three experiments. Statistical significance was assessed by the Student`s t test, where **p=<0.01vs control and *p=<0.05 vs control.

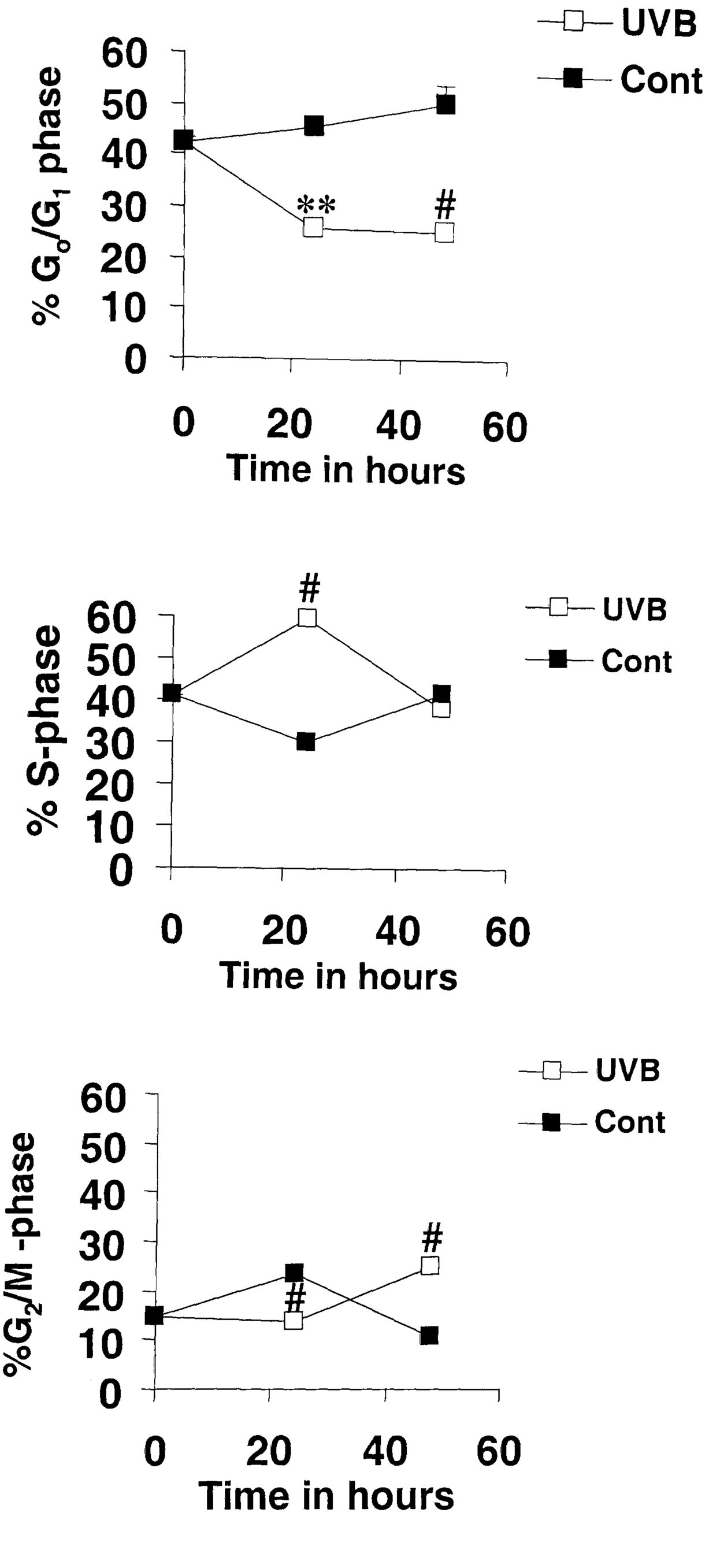


Figure 5.6 Time-dependent effect of UVB irradiation on SM1 cell cycle phases as assessed by flow cytometry. Exponentially growing cells were exposed to 50 J/m^2 of UVB or not exposed (Cont) for 48 hours, and the cells were harvested, stained with propidium iodide, and the % total proportion of each cell cycle phase was analysed by the SOBR algorithm, which is part of the DNA content analysis software. The results represent the mean±SEM of three experiments. Statistical significance was assessed using the Student`s t test, where **=p<0.01 vs control and #=p<0.001 vs control.

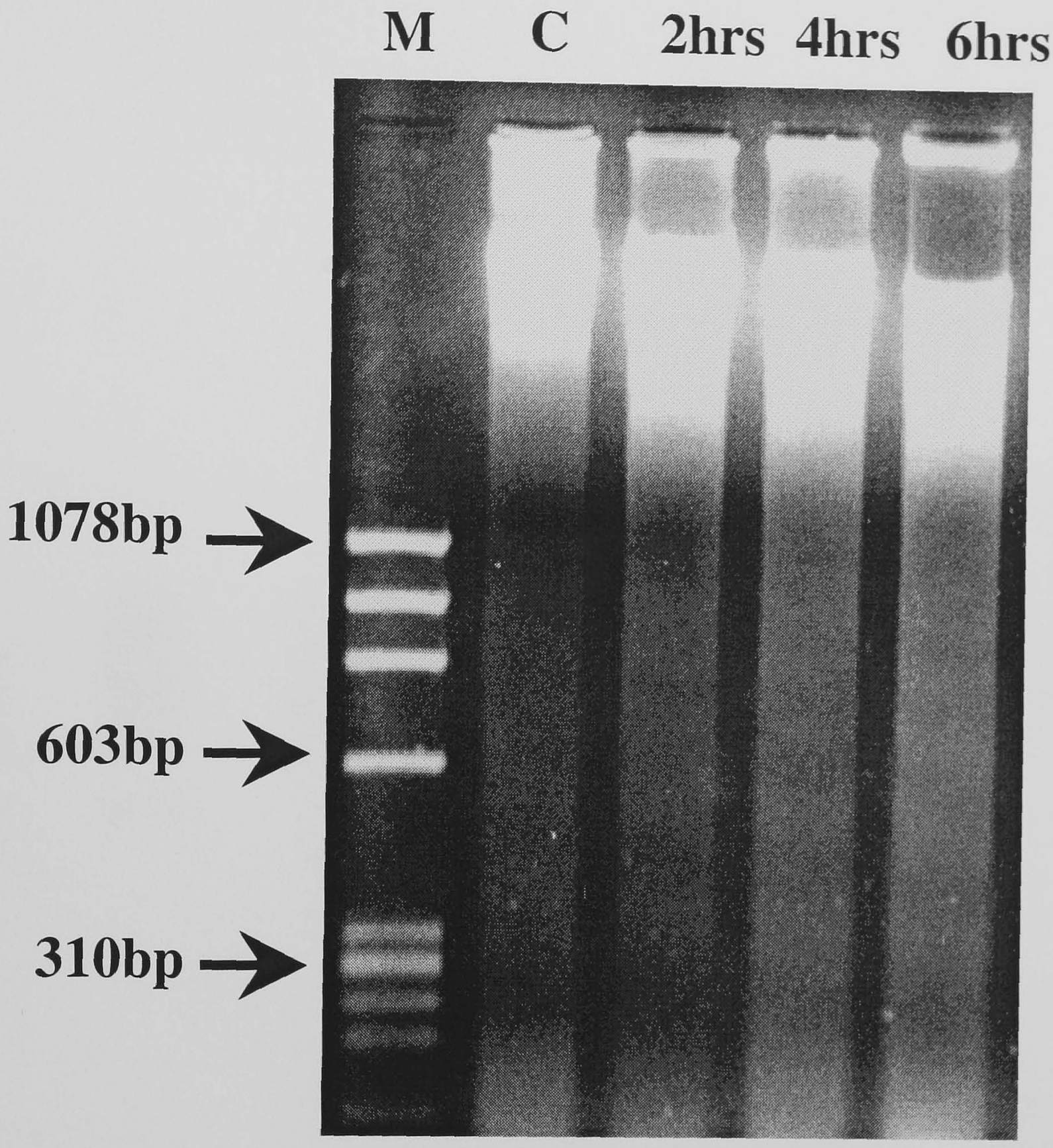


Figure 5.7 Time-dependent effect of UVB irradiation on DNA fragmentation in SM1 cells. Agarose gel (2%) (w/v) electrophoresis of DNA extracted from SM1cells not exposed to UVB (C) or treated with 50J/m^{2}of UVB irradiation for 2, 4, and 6 hours in 10% (v/v) FBS. Treatment was associated with a time-dependent increase in levels of DNA fragmentation, resulting in multiples of 180-200 base pair molecular weight fragments. Lane M indicates the DNA size marker, ϕX174 plasmid cut with *Hae* III (0.04mg/ml). The standard protocol for DNA extraction was used to extract the DNA from the cells. About 50µg of nucleic acid was loaded, and the gel was cast with Ethidium Bromide to visualise the DNA.

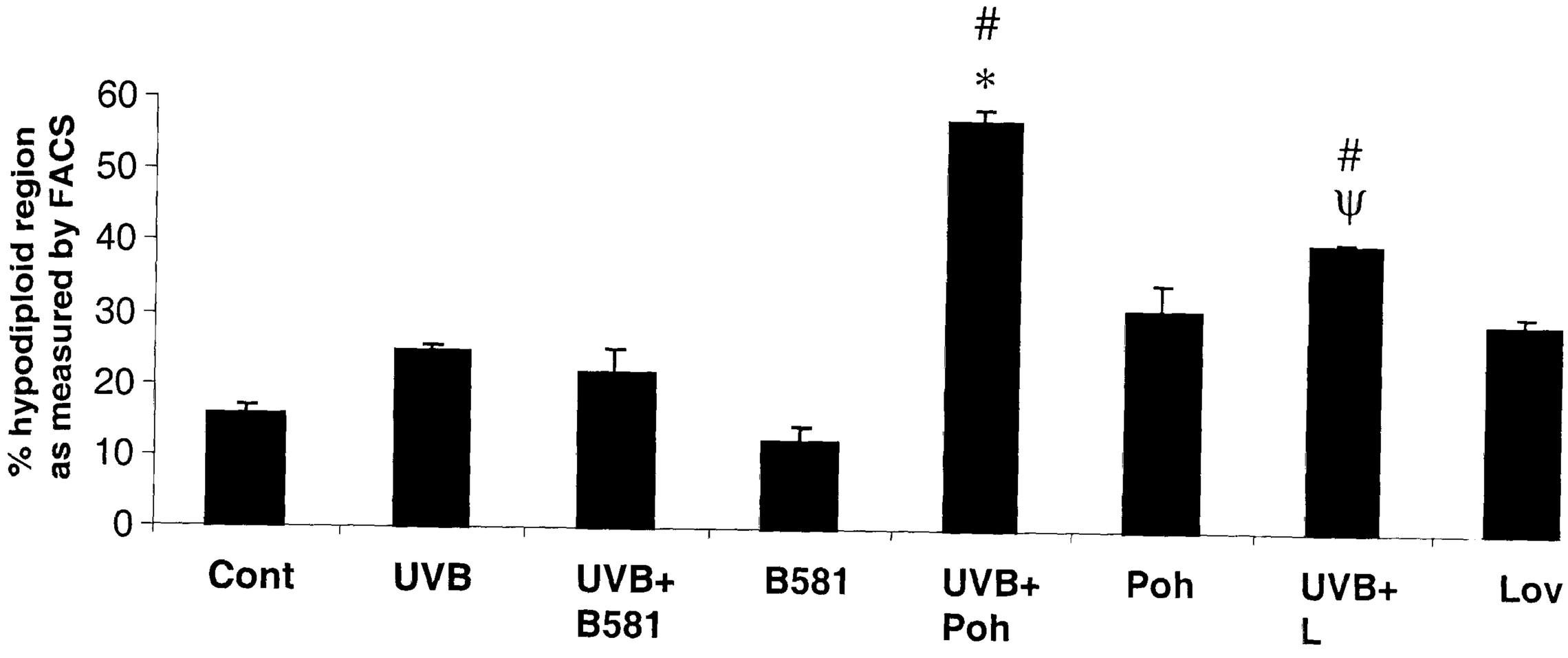


Figure 5.8 Effect of perillyl alcohol, farnesyl transferase inhibitor, B581 and lovastatin co-incubation of UVB treated cells on hypodiploid DNA content. Exponentially growing SM1 cells were either untreated (Cont) or irradiated with UVB ($50J/m^2$) and co-incubated either with 100μM farnesyl transferase inhibitor (B581), 2mM perillyl alcohol (Poh), or 10μM lovastatin (Lov) for 48 hours in 10% (v/v) FBS. Treatments with lovastatin were in 10% (v/v) dialysed FBS. The samples were then harvested, stained with propidium iodide and analysed through flow cytometry. The % proportion of total events of the hypodiploid region was measured. Results represent the mean±SEM of four experiments. Stastistical significance was assesed by ANOVA, followed by Tukey-Kramer multiple comparisons test where, #=$p<0.01$ vs UVB, *=$p<0.001$ vs Poh and ψ=$p<0.05$ vs Lov.

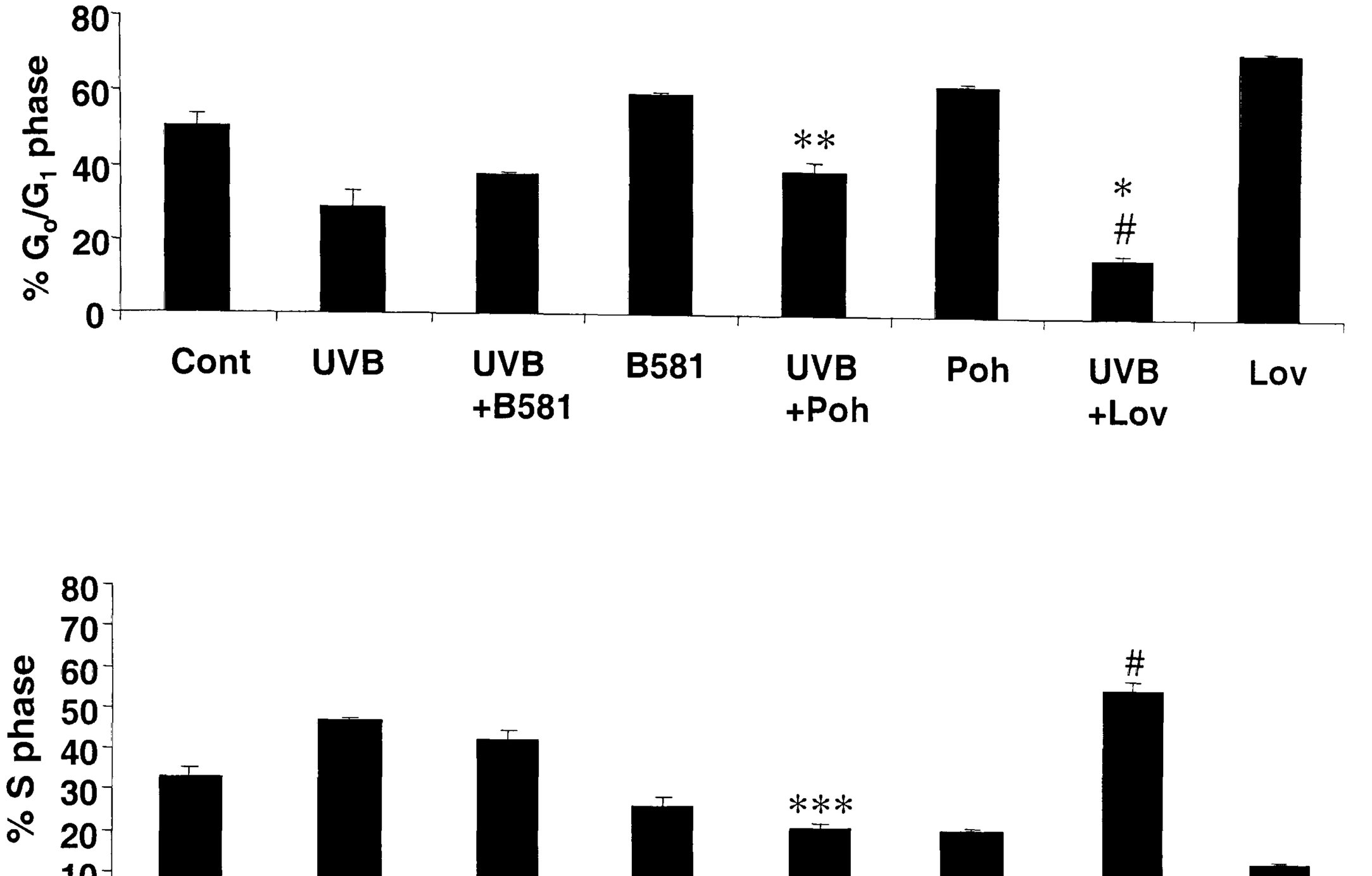


Figure 5.9 Effect of perillyl alcohol, farnesyl transferase inhibitor, B581, and lovastatin co-incubation of UVB treated cells on % proportion of cell cycle phases as assessed by flow cytometry. Exponentially growing SM1 cells were either untreated (Cont) or irradiated with UVB ($50J/m^2$) and co-incubated either with 100μM farnesyl transferase inhibitor (B581), 2mM perillyl alcohol (Poh), or 10μM lovastatin (Lov) for 48 hours in 10% (v/v) FBS. Treatments with lovastatin being in 10% (v/v) dialysed FBS. The samples were then harvested, stained with propidium iodide and analysed on the SOBR algorithm, as part of the DNA content analysis software. The data represent the % total proportion of each cell cycle phase, and the mean±SEM of three experiments. Stastistical significance was assessed by ANOVA, followed by Tukey-Kramer multiple comparisons test, where *=$p<0.05$ vs UVB. **=$p<0.001$ vs Poh, #=$p<0.001$ vs Lov and ψ=$p<0.01$ vs UVB.

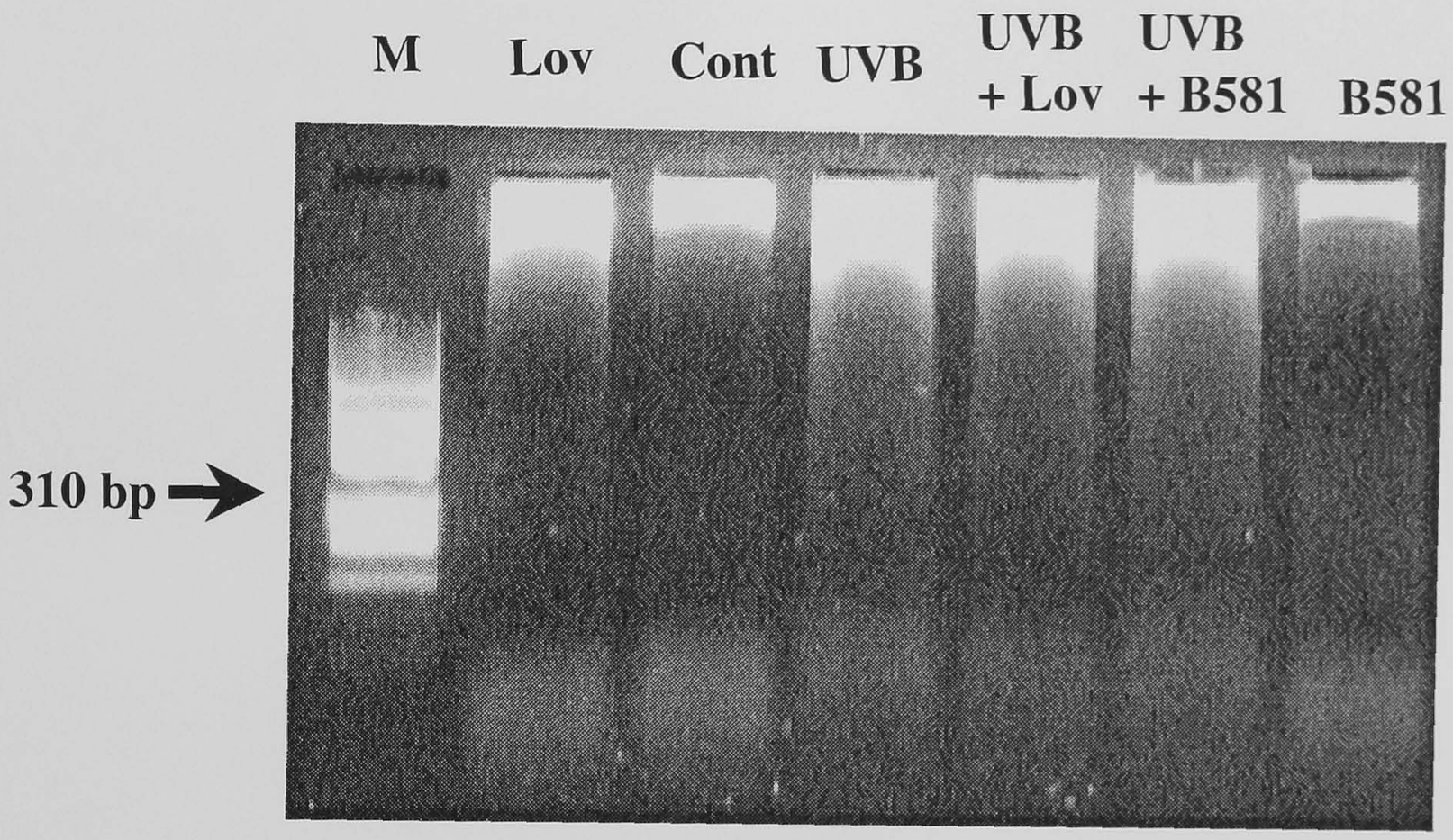


Figure 5.10 Effect of lovastatin, or the farnesyl transferase inhibitor on UVB-induced increase in DNA fragmentation. SM1 cells were untreated (Cont) or co-incubated either with 10μM lovastatin (Lov) or the farnesyl transferase inhibitor, B581 (100μM) after 50J/m^2 of UVB irradiation and incubated for 48 hours in 10% (v/v) FBS. The DNA was extracted and run on a 2% (w/v) agarose gel. However, the sensitivity of this technique may be too low to detect significant differences in hypodiploid DNA content as changes in DNA fragmentation.

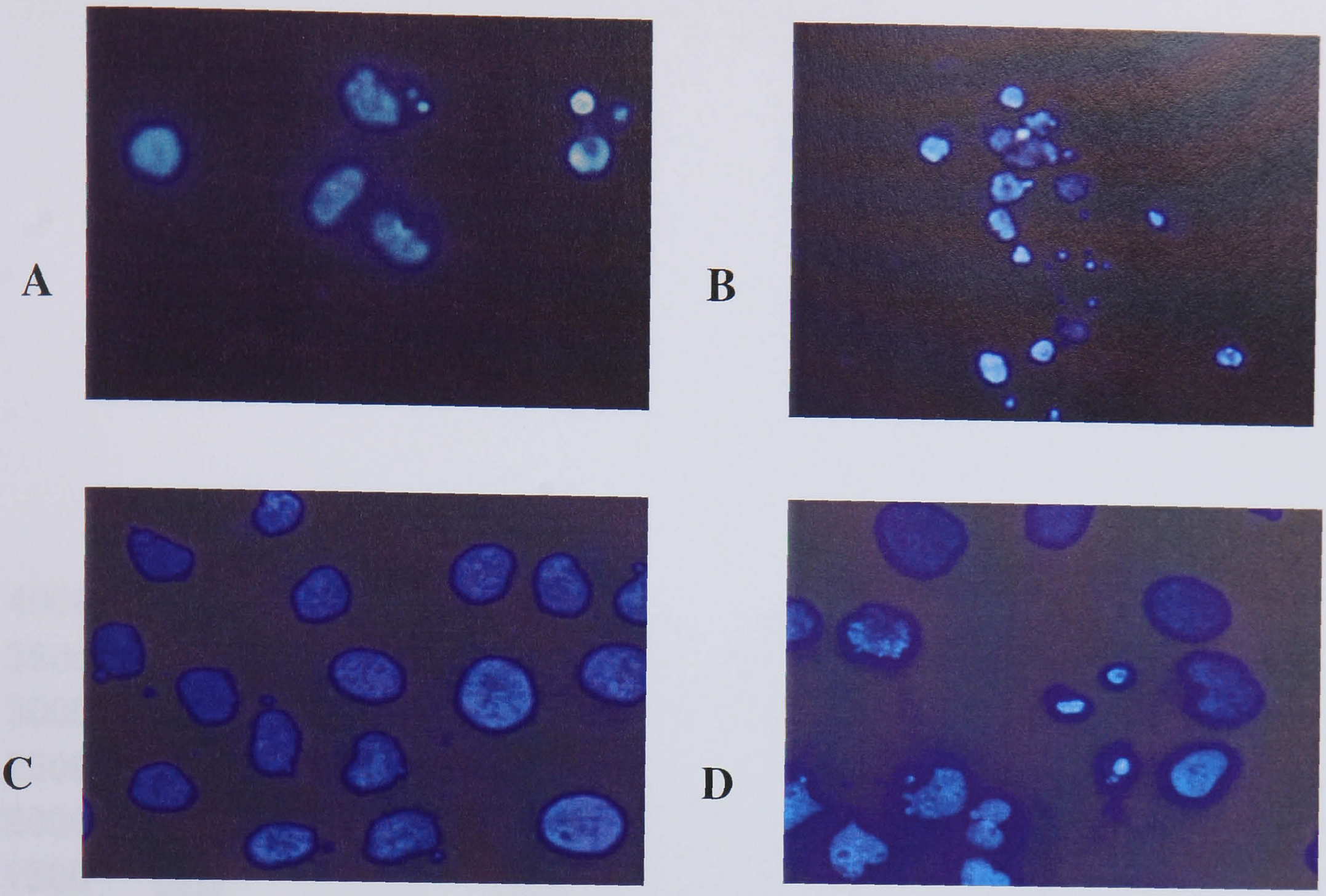


Figure 5.11 Cytochemical effects of perillyl alcohol, the farnesyl transferase inhibitor, B581, and lovastatin on UVB-induced DNA condensation in SM1 cells. Fluorescent photomicrographs of SM1 cells that have been stained with the fluorescent DNA-binding dye, DAPI, after **A)** UVB (50J/m^2) irradiation alone (original magnification x400) , or co-treatment of UVB irradiated cells with **B)** 10μM of lovastatin (original magnification x200) **C)** B581 (100μM), or **D)** 1mM of perillyl alcohol for 48 hours in 10% (v/v) FBS(original magnification x 400, respectively). The bright blue staining indicate areas of nuclear DNA condensation, usually a characteristic of apoptotic cells. The normal cells are distinct with large, uniformly stained nuclei.

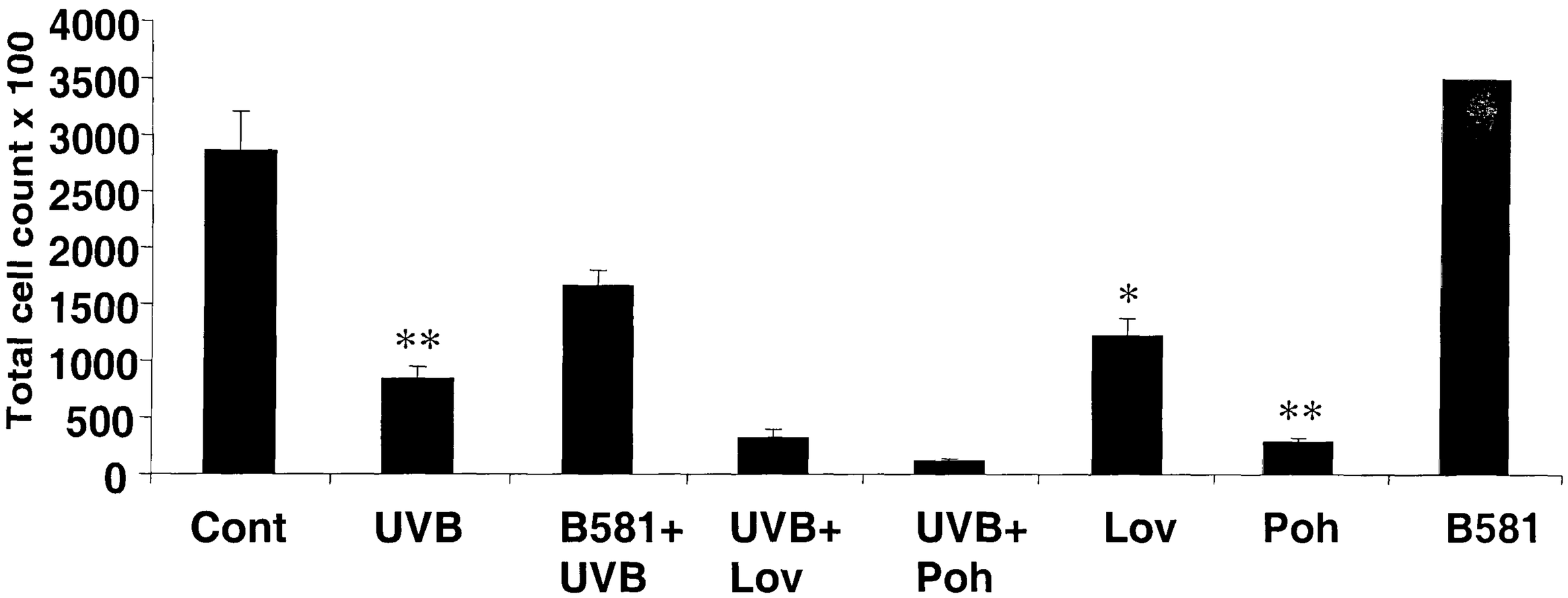


Figure 5.12 Effect of perillyl alcohol, the farnesyl transferase inhibitor, B581, and lovastatin on UVB-induced inhibition of cell proliferation in SM1 cells. Exponentially growing SM1 cells were untreated (Cont) or exposed to UVB alone ($50J/m^2$), or co-incubated either with 2mM perillyl alcohol (Poh), or 100μM farnesyl transferase inhibitor (B581), or with 10μM lovastatin (Lov) for 48 hours in 10 % (v/v) FBS. Dialysed FBS was used for all treatments with lovastatin. Results represent the mean±SEM of four experiments. Stastistical significance was assessed by ANOVA, followed by Tukey-Kramer multiple comparisons test wher, *=$p<0.01$ vs control and **=$p<0.001$ vs control.

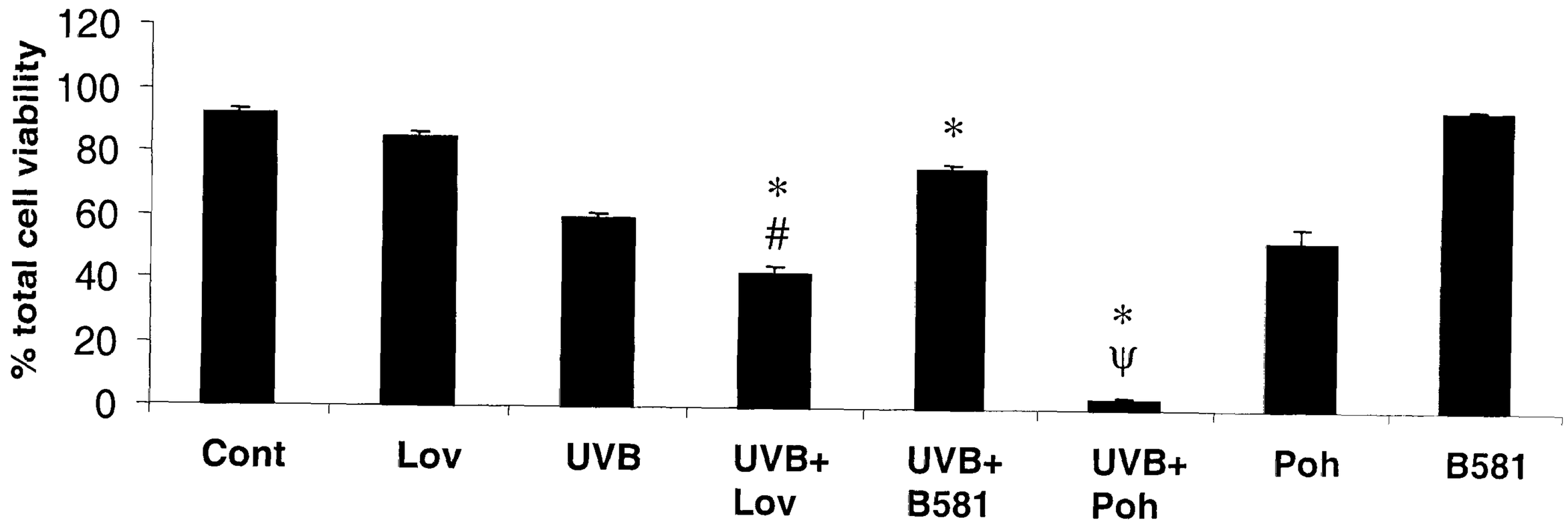


Figure 5.13 Effect of perillyl alcohol, the farnesyl transferase inhibitor, B581, and lovastatin on % total cell viability of SM1 cells exposed to UVB. Exponentially growing SM1 cells were not treated (Cont) or exposed to UVB alone or co-incubated with 2mM perillyl alcohol (Poh), 100μM of B581 or with 10μM lovastatin (Lov) for 48 hours in 10% (v/v) FBS. Percentage total cell viability was calculated every day after both the attached and the detached cells were pooled, spun down and resuspended in a 1:1 ratio (v/v) of Trypan blue : 10% (v/v) FBS. The number of viable cells (exclusion of Trypan blue) were calculated as a % proportion of the total number of cells using the Neubauer Haemocytometer. Stastistical significance was assessed by ANOVA, followed by Tukey-Kramer multiple comparisons test, where *=$p<0.01$ vs UVB, #=$p<0.001$ vs Lov and ψ=$p<0.001$ vs Poh.

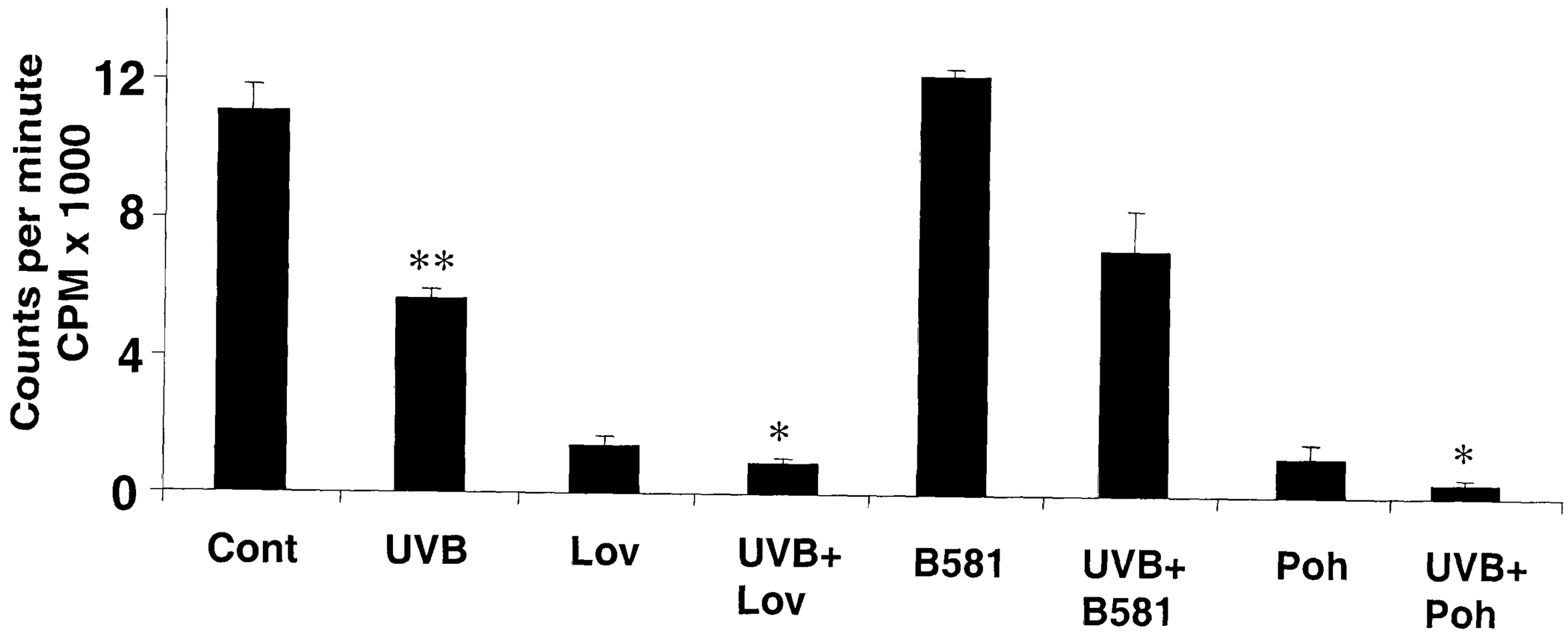


Figure 5.14 Effect of perillyl alcohol, farnesyl transferase inhibitor, and lovastatin on UVB-induced inhibition of thymidine incorporation in SM1 cells. Exponentially growing SM1 cells were untreated (Cont) or exposed to 50J/m^2 of UVB, and co-incubated either with 2mM perillyl alcohol (Poh), 100μM farnesyl transferase inhibitor (B581) or 10μM lovastatin (Lov) for 46 hours in 10% (v/v) FBS. The samples were then pulsed with [^{3}H] thymidine for 4 hours. The results represent the mean±SEM of three experiments. Stastistical significance was assessed by ANOVA, followed by Tukey-Kramer multiple comparisons test, where *=$p<0.001$ vs UVB, **=$p<0.001$ vs control.

5.1.1.3 Discussion

The results presented in this chapter indicate that UVB irradiation leads to inhibition of cell proliferation, DNA synthesis and is associated with apoptosis in transformed human VSM cells. The Ras superfamily of small GTPases have been implicated in signal transduction in response to DNA damaging agents. In this study, we used the isoprenyl transferase inhibitors perillyl alcohol, and B581, a farnesyl transferase inhibitor, to examine whether there will be any changes in the sensitivity of SM1 cells to UVB-induced cell death, inhibition of cell proliferation or DNA synthesis, when co-incubated with these reagents.

Garcia AM et. al., 1993; Cox A D et. al., 1994, first used B581 to demonstrate that this CAAX peptidomimetic compound specifically blocked signalling from the farnesylated form of oncogenic Ras protein, but not the geranylgeranylated form of oncogenic Ras, even though either form of Ras transfection led to transformation in NIH 3T3 cells. Although farnesyl transferase inhibitors have generally been used to induce apoptosis in tumour cells dependent on Ras for growth (**Gibbs JB and Oliff A, 1997; Barrington RE et. al., 1998**), addition of these inhibitors to normal cells was shown to have no effect on cell viability or cell growth (**James G L et. al., 1993**; **Kohl N E et. al., 1994**). This was an unexpected result, even though a mobility shift, implying inhibition of prenylation in both the wild type and oncogenic forms of Ras was observed (**James GL et al., 1993**). In fact, it was shown that the localisation or function of normal Ras proteins were not altered, although their farnesylation was blocked with a farnesyl transferase inhibitor (**Dalton MB et. al., 1995**). They showed that crucial cellular functions, such as cell growth and viability, including the membrane association of Ras were not compromised. Likewise, the farnesylation of other farnesylated proteins, like lamin B, was inhibited but their function remained unaltered. **Schafer WR, et. al., 1990** demonstrated results consistent with the latter, who showed that null mutations of the *RAM1* gene (the β subunit of yeast FPTase) were not lethal and cell growth was not compromised.

The actual reason for such an outcome is still unresolved, but it may be due to the existence of geranylgeranylated proteins, and the compensating role played by this alternative process of prenylation (**Whyte DB et. al., 1997**), as discussed in Chapter

3. Further evidence to justify this hypothesis comes from **James GL et. al., 1994**, who showed that when both untransformed and oncogenic H-Ras^{V12}-transformed Rat-1 cells were treated with a farnesyl transferase inhibitor, farnesylation was inhibited as expected, but there was no effect on cell viability or growth in untransformed cells, while the growth of transformed cells was markedly inhibited. However, the prenylation of cells transformed with a geranylgeranylated form of Ras, H-Ras$^{V12.\ L189}$ was not inhibited under the same circumstances. Similarly, they also demonstrated that the activity of many signalling proteins like MAP kinase and Raf was decreased as the farnesylation of oncogenic Ras proteins was inhibited, in a dose-dependent manner, in the transformed cells. In contrast, there was no significant difference in the activity of Raf or MAP kinase when the farnesylation of normal Ras was inhibited in untransformed cells.

Hence, it seems that changes in farnesylation, due to FPTase inhibitors, of normal Ras proteins does not seem to have any effect on crucial signalling processes in the cell. In contrast, oncogenic Ras-mediated activity, signalling and membrane association is known to be vitally dependent on farnesylation of the protein, as shown by **Hancock JF et. al., 1989.** Oncogenic Ras proteins, derived from oncogenic *ras* genes, are known to contain specific point mutations that abolish GTPase activity, such that the protein remains continually activated, resulting in transformation and cancerous growth (**Barbacid M, 1987**). One reason why signalling from oncogenic Ras is totally dependent on farnesylation, however, may be that in transformed, rapidly growing cells levels of farnesylated Ras are crucial and even partial inhibition retards growth. In non-transformed cells, however, there may be a degree of redundancy and effective "reserve" such that Ras signalling can proceed despite depressed total levels of farnesylated Ras protein (**Dalton MB et. al., 1995**). Furthermore, Ras turnover rates, and hence levels of new protein synthesis and farnesylation are likely to be much higher in rapidly growing cells. Finally, whilst farnesylation may be obligate for transformation where Ras performs an abnormal function it may not be crucial in non-transformed cell signalling.

Our results also suggest that inhibition of FTase is not lethal to the cell, at least over the time period studied. It is possible that GGTases, through evidence shown by other workers, might transfer geranylgeranyl pyrophosphate groups as direct substitutes for

the farnesyl moiety on proteins when farnesylation is inhibited . For example, the Rho1p and Cdc42p proteins from budding yeast *Saccharomyces cerevisiae* were shown to be utterly dependent on geranylgeranyl modification, such that inhibition of GGTase I in these organisms prevented growth (**Ohya Y et. al., 1993**). However, when C-terminal sequences of these proteins were altered such that they could only be modified with farnesyl transferase (FTase), then the activity of this enzyme normally not essential for growth became essential. Similar results were seen by **Miquel K et. al., 1997**, who demonstrated that a GGTase inhibitor, called GGTI-298, led to apoptosis in human lung adenocarcinoma cells, but an inhibitor of FFTase, FTI-277 did not lead to apoptosis.

Other workers have demonstrated that complete inhibition of H-Ras and K-Ras prenylation in the presence of either FTase and/or GGTase inhibitors was never achieved, indicating that these proteins were always prenylated in the presence of either prenyl transferase inhibitor (**Lerner EC et. al., 1997**). It is also interesting to note that lamin farnesylation and localisation were not disturbed, but oncogenic Ras farnesylation, and hence cell growth, were inhibited in human tumours treated with FPTase inhibitors (**Nagase T et. al., 1997**).

Our results indicate that UVB (about 314nm) irradiation of SM1 cells is associated with apoptosis, as revealed through DAPI and TUNEL staining, the DNA ladder assay, and as (indirectly) quantified by flow cytometry. However, exposure of SM1 cells to UVB irradiation was also associated with changes in the percentage proportion of cell cycle phases, as measured through the SOBR algorithm after flow cytometry. A dramatic reduction in G_o/G_1 phase was seen after UVB exposure, accompanied with a rise in S phase, as well as an increase in the proportion of the hypodiploid region, a marker of apoptosis, at 24 hours post-irradiation (**Figure 5.6 and 5.5**). The increase in S phase proportion may not reflect a true increase in S phase entry, or DNA synthesis, since [^{3}H] thymidine incorporation, (**Figure 5.14**), indicated a marked reduction in DNA synthesis levels after UVB exposure. This apparent increase in S phase could result from a disproportionate loss of cells in G_o/G_1 phase (through apoptosis) , leading to an apparent increase in cells in S phase despite reduced overall levels of [^{3}H] thymidine incorporation.

Interestingly, co-incubation of B581 with UVB treated cells was not associated with a significant change in levels of apoptosis in these cells, as depicted in **Figure 5.8**. Likewise, there was no significant change in levels of apoptosis in control untreated cultures when exposed to B581. No significant changes in any of the cell cycle phases, G_o/G_1, S or G_2/M phase were seen between the UVB and B581 co-treated cultures and those treated with UVB alone (**Figure 5.9**). Significant changes in these cell cycle phases were also absent after treatment with B581 alone with respect to untreated cultures. The DAPI stains of cultures co-treated with both UVB and B581 generally revealed normal, heterogenous, and uncondensed nuclei (**Figure 5.11**), although some apoptotic bodies, without any bright blue staining were seen. In terms of total cell counts, there was no significant change in cell numbers between cultures exposed to UVB alone and those co-treated with UVB and B581 (**Figure 5.12**). There was also no significant change in $[^3H]$ thymidine incorporation (**Figure 5.14**) in cultures treated with both UVB and B581, compared to those treated with UVB alone, and also after treatment with B581 alone, compared to untreated cultures. However, the Trypan blue exclusion (viability) assay indicated a significant increase in total percentage viability in cultures co-treated with both UVB and B581, with respect to those treated with UVB alone (**Figure 5.13**).

These results indicate that B581 has no substantial effect on SM1 cell growth or apoptosis, although percentage total cell viability seemed to be increased. The DAPI pictures also indicate normal, heterogenous nuclei. A similar response was reported by another group of workers (**Fokstuen T et. al., 1997**) with another farnesyl transferase inhibitor, BZA-5B. They observed a decreased number of cells with *in situ* DNA fragmentation positivity using the TUNEL reagent and increased cell viability with BZA-5B and cisplatin treatment.

In contrast to the effect of B581 on normal and UVB-induced apoptosis in SM1 cells, addition of perillyl alcohol, another prenyl transferase inhibitor, to UVB-induced cells was associated with enhanced apoptosis with respect to cultures exposed to UVB alone or perillyl alcohol alone (**Figure 5.8**). Significant increase in G_o/G_1 phase, but significant decrease in S and G_2/M phases were evident when cells were co-incubated with UVB and perillyl alcohol (**Figure 5.9**). This indicated that growth arrest at G_o/G_1 was enhanced in the presence of perillyl alcohol, while entry into S phase was

decreased, which was also confirmed by the [^{3}H] thymidine incorporation data (**Figure 5.14**). Levels of DNA condensation, as assessed by DAPI staining of cells, indicate that this morphological characteristic of apoptosis was increased under these conditions (**Figure 5.11**). However, cell proliferation was not significantly affected as the number of cells in UVB and perillyl alcohol co-treated cultures were not statistically less than cultures treated with UVB alone (**Figure 5.12**). In contrast, percentage total cell viability was also markedly decreased in UVB and perillyl alcohol co-treated cultures, compared to cultures treated with UVB or perillyl alcohol alone (**Figure 5.13**).

Likewise, addition of lovastatin to UVB treated cultures was associated with increased apoptosis, with respect to cultures treated with UVB or lovastatin alone (**Figure 5.8**). Under these circumstances, all the cell cycle phases, G_o/G_1, G_2/M and S phase were affected. The G_o/G_1 phase was significantly reduced in co-treated cultures with respect to cultures treated with UVB or lovastatin alone, while the S phase was significantly increased in co-treated cultures with respect to those treated with lovastatin alone (**Figure 5.9**). However, the G_2/M phase of co-treated cultures was increased with respect to both lovastatin or UVB alone treatments. These results indicate a selective loss of cells in G_o/G_1 phase through apoptosis, which may result in an apparent increase in S phase proportion as discussed above, since thymidine incorporation data show a clear inhibition of DNA synthesis under these circumstances (**Figure 5.14**).

However, a significant change in cell proliferation in UVB treated cultures, with respect to UVB and lovastatin co-treated cultures, was not seen (**Figure 5.12**), although a significant decrease in percentage total cell viability was observed (**Figure 5.13**). These data indicate that lovastatin treatment is associated with increased apoptosis in UVB treated cultures, but this does not seem to affect the cell numbers. Comparable results were also obtained by **Quiec D et. al., 1995**, who demonstrated that lovastatin enhanced the photocytotoxicity of UVA radiation towards cultured human keratinocytes. Likewise, results of **Vogt A et. al., 1996** also showed that a lovastatin-induced block in G_o/G_1 in mouse fibroblasts was released when co-incubated with mevalonate, and was reversed upon co-incubation with GGTI-298, but not with the farnesyl protein transferase inhibitor, FTI-277. Hence this FPTase

inhibitor had no effect on growth, just as B581 had no effect on growth in untreated, control SM1 cells.

In conclusion, the above results demonstrate that lovastatin, an HMG CoA reductase inhibitor and perillyl alcohol, a putative inhibitor of prenyl transferase interact additively with UVB in terms of apoptosis, and inhibition of DNA synthesis. This confirms that a depletion of geranyl geranyl pyrophosphates, either through lovastatin or through perillyl alcohol (a putative GGTase inhibitor) is associated with enhanced apoptosis in this cell type. In contrast, inhibition of farnesyl protein transferase does not seem to affect apoptosis, cell growth, DNA synthesis or viability in untreated cultures. Even following UVB irradiation it was not possible to discern an effect of the selective farnesyl transferase inhibitor, B581, on apoptosis, cell growth or DNA synthesis in these cells. Although B581 was associated with increased cell viability following UVB irradiation, the mechanism and significance of this observation remains unclear.

Chapter 6

Stimulation with platelet-derived growth factor-BB is associated with apoptosis in cultured primary human VSM cells derived from saphenous vein

6.1.1.1 Introduction

Platelet-derived growth factor (PDGF) was first discovered when serum from clotted blood was shown to stimulate proliferation of aortic vascular smooth muscle cells at a significantly greater rate than serum from platelet-free blood (**Ross R et. al., 1974**). Subsequently, platelets were found to be required for the growth of fibroblasts in culture (**Kohler N and Lipton A, 1974**).

Structurally, a PDGF molecule consists of a glycoprotein dimer of molecular weight 28-30 kDa, composed of two polypeptide chains. Two PDGF monomers exist, A and B. Two of the B monomers are linked by disulphide bonds to form one of the three isoforms, PDGF-BB, and depending on chain identity, the other isoforms are PDGF-AB or PDGF-AA (**Heldin CH, 1992**).

Platelet-derived growth factor-BB has been shown to be a potent inducer of DNA synthesis in many cell types, including human vascular smooth muscle cells (**Hughes A D et. al., 1995**). However, on its own, it is known to be a weak stimulator of mitosis, unless other "progression" factors like insulin, insulin-like growth factor, required for the successful completion of S phase are present in the exracellular milieu (**Olashaw N E et. al., 1987**; **Stiles C D, 1983**). Hence, it has been termed merely as a "competence" factor for growth–arrested, serum starved cells, since genes required for entry into the G_1 phase are upregulated when cells in growth arrest or G_0/G_1 phase are exposed to it (**Stiles CD et. al., 1979; Pledger WJ et. al., 1981).**

Addition of a PDGF antibody was shown to abrogate the accumulation of neointimal VSM cells *in vivo* after balloon injury of normal rat carotid artery, indicating that it could have chemoattractanct properties (**Ferns G A et. al., 1991**). *In vitro*, PDGF-BB was shown to lead to directional migration of VSM cells, but the intracellular signals elicited were distinct from those evoked during cell proliferation (**Bornfeldt K E et.**

al., 1995), as well as showing different concentration relationships, at least in human VSM cells (**Clunn G et. al., 1997**).

In the vascular system, this polypeptide is not only released from platelets, but also from endothelial cells, macrophages/monocytes and vascular smooth muscle cells (**Baumgartner and Hosang, 1988**). PDGF was found to be important not only during normal development of the vascular system (**Raff MC et. al., 1988; Yeh H-J et. al., 1991**) but also in the vascular response to injury and in the development of atherosclerosis (**Ross R, 1993**). Human carotid artery primary atherosclerotic lesions were shown to contain greater levels of PDGF-β chain gene transcript than normal artery tissues (**Barrett TB and Benditt EP, 1987**). Pronounced expression of β-type receptors for PDGF was seen on vascular smooth muscle cells in atherosclerotic plaques (**Rubin K et. al., 1988**). This protein was shown to be upregulated on the smooth muscle cells from the stage of macrophage infiltration (**Bohm M et. al, 1994**). Neointimal formation was shown to precisely correlate with PDGF receptor β subunit expression in an exponential fashion (**Sirois MG et. al., 1997**). It has been speculated that PDGF may be involved in the development of hyperplasia, which is frequently observed during vascular hypertrophy (**Campbell JH et. al., 1991**)

An interesting observation to note is that cells in tissues where PDGF is highly expressed tend to be localised in conditions unfavourable for cell growth. This indicates that PDGF may have a plethora of effects on the intracellular property of each cell, depending upon the extracellular or environmental context in which the cell is found.

Induction of apoptosis is known to be influenced by the presence of survival factors such as basic fibroblast growth factor (bFGF) (**Fox JC and Shanley JR, 1996**), and insulin-like growth factor (IGF-I) (**Bennett M R et. al., 1995**). PDGF-BB was reported to act as a survival factor in human cultured aortic and coronary arterial smooth muscle cells (**Bennett M R et. al., 1995**). However, it was also implicated in oncogenic transformation, especially in the formation of a functional vascular system required for tumour formation (**Forsberg K et. al., 1993; Westermark B et. al., 1993**).

Although the knowledge of intracellular signals responsible for cell survival and control of apoptosis in VSM cells is incomplete, our earlier studies with SM1 cells also implicated that a protein which may be geranylgeranylated may be required for survival in VSM cells. The small Ras-like GTPase Rho was shown to associate with the PDGF type-β receptor upon ligand binding (**Zubiaur M et. al., 1995**). The same molecule was shown to be required for G_1 progression (**Weber J D et. al., 1997**). Rapid induction of *rhoB* gene was also observed when quiescent rat fibroblasts were stimulated with PDGF (**Jahner D and Hunter T, 1991**).

In this study, we provide evidence that stimulation of quiescent human vascular smooth muscle cells with PDGF-BB in serum-free medium leads to apoptosis.

6.1.1.2 Results

6.1.2.2 *Cell death and entry into S phase after stimulation of confluent growth-arrested human VSM cells with PDGF-BB*

Primary human vascular smooth muscle cells derived from saphenous vein at passage 3 were growth arrested for 7 days in serum-free medium (NCTC-109, supplemented with BSA). The cells were then stimulated with PDGF-BB (at 20ng/ml) in serum-free medium over a period of 24 and 48 hours.

Morphological changes with the light microscope were not apparent (**Figure 6.1**). However, staining with the DNA-binding dye DAPI revealed many nuclei containing bright, condensed DNA (**Figure 6.2**).

Staining with the TUNEL reagent also revealed specific labelling around the edge of the nucleus (**Figure 6.3**).

Analysis of the cell cultures with flow cytometry after PI staining demonstrated that there was an increase in the percentage proportion of the hypodiploid region, characteristic of apoptosis (**Figure 6.4**). There was a significant increase in

hypodiploid DNA content from 2±1% in vehicle treated, control cultures to 24±6% in PDGF-BB treated cultures after 48 hours ($p<0.01$, $n=4$).

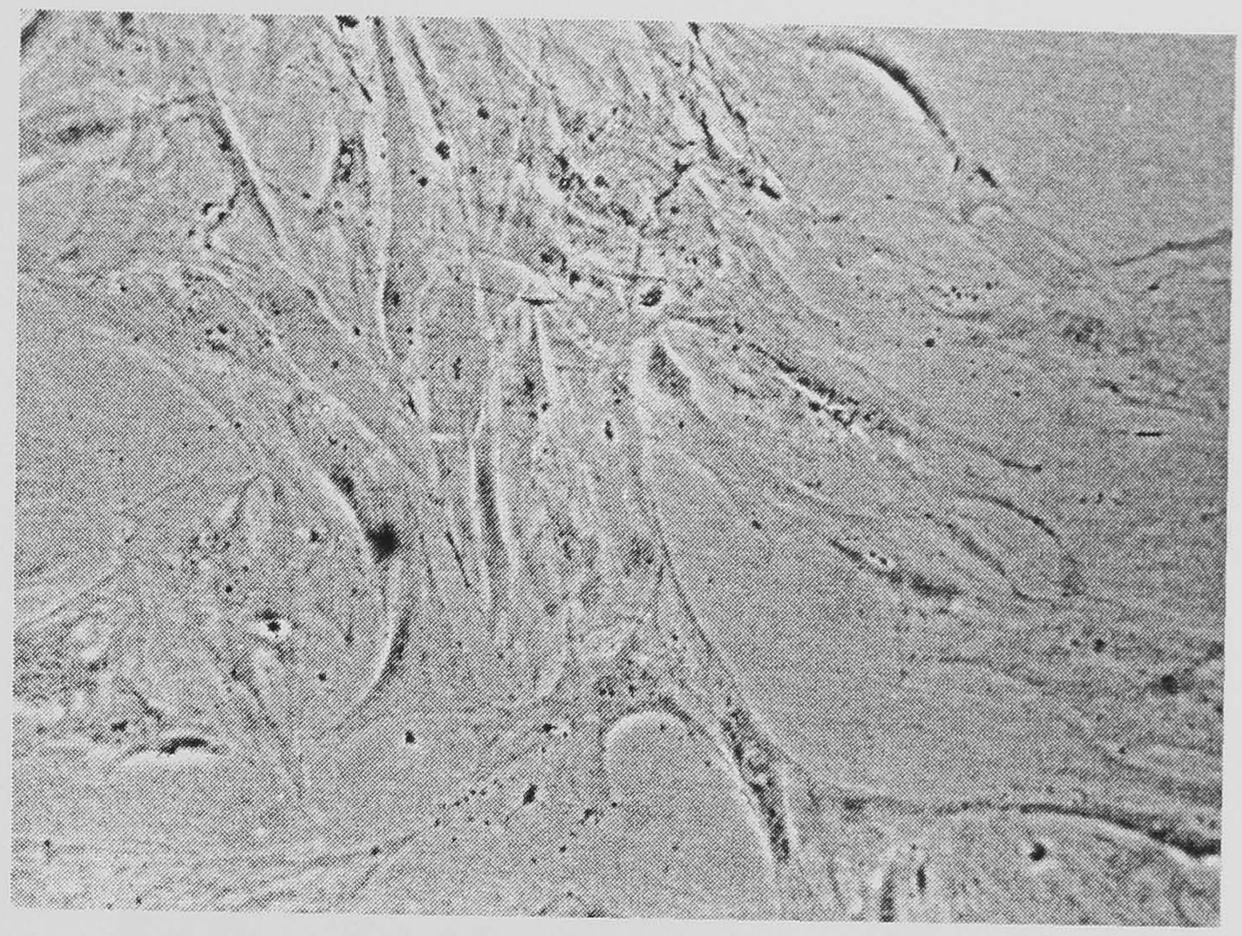
An increase in the proportion of the hypodiploid region was also confirmed with the characteristic DNA laddering pattern after gel electrophoresis (**Figure 6.5**).

Measurement of S phase proportion as part of cell cycle analysis with flow cytometry, indicted that there was a significant rise in S-phase of VSM cells after being exposed to PDGF-BB (**Figure 6.6**). Stimulation with PDGF-BB increased the proportion of cells in S-phase from 3±1% in control cultures to 8±1% in PDGF-BB exposed cultures at 24 hours ($p<0.05$, $n=4$).

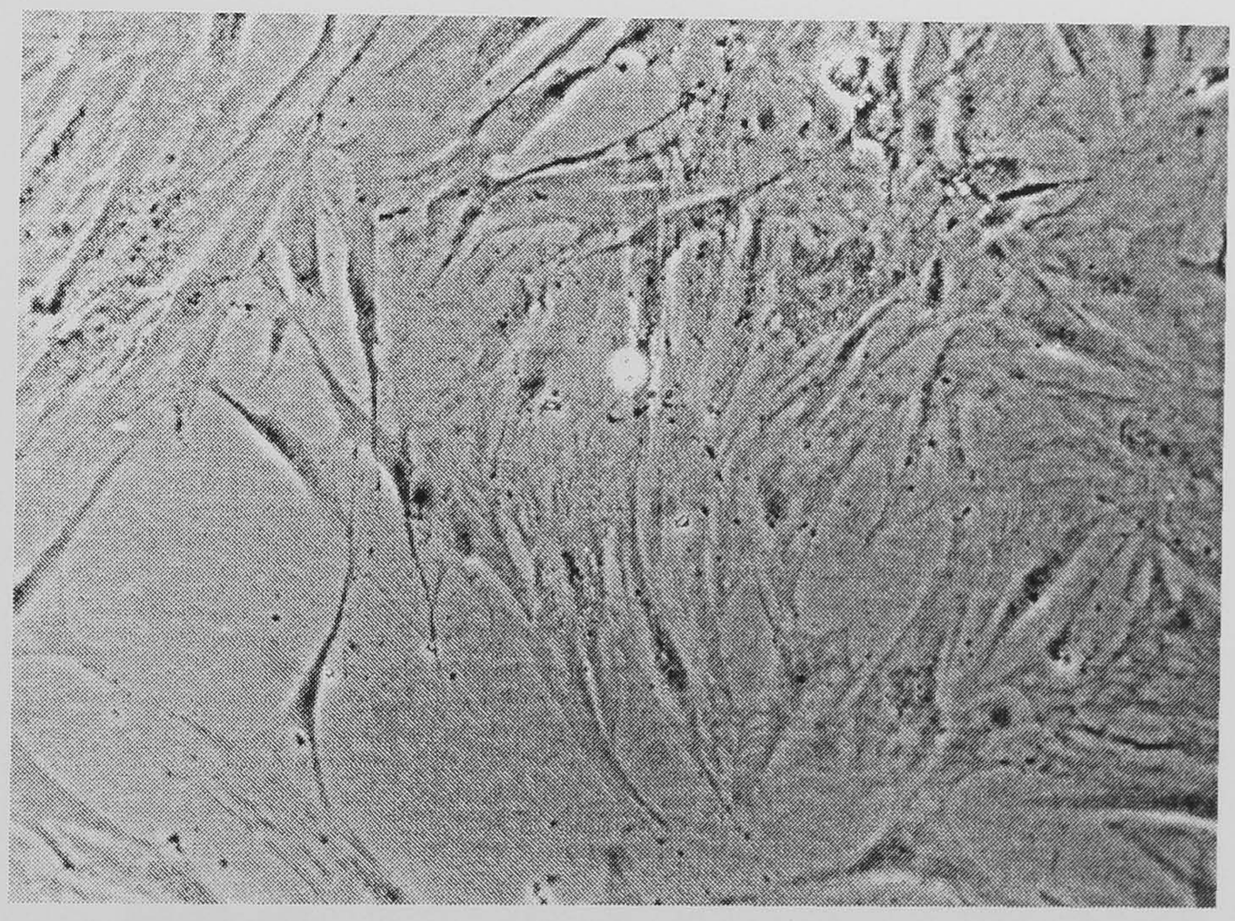
6.1.3.2 Effect of lovastatin on PDGF-BB-induced apoptosis and S phase entry in human VSM cells

Lovastatin (10μM) was co-incubated with PDGF-BB (20ng/ml) when cells were stimulated after growth arrest for 7 days. Co-incubation with lovastatin inhibited the increased proportion of the hypodiploid region, a marker of apoptosis, with respect to PDGF-BB alone treated cultures. DNA content of the hypodiploid region decreased from 24±6% in PDGF-BB treated cultures to 10±2.5% in cultures co-incubated with lovastatin and PDGF-BB ($p<0.01$, $n=4$). Treatment with lovastatin alone had no significant effect on the percentage of the hypodiploid region or on S phase in these cells (**Figure 6.6**).

Cytochemical staining with DAPI and TUNEL reagent confirmed that co-incubation of PDGF-BB treated cell cultures with lovastatin was associated with decreased levels of apoptotic cell death (**Figure 6.7 and 6.8, respectively**).



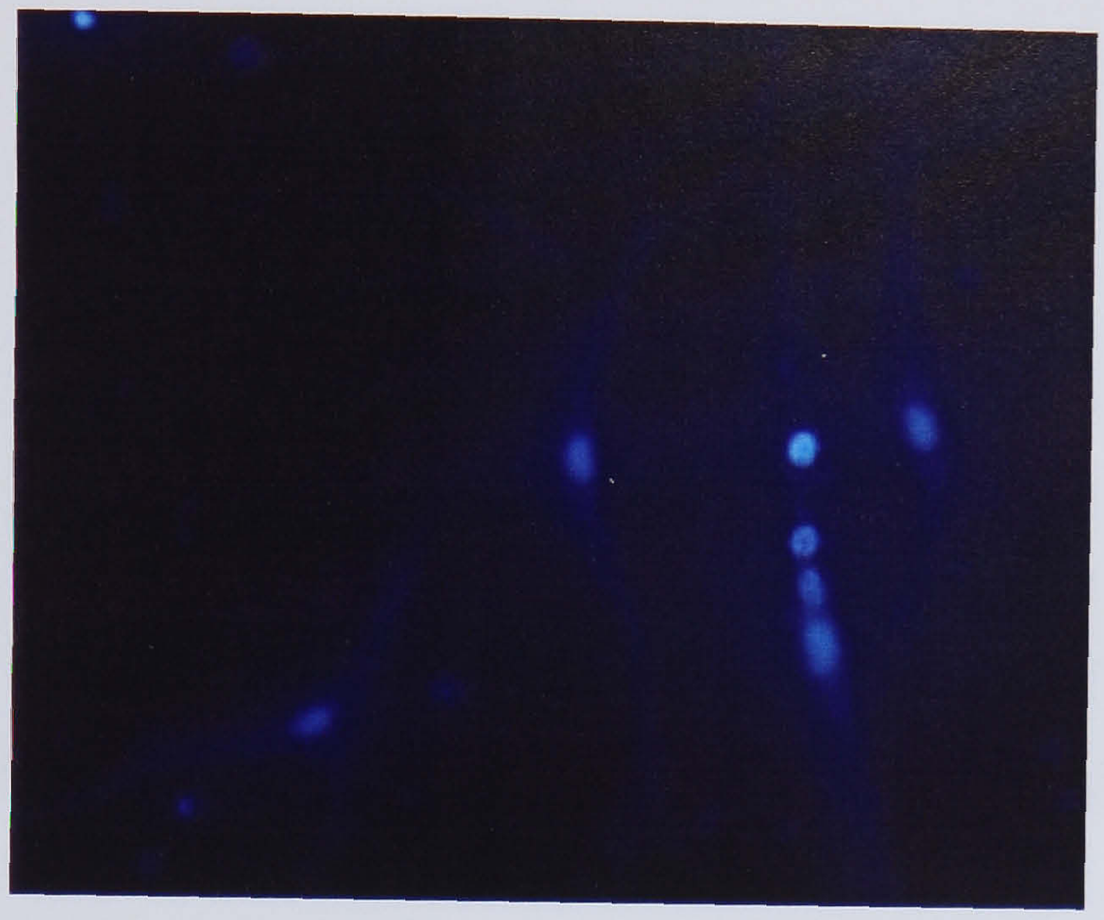
A



B

Figure 6.1 Morphological effects of PDGF-BB in growth-arrested primary human saphenous vein-derived smooth muscle cells in culture. Light microscopy photomicrographs of PDGF-BB-treated VSM cells, indicating the presence of some common morphological features of apoptosis, such as retracted cells and a rounded up cell **A**) growth-arrested human VSM cells in the absence of any treatment, in serum-free medium **B**) after treatment with 20ng/ml PDGF-BB for 48 hours (original magnification x100, respectively).

A



B

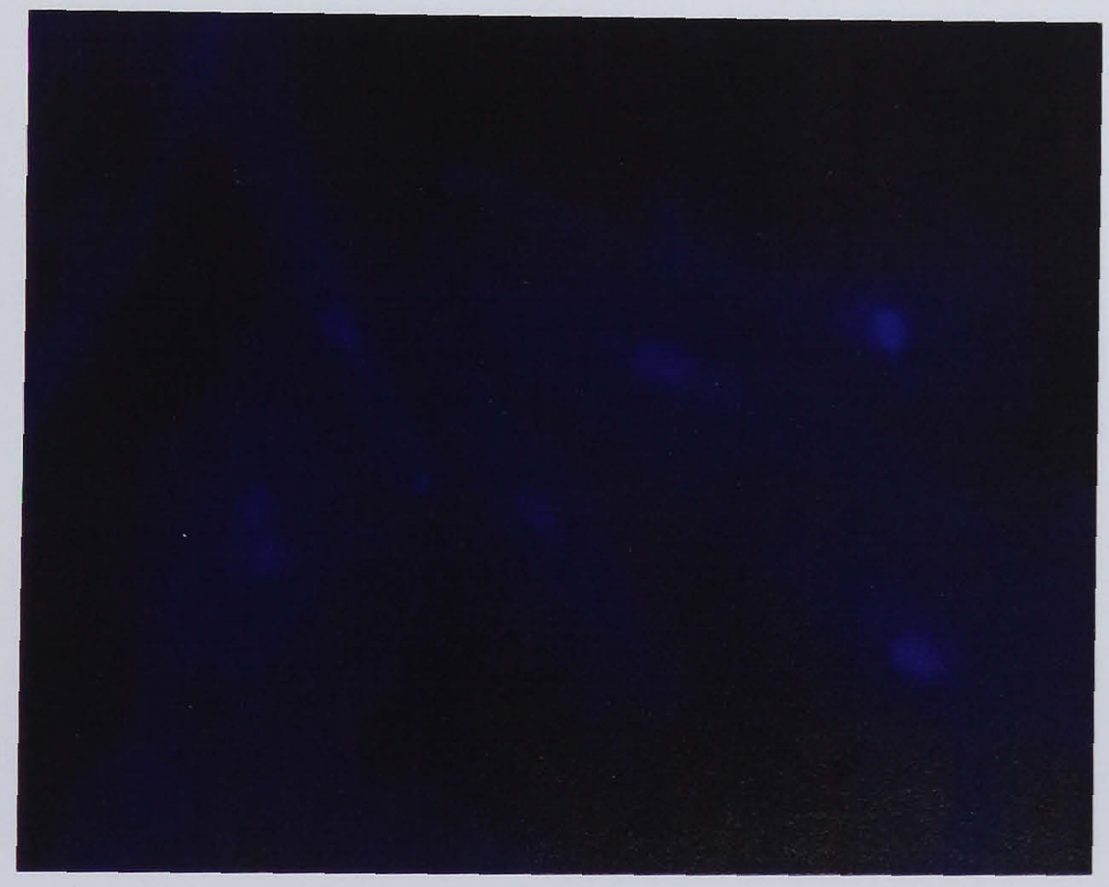
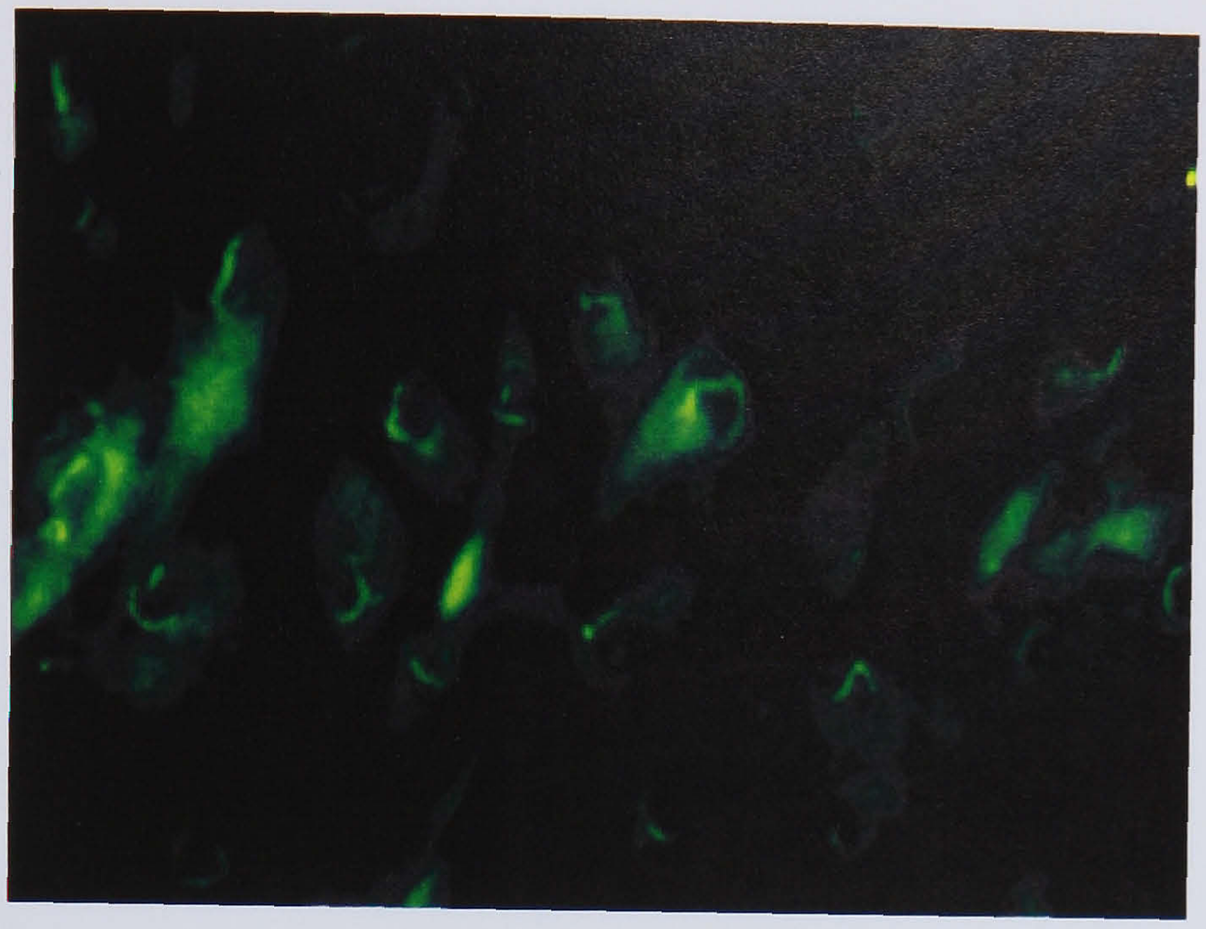


Figure 6.2 Cytochemical effects of stimulation of growth-arrested human VSM cells with PDGF-BB. Fluorescent photomicrographs of human VSM cells that have been stained with the fluorescent DNA-binding dye, DAPI, after treatment with **A)** 20ng/ml PDGF-BB of growth-arrested cells **B)** no treatment for 48 hours in serum-free medium (original magnification x 400). The bright blue staining indicate areas of nuclear DNA condensation, usually a characteristic of apoptotic cells.

A



B



Figure 6.3 Effects of PDGF-BB on fluorescent DNA fragmentation in growth-arrested human VSM cells. Growth-arrested human VSM cells were exposed to **A)** 20ng/ml PDGF-BB for 48 hours, and stained with the TUNEL reagent (transferase-mediated dUTP end-labelling) **B)** no treatment (original magnification x400). The bright green staining around the edges of the nuclei probably indicate the TUNEL-positive chromatin with DNA fragmentation. Positive staining is absent in the control samples (except for some background staining).

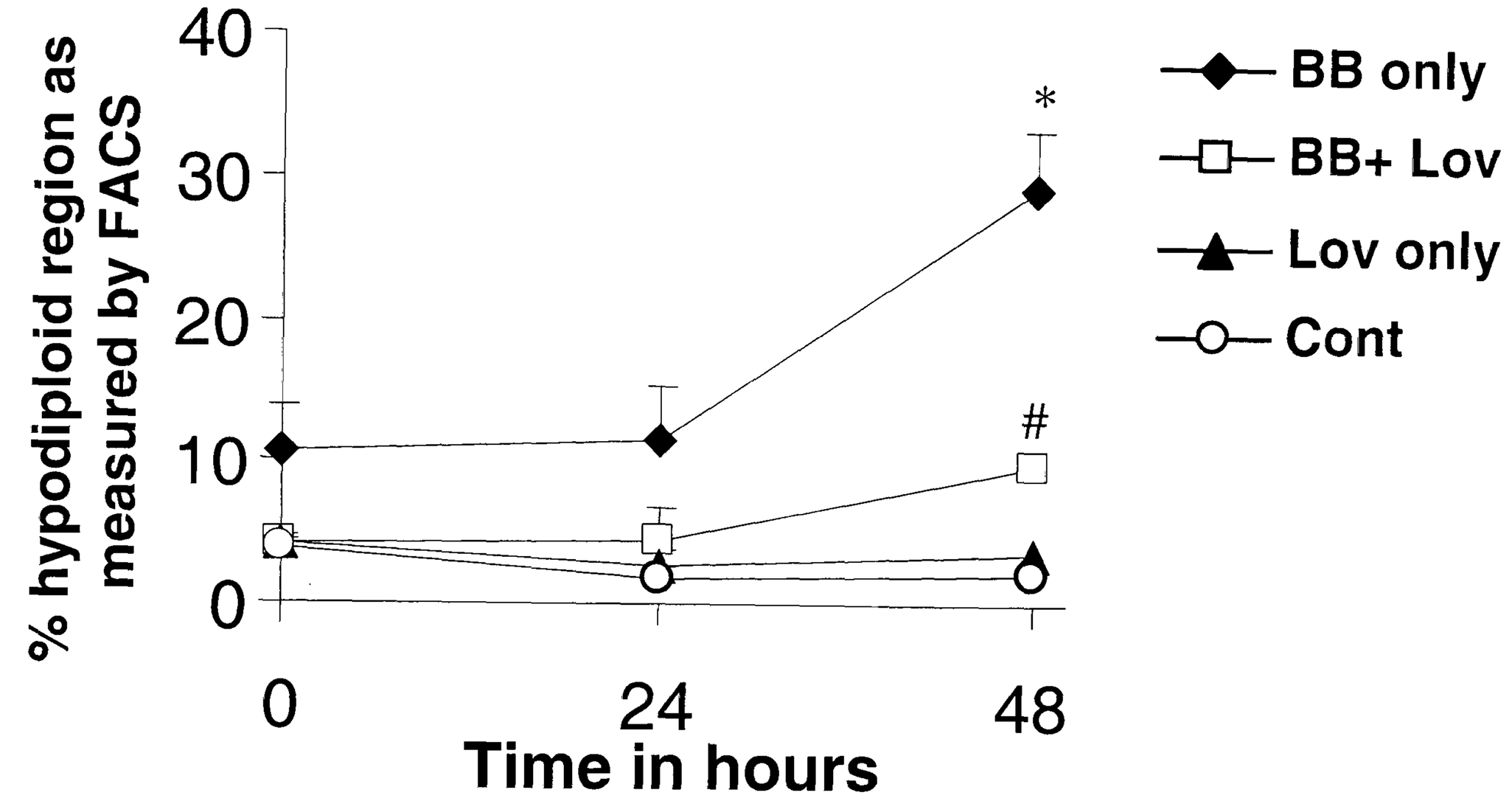


Figure 6.4 Effect of treatment of growth-arrested primary VSM cells with PDGF-BB, and co-incubation with lovastatin on hypodiploid DNA content of cultures. Growth-arrested primary human VSM cells were either exposed to 20ng/ml PDGF-BB (BB) alone, or co-incubated with PDGF-BB and lovastatin (10μM) (BB+Lov), or to lovastatin alone (Lov) or vehicle (Veh) alone for upto 48 hours in serum-free medium. The samples were then harvested, stained with propidium iodide and analysed through flow cytometry. The results represent % total proportion of the hypodiploid region and the mean±SEM of four experiments. Statistical significance was assessed by ANOVA, followed by the Tukey-Kramer multiple comparisons test, where *=$p<0.01$ vs control, and #=$p<0.01$ vs BB only.

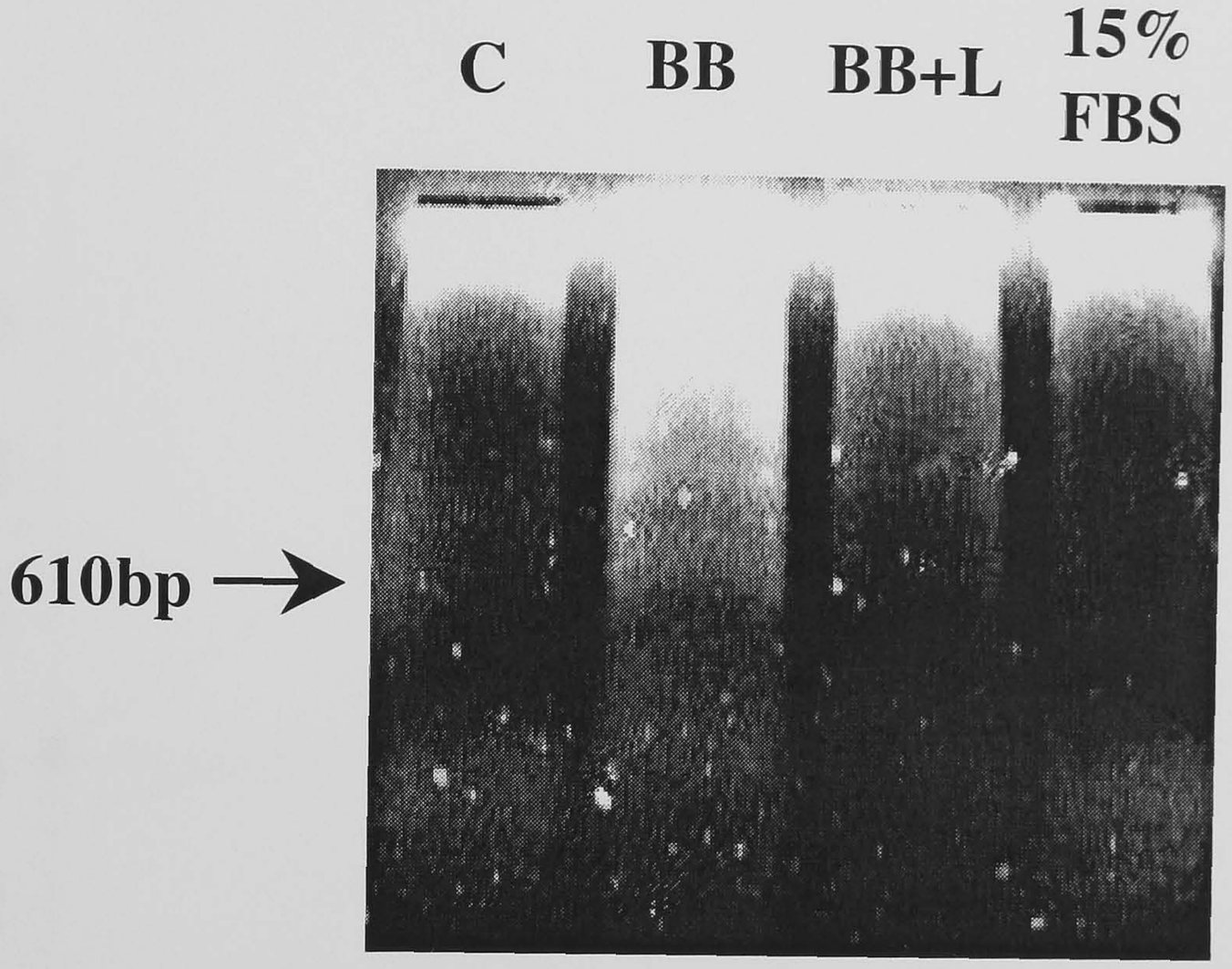


Figure 6.5 The effect of stimulation with PDGF-BB on DNA fragmentation in growth-arrested primary human VSM cells. Agarose gel (2%) (w/v) electrophoresis of DNA extracted from growth-arrested primary human VSM cells were either stimulated with 100ng/ml PDGF-BB alone (BB), co-treated with both 100ng/ml PDGF-BB and 10μM lovastatin (BB+Lov), no treatment (C) for 48 hours in serum-free medium or stimulated with 15% (v/v) FBS (15% FBS). Treatment with PDGF-BB alone was associated with an increase in levels of DNA fragmentation, resulting in high molecular weight DNA fragments. Lane M indicates the DNA size marker, ϕX174 plasmid cut with *Hae* III (0.04mg/ml). The final optimised procedure was used to extract the DNA from the cells, and the gel was cast with 1:10000 dilution of SYBR Green I dye and half of the total amount of extracted DNA was loaded onto the gel.

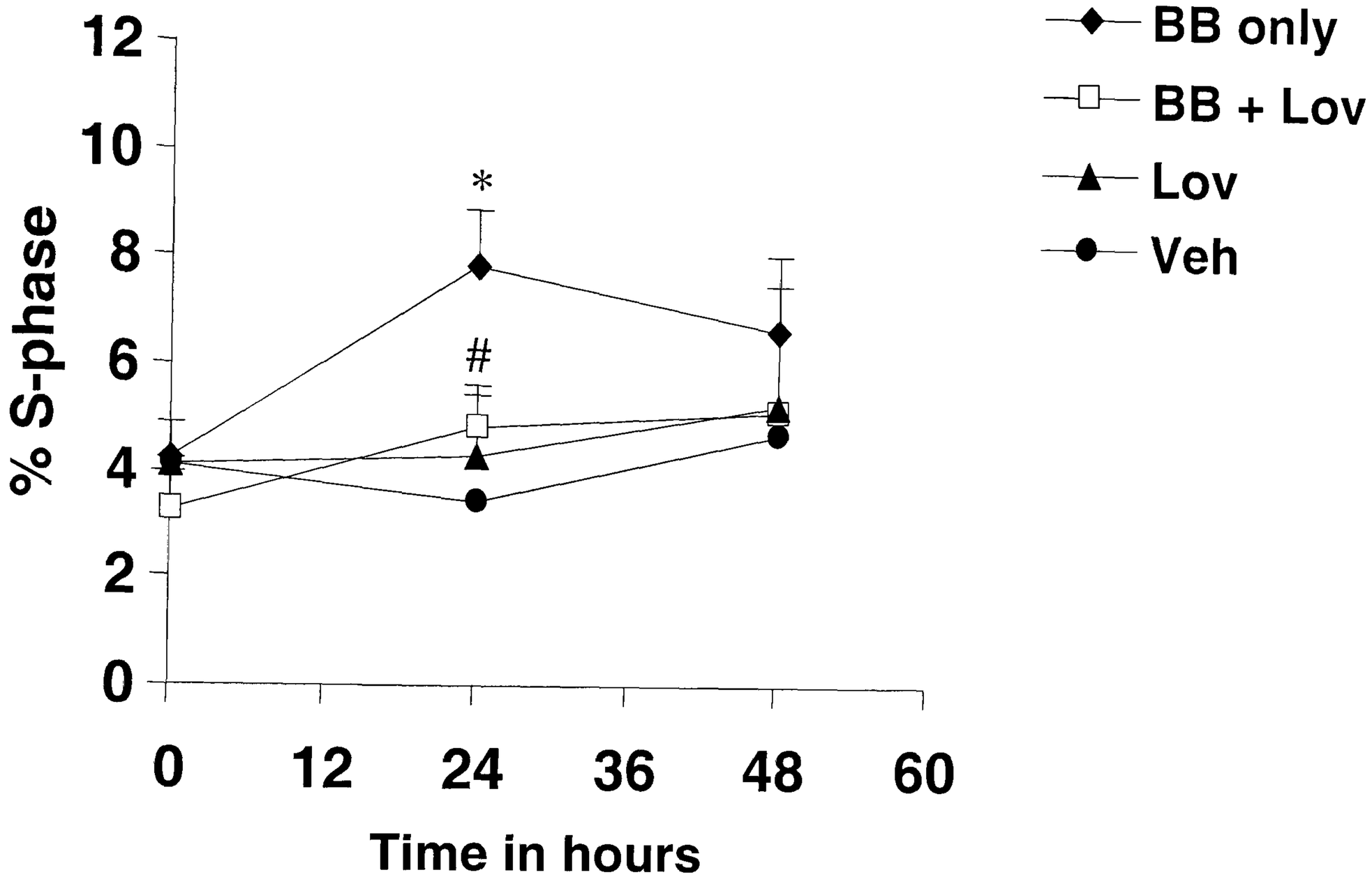
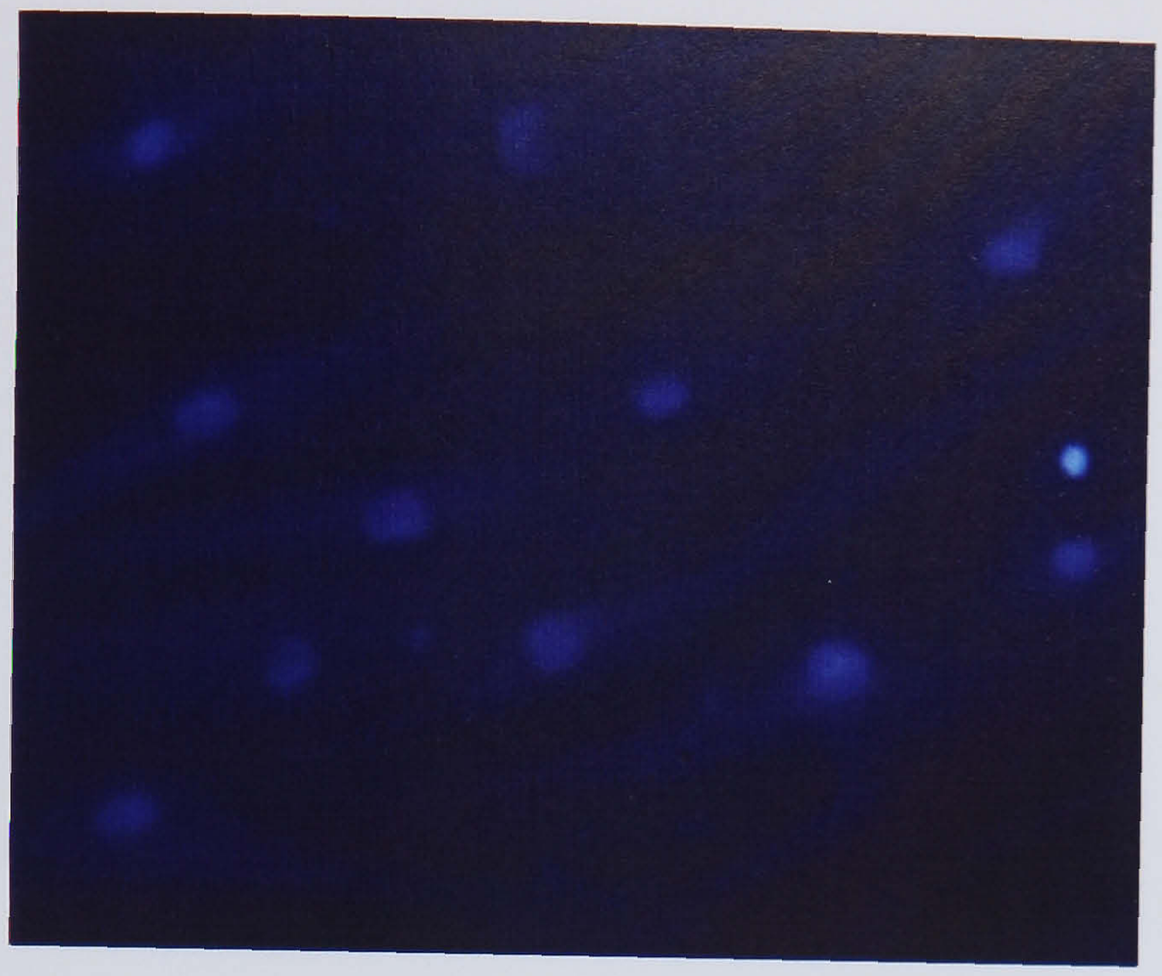
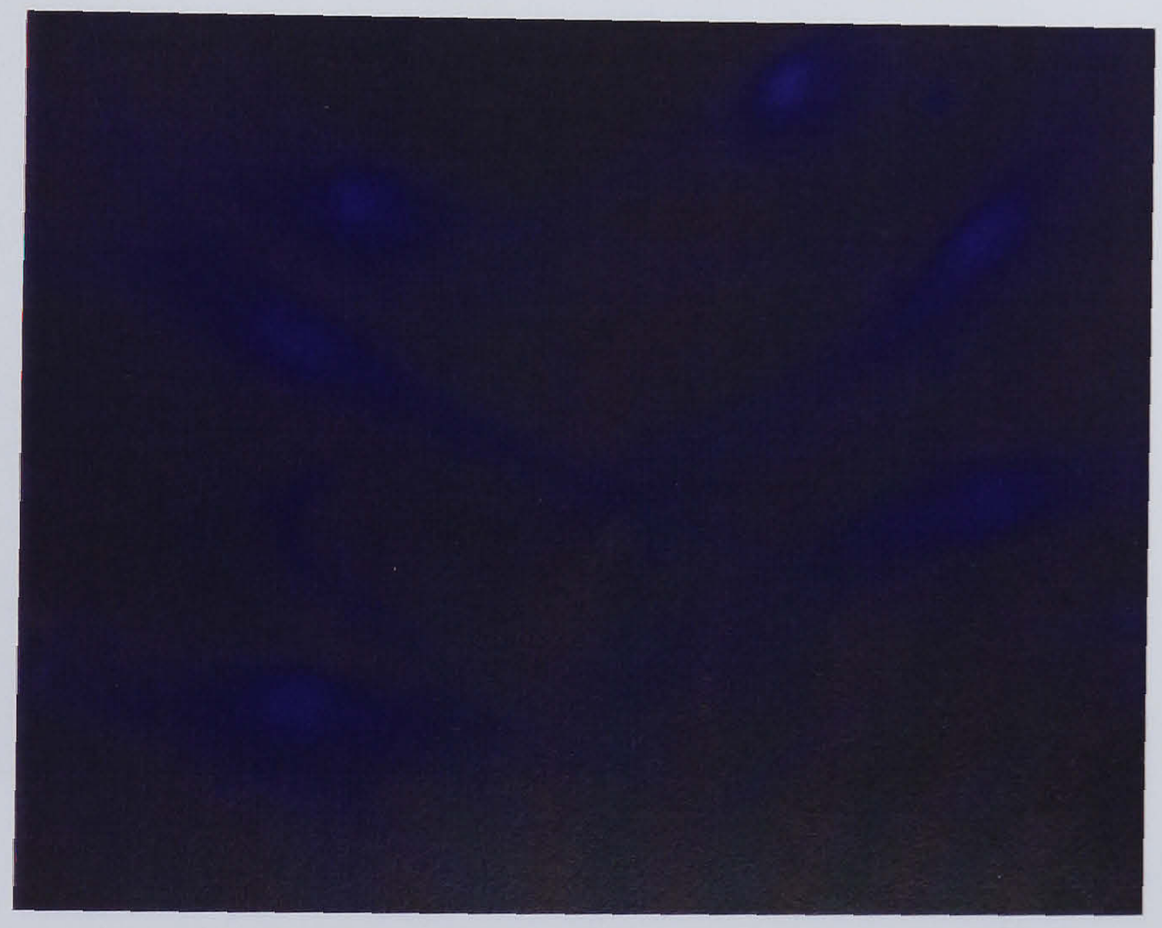


Figure 6.6 Effect of treatment of growth-arrested primary VSM cells with PDGF-BB, and co-incubation with lovastatin on cell cycle S-phase DNA content of cultures. Growth-arrested primary human VSM cells were either exposed to 20ng/ml PDGF-BB (BB) alone, or co-incubated with PDGF-BB and lovastatin (10μM) (BB+Lov), or to lovastatin alone (Lov) or vehicle alone (Veh) for upto 48 hours in serum-free medium. The samples were then harvested, stained with propidium iodide and analysed through flow cytometry. The results represent the mean±SEM of four experiments. Statistical significance was assessed by ANOVA, followed by Tukey-Kramer multiple comparisons test, where *=$p<0.05$ vs control, # =$p<0.01$ vs BB only.

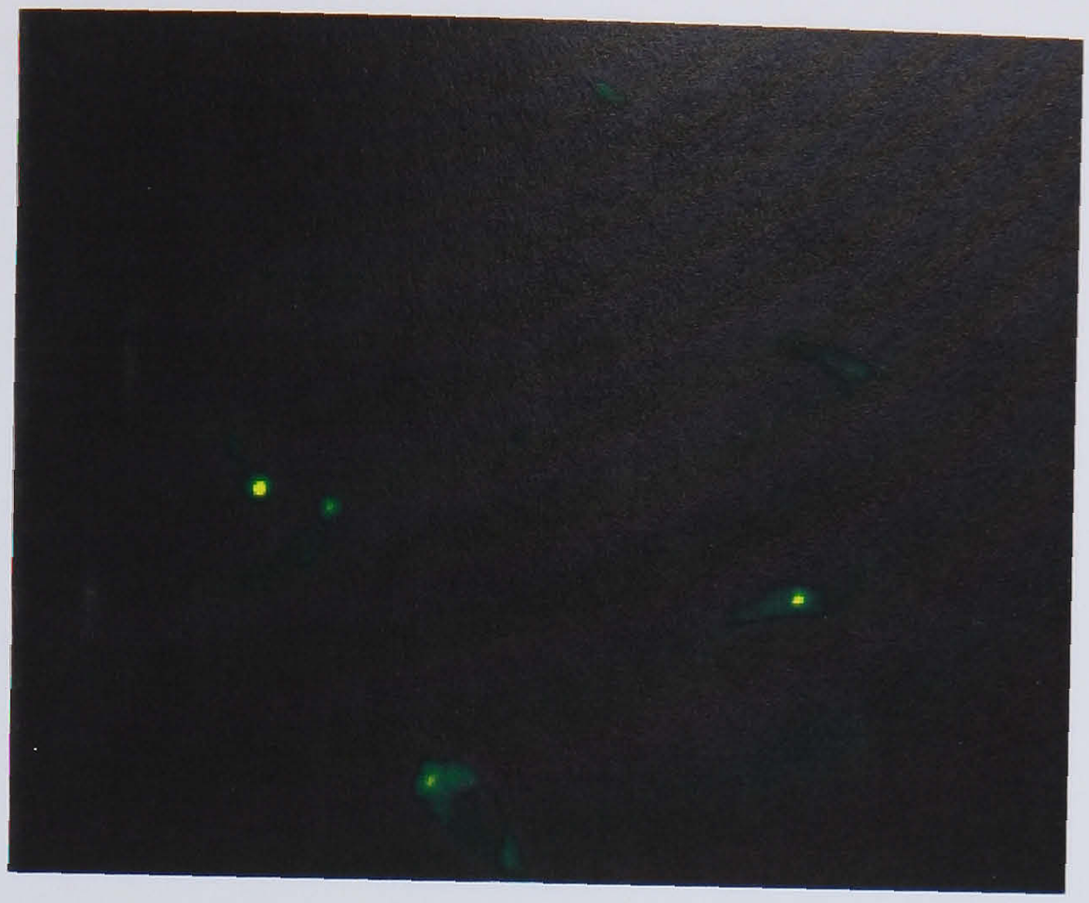


A



B

Figure 6.7 Cytochemical effects of co-stimulation of growth-arrested human VSM cells with PDGF-BB and lovastatin. Fluorescent photomicrographs of growth-arrested human VSM cells that have been stained with the fluorescent DNA-binding dye, DAPI, after treatment with **A**) 20ng/ml PDGF-BB and 10μM lovastatin **B)** 10μM lovastatin alone for 48 hours in serum-free medium (original magnification x 400). The bright blue staining indicate areas of nuclear DNA condensation, usually a characteristic of apoptotic cells. Normal nuclei are stained uniformly.



A



B

Figure 6.8 Effects of co-stimulation with both PDGF-BB and lovastatin on fluorescent DNA fragmentation in growth-arrested human VSM cells. Growth-arrested human VSM cells were exposed to **A)** 20ng/ml PDGF-BB and 10μM lovastatin for 48 hours, **B)** 10μM lovastatin alone fro 48 hours and stained with the TUNEL reagent (transferase-mediated dUTP end-labelling) (original magnification x 400). The bright green staining within the nuclei probably indicate the TUNEL-positive chromatin with DNA fragmentation.

6.1.1.3 Discussion

The diversity of cellular responses triggered after exposure of cells to PDGF, or any other specific extracellular stimulus, indicate that there is a significant degree of crosstalk and interdependence between the intracellular signal transduction pathways which are evoked (**Claesson-Welsh L, 1994**). Therefore, it is not surprising to note that interplay between both cell cycle and cell death signalling pathways occurs in cells. Cell cycle check points appear to link the cell cycle to apoptosis (**King K L and Cidlowski JA, 1995**), so that an inappropriate or deregulated stimulation of cell cycle components may lead to cell death.

For example, over-expression of *c-myc*, an early cell cycle specific gene, was shown to lead to apoptosis in rat fibroblasts under conditions of growth factor deprivation (**Evan GI et. al., 1992**). The expression of the *bcl-2* oncogene under similar conditions was shown to counteract the effect due to *c-myc* overexpression and the cells were rescued from apoptosis (**Bissonette RP et. al., 1992, Fanidi A et. al., 1992**). Similarly, apoptosis was induced in serum-starved, quiescent Rat-1a fibroblasts and in rat VSM cells following over-expression of *myc* (**Bennett MR et. al., 1994**; **Hoang A T et. al., 1994**). *C-myc* over-expression was associated with transcriptional upregulation of a host of other gene products induced during G_1 to S phase transition, such as the cyclins (**Jansen-Durr P et. al., 1993**). Under the latter circumstances, ectopic or inappropriate expression of c-myc protein was associated with a "false" entry into the G_1 phase, which culminated in apoptosis. Furthermore, the susceptibility of Ras transfected cells to apoptosis has been correlated with *c-myc* expression (**Arends M J et. al., 1993**). It is also interesting to note that deregulated expression of another transcription factor required for transactivation of genes in S phase transition, E2F-1, has also been associated with S-phase entry and apoptosis (**Qin X Q et. al., 1994; Fueyo J et. al. 1998**).

Upregulated expression of other cell proliferation associated oncogenes, such as, *c-fos* and *c-jun*, were observed after induction of apoptosis in interleukin-2 and interleukin-6-dependent myeloma cells (**Colotta F et. al., 1992**). Other early cell-cycle specific genes, including *cdc2*, the primary kinase active during mitosis, as well as the phosphorylated form of the Riboblastoma (Rb) susceptibility gene product, were also

detected soon after serum deprivation-induced apoptosis of density-arrested quiescent Swiss 3T3 cells (**Pandey S and Wang E, 1995**). These cells were dependent upon growth factors for their survival, hence apoptosis ensued 5-10 hours after withdrawal of growth-factor containing serum from the medium (**Tamm I and Kikuchi T, 1990**). **Pandey and Wang, 1995** also showed that serum-deprivation induced apoptosis was associated with very early [^{3}H]-thymidine and bromodeoxyuridine (BrdU) incorporation. Many of the BrdU-incorporated nuclei displayed the characteristic features of apoptosis, i.e. nuclear condensation and DNA fragmentation. To test whether DNA synthesis and DNA fragmentation were taking place at the same time in the same cells, they performed a double-labeling experiment for *in situ* detection of DNA fragmentation and BrdU incorporation. They observed co-localisation of both activities in some but not all cells, suggesting that in a significant fraction of density-arrested quiescent Swiss 3T3 cells, DNA synthesis and serum-deprivation-induced apoptosis, as assessed by DNA fragmentation, may be taking place simultaneously. The thymidine incorporation they had observed after serum withdrawal occurred after 3 hours; whereas the normal traversion time from G_o/G_1 phase to S phase (or initiation of DNA synthesis) was shown to be approximately 8-10 hours after induction with a mitogen (**Pandey S and Wang E, 1995**). This may indicate that the earlier initiation of DNA synthesis activity after serum deprivation may indicate an attempt at DNA repair in these cells. According to their results, there seemed to be a significant increase in DNA fragmentation 6 hours after serum deprivation, indicating that DNA repair may be activated in response to DNA damage. However, the attempt at DNA repair may remain too weak to overcome the magnitude of the DNA damage that eventually apoptosis ensues. Therefore, it is possible that part of the thymidine or BrdU incorporation they observe may be due to the endogenous terminal transferase activity from DNA repair.

Nonetheless, the workers had also observed the appearance of the proliferating cell nuclear antigen (PCNA) in the cells after serum deprivation. PCNA, otherwise known as DNA polymerase δ, is not usually associated with DNA repair, and was shown to be synthesised during mid and late G_1 phase in primary thyroid culture (**Baptist M et. al., 1993**). The presence of this component of the DNA synthesis machinery may actually indicate that net DNA synthesis may take place after serum

deprivation.Whether these two processes (either DNA synthesis or DNA repair, along with DNA fragmentation due to apoptosis) are taking place in the primary human VSM cells under the conditions of our experiments is unknown, but the possibility still remains.

PDGF stimulation on its own has been shown to function as a "competence" factor (**Stiles CD et. al., 1979;_Pledger WJ et. al., 1981**) in serum-starved, growth-arrested cells, where upregulation of the same set of immediate-early-response genes was seen during G_o/G_1 phase. These included genes such as *c-myc* (**Kelly K et. al., 1983**) and *c-fos* (**Greenberg ME and Ziff EB, 1984**). However, for progression beyond late G_1 phase, entry into S phase and ultimate cell division, PDGF-stimulated cells require additional "progression" factors such as insulin and insulin-like growth factor 1 (IGF-1) (**Olashaw N E et. al., 1987**; **Stiles C D, 1983**). PDGF-AA and IGF-1 were shown to act in a synergistic manner on VSM cell proliferation (**Thommes K B et. al., 1996**). Such a potentiating effect of IGF-1 and PDGF on VSM cells may have been accounted for by a significant increase in the Ras protein pool in cells treated with both IGF-1 and PDGF (**Goalstone M L et. al., 1998**). Although exposure of growth-arrested VSM cells to PDGF or EGF or IGF-1 alone was shown to stimulate DNA synthesis (or thymidine incorporation), simultaneous addition of all three factors had an additive effect on DNA synthesis (**Hwang D L et. al., 1992**). Hence, under these circumstances, co-stimulation with IGF-I prevented the apoptosis that may otherwise have occurred, possibly through the synergistic action of R-Ras (**Suzuki J et. al., 1998**). In fact, it is interesting to note that there was a transient induction of apoptosis in serum-starved glioma cells when they were exposed to insulin or IGF-I alone (**Yang B C et al., 1996**).

Members of the Ras superfamily of small GTPases, such as Ras, Rac and Rho, have been shown to act as molecular switches in intracellular signalling (**Olson M F et. al., 1998**). These GTPases were shown to be essential for regulation of cell proliferation, as the mitogenic response to a variety of growth factors can be blocked through inhibition of Ras function (**Mulcahy LS et. al., 1985**). Oncogenic Ras, but not normal Ras protein transfection of quiescent cells was associated with cell cycle entry (**Feramisco J R et. al., 1984**), while inhibition of proliferation of neuronally differentiated PC12 cells with a dominant negative Ras also prevented apoptosis in

response to nerve growth factor (NGF) in the same cells (**Ferrari G and Greene L A, 1994**).

Rho GTPase was shown to be required for G_1 to S phase transition in NIH 3T3 cells, mediated through the inhibition of the cyclin-dependent-kinase inhibitor, p21Waf1 (**Olson M F et. al., 1998**). Cyclin-dependent kinase inhibitors are activated through the presence or absence of phosphorylation on specific amino acid residues on the protein. Such phosphorylation and dephosphorylation is controlled through cyclin-dependent kinases, which in turn are regulated by inhibitors, like p27Kip1 or p21Waf1 (**Harper JW, 1997**). When Rho was active, p21Waf1 activity was inhibited, leading to S phase entry. It is interesting to note, however, that certain geranylgeranylated small GTPases, such as Cdc42 or Rac1, were shown to be required for nerve growth factor (NGF) withdrawal-induced apoptosis in rat sympathetic neurons (SCG) (**Bazenet C E et. al., 1998**). In their experiments, these workers demonstrated that expression of dominant negative mutants of Rac1 or Cdc42 lead to inhibition of apoptosis after NGF withdrawal.

Binding of growth factors such as platelet-derived growth factor (PDGF) onto its respective tyrosine kinase plasma membrane receptor, results in a complex series of events, including receptor dimerisation and stimulation of receptor tyrosine kinase activity, rapid autophosphorylation and subsequent recruitment of intracellular proteins (**Heldin C H et. al., 1998**). Treatment of NIH-3T3 cells with lovastatin, blocked PDGF receptor tyrosine autophosphorylation, and co-treatment with geranylgeraniol, but not with farnesol, reversed the lovastatin block (**McGuire T F et. al., 1996**). Likewise, treatment of the cells with a GGTase I inhibitor (GGTI-298) led to a strong inhibition in receptor tyrosine phosphorylation, while treatment with a FFTase inhibitor (FTI-277) had no effect. In contrast, using human saphenous vein smooth muscle cells (**Clunn GF et. al., 1998**) found that lovastatin did not affect tyrosine phosphorylation of the PDGF β receptor although inhibition of PDGF-induced calcium signalling was observed.

PDGF-induced Ras activation was shown to be required for G_1 progression in Chinese hamster embryo fibroblasts (IIC9 cells). Under these circumstances, stimulation of

Ras due to PDGF was coupled to RhoA activity and progression through the G_1 phase, while dominant negative forms of RhoA were associated with growth arrest (**Weber J D et. al., 1997**).

Transfection of a cultured VSM cell line (A10) with a dominant negative mutant ras protein (ras^{DN}) was associated with inhibition of DNA synthesis in response to PDGF and other growth factors (**Irani K et. al., 1994**). Inhibitors of HMG-CoA reductase inhibitors have also been reported to inhibit PDGF-induced mitogenesis (**Munro E et. al., 1994**) in VSM cells; again confirming and corroborating the key role of certain isoprenylated proteins, like the Ras-related small GTPases, in such a process.

To do justice to such cellular functions, it becomes important to understand what molecules are required to complete the transition into S and the latter phases of the cell cycle, and likewise which molecules, in the absence of the latter, would result in apoptosis. The complementary molecules required to complete transition of S phase and ultimately mitosis, are most probably upregulated when additional and distinct, "progression" factors are present in the medium or in the extracellular milieu.

It may be that under normal, optimal conditions when progression factors are present, apoptotic pathways are repressed to allow DNA synthesis and mitosis to proceed. Hence, the simultaneous presence of potentially "apoptotic" signals in the initial phases of cell cycle entry provide the safety mechanism for elimination or abortion of the entire cell, when the requisite signals to sustain cell proliferation are absent. Such a mechanism ensures the integrity of the tissue or organism as a whole is maintained, even though it is at the expense of cell loss.

The results presented in this study indicate that exposure of primary human VSM cells to PDGF-BB after growth-arrest in serum–free medium is associated with entry into S phase and apoptosis. However, when cells are co-incubated with both lovastatin and PDGF-BB after growth arrest, both entry into S phase and apoptosis were inhibited. One interpretation of these data is that growth arrest at a specific point in late G_1 phase by lovastatin will prevent apoptosis which would otherwise occur with progression through the cell cycle in the absence of survival factors. In the absence of this block, however, entry into a defective cell cycle leads to apoptosis in

these cells. In light of the discussion above, the deficiency is likely to be one or more of the survival signals, which probably stems from an inadequacy or lack of an appropriate extracellular stimulus. This proposal is consistent with previous studies showing that stimulation of quiescent cells with PDGF-BB alone is not enough for the successful completion of S phase. Although stimulation of the same growth-arrested saphenous vein-derived human VSM cells with PDGF-BB at 10ng/ml or 50ng/ml has been shown to stimulate DNA synthesis (**Hughes AD et. al., 1995**), the rate of cell proliferation in cells exposed to PDGF-BB alone was very low compared to the rate of cell proliferation when cells were grown in 15% (v/v) foetal bovine serum (**Patel MK et. al., 1997**). Hence, it seems likely that when PDGF is used alone, there is loss in cell numbers, and that few cells complete cell division at the end of the cell cycle. Such a cell proliferation response due to PDGF-BB was also seen by **Kim H R, et. al., 1995**, who demonstrated that in fact there was a loss in rat kidney fibroblast cell numbers over a period of 4 days when these cells were grown in PDGF-BB at 50ng/ml. This cell loss was associated with apoptosis. That stimulation of growth-arrested VSM cells with PDGF-BB leads to cell death by apoptosis was also observed by **Okura T et. al., 1998**, who reported that addition of PDGF-BB to growth-arrested rat VSM cells was associated with apoptosis in a time- and dose-dependent manner.

The ability of lovastatin to inhibit DNA synthesis (**Munro E et. al., 1994**) suggests that a protein dependent on isoprenylation, possibly a small GTPase like Rho, is required for entry into S phase. Whether this isoprenylated protein protein(s) is also actively required for apoptosis or simply permits progress through the cell cycle to a point where apoptosis results in the absence of survival factors is unknown.

This putative isoprenylated protein, possibly Rho, may be functionally involved in the regulation of the G_1 checkpoint before the successful initiation of DNA synthesis. The Rho protein has been shown to have close links with p21Waf1, the cyclin-dependent kinase inhibitor. When Rho protein signalling for cell cycle entry is inactivated, p21Waf1 was upregulated during growth arrest at the G_o/G_1 phase (**Olson MF et. al., 1998**). Interestingly, the p21Waf1 protein was associated with inhibition of apoptosis, as demonstrated by **Yu D et. al., 1998; Asada M et. al., 1998**, while cleavage of p21Waf1 protein was shown to be associated with an upregulated expression of cyclin-dependent kinases (CDK) during apoptosis of endothelial cells

(**Levkau B et. al., 1998**). CDK's are known to be required for transition from G_1 to S phase (**Rosenblatt J et. al., 1992**) and are also seen following induction of apoptosis in many cell types (**Meikrantz W et. al., 1994; Park DS et. al., 1998; Braun K et al., 1998**). Cyclin A in particular is activated during c-myc-induced cell death in serum-free medium (**Jansen-Durr P et. al., 1993**) and cell-cycle arrest prior to the appearance of cyclin A has been shown to protect cells from apoptosis (**Boehme SA and Leonardo MJ, 1993**). Furthermore transient expression of dominant negative mutants of CDK, especially CDK-cyclin A complexes, has been shown to suppress TNF-α-induced apoptosis in HeLa cells (**Meikrantz W and Schlegel R, 1996**). In view of these observations it is tempting to link the ability of lovastatin to inhibit PDGF-induced apoptosis with its potential ability to inhibit rho-dependent down regulation of p21Waf1. Further studies are clearly necessary to establish whether this is indeed the mechanism of lovastatin under these circumstances.

In retrospect, these results demonstrate the importance of the inter-relationship between apoptotic and proliferation pathways, confirming in a specific way that isoprenylated molecules, such as the Ras-related small GTPases, may play important roles in the optimal control of cell populations in tissues. The inhibition of such proteins may be associated with prevention or promotion of apoptosis, depending on the extracellular environment around the cell. The significance of PDGF-BB induced apoptosis in the cardiovascular system may become important during the exposure of medial VSM cells to the extracellular milieu released from macrophages after infiltration from the lumen. When exposed to a very high concentration of PDGF-BB released from macrophages, these medial cells, if assumed to be quiescent *in vivo*, may be triggered into apoptosis. Although concerted stimulation of cells with a multitude of growth or survival factors may take place under optimal conditions *in vivo*, excessive stimulation of cells with one or more survival factors, however, may take place in disease conditions, resulting in uncontrolled levels of cell death.

Such an isolated stimulation of quiescent VSM cells with a single dose of PDGF-BB, and possibly any other growth factor may be a good system to study the effects of a single growth factor on these cells. However, it becomes a major disadvantage when these results are extrapolated to the complex processes taking place *in vivo*. The

above results point to the hypothesis that cell apoptosis may be stimulated under deficient conditions for proper growth or survival, but we are still far from any conclusive evidence as to what is really taking place *in vivo*, especially under pathological circumstances.

These results also demonstrate the relative insensitivity of quiescent or growth arrested human VSM cells to apoptosis after exposure to lovastatin, unlike that of SM1 cells. One reason for this may possibly be due to the quiescent state of the primary human VSM cells at the time of exposure to lovastatin. During quiescence, the turnover rate of the mevalonate derived isoprenoids required for cell proliferation and survival signalling may be relatively less with respect to the continuous cell cycle activity in SM1 cells. Hence the lower turnover rate means that the depletion of the isoprenoids in the presence of lovastatin would not affect the apoptotic pathways in the quiescent primary human VSM cells.

In many clinical trials for the prevention of restenosis after coronary angioplasty, lovastatin treatment was not found to be significantly beneficial, at least in terms of the angiographic parameters measured with or without the drug (**Weintraub W S et. al., 1994; Beigel Y et. al., 1995**). Such outcomes may be accounted for by the results we observed in these primary human saphenous vein cells, since a quiescent phenotype could be comparable to the physiological state of medial SMC found in vessels *in vivo* (**Frid MG et al., 1997**). Nonetheless, other factors such as inaccessibility of the drug to the requisite target may also be another reason why no beneficial effects were observed.

Concluding Remarks and Future Work

The results of this study provide evidence that inhibition or depletion of certain isoprenoid derivatives of mevalonate may not only lead to cell death by apoptosis, as well as inhibition of cell proliferation and DNA synthesis, but also to inhibition of apoptosis under some circumstances. Certain prenylated proteins, such as the Ras-related small GTPases like, Rho have been proposed to be involved in these effects since such proteins play a role not only in signalling required for survival and proliferation, but also for the promotion of apoptosis. Due to lack of cell availability, no experiments on the effect of co-incubation of a geranygeranyl or farnesyl pyrophosphate with lovastatin after PDGF-BB induction of quiescent primary VSM cells were carried out. However, this could have revealed more information as to which prenoid moiety was required for apoptosis under these circumstances.

Work by **Munro E et. al., 1994** on the same human non-transformed VSM cell type (but different cell lines) indicated that there was a recovery of lovastatin-induced inhibition of DNA synthesis when co-incubated with farnesol, this result differs from the data using the SV-40 transformed human VSM cells. A possible reason for this is that the two cell types were treated under different circumstances. **Munro E et. al., 1994**, also did not use dialysed serum, therefore there may have been some mevalonate available in these studies. Under these circumstances supplementation with farnesol might allow all of this mevalonate to be utilised for generation of geranylgeranyl pyrophosphate. Nonetheless, more recent studies (Clunn GF, Lymn J, Patel MK, Hughes AD, unpublished data) have indicated that inhibition of PDGF-BB-induced DNA synthesis due to lovastatin, was recovered only when co-incubated with geranylgeranyl pyrophosphate in the absence of undialysed serum. Other groups have also found that co-incubation of pravastatin-treated VSM cells either with farnesol or geranylgeraniol isoprenoids led to recovery (or prevention of) pravastatin-induced apoptosis in cultured rat VSM cells (**Guijarro C et. al., 1998**). This requirement may have depended on the actual needs of the cells at that particular instance in culture.

The experiments of chapter 5, on the other hand, were carried out specifically to see the effects of a farnesyl transferase inhibitor (B581) on apoptosis, the cell cycle

phases, and on the effect of UVB in these cells. Since RhoB proteins, known to be farnesylated, were shown to be upregulated when cells were exposed to DNA-damaging agents, such as UVB and cisplatin, then it seemed interesting to see whether there was any inhibition of apoptosis in VSM cells exposed to a FTase inhibitor under these circumstances. For most measured parameters the FTase inhibitor, B581, had no effect, except for the percentage total cell viability. The total cell counts were also not significantly affected. The absence of a significant effect on any of the parameters measured by us indicates that cell growth and apoptosis is not affected by inhibition of farnesylation, as reported by many other workers. It further indicates that the inhibition of attachment of this post-translational modification can be compensated for in some way, or that it is not essential for survival. Such an effect of the FTase inhibitor on UVB-induced effects seems to be in direct contrast to the effects of lovastatin, and perillyl alcohol when co-incubated under the same conditions. This may be due to the depletion of the geranylgeranyl isoprenoid pool in the presence of lovastatin, and possibly due to inhibition of its transfer onto relevant proteins, as in the presence of perillyl alcohol.

A caveat in the method of measuring the relative levels of apoptosis in cultures is the use of a single fluorescent dye, which only provides a univariate analysis. This method is likely to provide us with an underestimate as to the actual levels of apoptosis in the cultures due to the possible appearance of certain "apoptotic" events in one of the cell cycle phases, rather than the hypodiploid region alone. Use of dual flow cytometric analysis that measures another parameter related to apoptosis, such as TUNEL staining may have revealed more information as to the extent of apoptosis under these conditions, but this could not be carried out.

It is interesting to note that FTase inhibitors do not affect the functional signalling mediated through normal Ras proteins or their localisation (**Dalton MB et. al., 1995**), but are associated with direct inhibition of oncogenic Ras protein action. The insensitivity of (non Ras-transformed) SM1 cell growth and apoptosis to inhibition of farnesylation could be due to the relatively lower turnover rates of the Ras GTPase proteins and functional redundancy in the system. Hence, the integrity of the system is not affected, although functional Ras proteins have been reduced. Alternatively, under these circumstances, it may be possible that Ras, or any other farnesylated

small GTPase, is geranylgeranylated as shown in human colon carcinoma cells (**Whyte BD et. al., 1997**). If this were the case, possibly oncogenic forms of Ras which comprise a mutant form of Ras protein (due to the specific mutation on the *ras* gene) may not undergo this prenylation or may not function as an oncogene unless farnesylated. Consequently all signalling through oncogenic Ras would cease when farnesylation is inhibited.

The effect of direct inhibition of Ras activity, either through antisense oligonucleotides against Ras or via transfection with dominant negative mutants, could also be carried out. This would confirm the contribution of Ras activity during prevention of, or promotion of apoptosis, e.g. in the case of PDGF-BB induction.
It is interesting to note that **Irani K et.al., 1994** found that stable transfection of VSM cells with dominant negative Ras (ras^{DN}) resulted in cell death.

It would also be interesting to see the effect of B581 co-incubation on PDGF-BB-induced apoptosis in primary cells. Finally, it would be interesting to know whether the prenylation of the small GTPases, such as Rho, in primary human VSM cells, changes according to whether it is involved in a pro-apoptotic signal or an anti-apoptotic signal (as in the presence of lovastatin)?

The evidence in this thesis thus points out to the possible opposing functions of a given prenylated protein(s) in signal transduction mechanisms involved in determining cell fate.

Critical appraisal of the studies undertaken and possible future work

The transformed HVSM cell line (SM1) utilized in our experiments was obtained after transfection with a temperature-sensitive replication-defective SV40 virus vector. These cells were established to be conditionally immortalised since a proliferative phenotype was expressed only under the permissive temperature (37°C) (Hsieh J-K *et al.*, Arterioscler. Thromb. Vasc. Biol. *in press*). Under these conditions, immortalisation was defined as the life span of the cell beyond 200 culture passages. Compared to the primary, non-transformed HVSM cells, SM1 cells are smaller in size, and the typical spindle morphology characteristic of normal non-transformed HVSM cells is absent. However, continual expression of smooth muscle specific cytoskeletal proteins including myosin heavy chain and alpha-actin was observed (Hsieh J-K *et al.,* Arterioscler. Thromb. Vasc. Biol. *in press*). These authors have additionally demonstrated that SM1 cells respond to PDGF-BB by increased DNA synthesis, although the response was 2-3 fold lower than in normal non-transformed HVSM cells. One reason for this result may be large T (LT)-antigen-induced down regulation of PDGF-BB receptor expression (Wang J L *et. al.* 1996).

Lovastatin has been demonstrated to be a potent competitive inhibitor of HMG-CoA reductase in rat liver microsomes with an estimated K_i of 0.64nM (Alberts *et. al.,* 1980). In another study, Bischoff *et. al.*, (1998) also isolated membrane-bound microsomal HMG-CoA reductase from rat liver to measure the inhibitory activity (IC_{50}) of lovastatin. The IC_{50} value in these studies was determined to be 77nM. The difference in the estimated potency of lovastatin is presumed to reflect differences in assay conditions. Such a discrepancy emphasizes the difficulty in extrapolating findings using (partially) purified enzyme systems to intact cells where concentrations of substrate and other factors influencing enzyme activity may not be fully known. The HMG-CoA reductase activity in SM1 cells under our experimental conditions was not measured. One of the main reasons for this was the lack of time available to establish a new method for measuring HMG-CoA reductase activity, which had not been used previously in our laboratory and for which there were no published methods using vascular smooth muscle cells. The concentrations of lovastatin used in our experiments were relatively large with respect to the IC_{50} measured *in vitro* examining HMG CoA reductase activity (see above) or for its reported potency as an inhibitor of sterol synthesis (~10nM) (Sinensky *et al.*, 1990). However it is

potency as an inhibitor of sterol synthesis (~10nM) (Sinensky *et al.*, 1990). However it is not dissimilar to the IC_{50} reported for lovastatin as an inhibitor of ras prenylation (2.6μM) in CHO-K1 and HeLa cells (Sinensky *et al.*, 1990). It has been suggested that the relative insensitivity of inhibition of mevalonate biosynthesis on prenylation reflects the lower K_m of the appropriate prenyl transferase compared with squalene synthase, thereby allowing the synthesis of isoprenoids under conditions of partial inhibition of mevalonate biosynthesis (Sinensky *et al.*, 1990).

The concentrations of perillyl alcohol used in our experiments (chapter 4) may not give an indication of the actual soluble concentration of perillyl alcohol used to treat the SM1 cells. These concentrations merely indicate the amount of the monoterpene added to the culture medium. Additionally, no attempt was made to measure the solubility of perillyl alcohol under the conditions used in our experiments. Some authors have used ethanol to increase the solubility of the monoterpene perillyl alcohol at 1000-fold final concentration, which was then added to the culture medium (Bardon S *et. al.*, 1998). Work by Gelb M H *et. al.*, 1995 indicated that both farnesylation (of ras p21) and geranylgeranylation (of G25K protein) were inhibited by perillyl alcohol *in vitro*. They found that the inhibitory activity (IC_{50} values) for perillyl alcohol inhibition were 1mM for protein farnesyl transferase (pftase) and 0.7mM for geranylgeranyl transferase (ggtase), where both the prenyl transferases were isolated from *S. cerevisiae* which correspond well with the potency of perillyl alcohol seen in the studies presented here.

The substrate specificity of perillyl alcohol has been relatively controversial. Perillyl alcohol was associated with inhibition of ubiquinone and cholesterol biosynthesis in cultured NIH3T3 cells (Ren Z, Gould MN, 1994). Initially, it was shown to inhibit the isoprenylation of both farnesylated and geranylgeranylated small G proteins (Crowell PL *et. al.*, 1994). This inhibition was selective for small G proteins and not for other larger isoprenylated proteins such as lamin B which are farnesylated (Crowell PL *et. al.*, 1992). Other workers demonstrated that both pftase and ggtase enzymes were inhibited by perillyl alcohol *in vitro* (Gelb MH et al., 1995), though subsequently it was reported that perillyl alcohol was a relatively selective inhibitor of type II ggtase, compared with fptase in NIH3T3 cells (Ren Z *et. al.*, 1997).

Nevertheless, it is important to note that the inhibition of these enzymes had hitherto not been correlated with apoptosis. Hence, there is no evidence in the literature suggesting that

the pro-apoptotic effect of perillyl alcohol is due to the inhibition of prenyl transferases. Taken in conjunction with the data derived from co-incubation of lovastatin with specific isoprenoids these data suggest, albeit indirectly, that the pro-apoptotic effect of perillyl alcohol on HVSM cells may be due to the inhibition of ggtase(s).

In order to better interpret the data showing the effect of co-incubation of mevalonate derivatives on lovastatin (Figure 3.11), it may be important to keep in mind the possible differential uptake of the isoprenoids into cells. Although no experimental evidence is as yet available, these phosphorylated isoprenoids most probably exist as micelles under *in vitro* conditions. The uptake of the shorter farnesyl pyrophosphate (Fpp) isoprenoids could be faster than the relatively longer geranylgeranyl pyrophosphate (GGpp) isoprenoids, although again, there is no evidence for this. If this were the case then the relative difference in the percentage of apoptosis after co-incubation of lovastatin-treated SM1 cells with Fpp or GGpp could be due to the different levels of uptake (Figure 3.11). However, according to the literature, the actual levels of uptake of these isoprenoids depends on the intracellular demand, whereby the levels of labelling of 21-28 kDa proteins with [H^3] Fpp becomes less than [H^3] GGpp in the presence of lovastatin (Danesi R *et. al.,* 1995). This is taken to indicate that uptake of isoprenoid is increased when the intracellular isoprenoid pool, especially that of the predominant prenyl substituent of proteins becomes depleted, which is the 20-carbon geranylgeranyl moiety (Farnsworth CC *et. al.,* 1990) and may imply a smaller cellular pool of GGpp.

Critical analysis of methods

Limitations and disadvantages of the DNA ladder assay

One of the major disadvantages of this method is that it is very time consuming, requires large amounts of DNA and yields inconsistent results. Additionally, the method is essentially qualitative, and the degree of DNA fragmentation (a marker of apoptosis) in a particular population cannot be quantified as directly as it can be using techniques like flow cytometry. Unfortunately, at the time of these studies this method was still considered a standard approach to establishing the existence of apoptosis in cell populations. Other more convenient methods have been developed recently and could be used to quantify the degree of DNA fragmentation in cell cultures in future studies. For example, in the cell death detection ELISA kit (Boehringer-Mannheim), oligonucleosomal

DNA fragments released from apoptotic cells are probed with a monoclonal anti-histone antibody, conjugated with the peroxidase enzyme. A substrate (2,2`-Azinodi-[3-ethylbenzthiazoline sulfonate] is then added to obtain a coloured product, which is measured by spectrophotometry and allows quantitation of the extent of DNA fragmentation.

Limitations of the Trypan blue exclusion/cell viability assay

This assay gives only a crude measure of the number of cells that are non-viable as a percentage of the total number of cells. Trypan blue will be taken up by non-viable cells with damaged plasma membranes, i.e. by cells at the final stage of apoptosis and/or necrotic cells. However, apoptotic cells are generally characterised as cells with intact plasma membranes, so these cells would be counted as viable cells with this assay. Hence, this assay gives an overestimate measure of the number of viable, non-apoptotic cells. Other methods for obtaining a better measure of cell viability exist. These include the LDH (lipid dehydrogenase) cytotoxicity test, where the LDH released by non-viable cells is measured, and also the MTT assay. The MTT assay could be the better of these, where MTT is taken up exclusively by metabolically active cells, which may also exclude cells undergoing apoptosis.

Contribution and possible future work

Work in this thesis indicates that depletion of GGpp isoprenoids due to lovastatin is associated with apoptosis, decreased DNA synthesis and cell proliferation in SV40 virus virus large T-antigen-transformed HVSM cells (SM1 cells). Likewise, a putative inhibitor of ggptase(s), perillyl alcohol, was also shown to lead to apoptosis in these cells. However, an inhibitor of fptase, B581, had no effect on cell growth or apoptosis in the same cells. In contrast, addition of lovastatin to quiescent, non-transformed HVSM cells was not associated with apoptosis. In addition, incubation of PDGF-BB with quiescent HVSM cells led to cell cycle entry and apoptosis. Co-incubation of quiescent HVSM cells with both PDGF-BB and lovastatin, however, led to inhibition of PDGF-BB–induced DNA synthesis and apoptosis. These experiments provide indirect evidence that derivatives of GGpp such as geranylgeranylated protein(s) are required for normal progress through the cell cycle and proliferation in the transformed HVSM cells. Inhibition of the mevalonate pathway is associated with increased apoptosis in these cells. In contrast inhibition of

HMG CoA reductase in HVSM cells does not appear to induce apoptosis. at least under the conditions studied, and indeed, prevents growth factor-induced apoptosis. Whether the inhibition of PDGF-induced apoptosis reflects the ability of lovastatin to prevent PDGF-induced entry into the cell cycle or alternatively a requirement for isoprenylation in the apopototic process in HVSMC remains uncertain.

Possibly, isoprenylated protein(s), such as the small GTPases, may function as "switch" proteins in cells, and may be involved in the promotion or inhibition of apoptosis when the necessary conditions arise (Olson MF *et. al.,* 1998). Although it may prove difficult to associate the identity of the isoprenylated protein(s) with apoptosis, future work must concentrate on identifying these prenylated proteins. One approach to this question could be to identify all the isoprenylated proteins through 2-dimensional SDS PAGE with immunoblotting and radiolabelling in the absence and presence of lovastatin and perillyl alcohol, respectively. Given the ever increasing number of small G proteins this would be a considerable undertaking. Nevertheless, such studies would allow the degree of isoprenylation (after labelling with [^{3}H] Fpp and GGpp) to be measured before and after the addition of lovastatin to SM1 cells. Proteins showing large changes in isoprenylation over the time period when apoptosis peaks would be anticipated to be those most likely to involved in apoptosis and/or inhibition of cell proliferation. Once the putative proteins were identified, then direct inhibitors of protein activity may be utilised to see the effects on apoptosis. For example, inhibitors of *rho* and other similar small GTPases, such as *C. botulinum* exoenzyme C3 transferase might be used in this way. Alternatively, antisense oligonucleotide inhibitors of the identified isoprenylated proteins could be used to inhibit specific proteins thought to participate in the apoptotic process.

ADDITIONAL REFERENCES

Alberts AW, Chen J, Kuron G, Hunt V, Huff J, Hoffman C, Rothrock J, et al. Mevinolin: A highly potent competitive inhibitor of hydroxymethylglutaryl-coenzyme A reductase and a cholesterol-lowering agent. *Proc. Natl. Acad. Sci. USA* , 1980 77 (7): 3957-3961.

Bischoff H, Angerbauer R, Boberg M, Petzinna D, Schmidt D, Steike W, Thomas G. Preclinical review of cerivastatin sodium- a step forward in HMG-CoA reductase inhibition. *Atherosclerosis*, 1998 (139), Suppl 1:S7-S13.

Bardon S, Picard K, and Martel P. Monoterpenes inhibit cell growth, cell cycle progression, and cyclin D1 gene expression in human breast cancer cell lines. *Nutrition and Cancer,* 1998 32(1): 1-7.

Ren Z, Gould MN. Inhibition of ubiquinone and cholesterol synthesis by the monoterpene perillyl alcohol. *Cancer Lett.* 1994 (76): 185-190.

Sinensky M, Beck L, Leonard S, Evans R. Differential inhibitory effects of lovastatin on protein isoprenylation and sterol synthesis. J. Biol. Chem. 1990: 19937-19941.

Wang JL, Nister M, Bongcamrudloff E, Ponten J, Westermark B. Suppression of platelet-derived growth factor alpha- and beta-receptor mRNA levels in human fibroblasts by SV40 T/T antigen. *J Cell Physiol.* 1996 (166): 12-21.

CORRECTIONS

P8	lane 11	.....DNA content of SM1 cells.
P14	lane 1	(terminal
P22	para2, lane 1	has > have
P22	para 3, lane 3	-end *(delete)*
P23	para 2, lane 3	*carry on after lane 2* As yet, no information is available on the temporal pattern of apoptosis during the development of the disease, although recent evidence.....
P24	para2, lane 3	*new paragraph*
P30	legend, lane 4	the <u>the</u> (*delete)*
	legend, lane 5	become/tightly
P36	para1, lane 6	on/to
	para1, lane 9	on/to
	para1, lane 18	Clarke s > Clarke S
	para 2, penultimate lane	on/to
p37	para 1, lane 2	on/to
p40	para 3, lane 1	on/to
p41	para1, lane 5	Raff M <u>C</u> (*insert*)
p42	para2, lane 2	and (*delete*) but
	para 2, lane5	Decremoux > DeCremoux
	para2, lane 15	....induction of apoptosis in <u>NIH3T3 cells</u>
p49	legend, lane 3	on/to
p50	legend, lane 3	ribosos<u>s</u>mes
	legend, lane 6	<u>s</u>ulphur, <u>c</u>ysteine (*small letters*)

p53 penultimate lane (*definition of G418*) G418 or geneticin, used to select the cells which have been transformed with a recombinant plasmid containing the SV40 LT antigen and the neomycin resistance gene

p56	para1, lane 1	on/to
	para 1, lane 3	on/to
	para 2, lane 12	on/to
p63	para 1, lane 6	on/to

p64	para 2, lane 4	5/minutes
p65	para 1, lane 2	seen in (*delete*) as the
	para 1, lane 5	on/to
p66	para 2, penultimate lane	on/to
p67	para 2, lane 1	on/to
	para 2, lane 3	on/to
	para 2, lane 9	trypsin-EDTA (0.25% (w/v)) was added, and once (*delete*) the cells were > until the cells were
p68	para 2, lane 7	on/to
	para 3, last lane	10μM lovastatin (*delete 100μM*)
p69	para5, lane 1	on/to
p70	para1, lane 7	on/to
p71	lane1	derived/from
p75	legend, lane 4	50μg (*delete 50mg*)
p76	legend, last lane	considerably
p77	legend, lane 4	relatively more easily (*delete*) detectable
p80	para 1, lane 3	Figure 3.9 > 3.10
p82	para1, lane1	10[]M > 10 μM
p85	legend, lane 6	original/magnification
p87	Figure 3.4	*lane M is absent*
p90	legend, lane 5	indicat > indicate
p99	legend, lane 3	10mM > 10μM
p100	legend, lane 1	lovastatin/on
p101	para 2, lane 5	SM1 cells
	para 3, lane 12	compounds
p102	para 3, last lane	pyrosphate > pyrophosphate
p103	para 2	*double spacing between para 1 and 2*
p106	para1, lane 8	it was also associated (*delete*) with apoptosis > and with apoptosis
p108	para 2, lane 1	in this chapter indicate that > in this chapter are consistent with the hypothesis that
p127	para 1, lane 7	RhoB was reported to be an immediate-early gene inducible by DNA damaging treatments
p132	para 4, lane 7	perillyl alcohol

p133 para 2, lane 13 There was no significant increase (*delete*) in thymidine > there was no significant change

p136 legend, lane 4 (v/v) FBS/ (original magnification x 400)

p140 legend, lane 3 50J/$m^2$of UVB > 50J/m^2 of UVB

p141 legend, lane 1 Figure 5.8 Effect (*double spacing*)

P142 Figure 5.9 change *** > Ψ

p148 para 1, lane 6 and B581, a farnesyl transferase inhibitor and lovastatin, to examine

p151 para 1, penultimate lane percentage cell viability

para 3, lane 4 A significant increase

p154 para 4, lane 3 chemoattractant properties

p155 para1, lane2 Clunn G F et. al., 1997

p168 para 1, lane 1 deprivation. //Whether these

para 2, lane 2 (Stiles CS et. al., 1979; _Pledger WJ et. al., 1981) (*delete the line*)

p169 para 3, lane 1 on/to

p171 para 2, lane 3 ….isoprenylated protein (*delete*) protein(s) is also..

p177 *insert Armstrong SA et. al., 1995*

p181 *insert Brown MS and Goldstein JL, 1980*

p189 *insert Goldstein JL and Brown MS, 1977*

p182 *insert Chen HW et. al., 1974*

p183 *insert Clunn GF et. al., 1998 (lovastatin and tyrosine phosphorylation)*

p185 *insert Endo A et. al., 1976*

p186 *insert Falke P et. al., 1989*

p194 *insert Kandutsch AA and Chen HW, 1977*

p195 *insert Kuroda Y et. al., 1993*

p199 *insert Muller R et. al., 1984*

p200 *insert Nakanishi M et. al., 1988*

pagliacci MC > Pagliacci MC

1991 > 1992 for Nicolletti I et. al.,

p204 *insert Reiss Y et. al., 1990*

p209 *insert Thompson NL et. al., 1986*

p210 *insert Weber JD et. al., 1997*

check whether Wang HC or Wang HG

BIBLIOGRAPHY

Adamson P, Marshall C J, Hall A, Tilbrook P A. Post-translational modifications of p21 rho proteins (1992a) *J Biol Chem,* 267(28): 20033-20038.

Adamson P, Paterson HF, Hall HF. Intracellular localisation of the p21rho proteins (1992b) *J Cell Biol,* 119(3): 617-627.

Afanasyev V N, Korol A B, Matylevich N P, Pechatnikov V A and Umansky S R The use of flow cytometry for the investigation of cell death (1993) *Cytometry,* 14(6): 603-609.

Altshuler DL, Ribeiro-Neto F. Mitogenic and oncogenic properties of the small G protein Rap1b (1998) *Proc Natl Acad Sci USA,* 95(13): 7475-7479.

Arends M J, Morris R G, Wyllie H. Apoptosis: The role of endonuclease (1990) *Am J Pathol,* 136(3): 593-608.

Arends MJ, McGregor AH, Toft NJ, Brown EJ, Wyllie AH. Susceptibility to apoptosis is differentially regulated by c-myc and mutated H-ras oncogenes and is associated with endonuclease availability (1993) *Br J Cancer,* 68(6): 1127-1133.

Arends MJ, McGregor AH, Wyllie AH. Apoptosis is inversely related to necrosis and determines net growth in tumours bearing constitutively expressed myc, ras, and HPV oncogenes *Am J Pathol,* (1994) 144(5): 1045-1057.

Asada M, Yamada T, Fukumuro K, Mizutani S. p21Cip1/WAF1 is important for differentiation and survival of U937 cells (1998) *Leukemia,* 12(12): 1944-1950.

Astruc M, Laporte M, Tabacik C, Crates de Paulet A. Effect of oxygenated sterols on 3-hydroxy-3-methylglutaryl coenzyme A reductase and DNA synthesis in phytohemagglutinin-stimulated human lymphocytes (1978) *Biochem Biophys Res Commun,* 85(2): 691-700.

Austin GE, Ratliff NB, Hollman J, Tabei S, Phillips DF. Intimal proliferation of smooth muscle cells as an explanation for recurrent coronary artery stenosis after percutaneous transluminal coronary angioplasty. (1985) *J Am Coll Cardiol,* 6(2): 369-375.

Azrolan N I, Coleman P S. A Discoordinate increase in the cellular amount of 3-hydroxy-3-methylglutarryl-CoA reductase results in the loss of rate-limiting control over cholesterogenesis in a tumour cell-free system (1989) *Biochem J,* 258(2): 421-425.

Baetta R, Donetti E, Comparato C, Calore M, Rossi A, Teruzzi C, Paoleti R, Fumagalli R, Soma MR. Proapoptotic effect of atorvastatin on stimulated rabbit smooth muscle cells (1997) *Pharmacol Res*, 36 (2): 115-121.

Ballantyne CM. Low-density Lipoproteins and risk for coronary artery disease (1998) *Am J Cardiol,* 82: 3Q-12Q.

Bansal N, Houle A G, Melnykovych G. Comparison of dexamethasone and lovastatin (mevinolin) as growth inhibitors in cultures of T-cell derived human acute leukemia cell lines (CEM) (1989) *Leuk Res,* 13(10): 875-882.

Baptist M, Dumont JE, Roger PP. Demonstration of cell cycle kinetics in thyroid primary culture by immunostaining of proliferating cell nuclear antigen: differences in cyclic AMP-dependent and –independen mitogenic stimulations (1993) *J Cell Sci,* 105 (Pt 1): 69-80.

Barbacid M. ras genes (1987) *Annu Rev Biochem,* 56: 779-827.

Barber LA, Spandau DF, Rathman SC, Murphy RC, Johnson CA, Kelley SW, Hurwitz SA, Travers JB. Expression of the platelet-activating factor receptor results in enhanced ultraviolet B radiation-induced apoptosis in a human epidermal cell line (1998) *J Biol Chem,* 273(30): 18891-18897.

Bardon S, Picard K, and Martel P. Monoterpenes inhibit cell growth, cell cycle progression, and cyclin D1 gene expression in human breast cancer cell lines (1998) *Nutr Cancer,* 32(1): 1-7

Barr PJ and Tomei LD. Apoptosis and its role in human disease (1994) *Biotechnology,* 12(5): 487-493.

Barrett TB and Benditt EP. sis (platelet-derived growth factor β chain) gene transcript levels are elevated in human atherosclerotic lesions compared to normal artery (1987) *Proc Natl Acad Sci USA,* 84(4): 1099-1103.

Barrington RE, Subler MA, Rands E, Omer CA, Miller PJ, Hundley JE, Koester SK, Troyer DA, Bearss DJ, Conner MW, Gibbs JB, Hamilton K, Koblan KS, Mosser SD, O'Neill TJ, Schaber MD, Senderak ET, Windle JJ, Oliff A, Kohl NE. A farnesyltransferase inhibitor induces tumour regression in transgenic mice harboring multiple oncogenic mutations by mediating alterations in both cell cycle control and apoptosis (1998) *Mol Cell Biol,* 18(1): 85-92.

Baumgartner HR and Hosang M. Platelets, platelet-derived growth factor and arteriosclerosis (1988) *Experientia,* 44(2): 109-112.

Bauriedel G, Schluckebier S, Hutter R, Welsch U, Kandolf R, Luderitz B, Prescott M F. Apoptosis in restenosis versus stable-angina atherosclerosis: implications for the pathogenesis of restenosis (1998) *Arterioscler Thromb Vasc Biol*, 18 (7): 1132-1139.

Bazenet CE, Mota MA, Rubin LL. The small GTP-binding protein Cdc42 is required for nerve growth factor withdrawal-induced neuronal death (1998) *Proc Natl Acad Sci USA,* 95(7): 3984-3989.

Beigel Y, Zafir N, Teplitzky Y, Newman Y, Gavish D, Wurzel M, Fainaru M. The effect of lovastatin on early restenosis (1995) *J Clin Pharmacol,* 35(6): 599-605.

Benditt EP. Implications of the monoclonal character of human atherosclerotic plaques (1977) *Am J Pathol,* 86(3): 693-702.

Bennett MR and Boyle JJ. Apoptosis of vascular smooth muscle cells in atherosclerosis (1998) *Atherosclerosis,* 138(1): 3-9.

Bennett MR, Evan GI, Newby AC. Deregulated expression of the *c-myc* oncogene abolishes inhibition of proliferation of rat vascular smooth muscle cells by serum reduction, interferon-γ, heparin and cyclic nucleotide analogues and induces apoptosis. (1994) *Circ Res,* 74(3): 525-536.

Bennett MR, Evan GI, Schwartz S. Apoptosis of rat vascular smooth muscle cells is regulated by p53-dependent and –independent pathways (1995) *Circ Res,* 77(2): 266-273.

Bennett MR, Evan GI, Schwartz SM. Apoptosis of human vascular smooth muscle cells derived from normal vessels and coronary atherosclerotic plaques (1995) *J Clin Invest,* 95(5): 2266-2274.

Bennett MR, Littlewood TD, Schwartz SM, Weissberg PL. Increased sensitivity of human VSM cells from atherosclerotic plaques to p53-mediated apoptosis (1997) *Circ Res,* 81(4): 591-599.

Bennis F, Favre G, Le Gaillard F, Soula G. Importance of mevalonate-derived products in the control of HMG-CoA reductase activity and growth of human lung adenocarcinoma cell line A549 (1993) *In J Cancer,* 55(4): 640-645.

Bissonnette RP, Echeverri F, Mahabubi A, Green DR. Apoptotic cell death induced by c-myc is inhibited by bcl-2 (1992) *Nature,* 359(6395): 552-554.

Bobak D, Moorman J, Guanzon A, Gilmer L, Hahn C. Inactivation of the small GTPase Rho disrupts cellular attachment and induces adhesion-dependent and adhesion-independent apoptosis (1997) *Oncogene,* 15(18): 2179-2189.

Bochaton-Piallat M L, Gabbiani F, Redard M, Desmouliere A, Gabbiani G. Apoptosis participates in cellularity regulation during rat aortic intimal thickening (1995) *Am J Pathol,* 146(5): 1059-1064.

Boehme SA and Leonardo MJ. Propriocidal apoptosis of mature T lymphocytes occurs at S phase of the cell cycle (1993) *Eur J Immunol,* 23(7): 1552-1560.

Bohm M, Blasius S, Roessner A. Immunohistochemical localisation of PDGF β, PDGF beta receptors and IGF-I receptors during atherogenesis (1994) *Zentralbl Pathol,* 140(4-5): 357-362.

Bordoulous S, Orend G, MacKenna DA, Pasqualini R, Rouslahti E. Fibronectin Matrix Regulates Activation of Rho and Cdc42 GTPases and cell cycle progression (1998) *J Cell Biol,* 143(1): 267-276.

Bornfeldt LE, Raines EW, Graves LM, Skinner MP, Krebs EG, Ross R. Platelet-derived growth factor. Distinct signal transduction pathways associated with migration versus proliferation (1995) *Ann N Y Acad Sci,* 766: 416-430.

Bourne HR, Sanders DA, Mc Cormick F. The GTPase superfamily: conserved structure and molecular mechanism (1991) *Nature,* 349(6305): 117-127.

Braun K, Holzl G, Pusch O, Hengstschlager M. Deregulated expression of CDK2- or CDK3-associated kinase activities enhances c-Myc-induced apoptosis (1998) *DNA Cell Biol,* 17(9): 789-798.

Brenner B, Kopenhoefer U, Weinstock C, Linderkamp O, LangF Gulbins E. Fas- or ceramide-induced apoptosis is mediated by a Rac 1-regulated activation of Jun N-terminal kinase p38 kinases and GADD153 (1997) *J Biol Chem,* 272 (35): 22173-22181.

Brown Ms, Faust JR, Goldstein JL, Kaneko I and Endo A. Induction of HMG-CoA reductase activity in human fibriblasts incubated with compactin (ML-236B), a competitive inhibitor of the reductase (1978) *J Biol Chem,* 253(4): 1121-1128.

Brown SB, Bailey K, Savill J. Actin is cleaved during constitutive apoptosis (1997) *Biochem J,* 323(Pt 1): 233-237.

Buttyan R, Zakeri Z, Lockshin R and Wolgemuth D. Cascade induction of *c-fos*, *c-myc*, and heat shock 70K transcripts during regression of the rat ventral prostate gland (1988) *Mol Endocrinol,* 2(7): 650-657.

Campbell JH, Tachas G, Black MJ, Cockerill G, Campbell GR. Molecular biology of vascular hypertrophy (1991) *Basic Res Cardiol,* 86 Suppl 1: 3-11

Casalone R, Granata P, Minelli E, Portentoso P, Giudici A, Righi R, Castelli P, Socrate A, Frigenio B. Cytogenetic analysis reveals clonal proliferation of smooth muscle cells in atherosclerotic plaques. (1991) *Hum Genet,* 87 (2): 139-143.

Casey PJ and Seabra MC. Protein prenyltransferases (1996) *J Biol Chem,* 271(10): 5289-5292.

Casey PJ, Solski PA, Der CJ and Buss JE p21ras is modified by a farnesyl isoprenoid (1989) *Proc Natl Acad Sci USA,* 86(21): 8323-8327.

Casey PJ. Lipid modifications of G proteins (1994) *Curr Opin Cell Biol,* 6 (2): 219-225.

Chan P. Cell biology of human vascular smooth muscle (1994) *Ann R Coll Surg Engl,* 76(5): 298-303.

Chan PC, Lafreniere R, Parsons HG. Lovastatin increases surface low density lipoprotein receptor expression by retarding the receptor internalisation rate in proliferating lymphocytes (1997) *Biochem Biophys Res Commun,* 235(1): 117-222.

Chang TH, Ray FA, Thompson DA, Schlegel R. Disregulation of mitotic checkpoints and regulatory proteins following acute expression of SV40 large T antigen in diploid human cells (1997) *Oncogene,* 14(20): 2383-2393.

Chen CY and Faller DV. Direction of p21ras-generated signals towards cell growth or apoptosis is determined by protein kinase C and Bcl-2 (1995) *Oncogene,* 11(8): 1487-1498.

Chen CY, Liou J, Forman LW, Faller DV. Differential regulation of discrete apoptotic pathways by Ras (1998) *J Biol Chem,* 273(27): 16700-16709.

Cheng S, Levy D. The effects of cell proliferation on the lipid composition and fluidity of hepatocyte plasma membranes (1979) *Arch Biochem Biophys,* 196(2): 424-429.

Cho A, Courtman D, Langille L. Apoptosis (programmed cell death) in arteries of neonatal lamb (1995) *Cir Res*, 76(2): 168-175.

Cho A, Mitchell L, Koopmans D, Langille BL. Effects of changes in blood flow rate on cell death and cell proliferation in carotid arteries of immature rabbits (1997) *Circ Res* 81(3): 328-337.

Choi KH, Kang SW, Lee SW, Lee HY, Han DS, Kang BS. The effect of lovastatin on proliferation of cultured rat mesangial and aortic smooth muscle cells (1995) *Yonsei Med J,* 36(3): 251-261.

Chuang TH, Hahn M, Lee JD, Danley DE, Bokoch GM. The small GTPase Cdc42 initiates an apoptotic signalling pathway in Jurkat T Lymphocytes (1997) *Mol Biol Cell,* 8(9): 1687-1698.

Claesson-Welsh L. Platelet-derived growth factor receptor signals (1994) *J Biol Chem,* 269(51): 32023-32026.

Clarke S. Protein isoprenylation and methylation at carboxyl-terminal cysteine residues (1992) *Ann Rev Biochem,* 61: 355-386.

Clowes AW, Clowes MM, Reidy MA. Kinetics of cellular proliferation after arterial injury. I. Smooth muscle growth in the absence of endothelium (1983) *Lab Invest,* 49(3): 327-333.

Clunn GF, Refson JS, Lymn JS, Hughes AD. Platelet-derived growth factor beta-receptors can both promote and inhibit chemotaxis in human vascular smooth muscle cells (1997) *Arterioscler Thromb Vasc Biol,* 17(11): 2622-2629.

Clunn GF, Lymn JS, Schachter M, Hughes AD. Differential effects of lovastatin on mitogen induced calcium influx in human cultured vascular smooth muscle cells (1997) *Br J Pharmacol* 121(8): 1789-1795.

Colotta F, Polentarutti N, Sironi M, Mantovani A. Expression and involvement of c-fos and c-jun protooncogenes in programmed cell death induced by growth factor deprivation of lymphoid cell lines (1992) *J Biol Chem,* 267: 18278-18283.

Compton MM. A biochemical hallmark of apoptosis: internucleosomal degradation of the genome (1992) *Cancer Metastasis Rev,* 11(2): 105-119.

Corcoran GB, Fix L, Jones DP, Moslen MT, Nicotera P, Oberhammer FA and Buttyan R. Apoptosis: Molecular control point in Toxicity. (1994) *Toxicol Appl Pharmacol*, 128 (2): 169-181.

Corsini A, Arnaboldi L, Raiteri M, Quarato P, Faggiotto A, Paoletti R, Fumagalli R. Effect of the new HMG-CoA reductase inhibitor cerivastatin (BAY W 6228) on migration, proliferation and cholesterol synthesis in arterial myocytes (1996) *Pharmacol Res,* 33(1): 55-61.

Corsini A, Mazzotti M, Raiteri M, Soma M R, Gabbiani G, Fumagalli R, Paoletti R. Relationship between mevalonate pathway and arterial myocyte proliferation: in vitro studies with inhibitors of HMG-CoA reductase (1993) *Atherosclerosis,* 101(1): 117-125.

Corsini A, Raiteri M, Soma M, Fumagalli R, Paoletti R. Simvastatin but not pravastatin inhibits the poliferation of rat aorta myocytes (1991) *Pharmacol Res,* 23(2): 173-180.

Corsini A, Raiteri M, Soma MR, Bernini F, Fumagalli R, Paoletti R.. Pathogenesis of atherosclerosis and the role 3-hydroxy-3-methylglutaryl coenzyme A reductase inhibitors (1995) *Am J Cardiol,* 76(2): 21A-28A.

Cotter TG and Martin SJ. "Techniques in Apoptosis, A User`s Guide" (1996) Portland Press Ltd., London, p93.

Cox AD, Garcia AM, Westwick JK, Kowalczyk JJ, Lewis MD, Brenner DA, Der CJ. The CAAX peptidomimetic B581 specifically blocks farnesylated, but not geranylgeranylated or myristylated, oncogenic ras signaling and transformation (1994) *J Biol Chem,* 269(30): 19203-19206.

Crick DC, Andres DA, Danesi R, Macchia M, Waechter CJ. Geranylgeraniol overcomes the block of cell proliferation by lovastatin in C6 glioma cells (1998) *J Neurochem,* 70(6): 2397-23405.

Crick DC, Andres DA, Waechter CJ. Geranylgeraniol promotes entry of UT-2 cells into the cell cycle in the absence of mevalonate (1997) *Exp Cell Res,* 231(2): 302-307.

Crick DC, Waechter CJ, Andres DA.. Utilization of geranylgeraniol for protein isoprenylation in C6 glial cells (1994) *Biochem Biophys Res Commun,* 205(1): 955-961.

Crompton T, Peitsch MC, MacDonald HR and Tschopp J. Propidium iodide staining correlates with the extent of DNA degradation in isolated nuclei (1992) *Biochem Biophys Res Commun,* 183(2): 532-537.

Crouch M F, Simson L. The G-protein G(i) regulates mitosis but not DNA synthesis in growth factor-activated fibroblasts: a role for the nuclear translocation of G(i) (1997) *FASEB J,* 11 (2): 189-198.

Crowell PL, Ren Z, Lin S, Vedejs E, and Gould MN. Structure-activity relationships among novel monoterpene inhibitors of small G-protein isoprenylation and cell proliferation (1994) *Biochem Pharmacol,* 47(8): 1405-1415.

Crowell PL. Monoterpenes in breast cancer chemoprevention (1997) *Breast Cancer Res Treat,* 46(2-3): 191-197.

Cuthbert JA and Lipsky PE. Inhibition by 6-fluoromevalonate demonstrates that mevalonate or one of the mevalonate phosphates is necessary for lymphocyte proliferation (1990) *J Biol Chem,* 265(310): 18568-18575.

Cutts J L, Scallen T J, Watson J, Bankhurst A D. Role of mevalonic acid in the regulation of natural killer cell cytotoxicity (1989) *J Cell Physiol,* 139(3): 550-557.

Cuvillier O, Pirianov G, Kleuser B, Vanek PG, Coso OA, Gutkind S, Spiegel S. Suppresion of ceramide-mediated programmed cell death with sphingosine-1-phosphate (1996) *Nature,* 381(658): 800-803.

Dalton MB, Fantle KS, Bechtold HA, De Maio L, Evans RM, Krystosek A, Sinensky M. The farnesyl protein transferase inhibitor BZA-5B blocks farnesylation of nuclear lamins and p21ras but does not affect their function or localisation (1995) *Cancer Res,* 55(15): 3295-3304.

Danesi R, McLellan CA, and Myers CE. Specific labeling of isoprenylated proteins: application to study inhibitors of the post-translational farnesylation and geranylgeranylation (1995) *Biochem Biophys Res Communs,* 206(2): 637-643.

Darzynkiewicz Z, Bruno S, Del Bino G, Gorczyca W, Hotz MA. Lassota P, Traganos F. Features of Apoptotic cells measured by Flow Cytometry (1992) *Cytometry,* 13(8): 795-805.

Davies MJ, Richardson PD, Woolf N, Katz DR, Mann J. Risk of thrombosis in human atherosclerotic plaques: role of extracellular lipid, macrophage and smooth muscle cell content (1993) *Br Heart J,* 69(5): 377-381.

De Cremoux P, Gauville C, Closson V, Linares G, Calvo F, Tavitian A, Olofsson B EGF modulation of the Ras-related RhoB gene-expression in human breast-cancer cell lines (1994) *Int J Cancer,* 59(3): 408-415.

Didsbury JR, Uhing RJ, Snyderman R. Isoprenylation of the low molecular mass GTP-binding proteins rac1 and rac2: Possible role in membrane localisation (1990) *Biochem Biophys Res Commun,* 171(2): 804-812.

Duggan DE, Chen IW, Bayne WF, et al. The physiological disposition of lovastatin (1989) *Drug Met Dispos,* 17(2): 166-173.

Elledge SJ. Cell cycle checkpoints: preventing an identity crisis (1996) *Science,* 274(5293): 1664-1672.

Endresen PC, Prytz PS, Aarbakke J. A new flow cytometric method for discrimination of apoptotic cells and detection of their cell cycle specificity through staining of F-actin and DNA (1995) *Cytometry,* 20(2): 162-171.

Engelberg D, Klein C, Martinetto H, Struhl K, Karin M. The UV response invovling the ras signalling pathway and AP-1 transcription factorsis conserved between yeast and mammals (1994) *Cell,* 77(3): 381-390.

Esteve P, del Peso L, Lacal JC. Induction of apoptosis by rho in NIH 3T3 cells requires two complementary signals. Ceramides function as a progression factor for apoptosis. (1995) *Oncogene,* 11(12): 2657-2665.

Evan GI, Wyllie AH, Gilbert CS, Littlewood TD, Land H, Brooks M, Waters CM, Penn LZ, Hancock DC. Inducion of apoptosis in fibroblasts by c-myc protein (1992) *Cell,* 69(1): 119-128.

Eves EM, Xiong W, Bellacosa A, Kennedy S G, Tsichlis P N, Rosner M R, Hay N Akt, a target of phosphatidylinositol 3-kinase, inhibits apoptosis in a differentiating neuronal cell line (1998) *Mol Cell Biol,* 18(4): 2143-2152.

Fairbanks KP, Witte L and Goodman DS. Relationship between mevalonate and mitogenesis in human fibroblasts stimulated with PDGF (1984) *J Biol Chem* 259(3): 1546-1551.

Fanidi A, Harrington EA, Evan GI. Co-operative interaction between c-myc and bcl-2 oncogenes (1992) *Nature,* 359 (6395): 554-556.

Farnsworth CC, Gelb MH, and Glomset SA. Identification of geranylgeranyl-modified proteins in HeLa cells (1990) *Science,* 247 (4940): 320-322.

Fenton RG, Kung HF, Longo DL, Smith MR. Regulation of intracellular actin polymerization by prenylated cellular proteins (1992) *J Cell Biol,* 117(2): 347-356.

Feramisco JR, Gross M, Kamata T, Rosenberg M, Sweet RW. Microinjection of the oncogene form of the human H-ras (T-24) protein results in rapid proliferation of quiscent cells (1984) *Cell*, 38(1): 109-117.

Ferns GA, Raines EW, Sprugel KH, Motani AS, Reidy MA, Ross R. Inhibition of neointimal smooth muscle accumulation after angioplasty by an antibody to PDGF (1991) *Science,* 253(5024): 1129-1132.

Ferrari G and Greene LA. Proliferative inhibition by dominant-negative Ras rescues naive and neuronally differentiated PC12 cells from apoptotic death (1994) *EMBO J,* 13(24): 5922-5928.

Fiorentini C, Fabbri A, Matarrese P, Falzano L, Boquet P, Malorni W. Hinderance of apoptosis and phagocytic behaviour induced by Escherichia coli cytotoxic necrotizing factor 1: two related activities in epithelial cells (1997) *Biochem Biophys Res Comm,* 241(2): 341-346.

Fischer TH, Gatling M N, Lacal J C, White G C 2d. rap1B, a cAMP-dependent protein kinase substrate, associates with the platelet cytoskeleton (1990) *J Biol Chem,* 265(32): 19405-19408.

Flemming W. Uber die Bildung von Richtungsfiguren in Saugethiereiern bein Untergang Graaf'scher Follikel (1885) *Arch Anat EntwGesch*, 221-224.

Flint O P, Masters B A, Gregg R E and Durham S K. HMG-CoA reductase inhibitor-induced myotoxicity: Pravastatin and Lovastatin inhibit the geranylgeranylation of low-molecular-weight proteins in neonatal rat muscle cell culture (1997) *Toxicol Appl Pharmacol,* 145(1): 99-110.

Flint O P, Masters B A, Gregg R E and Durham S K. Inhibition of cholesterol synthesis by squalene synthase inhibitors does not induce myotoxicity *in vitro* (1997) *Toxicol Appl Pharmacol,* 145(1): 91-98.

Fokstuen T, Rabo YB, Zhou JN, Karlson J, Platz A, Shoshan MC, Hansson J, Linder S. The Ras farnesylation inhibitor BZA-5B increases the resistance to cisplatin in a human melanoma cell line (1997) *Anticancer Res,* 17(4A): 2347-2352.

Forsberg K, Valyi-Nagy I, Heldin CH, Herlyn M, Westermark B. Platelet-derived growth factor (PDGF) in oncogenesis: development of a vascular connective tissue stroma in xenotransplanted human melanoma producing PDGF-BB (1993) *Proc Natl Acad Sci USA,* 90(2): 393-397.

Fox JC and Shanley JR. Antisense inhibition of basic firbroblast growth factor induces apoptosis in vascular smooth muscle cells (1996) *J Biol Chem,* 271(21): 12578-12584.

Fraker PJ, King LE, Lill-Elghanian D, Telford WG. "Quantification of Apoptotic Events in Pure and Heterogenous Polpulations of Cells Using the Flow Cytometry", (1995) Chp.4 in Methods in Cell Biology Vol. 46, p62.

Frid MG, Aldashev AA, Dempsey EC, Stenmark KR. Smooth muscle cells isolated from discrete compartments of the mature vascular media exhibit unique phenotypes and distinct growth capabilities (1997) *Cir Res,* 81(6): 940-952.

Fritz G, Kaina B, Aktories K. The ras-related small GTP-binding RhoB protein is immediate-early inducible by DNA damaging treatments (1995) *J Biol Chem,* 270(42): 25172-25177.

Fueyo J, Gomez-Manzano C, Yung WK, Liu TJ, Alemany R, Mc **Donnell TJ, ShiX, Rao JS, Levin VA, Kyritsis AP**. Overexpression of E2F-1 in glioma triggers apoptosis and suppresses tumour growth *in vitro* and *in vivo* (1998) *Nat Med,* 4(6): 685-690.

Fulton GJ, Barber L, Svendensen E, Hagen PO, Davies MG. Oral monoterpene therapy (perillyl alcohol) reduces vein graft intimal hyperplasia (1997) *J Surg Res,* 69(1): 128-134.

Furberg C D, Adams H P Jr, Applegate W B, Byington R P, Espeland M A, Hartwell T, Hunninghake D B, Lefkowitz D S, Probstfield J, Riley W A, et al. Effect of lovastatin on early carotid atherosclerosis and cardiovascular events. Asymptomatic Carotid Artery Progression Study (ACAPS) Research Group (1994) *Circulation,* 90(4): 1679-1687.

Garcia AM, Rowell C, Ackermann K, Kowalczyk JJ, Lewis MD. Peptidomimetic inhibitor of Ras farnesylation and function in whole cells (1993) *J Biol Chem,* 268(25): 18415-18418.

Garder A M and Johnson G L. Fibroblast growth factor-2 suppression of tumour necrosis factor alpha-mediated apoptosis requires Ras and the activation of mitogen-activated protein kinase (1996) *J Biol Chem,* 271(24): 14560-14566.

Gavrieli Y, Sherman Y, and Ben-Sasson SA. Identification of programmed cell death *in situ* via specific labelling of nuclear DNA fragmentation. (1992) *J Cell Biol*, 119 (3): 493-501.

Gelb MH, Tamanoi F,Yokoyama K, Ghomaschi F, Esson K, and Gould MN. The inhibition of protein prenyl transferases by oxygenated metabolites of limonene and perillyl alcohol (1995) *Cancer Lett,* 91(2): 169-175.

Geng YJ, Wu Q, Muszynski M, Hansson GK, Libby P. Apoptosis of vascular smooth muscle cells induced by *in vitro* stimulation with interferon-γ, TNF-α, and IL-1β (1996) *Arterioscler Thromb Vasc Biol,* 16(1): 19-27.

Ghosh PM, Mott GE, Ghosh Choudhury N, Radnik RA, Stapleton ML, Ghidoni JJ, Kreisberg JI. Lovastatin induces apoptosis by inhibiting mitotic and post-mitotic events in cultured mesangial cells. (1997) *Biochemica et Biophysica Acta – Molecular Cell Research*, 1359 (1): 13-24.

Ghosh R, Amstad P, Cerutti P. UVB-induced DNA breaks interfere with transcriptional induction of c-fos (1993) *Mol Cell Biol,* 13(11): 6992-6999.

Giambarella U, Yamatsuji T, Okamoto T, Matsui T, Ikezu T, Murayama Y, Levine MA, Katz A, Gautam N, Nishimoto I. G protein beta gamma complex-mediated apoptosis by familial Alzheimer's disease mutant of APP (1997) *EMBO J,* 16(16): 4897-4907.

Gibbs JB and Oliff A. Pharmaceutical research in molecular oncology (1994) *Cell,* 79(2): 193-198

Gibbs JB and Oliff A. The potential of farnesyltransferase inhibitors as cancer chemotherapeutics (1997) *Annu Rev Pharmacol Toxicol,* 37: 143-146.

Gjoerup O, Lukas J, Bartek J, Willumsen BM. Rac and Cdc42 are potent stimulators of E2F-dependent transcription capable of promoting retinoblastoma susceptibility gene product hyperphosphorylation (1998) *J Biol Chem,* 273(30): 18812-18818.

Glagov S, Weisenberg E, Zarins CK, Stankunavicius R, Kolettis GJ. Compensatory enlargement of human atherosclerotic coronary arteries (1987) *N Engl J Med,* 316(22): 1371-1375.

Glucksmann A. Cell deaths in normal vertebrate ontogeny (1951) *Biol Rev Camb Philos Soc,* 26: 59-86.

Goalstone ML, Natarajan R, Standley PR, Walsh MF, Leitner JW, Carel K, Scott S, Nadler J, Sowers JR, Draznin B. Insulin potentiates platelet-derived growth factor action in vascular smooth muscle cells (1998) *Endocrinology,* 139(10): 4067-4072.

Goldstein J L and Brown M S. Regulation of the mevalonate pathway (1990) *Nature,* 343(6257): 425-430.

Gomez J, Martinez AC, Fernandez B, Garcia A, Rebollo A. Critical role of Ras in the proliferation and prevention of apoptosis mediated by IL-2 (1996) *J Immunol,* 157(6): 2272-2281.

Gomez J, Martinez AC, Gonzalez A, Rebollo A. Dual role of Ras and Rho proteins: at the cutting edge of life and death (1998) *Immunol Cell Biol,* 76(2): 125-134.

Gomez J, Martinez C, Giry M, Garcia A, Rebollo A. Rho prevents apoptosis through Bcl-2 expression: implications for interleukin-2 receptor signal transduction (1997) *Eur J Immunol,* 27(11): 2793-2799.

Gong J, Traganos F, Darzynkiewicz Z. A selective procedure for DNA extraction form apoptotic cells applicable for gel electrophoresis and flow cytometry (1994) *Anal Biochem,* 218(2): 314-319.

Gordon D, Reidy MA, Benditt EP, Schwartz SM. Cell proliferation in human coronary arteries (1990) *Proc Natl Acad Sci USA,* 87(12) 4600-4604.

Green DR and Reed JC. Mitochondria and apoptosis (1998) *Science* 281(5381):1309-1312.

Green DR and Scott DW. Activation-induced apoptosis in lymphocytes (1994) *Curr Opin Immunol,* 6(3): 476-487.

Greenberg ME and Ziff EB. Stimulation of 3T3 cells induces transcription of the c-fos oncogene (1984) *Nature,* 311(5985): 433-438.

Grunler J, Ericsson J, Dallner G. Branch-point reactions in the biosynthesis of cholesterol, dolichol, ubiquinone and prenylated proteins (1994) *Biochim Biophys Acta,* 1212(3): 259-277.

Guenal I, Risler Y, Mignotte B. Down-regulation of actin genes precedes microfilament network disruption and actin cleavage during p53-mediated apoptosis (1997) *J Cell Sci,* 110 (Pt 4): 489-495.

Guijarro C, Blanco-Colio LM, Ortego M, Alonso C, Ortiz A, Plaza JJ, Diaz C, Hernandez G, Edigo J. 3-Hydroxyl-3-Methylgutarl coenzyme A reductase and isoprenylation inhibitors induce apoptosis of vascular smooth muscle cells in culture (1998) *Circ Res,* 83(5): 490-500.

Gulbins E, Coggeshall KM, Brenner B, Schlottmann K, Linderkamp O, Lang F Fas-induced apoptosis is mediated by activation of a Ras and Rac protein-regulated signalling pathway (1996) *J Biol Chem,* 271(42): 26389-26394.

Gutierrez L, Magee A I, Marshall C J, Hancock J F. Post-translational processing of p21 ras is two-step and involves carboxyl-methylation and carboxyl terminal proteolysis (1989) *EMBO J,* 8(4): 1093-1098.

Haag JD, Gould MN. Mammary carcinoma regression induced by perillyl alcohol, a hydroxylated analog of limonene (1994) *Cancer Chemother Pharmacol,* 34(6): 477-483.

Habenicht AJ, Glomset JA, Ross R. Relation of cholesterol and mevalonic acid to the cell cycle in smooth muscle and Swiss 3T3 cells stimulated to divide by platelet-derived growth factor (1980) *J Biol Chem,* 255(11): 5134-5140.

Hadrava V, Tremblay J, Hamet P. Abnormalities in growth characteristics of aortic smooth muscle cells in spontaneously hypertensive rats. (1989) *Hypertension,* 13 (6Pt1): 589-597.

Hamet P, Moreau P, Dam TV, Orlov SN, Tea BS, deBlois D, Tremblay J. The time window of apoptosis: a new component in the therapeutic strategy for cardiovascular remodelling (1996) *J Hypertens Suppl,* 14(5): 565-570.

Hamet P, Richard L, Dam T, Teiger E, Orlov S, Gaboury L, Gossard F, Tremblay J. Apoptosis in target organs of hypertension (1995) *Hypertension,* 26(4): 642-648.

Hamet P. Proliferation and apoptosis of vascular smooth muscle in hypertension (1995) *Curr Opin Nephrol Hypertension,* 4(1): 1-7

Han D, Haundenschild C, Hong M, Tinkle BT, Leon MB, Liau G. Evidence for apoptosis in a human atherosclerosis and in a rat vascular injury model (1995) *Am J Pathol,* 147(2): 267-277.

Hancock JF and Hall A. a novel role for RhoGDI as an inhibitor of GAP proteins (1993) *EMBO J* 12(5): 1915-1921.

Hancock JF, Magee AI, Childs JE and Marshall CJ. All ras proteins are polyisoprenylated but only some are palmitoylated (1989) *Cell,* 57(7): 11167-11177.

Hanke H, Karsch KR. Role of smooth muscle cell proliferation after balloon angioplasty (1992) *Herz.,* 17(5): 300-308.

Harper JW. Cyclin-dependent kinase inhibitors (1997) *Cancer Surv,* 29: 91-107.

Heldin CH, Ostman A, Ronnstrand L. Signal transduction via platelet-derived growth factor (1998) *Biochim Biophys Acta,* 1378(1): F79-F113.

Heldin CH, Ostman A, Westermark B. Structure of platelet-derived growth factor: implications for functional properties (1993) *Growth factors,* 8(4): 245-252.

Heldin CH. Structural and functional studies on platelet-derived growth factor (1992) *EMBO J,* 11(12): 4251-4259.

Hidaka Y, Eda T, Yonemoto M, Kamei T. Inhibition of cultured vascular smooth muscle cell migration by simvastatin (MK-733) (1992) *Atherosclerosis,* 95(1): 87-94.

Hirai A, Nakamura S, Noguchi Y, Yasuda T, Kitagawa M, Tatsuno I, Oeda T, Tahara K, Terano T, Narumiya S, Kohn LD, Saito Y. Geranylgeranylated rho small GTPase(s) are essential for the degradation of p27Kip1 and facilitate the progression from G_1 to S phase in growth-stimulated rat FRTL-5 cells (1997) *J Biol Chem,* 272(1): 13-6.

Hoang AT, Cohen KJ, Barrett JF, Bergstrom DA, Dang CV. Participation of cyclin A in myc-induced apoptosis (1994) *Proc Natl Acad Sci USA,* 91(15): 6875-6879

Hohl RJ and Lewis K. Differential effects of Monoterpenes and Lovastatin on Ras processing (1995) *J Biol Chem* 270(29): 17508-17512.

Hughes AD, Patel M, Wijetunge S, Clunn G, Schacter M. Comparison of effects of platelet-derived growth factor isoforms on siganlling and DNA synthesis of human cultured saphenous vein cells (1995) *J Cardiovasc Pharmacol,* 25(3): 481-485.

Hughes AD. The role of isoprenoids in vascular smooth muscle: potential benefits of statins unrelated to cholesterol lowering (1996) *J Hum Hypertens,* 10(6): 387-390.

Huot J, Houle F, Rousseau S, Deschesnes RG, Shah GM, Landry J. SAPK/p38-dependent F-actin reorganisation regulates early membrane blebbing during stress-induced apoptosis (1998) *J Cell Biol,* 143(5): 1361-1373.

Hwang DL, Latus LJ, Lev-Ran A. Effects of platelet-contained growth factors (PDGF, EGF, IGF-I, and TGF-beta) on DNA synthesis in porcine aortic smooth muscle cells in culture (1992) *Exp Cell Res,* 200 (2): 358-360.

Iimura O, Vrtovsnik F, Terzi F, Friedlander G. HMG-CoA reductase inhibitors induce apoptosis in mouse proximal tubular cells in primary culture. (1997) *Kidney International*, 52 (4): 962-972.

Indolfi C, Avvedimento EV, Rapacciuolo A, DiLorenzo E, Esposito G, Stabile E, Feliciello A, Mele E, Giuliano P, Condorelli G, et al., Inhibition of cellular ras prevents smooth muscle cell proliferation after vascular injury *in vivo* (1995) *Nat Med,* 1(6): 541-545.

Irani K, Herzlinger S, Finkel T. Ras proteins regulate multiple mitogenic pathways in A10 vascular smooth muscle cells (1994) *Biochem Biophys Res Commun,* 202(3): 1252-1258.

Isner J M, Kearnery M, Bortman S, Passeri J. Apoptosis in human atherosclerosis and restenosis (1995) *Circulation,* 91(11): 2703-2711.

Itoh Y, Kaibuchi K, Masuda T, Yamamoto T, Matsura Y, Maeda A, Shimizu K, Takai Y. Post-translational processing of ras p21 is critical for its stimulation of mitogen-activated protein kinase (1993) *J Biol Chem,* 268(5): 3025-3028.

Jahner D and Hunter T. The ras-related gene rhoB is an immediate-early gene inducible by v-Fps, epidermal growth factor, and platelet-derived growth factor in rat fibroblasts (1991) *Mol Cell Biol,* 11(7): 3682-3690.

James GL, Brown MS, Cobb MH, Goldstein JL. Benzodiazepine peptidomimetic BZA-5B interrupts the MAP kinase activation pathway in H-Ras-transformed Rat-1 cells, but not in untransformed cells (1994) *J Biol Chem,* 269 (44): 27705-27714.

James GL, Brown Ms, Goldstein JL. Assays for inhibitors of CAAX farnesyl transferase in vitro and in intact cells (1995) *Methods Enzymol,* 255: 38-46.

James GL, Goldstein JL, Brown MS, Rawson TE, Somers TC, McDowell RS, Crowley CW, Lucas BK, Levinson AD, Marsters JC Jr. Benzodiazepine peptidomimetics: potent inhibitors of ras farnesylation in animal cells (1993) *Science,* 260 (5116): 1937-1942.

James GL, Goldstein JL, Brown MS. Poly-L-Lysine and CVIM sequnces of K-RasB dictate specificity of prenylation and confer resistance to benzodiazepine peptidomimetic *in vitro* (1995) *J Biol Chem,* 270(11): 6221-6226.

Jansen-Durr P, Meichle A, Steiner P, Pagano M, Finke K, Botz J, Wessbecher J, Draetta G, Eilers M. Differential modulation of cyclin gene expression by myc (1993) *Proc Natl Acad Sci USA,* 90(8): 3685-3689.

Kamiya Y, Sakurai A, Tamura S, Takahashi N. Structure of rhodotorucine A, a novel lipopeptide, inducing mating tube formation in *Rhodosporidium toruloides.* (1978) *Biochem Biophys Res Commun,* 83(3): 1077-1083.

Kaneko I, Hazama-Shimada Y, Endo A. Inhibitory effects on lipid metabolism in cultured cells of ML-236B, a potent inhibitor of 3-hydroxy-3-methylglutaryl-coenzyme A reductase (1978) *Eur J Biochem,* 87(2): 313-321.

Kauffmann-Zeh A, Rodriguez-Viciana P, Ulrich E, Gilbert C, Coffer P, Downward J, Evan G. Suppresion of *c-myc*-induced apoptosis by Ras signalling through PI(3)K and PKB (1997) *Nature,* 385(6616): 544-548.

Kelly K, Cochran BH, Stiles CD, Leder P. Cell-specific regulation of the c-myc gene by lymphocyte mitogens and platelet-derived growth factor (1983) *Cell,* 35(3 Pt 2): 603-610.

Kerr JFR and Harmon BV. Definition and incidence of apoptosis: an historical perspective, In Tomei LD, Cope F (eds) (1991) "Apoptosis: The Molecular Basis of Death" Plainview, NY: Cold Spring Harbor press, pp5-29.

Kerr JFR, Wyllie AH, and Currie AR. Apoptosis: a basic biological phenomenon with wide-ranging implications in tissue kinetics. (1972) *Br J Cancer,* 26 (4): 239-257.

Keyomarsi K, Sandoval L, Band V, Parde AB. Synchronization of tumour and normal cells from G to multiple cell cylces by lovastatin (1991) *Cancer Res,* 51(3): 3602-3609.

Kim DN, Schmee J, Ho HT, Thomas WA. The "turning off" of excessive cell replicative activity in advanced atherosclerotic lesions of swine by a regression diet (1988) *Atherosclerosis,* 71(2-3): 131-142.

Kim HE, Han SJ, Kasza T, Ham R, Choi HS, Plamer KC, Kim HR. Platelet-derived growth factor (PDGF)-signaling mediates radiation-induced apoptosis in human prostate cancer cells with loss of p53 function (1997) *Int J Radiat Oncol Biol Phys,* 39(3): 731-736.

Kim HR, Upadhyay S, Li G, Palmer KC, Deuel TF. Platelet-derived growth factor induces apoptosis in growth-arrested murine fibroblasts (1995) *Proc Natl Acad Sci USA,* 92(21): 9500-9504.

King KL and Cidlowski JA. Cell cycle and apoptosis: common pathways to life and death (1995) *J Cell Biochem,* 58(2): 175-180.

King KL and Cidlowski JA. Cell cycle regulation and apoptosis (1998) *Annu Rev Physiol,* 60: 601-617

Kinoshita T, Yokota T, Arai K, Miyajima A. Regulation of Bcl-2 expression by oncogenic ras proteins in hematopoietic cells (1995) *Oncogene,* 10(11): 2207-2212.

Kobayashi S and Koike T. The molecular structure and biological significance of soluble Fas (1996) *Nippon Rinsho,* 54(7): 1741-1746.

Koch G, Benz C, Schmidt G, Olenik C, Aktories K. Role of Rho protein in lovastatin-induced breakdown of actin cytoskeleton (1997) *J Pharmacol Exp Ther,* 283(2): 901-909.

Kockx MM, Cambier BA, Bortier HE, De Meyer GR, Declercq SC, Van Cauwelaert PA, Bultinck J. Foam cell replication and smooth muscle cell apoptosis in human saphenous vein grafts (1994) *Histopathology,* 25(4): 365-371.

Kohl NE, Wilson FR, Mosser SD, Giuliani E, deSolms SJ, Conner MW, anthony NJ, Holtz WJ, Gomez RP, Lee TJ et al., Protein farnesyltransferase inhibitors block the growth of ras-dependent tumours in nude mice (1994) *Proc Natl Acad Sci USA,* 91(19): 9141-9145.

Kohler N and Lipton A. Platelets as a source of fibroblast growth-promoting activity (1974) *Exp Cell Res,* 87(2): 297-301.

Konstadoulakis MM, Kymionis GD, Karagiani M, Katergianakis A, Doundoulakis N, Pararas V, Koutselinis A, Sehas M, Peveretos P. Evidence of apoptosis in human carotid atheroma (1998) *J Vasc Surg,* 27(4): 733-739.

Kraemer PM and Bradbury EM. Abrogation of a kinase-mediated G1 cell cycle arrest point is a late event in the neoplastic progression of human fibroblasts transfected with the SV40 large T antigen gene (1993) *Exp Cell Res,* 207(1): 206-210.

Kramer M, Stein B, Mai S, Kunz E, Konig H, Loferer H, Grunicke HH, Ponta H, Herrlich P, Rahmsdorf HJ. Radiation-induced activation of transcription factors in mammalian cells (1990) *Radiat Environ Biophys,* 29(4): 303-313.

Kroemer G, Petit P, Zamzami N, Vayssiere JL, Mignotte B. The biochemistry of Programmmed cel death (1995) *FASEB J,* 9(13): 1277-1287.

Lacal JC. Regulation of proliferation and apoptosis by Ras and Rho GTPases through specific phospholipid-dependent signalling (1997) *FEBS Lett,* 410(1): 73-77.

Larsson O. Role of biosynthesis of cholesterol and isoprenoid derivatives in regulation of G_1 progression and cell proliferation of 3T6 cells (1987) *J Cell Physiol,* 133(1): 163-168.

Lazebnik YA, Cole S, Cooke CA, Nelson WG, Earnshaw WC. Nuclear events of apoptosis in vitro in cell-free mitotic extracts: a model system for analysis of the active phase of apoptosis (1993) *J Cell Biol,* 123(1): 7-22.

Lerner EC, Qian Y, Hamilton AD, Sebti SM. Disruption of oncogenic K-Ras4B processing and signaling by a potent geranylgeranyl transferase I inhibitor (1995) *J Biol Chem,* 270(45): 26770-26773.

Lerner EC, Zhang TT, Knowles DB, Qian Y, Hamilton AD, Sebti SM. Inhibition of the prenylation of K-Ras, but not H- or N-Ras, is highly resistant to CAAX peptidomimetics and requires both a farnesyltransferase and a geranylgeranyltransferase I inhibitor in tumour cell lines (1997) *Oncogene,* 15(11): 1283-1288.

Levitzki A. Signal-transduction therapy. A novel approach to disease management (1994) *Eur J Biochem,* 226(1): 1-13.

Levkau B, Koyama H, Raines EW, Clurman BE, Herren B, Orth K, Roberts JM, Ross R. Cleavage of p21Cip/WAF1 and p27Kip1 mediates apoptosis in endothelial cells through activation of Cdk2: role of a caspase cascade (1998) *Mol Cell,* 1(4): 553-563.

Libby P, Warner SJ, Salomon RN, Birinyi LK. Production of platelet-derived growth factor-like mitogen by smooth muscle cells from human atheroma (1988) *N Eng J Med,* 318(23): 1493-1498.

Lopez-Candales A, Holmes DR, Liao S, Scott MJ, Wickline SA, Thompson RW. Decreased vascular smooth muscle cell density in medial degeneration of human abdominal aortic aneurysms. (1997) *Am J Pathol,* 150(3): 993-1007.

Lutz RJ, McLain TM, Sinesky M. Feedback inhibition of polyisoprenyl pyrophosphate synthesis form mevalonate *in vitro*. Implications for protein prenylation (1992) *J Biol Chem,* 267(12): 7983-7986.

MacLellan WR, Schneider MD. Death by design. Programmed Cell Death in Cardiovascular Biology and Disease (1997) *Circ Res,* 81(2): 137-144.

Maeda S, Suzuki A, Lin KH, Inagaki H, Saito I. DNA fragmentation induced in high-cell-density culture of primary rat hepatocytes is an active process dependent on energy availability, gene expression, and calmodulin (1995) *J Biochem (Tokyo)*. 118(6): 1161-1165

Maltese W A and Sheridan K M. Differentiation of neuroblastoma cells induced by an inhibitor of mevalonate synthesis: relation of neurite outgrowth and acetylcholinesterase activity to changes in cell proliferation and blocked isoprenoid synthesis (1985) *J Cell Physiol,* 125(3): 540-548.

Maltese W A and Sheridan K M. Isoprenoid modification of G25K(Gp), a low molecular mass GTP-binding protein distinct from p21ras (1990) *J Biol Chem,* 265 (29): 17883-17890.

Maltese W A and Sheridan K M. Isoprenylated proteins in cultured cells: subcellular distribution and changes related to altered morphology and growth arrest induced by mevalonate deprivation (1987) *J Cell Physiol,* 133 (3): 471-481.

Maltese W A, Defendi R, Green R A, Sheridan K M, Donley D K.. Suppression of murine neuroblastoma growth in vivo bu mevinolin, competitive inhibitor of 3-hydroxy-3-methylglutaryl CoA-reductase (1985) *J Clin Invest,* 76(5): 1748-1754.

Maltese W A. Post-translational modification of proteins by isoprenoids in mammalian cells (1990) *FASEB J,* 4(15): 3319-3328.

Maltese WA and Sheridan KM. Differentiation of neuroblastoma cells induced by an inhibitor of mevalonate synthesis: relation of neurite outgrowth and acetylcholinesterase activity to changes in cell proliferation and blocked isoprenoid synthesis (1985) *J Cell Physiol,* 125(3): 540-558.

Malumbres M, Pellicer A. Ras pathways to cell cycle control and cell transformation (1998) *Front Biosci,* 3: D887-D912.

Majno G and I Joris. Apoptosis, Oncosis, and Necrosis (1995) *Am J Pathol,* 146(1): 3-15.

Marshall CJ. Protein prenylation: A mediator of protein-protein interactions (1993) *Science* 259(5103): 1865-1866.

Massy ZA, Keane WF, Kasiske BL. Inhibition of the mevalonate pathway: benefits beyond cholesterol reduction? (1996) *Lancet,* 347(8994): 102-103.

Matzno S, Yamauchi T, Gohda M, Ishida N, katsuura K, Hansaki Y, Yokunaga T, Itoh H, Nakamura N. Inhibition of cholesterol biosynthesis by squalene epoxidase inhibiotr avoids apoptotic cell death in L6 myoblasts (1997) *J Lipid Res,* 38(3): 1639-1648.

McConkey D J, Hartzell P, Amador-Perez J F, Orrenius S, Jondal M. Calcium-dpendent killing of immature thymocytes by stimulation via the CD3/T cell receptor complex (1989) *J Immunol,* 143(6): 1801-1806.

McConkey DJ, Zhivotovsky B, and Orrenius S. Apoptosis - Molecular mechanisms and biomedical implications. (1996) *Molec Aspects Med*, 17 (1): 1-110.

McCormick F. Signal transduction. Why Ras needs Rho (1998) *Nature,* 394(6690): 220-221.

McGuire T F and Sebti S M. Geranylgeraniol potentiates lovastatin inhibition of oncogenic H-Ras processing and signalling while preventing cytotoxicity (1997) *Oncogene,* 14(3): 305-312.

McGuire TF, Qian Y, Vogt A, Hamilton AD, Sebti SM. Platelet-derived growth factor receptor tyrosine phosphorylation requires protein geranylgeranylation but not farnesylation (1996) *J Biol Chem,* 271(44): 27402-27407.

Meikrantz W and Schlegel R. Suppression of apoptosis by dominant negative mutants of cyclin-dependent protein kinases (1996) *J Biol Chem,* 271(17): 10205-10209.

Meikrantz W, Gisselbrecht S, Tam SW, Schlegel R. Activation of cyclin-A dependent protein kinases during apoptosis (1994) *Proc Natl Acad Sci USA,* 91(9): 3754-3758

Meikrantz W and Schlegel R. Apoptosis and the cell cycle (1995) *J Cell Biochem,* 58(2): 160-174.

Mills JC, Stone NL, Erhardt J, Pittman RN. Apoptotic membrane blebbing is regulated by myosin light chain phosphorylation (1998) *J Cell Biol,* 140(3): 627-636.

Mills JJ, Chari RS, Boyer IJ, Gould MN, Jirtle RL. Induction of apoptosis in liver tumours by the monoterpene perillyl alcohol (1995) *Cancer Res,* 55(5): 979-983.

Miquel K, Pradines A, Sun J, Qian Y, Hamilton AD, Sebti SM, Favre G. GGTI-298 induces G_0/G_1 block and apoptosis whereas FTI-277 causes G_2/M enrichment in A549 cells (1997) *Cancer Res,* 57(10): 1846-1850.

Mizuno T, Kaibuchi K, Yamamoto T, Kawamura M, Sakoda T, Fujioka H, Matsuura Y, Takai Y. A stimulatory GDP/GTP exchange protein for smg p21 is active on the post-translationally processed form of c-Ki-ras p21 and rhoA p21 (1991) *Proc Natl Acad Sci USA,* 88(15): 6442-6446.

Moore K A, Sethi R, Doanes A M, Johnson T M, Pracyk J B, Kirby M, Irani K, Goldsmidt-Clermont P J, Finkel T. Rac 1 is required for cell proliferation and G_2/M progression (1997) *Biochem J,* 326 (Pt1): 17-20.

Moores SL, Schaber MD, Mosser SD, Rands E, O'Hara MB, Garsky VM, Marshall MS, Pompliano DL, Gibbs JB. Sequence dependence of protein isoprenylation (1991) *J Biol Chem,* 266(22): 14603-14610.

Moreau P, Tea BS, Dam TV, Hamet P. Altered balance between cell replication and apoptosis in hearts and kidneys of newborn spontaneously hypertensive rat (SHR) (1997) *Hypertension,* 30[3 part 2]: 720-724.

Motulsky, H. Intuitive Biostatistics. Oxford University Press, Inc. 1995.

Mulcahy LS, Smith MR, Stacey DW. Requirement for ras proto-oncogene function during serum-stimulated growth of NIH 3T3 cells (1985) *Nature,* 313(5999): 241-243

Mumby S M, Casey P J, Gilman A G, Gutowski S and Sterweis P C. G-protein gamma subunits contain a 20-carbon isoprenoid (1990) *Proc Natl Acad Sci USA,* 87(15): 5873-5877.

Munro E, Patel M, Chan P, Betteridge L, Clunn G, Gallagher K, Hughes AD, Schachter M, Wolfe J, Sever P. Inhibition of human vascular smooth musce cell proliferation by lovastatin: the role of isoprenoid intermediates of cholesterol synthesis. (1994) *Eur J Clin Invest*, 24(11): 766-772.

Murray A and Hunt T. The Cell Cycle (1993) New York: Oxford University Press. 251pp.

Murray A. Cell cycle checkpoints (1994) *Curr Opin Cell Biol,* 6(6): 872-876.

Nagase T, Kawata S, Tamura S, Matsuda Y, Inui Y, Yamasaki E, Ishiguro H, Ito T, Miyagawa J, Mitsui H, Yamamato K, Kinoshita M, Matsuzawa Y. Manumycin and gliotoxin derivative KT7595 block Ras farnesylation and cell growth but do not disturb lamin farnesylation and localisation in human tumour cells (1997) *Br J Cancer,* 76(8): 1001-1010.

Newby AC and George JS. Proliferation, migration, matrix turnover, and death of smooth muscle cells in native coronary and vein graft atherosclerosis (1996) *Curr Opin Cardiol,* 11(6): 574-582.

Newman C and Magee AI. Post-translational processing of the ras superfamily of small GTP-binding proteins (1993) *Biochim Biophys Acta,* 1155(1): 79-96.

Nicoletti I, Migliorati G, pagliacci MC, Grinani F and Riccardi C. A rapid and simple method for measuring thymocyte apoptosis by propidium iodide staining and flow cytometry (1991) *J Immunol Methods,* 149(2): 271-279.

Nobes CD and Tolkovsky AM. Neutralizing anti-p21ras Fabs suppress rat sympathetic neuron survival induced by NGF, LIF, CNTF and cAMP (1995) *Eur J Neurosci,* 7(2): 344-350.

Noguchi Y, Nakamura S, Yasuda T, Kitagawa M, Kohn LD, Saito Y, Hira A. Newly synthesised RhoA, not Ras, is isoprenylated and translocated to membranes coincident with progression of the G_1 to S phase of growth-stimulated rat FRTC-5 cells. (1998) *J Biol Chem,* 273(6): 3649-3653.

Nunez G, Benedict MA, Hu Y, Inohara N. Caspases: proteases of the apoptotic pathway (1998) *Oncogene* 17(25): 3237-3245.

O'Brien ER, Alpers CE, Stewart DK, Ferguson M, Tran N, Gordon D, Benditt EP, Hinohara Y, Simpson JB, Schwartz SM. Proliferation in primary and restenotic coronary atherectomy tissue: Implications for anti-proliferative therapy (1993) *Circ Res,* 73(2): 223-231.

Oberhammer F, Bursch W, Tiefenbacher R, Froschl G, Pavelka M, Purchio T, Schulte-Hermann R. Apoptosis is induced by transforming growth factor-beta 1 within 5 hours in regressing liver without significant fragmentation of the DNA (1993) *Hepatology,* 18(5): 1238-1246.

Ohya Y, Qadota H, Anraku Y, Pringle JR, Botstein D. Suppression of yeast geranylgeranyl transferase I defect by alternative prenylation of two target GTPases, Rho1p and Cdc42p (1993) *Mol Biol Cell,* 4(10): 1017-1025.

Okura T, Igase M, Kitami Y, Fukuoka T, Maguchi M, Kohara K, Hiwada K Platelet-derived growth factor induces apoptosis in vascular smooth muscle cells: roles of the Bcl-2 family (1998) *Biochim Biophys Acta,* 1403(3): 245-253.

Olashaw NE, Van Wyk JJ, Pledger WJ. Control of late G_0/G_1 progression and protein modification by SmC/IGF-I (1987) *Am J Physiol,* 253(4Pt1): C575-C579

Olson MF, Ashworth A, Hall A. An essential role for Rho, Rac, and Cdc42 GTPases in cell cycle progression through G_1 (1995) *Science,* 269(5228): 1270-1272.

Olson MF, Paterson HF, Marshall CJ. Signals from Ras and Rho GTPases interact to regulate expression of p21Waf1/Cip1 (1998) *Nature,* 394(6690): 295-299.

Oltvai Z N, Milliman C L, Korsmeyer S J. Bcl-2 heterodimerizes *in vivo* with a conserved homolog, Bax, that accelerates programmed cell death (1993) *Cell,* 74(4): 609-619.

Orekhov AN, Tertov VV, Kudryashov SA, Khashimov KhA, Smirnov VN. Primary culture of human aortic intima cells as a model for testing anti-atherosclerotic drugs. Effects of cyclic AMP, prostaglandins, Calcium antagonists, antioxidants, and lipid-lowering agents (1986) *Atherosclerosis,* 60(2): 101-110.

Ormerod M G, Collins M K L, Rodriguez-Tarduchy G and Robertson D. Apoptosis in interleukin-3-dependent haemopoietic cells: quantitation by two flow cytometric methods (1992) *J Immunol Methods,* 153(1-2): 57-65.

Padayatty SJ, Marcelli M, Shao TC, Cunningham GR. Lovastatin–induced apoptosis in prostate stromal cells. (1997) *J Clinl Endocrinol Metab*, 82 (5): 1434-1439.

Pandey S and Wang E. Cells en route to apoptosis are characterised by the upregulation of c-fos, c-jun, cdc2, and RB phosphorylation, resembling events of early cell-cycle traverse (1995) *J Cell Biochem,* 58(2): 135-150.

Pappu AS, Illingworth DR. Contrasting effects of lovastatin and cholestyramine on low-density lipoprotein cholesterol and 24 hours urinary mevalonate excretion in patients with heterozygous familial hypercholesterolemia (1989) *J Lab Clin Med.* 114(5): 554-562.

Park DS, Morris EJ, Padmanabhan J, Shelanski ML, Geller HM, Greene LA Cyclin-dependent kinases participate in death of neurones evoked by DNA-damaging agents (1998) *J Cell Biol,* 143(2): 457-467.

Pascal M, Sepulchre C, Chazan JB, Majoie B. Evidence for the inhibition of platelet-derived growth factor induced rat smooth muscle cell DNA synthesis by fenofibric acid at the G_o/G_1 cell cycle level (1983) *Life Sci,* 33(10): 925-933.

Patel MK, Lymn JS, Clunn GF, Hughes AD. Thrombospondin-1 is a potent mitogen and chemoattractant for human VSM cells (1997) *Arterioscler Thromb Vasc Biol,* 17(10): 2107-2114.

Peeper DS, Upton TM, Ladha MH, Neuman E, Zalvide J, Bernards R, De Caprio JA, Ewen ME. Ras signalling linked to the cell-cycle machinery by the retinoblastoma protein (1997) *Nature,* 386(6621): 177-181.

Perez-Sala D and Mollinedo F. Inhibition of isoprenoid biosynthesis induces apoptosis in human promyelocytic HL-60 cells (1994) *Biochem Biopys Res Comm,* 199(3): 1209-1215.

Perlman H, Maillard L, Kransinski K, Walsh K. Evidence for the rapid onset of apoptosis in medial smooth muscle cells after balloon injury (1997) *Circulation,* 95 (4): 981-987.

Petrocelli T, Poon R, Drucker DJ, Slingerland JM, Rosen CF. UVB irradiation induces p21Cip1/WAF1 and mediates G_1 and S phase checkpoints (1996) *Oncogene,* 12 (7): 1387-1396.

Pickering JG, Weir L, Rosenfield K, Stetz J, Jekanowski J, Isner JM. Smooth muscle cell outgrowth from human atherosclerotic plaque: implications for the assessment of lesion biology (1992) *J Am Coll Cardiol,* 15; 20(6): 1430-1439.

Pledger WJ, Hart CA, Locatell KL, Scher CD. Platelet-derived growth factor-modulated proteins: constitutive synthesis by a transformed cell line (1981) *Proc Natl Acad Sci USA,* 78(7): 4358-4362.

Pollard JW and Walker JM. Animal Cell Culture (Vol 5) (1989) in *Methods in Molecular Biology*; Humana Press, Clifton, New Jersey, p6.

Pollman MJ, Hall JL, Mann MJ, Zhang L and Gibbons GH. Inhibition of neointimal cell bcl-x expression induces apoptosis and regression of vascular disease (1998) *Nat Med,* 4 (2): 222-227.

Qin XQ, Livingston DM, Kaelin WG Jr, Adams PD. Deregulated transcription factor E2F-1 expression leads to S-phase entry and p53-mediated apoptosis (1994) *Proc Natl Acad Sci USA,* 91(23): 10918-10922.

Quesney-Huneeus V, Galick H A, Siperstein M D, Erickson S K, Spencer T A, Nelson J A. The dual role of mevalonate in the cell cycle (1983) *J Biol Chem,* 258(1): 378-385.

Quesney-Huneeus V, Wiley MH and Siperstein MD. Essential role for mevalonate synthesis in DNA replication (1979) *Proc Natl Acad Sci USA,* 76(10): 5056-5060.

Quiec D, Maziere C, Auclair M, Santous R, Gardette J, Redziniak G, Franchi J, Dubertret L, Maziere JC. Lovastatin enhances the photocytotoxicity of UVA radiation towards cultured N.C.T.C. 2544 human keratinocytes; prevention by cholesterol supplementation and by a cathepsin inhibitor (1995) *Biochem J,* 310 (Pt 1): 305-309.

Rabinovitch PS. "Analysis of flow cytometric DNA histograms" Chp. 3 in Cell Growth and Apoptosis (A Practical Approach) (1996) ed. by Studzinski GP, Practical Approach Series IRL Press, p45.

Raff MC, Lillien LE, Richardson WD, Burne JF, Noble MD. Platelet-derived growth factor from astrocytes drives the clock that times oligodendrocyte development in culture (1988) *Nature,* 333(6173): 562-565.

Raff MC. Social controls on cell survival and cell death (1992) *Nature*, 356(6368): 397-400.

Rando RR. Chemical biology of isoprenylation/methylation (1996) *Biochemica et Biophysica Acta* 1300(1): 5-16.

Rattis FM, Cocha M, Dalbiez-Gauhier C, Courtellemont P, Schmitt D, Peguet-Navarro J. Effects of ultraviolet B radiation on human Langerhans cells: functional alteration of CD86 upregulation and induction of apoptotic cell death (1998) *J Invest Dermatol,* 111(3): 373-379.

Reddy BS, Wang CX, Samaha H, Lubet R, Steele VE, Kelloff GJ, Rao CV Chemoprevention of colon carcinogenesis by dietary perillyl alcohol (1997) *Cancer Res*, 57(3) : 420-425.

Reed SI. Control of the G_1/S transition (1997) *Cancer Surv*, 29: 7-23.

Reedquist KA, Pope TK, Roess DA. Lovastatin inhibits proliferation and differentiation and causes apoptosis in lipopolysaccharide-stimulated murine B-cells. (1995) *Biochem and Biophys Research Communs*, 211 (2): 665-670.

Refson JS, Schachter M, Patel MK, Hughes AD, Munro E, Chan P, Wolfe JH, Sever PS. Vein graft stenosis and the heparin responsiveness of human vascular smooth muscle cells (1998) *Circulation*, 97(25): 2506-2510.

Ren Z, Elson CE, and Gould MN. Inhibition of type I and type II geranylgeranyl protein transferase by the monoterpene perillyl alcohol in NIH3T3 cells (1997) *Biochem Pharmacol*, 54(1): 113-120.

Resh MD. Regulation of cellular signalling by fatty acid acylation and prenylation of signal trasduction proteins (1996) *Cell Signal*, 8(6): 403-412.

Ripple GH, Gould MN, Stewart JA, Tutsch KD, Arzoomanian RZ, Alberti D, Feierabend C, Pomplum M, Wilding G, Bailey HH. Phase I clinical trial of perillyl alcohol administered daily (1998) *Clin Cancer Res*, 4(5): 1159-1164.

Rosenblatt J, Gu Y, Morgan DO. Human cyclin-dependent kinase 2 is activated during the S and G_2 phases of the cell cycle and associates with cyclin A (1992) *Proc Natl Acad Sci USA*, 89(7): 2824-2828.

Ross R, Glomset J, Kariya B, Harker L. A platelet-dependent serum factor that stimulates the proliferation of arterial smooth muscle cells *in vitro* (1974) *Proc Natl Acad Sci USA*, 71(4): 1207-1210.

Ross R. The pathogenesis of atherosclerosis: A perspective for the 1990's. (1993) *Nature*, 362(6423): 801-809.

Ross R. Atherosclerosis – an inflammatory disease (1999) *N Engl J Med* 340(2): 115-126.

Roullet J B, Xue H, Pappu A S, Roullet C, Holcomb S, McCarron D A. Mevalonate availability and cardiovascular functions (1993) *Proc Natl Acad Sci USA*, 90(24): 11728-11732.

Roussillon S, Astruc M, Defay R, Tabacik C, Descomps B, Crastes de Paulet A DNA and cholesterol biosynthesis in synchronised embryonic rat fibroblasts I. Temporal relationships between HMG-CoA reductase activity, sterol biosynthesis and thymidine incorporation into DNA (1983) *Biochem Biophys Acta,* 763(1): 1-10.

Rowell C A, Kowalczyk J J, Lewis M D, Garcia A M. Direct demonstration of geranylgeranylation and farnesylation of Ki-ras *in vivo* (1997) *J Biol Chem,* 272(22): 14093-14097.

Rubin K, Tingstrom A, Hansson GK, Larsson E, Ronnstrand L, Klareskog L, Claesson-Welsh L, Heldin CH, Fellstrom B, Terracio L. Induction of β-type receptors for platelet-derived growth factor in vascular inflammation: possible implications for development of vascular proliferative lesions (1988) *Lancet,* 1(8599): 1353-1356.

Rudin CM and Thompson CB. Apoptosis and disease: regulation and clinical relevance of programmed cell death (1997) *Annu Rev Med*, 48: 267-281.

Rufini S, Rainaldi G, Abbracchio MP, Fiorentini C, apri M, Franceschi C, Malorni W. Actin Cytoskeleton as a target for 2-chloroadenosine: evidence for induction of apoptosis in C2C12 myoblastic cells (1997) *Biochem Biophys Res Commun,* 238(2): 361-366.

Sakai N, Ogiso Y, Fujita H, Watari H, Koike T, Kuzumaki N. Induction of apoptosis by a dominant negative H-Ras mutant (116Y) in K562 cells (1994) *Exp Cell Res,* 215(1): 131-136.

Sata M, Perlman H, Muruve DA, Silver M, Ikebe M, Libermann TA, Oettgen P, Walsh K. Fas ligand gene transfer to the vessel wall inhibits neointima formation and overrides the adenovirus-mediated T cell response (1998) *Proc Natl Acad Sci USA,* 95(3): 1213-1217.

Sawamura M, Li N, Nara Y, Yamori Y. Proliferation effect of mevalonate metabolites other than isoprenoids on cultured vascular smooth muscle cells (1993) *Clin Exp Pharmacol Physiol,* 20 (7-8): 509-514

Schaefer HE. Proliferation versus atrophy - the ambivalent role of smooth muscle cells in atherosclerosis (1994) *Basic Res Cardiol,* 89 Suppl 1: 47-58.

Schafer WR, Trueblood CE, Yang CC, Mayer MP, Rosenberg S, Poulter CD, Kim SH, Rine J. Enzymatic coupling of cholesterol intermediates to a mating pheromone precursor and to the ras protein (1990) *Science,* 249(4973): 1133-1139.

Schmidt R A, Glomset J A, Wight T N, Habenicht A J, Ross R. A study of the influence of mevalonic acid and its metabolites on the morphology of Swiss 3T3 cells (1982) *J Cell Biol,* 95(1): 144-153.

Schmidt RA, Schneider CJ and Glomset JA. Evidence for post-translational incorporation of a product of mevalonic acid into Swiss 3T3 cell proteins (1984) *J Biol Chem,* 259(16): 10175-10180.

Schulz S, Buhling F, Ansorge S. Prenylated proteins and lymphocyte proliferation: inhibition by d-limonene related monoterpenes (1994) *Eur J Immunol,* 24(2): 310-307.

Schwartz SM, Reidy MA, O'Brien ERM. Assessment of factors important in atherosclerotic occlusion and restenosis (1995) *Thromb Haemost,* 74(1): 541-551.

Schwatrz SM and Murry CE. Proliferation and the monoclonal origins of atherosclerotic lesions (1998) *Annu Rev Med* 49: 437-460.

Sepp-Lorenzino L, Rao S, Coleman PS. Cell-cycle-dependent, differential prenylation of proteins (1991) *Eur J Biochem,* 200(2): 579-590.

Seronie-Vivien S, Pradines A, Couderc B, Clamagirand C, Berg D, Soula G, Favre G. Reversion of transformed phenotype of human adenocarcinoma A549 cells by expression of 3-hydroxy-3-methylglutaryl coenzyme A reductase complementary DNA (1995) *Cell Growth Differ,* 6(11): 1415-1423.

Shi Y, Glynn JM, Guilbert LJ, Cotter TG, Bissonette RP and Green DR. Role for *c-myc* in activation-induced apoptotic cell death in T cell hybridomas. (1992) *Science,* 257(5067): 212-214.

Shindo Y and Hashimoto Y. Ultraviolet B-induced cell death in four cutaneous cell lines exhibiting different enzymatic antioxidant defences: involvement of apoptosis (1998) *J Dermatol Sci,* 17(2): 140-150.

Shirataki H, Kaibuchi K, Hiroyishi M, Isomura M, Araki S, Sasaki T, Takai Y Inhibition of the action of the stimulatory GDP/GTP exchange protein for smg p21 by the geranylgeranylated sythetic peptides designed from its C-terminal region (1991) *J Biol Chem,* 266(31): 20672-20677.

Sinensky M and Logel J. Defective macromolecule synthesis and cell-cycle progression in a mammalian cell starved for mevalonate (1985) *Proc Natl Acad Sci USA* 82(10): 3257-3261.

Sirois MG, Simons M, Edelman ER. Antisense oligonucleotide inhibition of PDGFR-beta receptor subunit expression directs suppression of intimal thickening (1997) *Circulation,* 95(3): 669-676.

Skalka M, Cejkova M and Matyasova J. The sensitivity of chromatin from thymuses and spleens of irradiated mice to alkaline solutions. (1976) *Folia Biol (Praha),* 22 (5): 335-342.

Slomp J, GittenbergerdeGroot AC, Glukhova Ma, van Munsteren J C, Kockx MM, Schwartz SM, Koteliansky VE. Differentiation, dedifferentiation, and apoptosis of smooth muscle cells during the development of the human ductus arteriosus (1997) *Arterioscler Thromb Vasc Biol,* 17(5): 1003-1009.

Smith A and Haaf T. DNA nicks and increased sensitivity of DNA to fluorescence in situ end labeling during functional spermiogenesis (1998) *Biotechniques* 25(3): 496-502.

Spiegel A M, Backlund P S, Butyrinski J E, Jones T L Z, Simonds W F. The G protein connection: molecular basis of membrane association (1991) *Trends Biochem Sci,* 16(9): 338-341.

Stark WW Jr, Blaskovich MA, Johnson BA, Qain Y, Vasudevan A, Pitt B, Hamilton AD, Sebti SM, Davies P. Inhibiting geranylgeranylation blocks growth and promotes apoptosis in pulmonary vascular smooth muscle cells (1998) *Am J Physiol,* 275(1 Pt 1): L55-L63.

Steg PG, Tahlil O, Aubailly N, Caillaud JM, Dedieu J F, Berthelot K, Le Roux A, Feldman L, Perricaudet M, Denefle P, Branellec D. Reduction of restenosis after angioplasty in an atheromatous rabbit model by suicide gene therapy (1997) *Circulation,* 96(2): 408-411.

Stiles CD, Capone GT, Scher CD, Antoniades HN, Van Wyk JJ, Pledger WJ. Dual control of the cell growth by somatomedins and platelet-derived growth factor (1979) *Proc Natl Acad Sci USA,* 76(3): 1279-1283.

Stiles CD. Molecular biology of platelet-derived growth factor (1983) *Cell*, 33(3): 653-655.

Stokoe D, MacDonald S G, Cadwallader K, Symons M, Hancock J F. Activation of Raf as a result of recruitment to the plasma membrane (1994) *Science*, 264(5164): 1463-1467

Stryer L, 1995. *Biochemistry* 4th edition. WH Freeman and Company, New York. p693.

Sun XF, Ekberg H, Zhang H, Carstensen JM, Nordenskjold B. Overexpression of ras is an independent prognostic factor in colorectal adenocarcinoma (1998) *APMIS* 106(6): 657-664.

Suzuki J, Kaziro Y, Koide H. Synergistic action of R-Ras and IGF-I on Bcl-xL expression and caspase-3 inhibition in BaF3 cells: R-Ras and IGF-I control distinct anti-apoptotic kinase pathways (1998) *FEBS Lett*, 437(1-2): 112-116.

Tagami M, Yagamata K, Nara Y, Fujino H, Kubota A, Numano F, Yamori Y. Ultrastructural analysis of survival in cultured smooth muscle cells isolated from stroke-prone spontaneously hypertensive rats: effect of growth factors (1996) *Cell Tissue Res*, 285(2): 205-215.

Tamm I and Kikuchi T. Insulin-like growth factor-I (IGF-I), insulin, and epidermal growth factor (EGF) are survival factors for density-inhibited, quiescent Balb/c-3T3 murine fibroblasts (1990) *J Cell Physiol*, 143(3): 494-500.

Tanaka T, Tatsuno I, Noguchi Y, Uchida D, Oeda T, Narumiya S, Yasuda T, Higashi H, Kitagawa M, Nakayama K, Saito Y, Hirai A. Activation of cyclin-dependent kinase 2 (Cdk2) in growth-stimulated rat astrocytes. Geranylgeranylated Rho small GTPase(s) are essential for the induction of cyclin E gene expression (1998) *J Biol Chem*, 273(41): 26772-26778.

Tatsuno I, Tanaka T, Oeda T, Yasuda T, Kitagawa M, SaitoY, Hirai A. Geranylgeranyl pyrophosphate, a metabolite of mevalonate, regulates the cell cycle progression and DNA synthesis in human lymphocytes (1997) *Biochem Biophys Res Commun*, 241(2): 376-382.

Taylor AJ, Farb AA, Angello DA, Burwell LR, Virmani R. Proliferative activity in coronary atherectomy tissue. Clinical, histopathologic and immunohistochemical correlates (1995) *Chest,* 108(3): 815-820.

Telford W G, King L E and Fraker P J. Evaluation of glucocorticoid-induced DNA fragmentation in mouse thymocytes by flow cytometry (1991) *Cell Prolif,* 24(5): 447-459.

Thommes KB, Hoppe J, Vetter H, Sachinidis A. The synergistic effect of PDGF-AA and IGF-I on VSMC proliferation might be explained by the differential activation of their intracellular signalling pathways (1996) *Exp Cell Res,* 226(1): 59-66

Tieger E, Than VD, Richard L, Wisnewsky C, Tea BS, Gaboury L, Tremblay J, Schwartz K, Hamet P. Apoptosis in pressure overload-induced heart hypertrophy in the rat (1996) *J Clin Invest,* 97(12): 2891-2897.

Tobert J A, Hitzenberger G, Kukovetz W R, Holmes I B, Jones K H. Rapid and substantial lowering of human serum cholesterol by mevinolin (MK-803), an inhibitor of hydroxymethylglutaryl-coenzyme A reductase (1982) *Atherosclerosis,* 41(1): 61-5.

Tobert J A. New developments in lipid-lowering therapy: the role of inhibitors of hydroxymethylglutaryl-coenzyme A reductase (1987) *Circulation,* 76(3): 534-538.

Trent JC 2nd, McConkey DJ, Loughlin SM, Harbison MT, Fernandez A, Ananthaswamy HN. Ras signaling in tumour necrosis factor-induced apoptosis (1996) *EMBO J,* 15(17): 4497-4505.

Ucker DS, Obermiller PS, Eckhart W, Apgar JR, Berger NA, Meyers J. Genome digestion is a dispensable consequence of physiological cell death mediated by cytotoxic T lymphocytes (1992) *Mol Cell Biol,* 12(7): 3060-3069.

Vaughan CJ, Murphy MB, Buckley BM. Statins do more than just lower cholesterol (1996) *Lancet,* 348 (9034): 1079-1082.

Vaux DL. Towards an understanding of the molecular mechanisms of physiological cell death (1993) *Proc Natl Acad Sci USA*, 90 (30): 786-789.

Velican C and Velican D. Study on the onset of atherosclerotic lesions in human coronary arteries (1979) *Med Interne,* 17(2): 131-149.

Villaschi S and Spagnoli LG. Autoradiographic and ultrastructural studies on the human fibro-atheromatous plaque. (1983) *Atherosclerosis,* 48(1): 95-100.

Virchow R. Cellular Pathology as based upon Physiological and Pathological Histology. (1859) ed.2 Translated from German by B Chance. Reproduced by Dover Publications, New York, 1971, 356-382.

Vogt A, Qian Y, Mc Guire TF, Hamilton AD, Sebti SM. Protein geranylgeranylation, not farnesylation, is required for the G_1 to S phase transition in mouse fibroblasts (1996) *Oncogene,* 13(9): 1991-1999.

Voisard R, Dartsch PC, Seitzer U, Roth D, Kochs M, Hombach V. [Cell culture as pre-screening system for drug prevention of restenosis]? Article in German (1991) *Vasa Suppl,* 33: 140-141.

Walter SV and Hamet P. Enhanced DNA synthesis in heart and kidney of newborn spontaneously hypertensive rats. (1986) *Hypertension,* 8(6): 520-525.

Wang H C, Millan J A, Cox A D, Der C J, Rapp U R, Beck T, Zha H, Reed J C R-ras promotes apoptosis caused by growth factor deprivation via a Bcl-2 suppressible mechanism (1995) *J Cell Biol,* 129(4): 1103-1114.

Wani M A, Denko N C, Stambrook P J. Expression of rap1 suppresses genomic instability of H-ras transformed mouse fibroblasts (1997) *Somat Cell Mol Genet,* 23(2): 123-133.

Weintraub WS, Boccuzzi SJ, Klein JL, Kosinski AS, King SB 3rd, Ivanhoe R, Cedarholm JC, Stillabower ME, Talley JD, DeMaio SJ, et al., Lack of effect of lovastatin on restenosis after coronary angioplasty. Lovastatin Restenosis Trial Study Group (1994) *N Engl J Med,* 331(20): 1331-1337.

Westermark B, Heldin CH. Platelet-derived growth factor. Structure, function and implications in normal and malignant cell growth (1993) *Acta Oncol,* 32(2): 101-105.

Whyte DB, Kirschmeier P, Hockenberry TN, Nunez-Oliva I, James L, Catino JJ, Bishop WR, Pai JK. K-and N-Ras are geranylgeranylated in cells treated with farnesyl protein transferase inhibitors (1997) *J Biol Chem,* 272(22): 14459-14464.

Wyllie A H, Rose K A, Morris R G, Stell C M, Foster E, Spandidos D A. Rodent fibroblasts tumours expressing human myc and ras genes: growth, metastasis and endogenous oncogene expression (1987) *Br J Cancer,* 56(3): 251-259.

Wyllie AH, Morris RG, Smith AL, and Dunlop D. Chromatin cleavage in apoptosis: association with condensed chromatin morphology and dependence on macromolecular synthesis. (1984) *J Pathol*, 142 (1): 67-77.

Wyllie AH. Glucocorticoid-induced thymocyte apoptosis is associated with endogenous endonuclease activation (1980) *Nature,* 284 (5756): 555-556.

Yamada T, Ohyama H, Kinjo Y, and Watanabe M. Evidence for the internucleosomal breakage of chromatin in rat thymocytes irradiated *in vitro*. (1981) *Radiat Res*, 85 (3): 554-553.

Yamane H K, Farnsworth C C, Xie H Y, Evans T, Howald W N, Gelb M H, Glomset J A, Clarke S, Fung B K. Membrane-binding domain of the small G protein G25K contains an S-(all-trans-geranylgeranyl) cysteine methyl ester at its carboxyl terminus (1991) *Proc Natl Acad Sci USA,* 88(1): 286-290.

Yamane HK, Fung BK-K. The membrane-binding domain of a 23-kDa G protein is carboxyl methyalted (1989) *J Biol Chem,* 264(33): 20100-20105.

Yamori Y, Igawa T, Kanbe T, Kihara M, Nara Y, Hovie R. Mechanisms of structural vascular changes in genetic hypertension: analyses on cultured vascular smooth muscle cells from spontaneously hypertensive rats (1981) *Clin Sci,* 61(suppl 7): 121s-123s.

Yang BC, Chang HM, Wang YS, Chen RF, Lin SJ. Transient induction of apoptosis in serum-starved glioma cells by insulin and IGF-I (1996) *Biochim Biophys Acta,* 1314(1-2): 83-92.

Yang Y, Yu J, Field J. Signals from the ras, rac, and rho GTPases converge on the Pak protein kinase in rat-1 firbroblasts (1999) *Mol Cell Biol* 19(3): 1881-1891.

Yeh H-J, Ruit KG, Wang Y-X, parks WC, Sinder WD and Deuel TF. PDGF A-chain gene is expressed by mammalian neurons during development and in maturity (1991) *Cell,* 64(1): 209-216.

Yokoyama K and Gelb MH. Purification of a mammalian protein geranylgeranyl transferase. Formation and catalytic properties of an enzyme-geranylgeranyl pyrophosphate complex (1993) *J Biol Chem,* 268(6): 4055-4060.

Yoshida Y, Kawata M, Katayama M, Horiuchi H, Kita Y and Takai Y. A geranylgeranyltransferase for rhoA p21 distinct from the farnesyltransferase for ras p21S (1991) *Biochem Biophys Res Commun,* 175(2): 720-728.

Yu D, Jing T, Liu B, Yao J, Tan M, Mc Donnell TJ, Hung MC. Overexpression of ErbB2 blocks Taxol-induced apoptosis by upregulation of p21Cip1, which inhibits p34Cdc2 kinase (1998) *Mol Cell,* 2(5): 581-591.

Zamai L, Falcieri E, Zauli G, Cataldi A, and Vitale M. Optimal detection of apoptosis by flow cytometry depends on cell morphology (1993) *Cytometry,* 14(8): 891-897.

Zhang FL and Casey PJ. Protein isoprenylation: molecular mechanisms and functional consequences (1996) *Ann Rev Biochem,* 65: 241-269.

Zhang FL, Kirschmeier P, Carr D, James L, Bond RW, Wang L, Patton R, Windsor WT, Syto R, Zhang R, Bishop WR. Characterisation of Ha-ras, N-ras, Ki-Ras4A, and Ki-Ras4B as *in vitro* substrates for farnesyl protein transferase and geranylgeranyl protein transferase type I (1997) *J Biol Chem,* 272(15): 10232-10239.

Zhivotovsky BD, Zvonareva NB, and Hanson KP. Characteristics of rat thymus chromatin degradation products after whole body X-irradiation. (1981) *Int J Radiat Biol*, 39 (4): 437-440.

Ziman M, Preuss D, Mulholland J, O'Brien JM, Botstein D, Johnson DI Subcellular localisation of cdc42p, a *Saccharomyces cerevisae* GTP-binding protein involved in the control of cell prolarity (1993) *Mol Cell Biol,* 4(12): 1307-1316.

Zubiaur M, Sancho J, Terhorst C, Faller DV. A small GTP-binding protein, Rho, associates with the platelet-derived growth factor type-beta receptor upon ligand binding (1995) *J Biol Chem,* 270(29): 17221-17228.

Publications relating to this thesis

1. **Unlu S, Mason CD, Hughes AD**. Action of a statin on apoptosis in human vascular smooth muscle cells (1997) *Hypertension* 30(4): p70.

2. **Unlu S, Demoliou-Mason C, Schacter M, Hughes AD**. Action of lovastatin on cell death in cultured SV-40 transformed human vascular smooth muscle cells (1997) *Br J Pharmacol* 122(SS): P368.

3. **Unlu S, Demoliou-Mason C, Hughes AD**. Action of perillyl alcohol on growth and apoptosis in SV-40 transformed human vascular smooth muscle cells (1998) *Hypertension* 32(4): p106.

4. **Unlu S, Mason CD, Schachter M, Hughes AD**. Interactions between HMG-CoA reductase inhibition and UVB irradiation on proliferation and apoptosis in SM1 smooth muscle cells (1998) *Biochem Soc Trans* 26(4): S322.

5. **Unlu S, Mason CD, Hughes AD**. Role of isoprenylation in the inhibitory action of lovastatin on proliferation of SV40 immortalised human saphenous vein smooth muscle cells (1998) *Biochem Soc Trans* 26(4): S324.

6. **Unlu S, Mason CD, Hughes AD**. Platelet-derived growth factor-BB induces apoptosis in cultured vascular smooth muscle cells derived from human saphenous vein (1998) *Biochem Soc Trans* 26(4): S325.

APPENDIX

Appendix I

All cuture media and reagents were stored at 4^0C.

Transport medium

All vascular samples were transported in this medium before the explant technique was carried out. To 845 ml of sterile deionised water, the following were added:

HBSS (10x)	100ml
1M HEPES (pH 7.3)	25ml
Penicillin/Streptomycin (10000IU/ml)/(10000mg/ml)	10ml
Kanamycin (10mg/ml)	10ml
Fungizone (250mg/ml)	5ml
Sodium Bicarbonate (7.5%w/v)	5ml

Condition medium

This consists of a 1:1 mixture of 15% (v/v) FBS from cell culture and fresh 15%(v/v) FBS culture medium

Sterile Foetal Bovine Serum (mycoplasma and virus screened)

Purchased from Life Technologies Ltd.(Paisley, UK). Stock stored at –20°C.

Dolbecco's Modified Eagle's Medium (DMEM) for primary human vascular smooth muscle (VSM) cells

Purchased from Life Technologies Ltd. (Paisley, UK), it contains 25mM HEPES, 4mM Glutamax-I, without Sodium Pyruvate. To make up 15% (v/v) FBS, the following were added to 500ml of DMEM:

Sodium Pyruvate (100mM)	6.04ml
Penicillin/Streptomycin (10000IU/ml)/(10000mg/ml)	6.04ml
Gentamicin (10mg/ml)	1.5ml
Foetal bovine serum	90.6ml

Dolbecco's Modified Eagle's Medium (DMEM) for SV-40 large T antigen transformed human VSM cells (SM1 cells)

Purchased from Life Technologies Ltd. (Paisley, UK), it contains 25mM HEPES, 4mM Glutamax-I, without Sodium Pyruvate. To make up 10% (v/v) FBS, the following were added to 500ml of DMEM:

Sodium Pyruvate (100mM)	5.69ml
Penicillin/Streptomycin	

(10000IU/ml)/(10000mg/ml)	5.0ml
Geniticin (G418 at 100mg/ml in PBS)	1.12ml
Foetal bovine serum	57.3ml

For 10% dialysed (v/v) FBS, normal serum was replaced with dialysed serum.

Synthetic serum-free medium (NCTC-109 medium) for the primary human VSM cells

Purchased from Life Technologies Ltd., this medium contains Sodium Bicarbonate ($NaHCO_3$) and other inorganic salts, all the L-amino acids, all the known vitamins, coenzymes, antioxidants and nucleic acid derivatives. It does not contain Glutamax-I nor Sodium Pyruvate. 500ml of NCTC-109 medium was supplemented with BSA (2.5mg/ml, final concentration), from Boehringer Mannheim (W. Germany) and the following:

Gentamicin (10mg/ml)	1ml
Penicillin/ Streptomycin	5ml
HEPES (1M)	13ml
L-Glutamine (200mM)	10.5ml
Bovine Serum Albumin (BSA)	1.32g

Synthetic serum-free medium (NCTC-109 medium) for the SV-40 large T antigen transformed human VSM cells

The same as above, but this time 500ml of NCTC-109 medium was supplemented with:

Penicillin/ Streptomycin	5ml
Geniticin (100mg/ml in PBS)	1.12ml
HEPES (1M)	13ml
L-Glutamine (200mM)	10ml
Bovine Serum Albumin (BSA)	1.32g

Supplemented serum-free medium without BSA for thymidine incorporation in SM1 cells

500ml of standard DMEM with Glutamax-I and HEPES from Life Technologies was supplemeted with:

Transferrin (4mg/ml)	625µl
Selenium (100µM)	500µl
Insulin (1µM)	500µl
Geniticin (100mg/ml)	1.12ml

Hank's Buffered Salt Solution (HBSS x10)

This was purchased from Life Technologies (Paisley, UK).

Trypsin-EDTA solution

This is a mixture of trypsin at 0.25% (w/v) in 1mM EDTA and PBS-A solution:

Stock trypsin solution (10x)	1vol
10mM EDTA solution in PBS-A (10x)	1vol
PBS-A	8vol

Appendix II

Tris-EDTA pH 8.0 (TE pH 8.0)

To 100ml of deionised water, the following reagents, both purchased as Molecular Biology (MB) grade from Sigma Chem. Co. Ltd., UK were added:

Tris-HCl pH8.0 (1M)	1ml
EDTA pH8.0 (500mM)	0.2ml

The solution was then pHed to pH 8.0, and stored at room temperature.

Tris-acetate-EDTA (50x TAE buffer)

To 500ml of deionised water, the following were added:

Tris base	242g
Glacial acetic acid	57.1 ml
EDTA pH 8.0 (500mM)	100ml

DNA gel loading buffer (6x)

Purchased from Sigma Chem Co., UK as a MB grade reagent, with the following composition:

Bromophenol blue	0.25% (w/v)
Xylene Cyanol	0.25% (w/v)
Sucrose in H_2O	40% (w/v)

5M Sodium Chloride solution (NaCl, M_r=58.44g)

Purchased as an MB grade reagent from Sigma Chem Co. Ltd, UK.
14.6g of the pure salt was dissolved in 50 ml of deionised water

Lysis buffer

This buffer was made up from the following MB grade reagents from Sigma Chem Co., UK, dissolved in 200ml of deionised water:

HEPES, pH7.2 (200mM)	2ml
Potassium Chloride (KCl) (50mM)	20ml
Magnesium Chloride ($MgCl_2$) (100mM)	2ml
NP-40 (10% w/v)	10ml

Sodium Deoxycholate (10% w/v)	2ml
EDTA (500mM)	4ml

Phenol:Chloroform (1:1)

This was purchased from Sigma Chem Co.,UK (MB grade) and stored at 4^{0}C.

IGEPAL CA-630

This is a non-ionic detergent, purchased from Sigma Chem Co., UK, and made up to 0.25% in deionised water.

Proteinase K

This was purchased from Sigma Chem Co., UK. It was made up in deionised water first as 50µg/ml (for the standard salting out procedure for DNA extraction), but later as 1mg/ml (for the final procedure).

Ribonuclease A (RNase A)

This was also purchased from the Sigma Chem Co., UK. It was first made up to 10µg/ml in TE (pH 8.0) buffer for the standard salting out method, but later as 1mg/ml in TE buffer for the final optimised procedure.

DNA weight marker, ϕX174 RF DNA Hae III fragments

This was purchased from Life Technologies (Paisley, UK). The stock (0.5mg/ml) was dissolved in 10mM Tris-HCL (pH 7.4), 5mM NaCl, 0.1mM EDTA. The re-constituted working concentration was 0.04mg/ml:

Stock (0.5mg/ml)	20µl
Filtered deionised H_2O	188.3µl
GLB (gel loading buffer)	41.7µl

The stock marker, and the above diluted solution were usually stored at –20°C and 5µl of the above solution was loaded onto each gel before the samples were run.

Ethidium Bromide

A stock of 0.5 mg/ml was purchased as an MB grade reagent from Sigma Chem Co., UK and stored at 4^{0}C.

SYBR Green I dye

This was purchased from Flowgen, UK and diluted by 1:10000 into the appropriate volume of 2% agarose, and mixed in polypropylene vials, in order to cast a 3-4mm thick gel.

Phosphate-Citrate buffer (pH 7.8)

The following reagents were purchased as MB grade reagents from the Sigma Chem. Co., Ltd and made up as:

Sodium Hydrogenphosphate ($NaHPO_4$) (0.2M)	192 vols
Citric acid, pH 7.8 (0.1M)	8 vols

80% Isopropanol-2

This was purchased from BDH (Poole, UK), and diluted with deionised water to 80%.

BIBL
LONDON
UNIV.